Multimodal Cue Integration in Balance and Spatial Orientation

Shamim Quadir

This thesis is submitted for the degree of Doctor of Philosophy

Imperial College London

Department of Neuro Otology

This thesis constitutes the author's original work, all else is appropriately referenced.

Abstract

The global objective of this thesis was to make a significant contribution to our understanding of how the human brain integrates multisensory, multimodal information to inform our motion through space. The primary objectives were to discern whether visual system differentially encodes visual motion coherence and how both allocentric visual cues interact with vestibular system to tell us where and when we are in physical space. A secondary objective was to develop current techniques for the recording and analysis of visuo-vestibular sensory information for the purpose of multisensory, multimodal integration.

I studied the response of cortical visual motion area V5/MT+ to random dot kinematograms (RDK) of varying motion coherence, from complete coherence to random. I used the probability of observing TMS (transcranial magnetic stimulation) evoked phosphenes before and after the RDK as a measure of cortical excitability change. I could not show what I had hypothesised: that coherent and random motion elicited a similar net effect upon V5/MT+ excitability, with intermediary coherences of motion having comparatively less effect. However, I argue that a large factor was insufficient sample size to find the effects given the analyses used. The results do show trends consistent with coherent and random net effects being achieved by different modes of cortical activation, and the study will inform future investigation with the paradigm used. I also measured cortical excitability change at a range of relative TMS intensities. This elicited a significant differential effect consistent with the theory that TMS facilitates neurons as a function of the amount of signal they carry.

In a separate TMS evoked phosphene study, I show an interaction between whole body rotation in yaw and the ability to observe phosphenes in V5/MT+; as a function of the TMS intensity used and the velocity of whole body rotation used, relative to perceptual thresholds. As I found no main effects, I could not show whether the findings were consistent with a model of reciprocal visual and vestibular cortical inhibition. My work can be considered a feasibility study to inform further investigation.

I also used a visual-vestibular mismatch paradigm to probe how erroneous visual landmark cues update veridical vestibular estimates of angular position and motion duration. I used visual masking to reduce the reliability of the visual landmark cues, prevent visual capture and to also elicit subliminal encodement. I found that reversion to vestibular estimates of angular position was made as a function of the noise inherent in the masked visual landmark cues. I found that it was possible to subliminally encode visual landmarks to update vestibularly derived estimates of motion duration.

Lastly, I investigated the combination of a two-interval forced choice technique to record estimates of vestibularly derived angular position and a Bayesian Inference technique to parameterize the characteristics of the angular position estimates. I show this combination provides accurate estimates at the subject level and is suitable for incorporation in a Bayesian inference model of multimodal integration.

The hypothesis I aim to test in the future is that if visual landmark and vestibular cues of angular position operate within different spatial reference frames, they cannot be optimally integrated in the brain analogous to a Bayesian Inference model of the multimodal integration.

Acknowledgements

My thanks go to my supervisors Dr. Barry Seemungal and Professor Adolfo Bronstein who have afforded me so much of their time, expertise and guidance throughout my doctoral journey. I thank Professor Michael Gresty whom I consider my third supervisor. He freely offered his expertise, his encouragement and tips on sailing. I thank David Buckwell and Mary Faldon for being technically impeccable. I thank Professor John Golding for sharing his vast statistical knowledge, always delivered with good humour and words of support. I thank Lorna Stevenson for making all matters administrative resolve like magic and for her ineffable good humour. I thank José, Erica and Korina for their invaluable friendship and quick wit. I send a huge thanks to Sofia Nousi who made the perfect partner in crime. She was always there to help in those hours of need, and at all other times keep me in line.

Lastly, I would like to thank both my grandfather, Neville, and my dear friend Irina, both of whom gave me their unfaltering support in pursuing this doctorate.

Contents

Figures

Tables

Abbreviations

A/V/L/C/MIP	Anterior/Ventral/Caudal/Lateral/Medial intraparietal cortex (within intraparietal sulcus of posterior parietal cortex)
BA	Brodmann area
CIP	Caudal interparietal cortex (within intraparietal sulcus of posterior parietal cortex)
CRT	Cathode Ray Tube
fMRI	Function Magnetic Resonance Imaging
GVS	Galvanic stimulation
IPS	Intraparietal sulcus
LGN	Lateral Geniculate Nucleus
MCMC	Monte Carlo Markov Chain
MDK	Moving dot kinematogram (non-random variant of RDK)
MEG	Magnetoencephalography
MLF	Medial longitudinal fasciculus
MOBS	Modified Binary Search
OBE	Out of body experience
PEST	Parameter Estimation by Sequential Testing
PET	Positron Emission Tomography
PIVC	Posterior insular vestibular cortex
PPC	Posterior parietal cortex
rANOVA	Repeated Measures Analysis of Variance
rTMS	Repetitive transcranial magnetic stimulation
SOA	Stimulus Onset Asynchrony
TPJ	Tempo-parietal junction
VOR	Vestibulo-ocular reflex
2IFC / 2AFC	Two-interval forced choice / Two-alternative forced choice

Chapter 1.

Introduction

1.1. The human visual system and the processing of visual motion

Introduction

The human visual system is essential for accurate balance and spatial orientation in man. We generally assume that our percept of physical space is veridical, yet we construct a percept of the outside world from one or more sensory modalities which is generally non-veridical (Volcic and Kappers, 2008). Our vision is the most reliable of our senses involved in the perception of where we are in space (Hansson et al., 2010). Consequently, it affords us the most near-veridical estimate of the outside world. It is able to guide us by encoding the position of the objects around us, calculating the spatial relationships between these objects, but also the spatial relationship of these objects to our own body position. Consequently, by comparison of egocentric and allocentric reference frames, our visual system allows us to make complex spatial judgements to navigate physical space (Klatzky, 1998). The visual system also takes advantage of non-object based cues from optic flow, which takes the form of visual motion cues as the body moves relative to its visual environment, which is within an egocentric reference frame (Smith et al., 2006).

Visual space and field maps

Humans are binocular in that we have two eyes which our brains control in concordance to afford us a single, three dimensional percept of the world. Due to the optics of the eye, light from our environment is mapped onto the retina upside

down and back to front. This retinal map is encoded by myriad photoreceptors within the retina. These feed into neurons which cumulatively combine their information to feed further into the brain in a sequential process of converging neuronal firing. Put simply, a cluster of neighbouring photoreceptors at the retina will capture the light from a particular area of visual space. The output of this cluster will converge onto a single neuron. This neuron will in turn be clustered with adjacent neurons at the same level of visual processing, outputs of which will be clustered together onto a single neuron further upstream and so on to higher levels of visual processing. It therefore follows that the further upstream the visual signals travel, the more distributed the neuronal information can become and the larger a neuron's receptive field (the area of visual space in which a stimulus will modulate the firing of that neuron). This information maintains the topographic relationship of adjacent points in visual space in often adjacent and at least spatially compartmentalised neurons in the brain (Kolster et al., 2010). Thus, these clusters of neurons, in the multiple brain areas they are found, are said to contain 'visual field maps' or 'retinotopic maps' of the initial retinal information (Wandell et al., 2005).

Primary visual cortex (V1)

The main visual processing areas of the brain are found at and clustered near the occiput in the visual cortices. The human cortex can be considered a folded sheet of neurons about 2.5mm thick and composed of columns of neurons with similar tuning properties (Fischl and Dale, 2000). The primary visual cortex (area V1 or striate cortex) is the crux of all visual processing in the brain and its neurons are tuned to changes in visual orientation, spatial frequencies, colour and ocular dominance (Das, 2000). It receives external (bottom-up) neural signals from the eyes through pathways that traverse the lateral geniculate nucleus (LGN) in the thalamus and the

superior colliculus in the basal ganglia. It holds recurrent pathways with other cortical areas (Bullier, 2001, Block, 2005). This two way communication is known as recurrent feedback. The main channels by which these areas communicate with V1 are the magnocellular and parvocellular pathways (Nealey and Maunsell, 1994, Vidyasagar et al., 2002). The magnocellular pathway transmits colour, visual acuity and high-grade black and white information and is considered a fast pathway (high bandwidth) due to the comparatively large size of its receptive fields from the retina and LGN. The parvocellular pathway transmits transient, motion related low-grade black and white information and it is considered quite a slow neural pathway (low bandwidth) given the small size of its receptive fields (Maunsell et al., 1999).

Area V1 is the last stage in bottom-up visual processing at which there is a continuous retinotopic map of the visual field; lower visual areas such as the LGN have very discrete retinotopic maps, whereas in higher cortical areas the maps are compartmentalised (Rosa, 2002). The lower calcarine sulcus contains V1 neurons which encode for the upper visual field, above the visual horizon, whilst those in the upper calcarine sulcus encode for the lower visual field. In addition, those neurons in the anterior calcerine sulcus encode for the peripheral field, whilst those in the posterior calcerine sulcus encode for central vision. Indeed there are a proportionally greater concentration of neurons dedicated to fine central vision than peripheral vision, a phenomena known as cortical magnification. (Horton and Hoyt, 1991, McFadzean et al., 1994). Area V1 is subdivided into 6 layers each functionally distinct. Signals from the LGN arrive in layer 4. Specifically, sublayers 4cβ and 4cα receive magnocellular and parvocellular input respectively. From here there can be considered two visual pathways that project from V1 to other exstriate cortical areas (Mishkin and Ungerleider, 1982, Ungerleider and Haxby, 1994). The

ventral pathway is associated with object recognition and long term memory, thus 'what' is perceived from the visual environment (Braddick et al., 2000, Bar et al., 2001, Barker and Warburton, 2011). The ventral pathway proceeds sequentially from area V1 to V2 to V4, among other interactions and downward to the temporal lobe. The dorsal pathway is associated with the spatial localisation of visual stimuli, thus 'where' things are perceived in the visual environment (Courtney et al., 1996, Broadbent et al., 2004). The dorsal pathway proceeds sequentially from area V1 to area V5/MT+ in the occipital cortex onto areas such as MST (medial superior temporal area), VIP (ventral intraparietal cortex) and LIP (lateral intraparietal cortex) and MIP (medial intraparietal cortex) in the posterior parietal cortex (PPC) (Thut et al., 2005). A gross division of the ventral and dorsal pathways is illustrated in Figure 1.1.

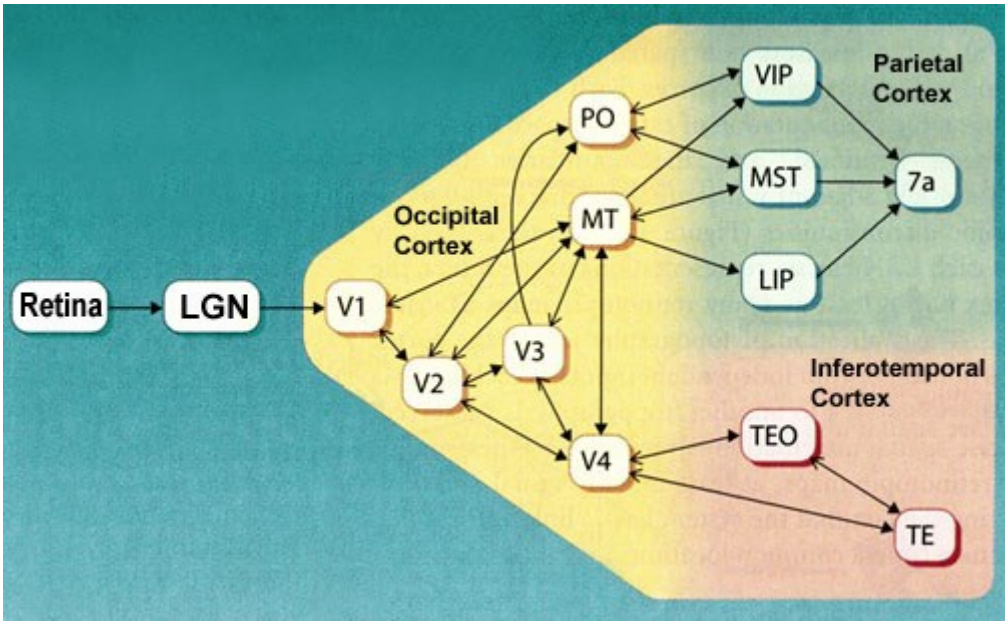

Figure. 1.1. OUTLINE OF THE CORTICAL INTERACTIONS BETWEEN VENTRAL AND DORSAL PATHWAYS. (McGill University, 2013)

In this thesis I am mainly concerned with interactions in the dorsal pathway, specifically area V5/MT+ which is responsible for the processing of visual motion. However, this does not preclude interactions in the ventral pathway. Indeed, I use visual stimuli based on allocentric cues (visual cues of objects/landmarks in space) which warrant interactions between the ventral and dorsal pathways (Klatzky, 1998). This is in addition to the more traditional use of optic flow as a visual stimulus. Optic flow is the global motion of visual stimuli across the retina (*see fig. 1.2.*) and does not require object recognition (Smith et al., 2006).

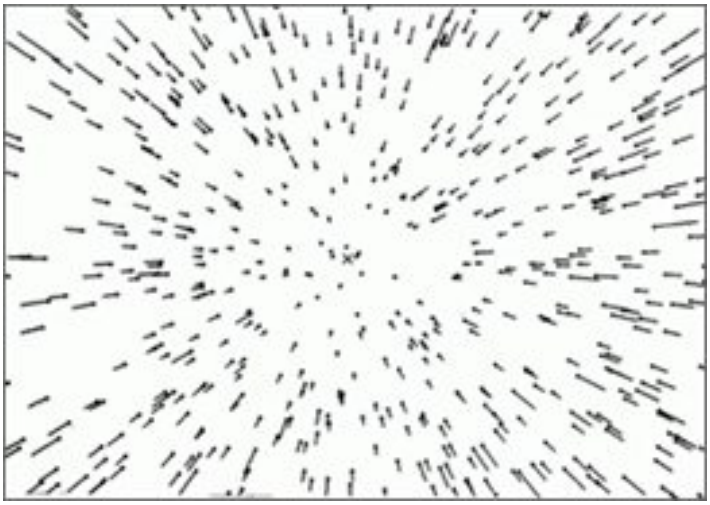

Figure 1.2. SIMULATION OF AN OPTIC FLOW FIELD IN THE FRONTAL PLANE (West Virginia University, 2013).

Medial Temporal area (V5/MT+)

Visual motion stimuli are processed in the primary visual cortex (V1) as well as medial temporal area (V5/MT+). Area V5/MT+ specifically encodes visual motion only. It receives largely magnocellular input, which is consistent with its function of processing first order visual motion based on luminance contrasts (Baloch et al., 1999).

The encoding of first order visual motion is a well understood neuronal function based on temporal changes in luminance between adjacent points in space. This can be either beta movement (Buckingham, 1987), where adjacent points consecutively illuminate, then darken creating the illusion of movement, much like an animation; or the phi phenomenon (Steinman et al., 2000), where the regular sequential illumination and darkening of adjacent points in space creates an illusion of movement – the motion perceived is that of the darkened (or background) space within the field of luminant points. The phi phenomenon requires a faster alternation of states than beta movement for the illusion to work and motion to be perceived.

Second order motion is defined as motion that incurs no change in luminance, and is based on moving contours of differing contrasts or textures. It requires higher order processing than first order motion and it is suggested that much of this takes place prior to arrival at V5/MT+ and in the ventral pathway of the visual system *(Watanabe et al., 2002).* It is suggested that both types of visual motion are fully combined by the time they reach the level of V5/MT+ (Smith et al., 1998). Comprehensive study of the monkey analogue (V5/MT) of human visual area V5/MT+ forms much our knowledge of how this visual area may function. In the macaque monkey, V5/MT is located in the posterior bank of the caudal superior temporal sulcus (Gattass and Gross, 1981), it contains a topographic representation of the contralateral visual field and receives direct projections from visual areas V1 and V2 (Dubner and Zeki, 1971, Ungerleider and Haxby, 1994). Electrophysiological recordings show that the most prominent feature of V5/MT is that some 95% of its neurons are markedly direction selective to simple visual motion, that is motion that follows a linear path in a frontal plane. Interestingly, this is in the context of being conspicuously absent of selectivity for form or for colour (Zeki, 1974, Maunsell and Van Essen, 1983, Ungerleider and

Haxby, 1994). Furthermore it has also been shown that 83% of V5/MT neurons are also selective for orientation of flashed stationary bar/slit stimuli, and indeed that there can be delineated two types of V5/MT neuron. Type I neurons are those which respond maximally to stationary bar stimuli which are presented perpendicular to their 'preferred' direction of motion, and Type II neurons are those which respond maximally when stationary bar stimuli are presented parallel to their preferred direction of motion (Albright, 1984). In addition, it has been shown that V5/MT response to static stimuli is far weaker than to motion stimuli (Albright, 1984, Marcar et al., 1995).

Many human studies define the V5/MT+ complex by use of a motion localizer (ML) test, whereby a motion stimulus is presented and regions of cortical activity measured, for example, with positron emission tomography (Zeki et al., 1991) or with fMRI (Tootell et al., 1995). In a recent study using fMRI it has been shown that the V5/MT+ complex accounted for 70% of motion localizer activation. In the same study it was shown that monkey V5/MT and human V5/MT+ share functional properties of their receptive field size, their response to moving and static stimuli, in addition to their encoding of three dimensional structure from motion. In combination with similarities in their retinotopic organisation and topological neighbourhood of cortex, it was concluded that they are indeed homologous (Kolster et al., 2010).

Medial Superior Temporal area (MST)

Human MST receives its primary input from area V5/MT+. fMRI shows that it responds strongly to activation of the ipsilateral hemifield and that this is dependent upon the nature of the optic flow structure presented. Optic flow fields are global patterns of apparent visual motion caused by an observer moving relative to their

environment and can be simulated in the laboratory. One study showed that the strongest response of human MST was produced by complex flow combining elements of expansion, contraction and rotation. Weaker responses were produced from single elements, and rigid translatory flow and random flow gave responses that were weaker still. Thus suggesting that human MST is specialized in encoding properties of global optic flow (Smith et al., 2006).

Neurons of MSTd respond to the patterns of visual motion that comprise optic flow (planar, radial and circular); they have very large receptive fields which are typically of a quadrant of the visual field to encompass global visual motion; some are modulated by changing the centre/source of optic flow, consistent with a new heading direction; and some correct for pursuit eye movements made relative to the mean heading direction (Duffy and Wurtz, 1997). To a lesser extent, MSTd also encodes for heading direction cues caused by vestibular stimuli. A neuronal recording study showed that 48% of the population sampled responded to optic flow stimuli, whilst 24% responded to translational motion, i.e. vestibular stimulation. These vestibular encoding neurons are more distributed than those that encode for elements of optic flow and it is not thought MSTd is a primary site for integration of these visual and vestibular heading cues (Gu et al., 2008, Gu et al., 2012). MSTd is discussed further in Chapter 2.

1.2. The human vestibular system and its multimodal cortical interactions

The human vestibular system consists of the peripheral sensing apparatus of the inner ear and the neural structures in the brain which co-ordinate vestibular input with the other senses and perceptual areas of the brain.

The relay stations of the human vestibular system are the vestibular nuclei of the brainstem. These route afferent signals from the peripheral vestibular sensory apparatus and maintain constant dialogue with other parts of the CNS such as the vestibulo-cortical areas, the cerebellum of the brain and tracts of the spinal cord (Wilson et al., 1967, Wilson and Yoshida, 1969, Minor et al., 1990, Guldin et al., 1992, Matesz et al., 1997).

Integration of multimodal signals such as from the visual and vestibular senses, involves communication between myriad brain areas. Those that encode for single sensory signals and those that have truly multimodal properties. There is a constant interplay between these brain areas and it is speculated that such recurrent processing gives rise to conscious perception of sensory stimuli (Lamme and Roelfsema, 2000, Lamme et al., 2000, Block, 2005).

Peripheral vestibular sensory organs

Humans possess a vestibular system that is capable of sensing acceleration of the head through space in terms of rotational and also linear motion.

Vestibular transduction of rotational motion

Rotational motions of the head are transduced by the crista ampullaris, which are sensors located in the inner ear connected to the vestibular nerve. Each crista is housed at the end of a 'semi'-circular canal which contains a fluid called endolymph. With movement of the head, the canal is rotated in space and the inertial motion of this fluid displaces the crista and thus modulates the afferent activity of the vestibular nerve in response to acceleration of the head in the plane of the canal. There are three cristae in each ear, and they are oriented such that their semi-circular canals are aligned almost orthogonally. This allows sensation of head acceleration in all three dimensions of space (Hasegawa, 1970).

Vestibular transduction of linear motion

Linear motions of the head are transduced by the otolith organs, namely the utricle and saccule. These contain hair cells whose apical surface is covered in stereocilia, which in turn are coated in crystals called otolith. Stereocilia are prong like structures and the inertia of the otolith causes the stereocilia to bend in surrounding endolymph. This in turn modulates the activity of the hair cells and connected afferent nerve. The utricle and saccule are oriented such that the utricle senses horizontal linear accelerations of the head, and the saccule senses vertical linear acceleration (Fluur, 1970, Campos et al., 1990, Clarke et al., 2003).

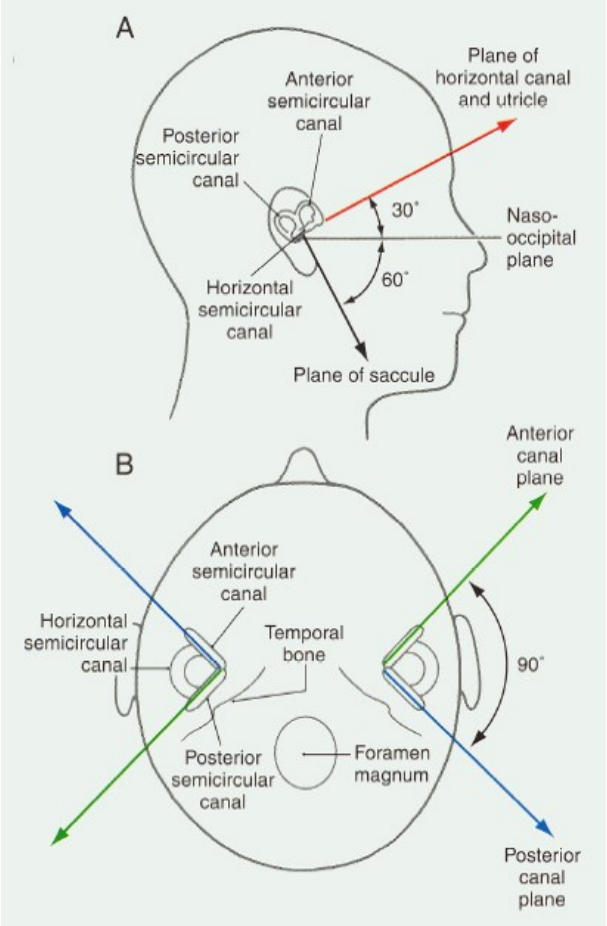

Figure. 1.3. ORIENTATION OF THE SEMI-CIRCULAR CANALS IN THE HEAD. Panel A. Orientation in the sagittal plane. Panell B. Orientation in the transverse plane (Magnum, 2009).

Whilst the semicircular canals and otolith organs are surrounded in endolymphatic fluid, both are contained in the membranous labyrinth of the inner ear. This in turn floats in a fluid called perilymph within the bony labyrinth of the inner ear, which protects the sensitive vestibular apparatus (Asher and Sando, 1981).

Vestibular nuclei

Afferent signals from the vestibular apparatus (semi-circular canals and otoliths) are transmitted via the vestibular nerve to the brainstem. The vestibular nerve is part of the VIII cranial nerve (vestibulocochlear nerve) and further branches its peripheral

fibres into the superior branch, ending in the utricle and the ampullae of the horizontal and superior semi-circular canals; the inferior branch ends in the saccule; the posterior branch ends in the poster semicircular canal (Suarez et al., 1997).

At the brainstem, the vestibular nerve primarily synapses in one of four vestibular nuclei: the superior, lateral, medial and inferior nuclei. From these nuclei, 2nd order afferent nerves synapse to other parts of the CNS via the medial longitudinal fasciculus (MLF). The descending pathway of the MLF contains the lateral and medial vestibulospinal tracts emanating from the lateral and medial vestibular nuclei, respectively. The lateral vestibulospinal tract innervates motorneurons in the leg and trunk areas to maintain upright posture with head movement. The medial vestibulospinal tract projects to the ventral horn of the cervical spinal cord and innervates motorneurons in the neck muscles with head movement (Wilson and Yoshida, 1969). The ascending pathway of the MLF emanates from 2nd order afferents in the superior and medial nuclei upward to synapse with the abducens (cranial nerve VI) trochlear (cranial nerve IV) and oculomotor (cranial nerve III) nuclei. These neural connections are concerned with eye movement in response to head movement and constitute most of the neural substrate for the vestibulo-ocular reflex which is discussed in the next section. (Barmack, 2003, Highstein and Holstein, 2006)

Vestibulo – ocular reflex (VOR)

The VOR acts to stabilise the gaze of the eyes with head movement. Without this reflex intact, such as in cerebellar stroke, the eyes cannot maintain their position during head motion and the sufferer experiences a visual disturbance known as oscillopsia; that is an oscillation of the visual field with head motion (Wist et al., 1983,

Grunfeld et al., 2000). An example would be that the up and down motion of the head during walking would not be compensated by eye movement, and thus the sufferer would perceive their visual field to oscillate up and down. The VOR compensates for head motion in three planes of motion: horizontal, vertical and torsional. The gain for the reflex eye movement opposing head motion is 1 in the horizontal and vertical planes and 0.1 in the torsional plane (Crawford and Vilis, 1991, Crawford et al., 1991).

Cerebellum

The cerebellum is extensively folded and consists of white matter enveloped in a covering of outer grey matter. At its midline is an area known as the vermis, which buds two small bulbs on either side, the anterior of which is the cerebellar peduncle and the posterior lateral bulb is called the flocculus. The flocculus and that part of the vermis connected to it are known as the flocculonodular lobe. Some vestibular afferents travel directly from the peripheral vestibular apparatus, through the inferior cerebellar peduncle of the brainstem to the cerebellum, most 1st order afferents synapse in the medial and inferior vestibular nuclei and thereafter ascend to the inferior cerebellar peduncle. Most of these afferents synapse primarily in the flocculonodular lobe (Ruwaldt and Snider, 1956, Ito et al., 1982, Carleton and Carpenter, 1984). The flocculus is imperative for cancelling the input of the VOR on passive head rotation, but is not involved in the cancellation of the VOR during active gaze pursuit (Belton and McCrea, 2000).

Parieto-insular vestibular cortex (PIVC)

The parieto-insular vestibular cortex (PIVC) plays a critical role in the cortical vestibular network. It was first defined and subsequently extensively studied in

monkey, and key characteristics are that PIVC is activated bilaterally to unilateral vestibular stimulation and is not specifically vestibularly but multimodally connected (Guldin and Grüsser, 1998). With galvanic vestibular stimulation (GVS) in humans it is proposed to be cytoarchitecturally analogous to posterior parietal operculum (OP2) (Eickhoff et al., 2006). The human PIVC has been confirmed in multiple brain imaging studies in response to caloric irrigation and with a bias to right hemisphere activation (irrespective of laterality of caloric), consistent with a right biased asymmetrical cortical spatial network (Lobel et al., 1999, Fasold et al., 2002).

Temporo-Parietal Cortex

The temporo-parietal junction (TPJ) is a multisensory area with strong vestibular input, implicated in the encoding of self-motion and being critical to our perception of our position in space from a first person perspective (Lenggenhager et al., 2006, Ionta et al., 2011). Such an implication has been derived from OBE (out of body experiences) of patients after suffering damage to the TPJ (Blanke et al., 2002, Blanke et al., 2004, Blanke et al., 2005, De Ridder et al., 2007) and through MBD (mental ball dropping) studies in healthy subjects in which synchrony of sensory stimuli caused perceptual conflict of body position (Lenggenhager et al., 2009, Ionta et al., 2011).

Hippocampus & entorhinal cortex

The mammalian hippocampal & entorhinal complex processes an animal's position and heading direction in a known environment (Taube, 1998). They contain place cells which modulate their firing with respect to specific locations (O'Keefe, 1976, McNaughton et al., 1983, O'Keefe and Burgess, 2005); head direction cells which respond to orientation in space (Taube et al., 1990, Sharp et al., 1996, Taube and

Bassett, 2003). Place cells are primarily modulated by visual cues. Whilst calibrated with visual cues, heading direction cells are primarily modulated by vestibular cues. A third type of cell which processes spatial information is the grid cell. It is thought that grid cells process global position as their receptive fields are dispersed over an entire environment. Grid cells do not require visual cues to function, although are calibrated by them (Hafting et al., 2005). Although the interaction is unclear, many models of these three types of spatial processing cell suggest that visual, vestibular and also proprioceptive cues from place and heading direction cells modulate the matrix of grid cells; which in turn constitute a map of egocentric space (O'Keefe and Burgess, 2005). Border cells have also recently been reported which are sensitive to borders in the environment (Solstad et al., 2008).

Posterior Parietal Cortex (PPC)

The PPC is a multimodal sensorimotor area which incorporates visual, vestibular, auditory and somatosensory and 'efferent copy' cues to elicit an appropriate, spatially directed motor output. Parietal area 7a and areas in the intraparietal sulcus of the PPC are explicitly implicated in this function (Andersen et al., 1997, Mesulam, 1998, Colby and Goldberg, 1999). The intraparietal sulcus constitutes five functionally distinct areas: the ventral (VIP); lateral (LIP); medial (MIP); anterior (AIP) and caudal (CIP) intraparietal cortices. Neurones encoding for vestibular motion signals have been found in the AIP,VIP and MIP (Guldin and Grüsser, 1998, Bremmer et al., 2002a, Klam and Graf, 2003). The VIP is strongly involved in encoding self-motion. Its neurons are primarily responsive to large field, optikinetic visual motion, but also respond to vestibular rotary motion (Bremmer et al., 2002b) and tactile input (Duhamel et al., 1998). Neuro-anatomical studies confirm this multi modal sensory input (Lewis and Van Essen, 2000). It has also been shown that the

fields of LIP and area 7a are referenced to ego-centric and allocentric frames of spatial orientation, respectively (Snyder et al., 1998). VIP and MIP are implicated in differential firing between active and passive vestibular stimulation; specifically neurones may switch between directional sensitivity between each type of stimulation (Klam and Graf, 2003).

Dorsal medial superior temporal cortex (MSTd) and spatial visuo-vestibular interactions in the macaque and human

The dorsal medial superior temporal cortex (MSTd) is thought to be important for heading perception as neurons in this area respond to vestibular signals as well as optic flow. Studies of visuo-vestibular interactions in the awake macaque have combined egocentric visual (optic flow) and vestibular cues (translational horizontal motion on a moving platform). Recording techniques included subjective 2IFC (two-interval forced choice) discrimination tasks (in which the macaque makes a saccade to the left or right to indicate its decision) and electrode recordings. Area MSTd receives the bulk of its input from visual area V5/MT. The role of MSTd in visuo-vestibular integration has been elucidated through a number of studies (Gu et al., 2007, Gu et al., 2008, Fetsch et al., 2009) and although vestibular processing is weakly present as compared to visual, it does not appear to be the primary site for visuo-vestibular integration (Gu et al., 2012). Although some studies suggest non visual input to closely related area V5/MT (Nadler et al., 2008, Seemungal et al., 2012) there is also strong evidence that vestibular input is not independently processed here (Chowdhury et al., 2009, Nadler et al., 2009). Comparable to macaque MSTd, a recent study suggests that human MST (hMST) is strongly

activated with galvanic stimulation in the dark, but that human V5/MT+ is not; expounding vestibular input to hMST but not V5/MT+ (Smith et al., 2012).

Reciprocal inhibition of visual and vestibular cortices in human self-motion perception

This theory was originally proposed from psychophysical experiments comparing egocentric (self) to allocentric motion (object based) with concurrent visuo-vestibular stimulation (Probst et al., 1985, Probst et al., 1986), then later supported by PET responses to visual vection and vestibular stimuli (Wenzel et al., 1996, Bense et al., 2001, Bottini et al., 2001, Brandt et al., 2003, Stephan et al., 2005, Dieterich and Brandt, 2008). The theory suggests that dependent upon whether visual or vestibular cortex is activated, the other is inhibited. The rationale being that to avoid a potentially confusing sensory mismatch, the brain will use the dominant sensory signal to the detriment of the other. However, other studies show no effect of vestibular stimulation on visual cortex (Iida et al., 1997, Lobel et al., 1998, Suzuki et al., 2001, Engelhardt et al., 2007). It is also unclear how this reciprocal inhibition may be reconciled with the dearth of literature espousing optimum integration of multimodal sensory stimuli; which argues that the precision of any spatial judgement can only be enhanced with additional sensory information (Ernst and Banks, 2002, Kording and Wolpert, 2004, Fetsch et al., 2009).

1.3. Multimodal Sensory Integration and the Psychometric Function

It was previously thought that vision would always dominate the other senses in what was termed visual capture (Pavani et al., 2000). Although some studies continue to probe this phenomena (Sanabria et al., 2004) many have reduced the interaction to the brain weighting the relative reliabilities of any sensory cues in a statistically optimal fashion. It is widely accepted that the brain is capable of near-optimal integration of stimuli from two of our senses (bimodal integration) (Ernst and Banks, 2002, Kording and Wolpert, 2004, Angelaki et al., 2009a). Indeed, with this approach, it has been shown that vision can also be 'captured' by other sensory stimuli given the right conditions (Alais and Burr, 2004)

Maximum likelihood estimation

Maximum likelihood estimation (MLE) is a process by which characteristics, such as the mean (μ) and the variance (σ) of an assumed, usually normally distributed population of data is inferred from a sample data set. It works on the principle that the probability of the observed data is given the maximum likelihood to have occurred in the context of the underlying statistical model used (Wichmann and Hill, 2001a).

The psychometric function

Psychometric functions describe human responses to sensory stimuli. They are generally sigmoidal in shape, such as a logistic function or cumulative Gaussian dependent upon the model fit used. Two key classes of psychometric function exist and require different assumptions when creating such a model fit.

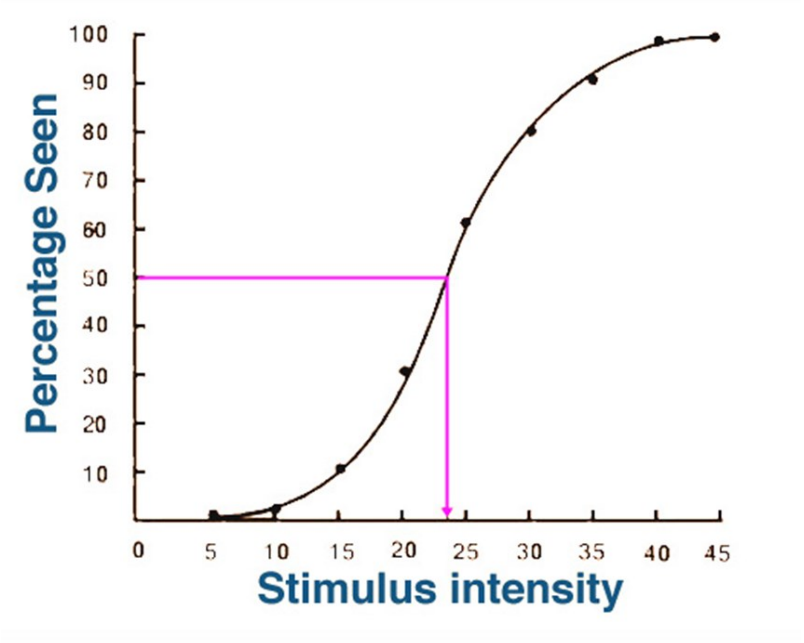

Figure 1.4. EXEMPLAR PSYCHOMETRIC FUNCTION FOR A YES/NO, SENSORY THRESHOLD TASK. Sigmoid shape of function fits the data points. Horizontal axis represents the intensity of stimulus. Vertical axis represents the number of 'yes' observations made out of the total number of observations. Each data point evenly spaced on the horizontal axis representing method of constant stimuli used. Pink lines represent the 50% sensory threshold/absolute threshold to observing the stimulus, here at an intensity of 23.5 arbitrary units. (Kalloniatis and Luu, 2013).

Psychometric Function of a sensory detection task using 'yes/no' design

The first type of psychometric function describes the relationship between the magnitude of a sensory stimulus and an observer's ability to perceive the stimulus. The data for such a psychometric function is collected in a yes/no response experimental design, where a subject responds yes or no to observing a stimulus. The stimulus is delivered over a range of intensities, and multiple times at each intensity using the method of constant stimuli (Fernberger, 1949, Herrick, 1967). Consequently the 'probability' of observing the stimulus (i.e. the number of times a 'yes' observation was made divided by the total number of observations) can be made for each stimulus intensity and plotted as function of that stimulus intensity. The point of inflection of the graph is generally taken as the absolute sensory threshold to a stimulus, i.e. the 50% chance level of perceiving a stimulus (Klein, 2001).

Psychometric function of a discrimination task using two-alternative forced choice design

The second type of psychometric function describes the relationship between a sensory stimulus and an observer's ability to discriminate between two magnitudes of that stimulus. The data for such a psychometric function is collected in a two forced choice experimental design in which the observer is 'forced' to choose between two stimuli of differing magnitude. The stimuli may be presented together, termed two-alternative forced choice (2AFC) or consecutively, termed two interval forced choice (2IFC). Dependent upon the requirements of the task, either

technique can be used. The outcome of the forced choice is predicated upon the question asked, i.e. which alternative/interval appeared larger/stronger or smaller/weaker. Part of the experimental design is that one of the alternatives/intervals is always kept constant. This will be termed the 'standard' stimulus. The other alternative/interval involved in the forced choice varies about the 'standard' stimulus at equally spaced increments using the method of constant stimuli. This alternative/interval will be termed the 'comparison'. The probability of choosing the 'comparison' over the 'standard' stimulus can then be plotted as a function of the stimulus. The point of inflection of the graph in such a discrimination task is known as the Point of Subjective Equality (PSE). It may or may not occur at the 'standard' stimulus magnitude, depending upon whether there is any bias in the observer (Ernst and Banks, 2002).

Using two-alternative forced choice design to estimate optimal multimodal integration

The data required is recorded from three separate discrimination tasks with feedback from each sensory cue alone and then both combined. As an example, let us consider the bimodal integration of vestibular and visual cues. A first 2IFC discrimination task could be rotating a subject in a chair a fixed angle to the left (or to the right) twice, then asking them which interval was longer. Using the method of constant stimuli, the task could be repeated at different comparison angle magnitudes and a psychometric function populated and model fit applied. If performed in the dark and assuming the chair is vibrationless, the subject would only use their vestibular sense to make this judgement making this the vestibular task.

To interrogate visual cues alone, one could theoretically keep the chair stationary and rotate the room (or visual scene) around the subject to the left (or right) and then ask the subject which of two disparate intervals was longer again to derive a psychometric function of this measure also. This would constitute the vision only cue condition.

When both visual and vestibular cues are used in a combined discrimination task (bimodal task), the theory is that the brain will try and use both types of cue and weight each according to its reliability. Specifically, reliability is synonymous with the inverse of the variance (the 'precision') of each sensory estimate, which were estimated in the unimodal, sensory cues tested independently tasks. A tip worth noting is that in our example the mean angular chair rotations, i.e. the 'standard' stimuli for the vestibular only condition and visual only condition, should be disparate enough that the psychometric functions of each do not overlap. This is a useful experimental step. As will be described formulaically, if the visual and vestibular cues are to be combined optimally, the mean of the combined cues should be a clear intermediary value between those of the single cue conditions. Furthermore, the variance of the combined condition should always be smaller than the variance of either sensory cue alone. The rationale for this can be explained formulaically (Ernst and Banks, 2002) where sensory cues *i* and *j* can be considered analogues for the visual and vestibular senses :

$$\hat{S}_i = f_i(\mathrm{S}) \qquad (1)$$

From (1) an environmental attribute can be given by *S* and the function by which the nervous system processes this attribute as *f*. It then follows that $\hat{S}_i$ is the estimate of *S* by the sensory cue (*i)*

$$\hat{S} = \sum_i w_i \hat{S}_i \text{ where } w_i = \frac{1/\sigma_i^2}{\sum_j \sigma_j^2} \quad (2)$$

Assuming that the transduction of S is corrupted by Gaussian, independent noise to give the estimate $\hat{S}_i$; that the variance of this noise is denoted by σ_i^2; and that the Bayesian prior (the a-priori expectation of the brain) is uniform, then equation (2) is the MLE of $\hat{S}$ by sense (i) and a similar equation with i and j subscripts reversed holds true for sense (j).

$$\sigma_{i,j}^2 = \frac{\sigma_i^2 \sigma_j^2}{\sigma_i^2 + \sigma_j^2} \quad (3)$$

The MLE rule also dictates that the optimal estimate is the estimate with lowest variance, and this is achieved by an addition of the sensory estimates weighted by the normalised reciprocal of their variances (3).

Bayesian Inference – prior experience and current evidence

Our perception of the outside world is formed not only from the current evidence around us, but from what we have learnt from prior experience. We integrate both to form percepts of our environment, and to make decisions about how we navigate through space. Bayesian inference helps explicate this interaction and is structured around Bayes theorem which was first suggested by the Reverend Thomas Bayes (1701-1761) and further developed by Pierre-Simon Laplace (Laplace, 1814). The formula for Bayes Theorem can be stated as such:

$$P(H|E) = \frac{P((E|H))P(H)}{P(E)} \quad (4)$$

Where:

$P(H|E)$ = is known as the 'posterior', and it is the outcome of bayes theorem. It tells us the probability of hypothesis H given the evidence E.

$P(E|H)$= is known as the 'likelihood' and it is the probability of observing the evidence E given the hypothesis H

$P(H)$= known as the 'prior' and is the initial degree of belief in the hypothesis H, which exists before the evidence E is presented.

$P(E)$= this is the evidence and is not dependent upon the hypothesis made. It is also known as the 'marginal likelihood'.

An appropriate way to consider this is an iterative process by which the prior and the evidence combine to update the posterior, which in turn becomes the new prior. Therefore, in the initial case there may be no prior, the first posterior being formed from the first piece of evidence. In any case, any initial prior would be polluted over time with updating by evidence, such that it should become of minimal consequence.

In the context of spatial navigation, evidence and prior can be considered to reflect the spatial elements of position, velocity or duration. Such estimates of these elements can be considered as distributions of continuous data which reflect the 'uncertainty' in each estimate. To clarify this, when we encode sensory evidence, there will always be a degree of uncertainty with which this is achieved. It is born from the quality of the environmental cues and the precision of the neural structures transducing them. It follows that this uncertainty is transferred to the prior and hence

the posterior; consequently, Bayesian analysis takes the form of the development and analysis of continuous distributions of data.

Psychometric function fitting using Bootstrapped MLE or Bayesian Inference

All psychometric functions created in this thesis were analysed with a psychometric function fitting program, Psignifit (Wichmann and Hill, 2001b). I was able to fit data via a bootstrap method, involving Maximum Likelihood Estimation, or a more sophisticated method which utilised Bayesian Inference to obtain a potentially more accurate fit (Kuss et al., 2005). Furthermore, I could use the program to assess the deviance value (D) of the data fit from the ideal model fit, and estimate the 95% confidence intervals of the bootstrapped MLE or Bayesian inference fit, and show whether or not the data was modelled correctly.

Exemplar Bayesian Inference model

In a Bayesian inference model the number of priors required is based upon whether the task being sampled from is a forced choice design or a stimulus detection (yes/no) task. Here I describe a yes/no task which takes four parameters requiring a prior to be set for each (a forced choice task requires only three priors which shall be explained shortly).

The first parameter sets the prior for the midpoint (m) of the psychometric function model, which can be considered the 50% ‘threshold’. The psychometric function is

also corrupted by Gaussian noise of some variance, which we model here as $\sigma^2 = 3$. Hence the first prior takes the form of a Gaussian distribution (0.5, 3).

The second parameter defines the 'width' (w) of the interval upon which the psychometric function rises. In our case this is described by a gamma distribution with shape (k = 1) and scale parameters (θ = 3) hence, denoted as Gamma (1, 3).

The third parameter defines the lapse rate (λ) of subjects, which could be considered the proportion of trials where the subjects lose attention. In Bayesian analysis, a common method to model this is the beta distribution, the conjugate prior probability distribution of the Bernoulli, binomial and geometric distributions, and which suitably describes the random behaviour of proportions and probabilities (Aitken, 1999). The beta distribution Beta(α, β) is continuous and defined on the interval [0,1] parameterized by two positive shape parameters, denoted by α and β, which control the shape of the distribution. This distribution can be applied to the lapse rate during phosphene perception by the following relationships:

For Beta (α, β)

$$\text{lapses} = \alpha - 1 \quad (1)$$

$$\text{non-lapses} = \beta - (\alpha - 1) \quad (2)$$

The benefit of using this distribution is that it does not have a cut off value at which the probability of lapsing upon an observation drops drastically, for example, a uniform prior that strictly describes a lapse rate of between 0 and 10% as equally likely, but any other probability having zero probability, could be parameterized as

the uniform distribution (0, 0.1). However this would mean that a lapse rate of 10.2% for example, is considered impossible, which is impractical.

According to (Kuss et al., 2005) a lapse rate of 10% is well modelled by a Beta(2,20) distribution, thus this was used as the prior for a reasonably alert, human subject to lapse in their attendance to phosphene perception in Chapter 5.

The fourth parameter defines the guessing rate (γ) for subjects, again with a Beta distribution and here it is simply set to the lapse rate (λ). It is worth noting that forced choice tasks do not require this parameter as guess rate is set be the degrees of freedom of the forced choice, .e.g. two forced choice designs have a guessing rate of 50%. The yes/no design means the psychometric function is parameterized over the interval [0,1] as subjects either observe a stimulus (yes) or do not observe a stimulus (no).

It is also worth noting that the 'fit' of the psychometric function is based on five parameters

$$\Psi(x;\omega) = \gamma + (1-\gamma-\lambda)F(x;\xi,\rho), \omega = (\xi,\rho,\lambda,\gamma) \quad (3)$$

Where:

x = stimulus intensity

ω = parameter vector

ξ, ρ = shape parameters

γ = guessing rate parameter (in forced choice tasks this is fixed)

λ =lapse rate parameter

1.4. Aims and hypotheses of this thesis

The primary objectives of this thesis are to discern how visual system differentially encodes visual motion coherence and how both egocentric and allocentric visual cues interact with vestibular system to tell us where and when we are in physical space. A secondary objective is to develop current techniques for the recording and analysis of visuo-vestibular sensory information for the purpose of multisensory, multimodal integration.

Chapter 2 investigates the use of a two-interval forced choice method (2IFC) to describe vestibular angular position estimates in yaw. The aim is to discern whether such a method is feasible to model responses at the level of an individual subject; the hypothesis is that this method would afford a model fit with parameters accurate enough to be used in wider Bayesian analysis with much larger sample sizes.

Chapter 3 investigates the use of visual masking to reduce reliability of visual landmark encodement, in a visuo-vestibular spatial orientation paradigm. The aim is to elucidate the mechanisms which drive allocentric visual and egocentric, vestibular interactions in estimation of angular position and duration in yaw. The hypothesis is that reduced visual reliability will lead to an increased bias toward vestibularly derived estimates of angular position and duration.

Chapter 4 investigates the use of transcranial magnetic stimulation to probe visual cortical excitability in visual motion area, V5/MT, in response to visual motion. The aim is to understand how coherence (‘noisiness’) of the motion signal differently activates V5/’MT. The hypothesis is that middle-range coherence of visual motion,

between complete coherence and random motion, will cause the maximal increase in excitability of V5/MT.

Chapter 5 like Chapter 4, investigates V5/MT excitability as measured by TMS, but under real-world vestibular stimulation in yaw. The aim is to discern how V5/MT excitability is modulated by such vestibular stimulation, free of confounding corollaries endemic to caloric irrigation, namely vertigo and nausea. The hypotheses are that real-world vestibular stimulation will incur a dose-dependent increase in concurrent V5/MT excitability; and that increased intensity of TMS used will reduce the effects of vestibular stimulation in a dose dependent fashion.

Chapter 2.

A two-interval forced choice method (2IFC) using Bayesian Inference to describe vestibular angular position estimates in yaw.

Summary

The method of constant stimuli was used within a two-interval forced choice design (2IFC). This was used to capture the psychometric functions of two independent subjects' vestibular estimates of their angular position in yaw. A Bayesian inference model was used to estimate mean and further important parameters of these angular position estimates. For an acceptable model fit, key measures which must be satisfied are converged Markov Chains, and acceptable deviance (D) values. The degree to which the Markov Chains converged is measured by a regression value *R* and in all cases the chains converged within the critical *R* value (R_{crit}) = 1.2. *R* = 1.00 for Subject A., and *R* = 1.02 for Subject B. The deviance (D) of the model is the difference in model fit between the data of the subject and that of the ideal model fit. D = 11.09 for Subject A and D = 11.49 for Subject B. These deviances were well within the maximal deviance permissible (D ≈ 40) for a 'good' model fit (see fig. 7.3.).

Introduction

Of all human senses, the vestibular sense must be the strangest. We only become aware of it when it goes awry, such as after being spun too fast on a theme park ride or, more insidiously, in disease states. Although the mechanisms involved in transducing vestibular signals are well known (Highstein et al., 2005), comparatively little is known about our vestibular percept. In recent years a haptic method of measuring vestibular perception of angular velocity has been developed. In this, subjects manually turn a wheel in keeping with their perception of self-rotation (Cousins et al., 2013). Furthermore, additional haptic methods of recording analogue measures of the corollaries of the head velocity signal, namely duration of rotation and angular position have also been developed *(see Chapter 4. methods*).

However, generally in psychophysics, forced choice methods are the most common way to elicit responses to sensory stimuli from either animals or humans (Bogacz et al., 2006). A critical utility of these methods is to be able to ascertain subjective ability to perceive a stimulus at a range of intensities without interference from motor noise; a problem endemic to analogue response methods (Sherback et al., 2010). In some two-forced choice designs, subjects may be presented with two stimuli simultaneously and be forced to make a choice between them (two *alternative* forced choice design [2AFC]). In others, the stimuli maybe presented consecutively in time and the subject made to make a choice between the intervals (two *interval* forced choice design [2IFC]).

In this chapter, I assess the suitability of a 2IFC method to determine discrimination thresholds for vestibular perception of changes in angular position (with stimulation of the semi-circular canals), using the method of constant stimuli (Fernberger, 1949,

Herrick, 1967) and Bayesian inference techniques (Kuss et al., 2005). Similar techniques have been used in the macaque for translational whole body motion (stimulating the vestibular otolith organs) to assess discrimination of heading direction relative to the sagittal plane (Angelaki et al., 2011), but not rotation in yaw such as in the current study. Such methods of constant stimuli use subject 2IFC responses to populate psychometric functions (*see Chapter 3.*). Psychometric functions are a graphic representation of how a subject responds to a sensory stimulus. They are generally sigmoidal in shape which reflects minimal changes in sensory response at the extremes of perception, and maximal changes in sensory response about an intermediary, threshold value (Lam et al., 1999, Klein, 2001). A psychometric function may describe the behaviour of a subject about a sensory threshold, whereby the lower limit of the function is where they just sense a stimulus, and the upper limit where they always perceive a stimulus (Bouman, 1955) (*see Chapter 5.*). However, in the current study the psychometric function describes the behaviour of a subject about a discrimination threshold. Here, with the comparison of two stimuli, the point at which both are perceived as the same equals the median point of the psychometric function, known as the PSE (position of subjective equality). If one of the stimuli is increased or decreased relative to the other, these relationships tend from the PSE to the extremes of the function, where a larger disparity incurs a larger, non-chance likelihood of perceiving the difference between stimuli (*see Chapter 3.*)(Herrick, 1967).

Forced choice experimental design and the utility of the psychometric function underpin analyses involving Bayesian Inference, which itself is a powerful tool to model the ability of the brain to discern whether two or more sensory cues are being

combined optimally as a function of their respective variance (*see Chapter 3.*) (Ernst and Banks, 2002).

Methods

Subjects

2 subjects, 1 female (mean age 23 .5 years, range 0.2 years), took part in this study. Both were naïve to the objectives of the study.

Apparatus

The equipment comprised a vibration-less motorised chair under computer control, which was free to rotate in the horizontal plane. All rotations were of a half raised cosine waveform of and under position control of the computer, meaning feedback of the angular chair position governed the magnitude of the stimulus (angular velocity) input. All rotations were of peak velocity 60°/s and time modulated to achieve required position, e.g. 45° rotation lasted 1.5s, 60° rotation lasted 2s and 75° rotation lasted 2.5s. Loudspeakers mounted on the chair provided white noise to eliminate ambient, spatial auditory cues. Subject psychophysical responses were recorded via twin push button (*see fig.7.1.*) Psychometric function fitting was performed in Psignifit (Wichmann and Hill, 2001a).

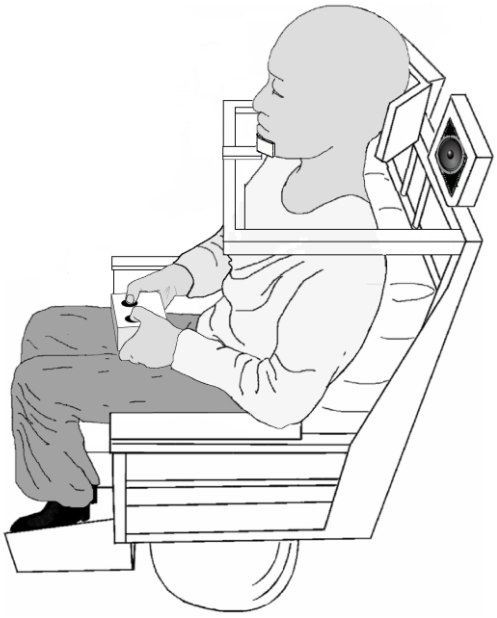

Figure 2.1. Left and Right push buttons to indicate 1st and 2nd interval forced responses, respectively. Chin and head rests maintain head ear canal orientation. Loudspeakers provide white noise.

Procedure

At the start of each trial, the subject faced a visual landmark which indicated their initial, datum position. The lights were turned off and the subject rotated in darkness to an unknown excursion position. The subject was then rotated back in the dark to the initial datum position and the lights turned on, allowing the subject to see the datum visual landmark again. This outbound then inbound rotation is termed an interval. Paired intervals were performed with disparate excursion positions in each interval. At the end of both intervals of the pair, the subject indicated which excursion position they perceived as further, either the 1st interval excursion (left button press) or the 2nd interval excursion (right button press).

Paired intervals were a comparison of a control interval in which the excursion position was always 60° from the initial datum position (termed the 'standard'

stimulus) and an interval in which the excursion position varied from 60° (termed the 'comparison' stimulus). There were 11 different comparison stimuli. The 'comparison' stimulus was either smaller than the standard stimulus (45˚, 48˚, 51˚, 54˚, 57˚) the same magnitude (60˚) or larger (63˚, 66˚, 69˚, 72˚, 75˚).

Each paired interval of standard vs. comparison stimulus was repeated 12 times, with the order of presentation equally balanced between intervals. Therefore, in half of trials the standard stimulus came in the first interval, and in the remaining half the comparison stimulus came in the first interval. The order of presentation of paired intervals was randomised between left and right chair rotation and interval in which the standard stimulus was delivered. In total, each subject experienced 264 paired intervals. 24 paired intervals for 11 standard vs. comparison stimuli conditions.

To populate a psychometric function for each subject, the yes/no, subject response data was converted into a probability of perceiving the standard stimulus as longer than the comparison stimulus at each of the 11 magnitudes of comparison stimulus tested. The comparison angle was plotted on the x-axis of the function and the probability of perceiving the standard stimulus as longer was plotted on the y-axis. The 11 data points were fit to the psychometric function using a Bayesian Inference model (*see chapter 1, section 1.3.*) (Kuss et al., 2005).

A.

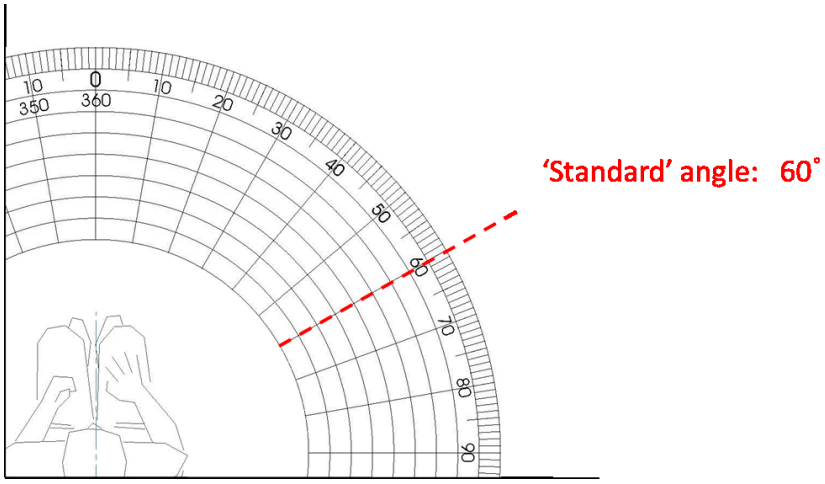

B.

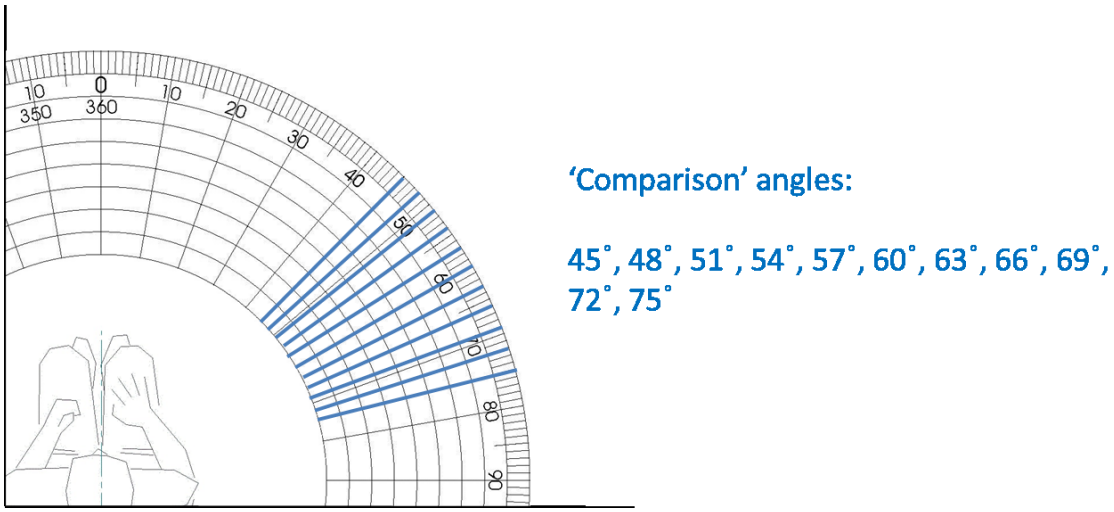

Figure 2.2. APPLICATION OF METHOD OF CONSTANT STIMULI TO CHAIR ROTATIONS. Panel A. Overhead view of initial chair position relative to the 'standard' 60° final excursion angular position (red dotted line). Panel B. Overhead view of initial chair position relative to the comparison final excursion angular position. Range 45°-75° at 3 intervals. Total of 11 comparators (blue solid lines).

Results

Psychometric functions of discrimination thresholds

In each case, both subjects were an excellent fit to the Bayesian Inference model used to perform the psychometric fit. The deviance (D) of the model is the difference in model fit to the data of the subject and that of the ideal model fit. D = 11.09 for Subject A and D = 11.49 for Subject B. These deviances were well within the maximal deviance permissible (D ≈ 40) for a 'good' model fit (see fig. 2.3.).

A.

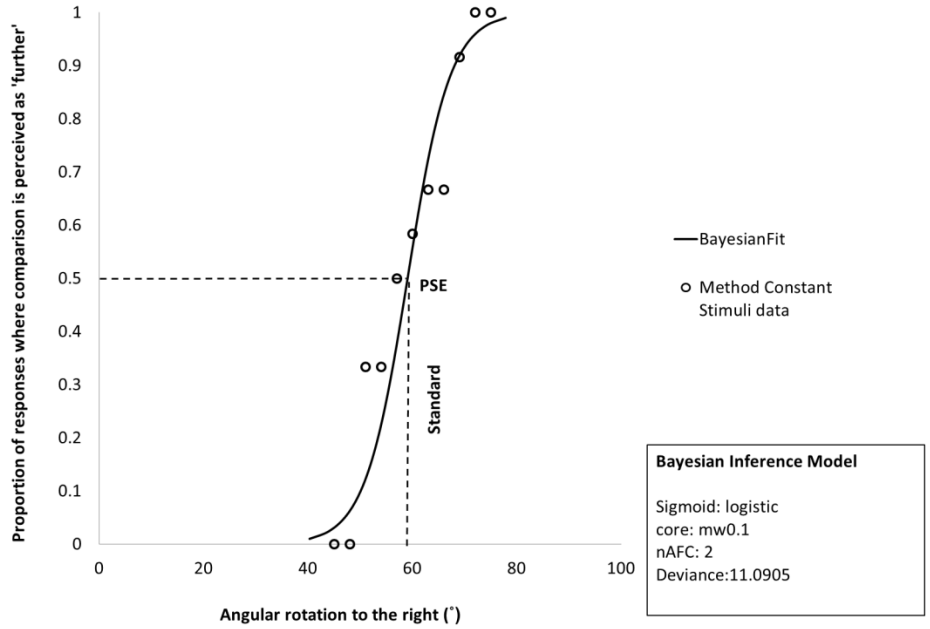

B.

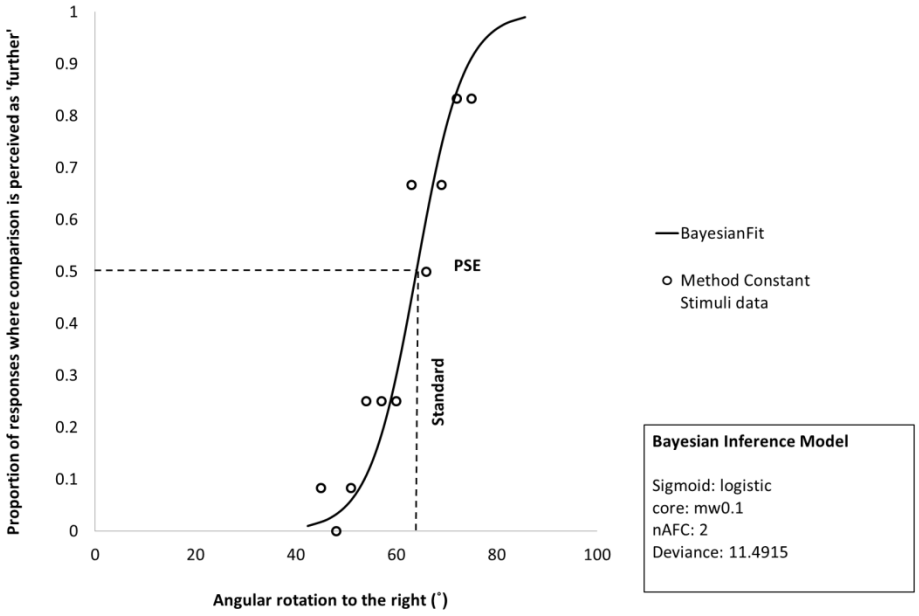

Figure 2.3. PSYCHOMETRIC FUNCTIONS OF ANGULAR POSITION ESTIMATES. Panel A. Psychometric function fit to method of constant stimuli data for Subject A. Panel B. Psychometric function fit to method of constant stimuli data for Subject B. Each function describes a two-interval forced choice (2IFC) experiment modelled as two-alternative forced choice (2AFC). PSE = Point of Subjective Equality. The 'standard' is the 60˚ angular rotation stimulus randomly compared in turn with the 'comparison'

angular rotation stimuli. The logistic sigmoid and mw0.1 core describe the shape of the psychometric function (*see Chapter 1, section 1.3.*). Deviance is the difference between the fit of the data to the model, and a perfect fit to the 'full' model.

Model Convergence

The Bayesian Inference model used utilises a method of random sampling to validate the accuracy of the estimated (posterior) distribution of the sample data. Known as a Markov Chain Monte Carlo (MCMC) method (Kuss et al., 2005, Toft et al., 2007), a series of three Markov Chains, each of 2000 random samples were compared for convergence onto a mean (μ) of the estimated distribution of the model. The degree to which the Markov Chains converged is measured by a regression value *R* and in all cases the chains converged within the critical *R* value (R_{crit}) = 1.2. *R* = 1.00 for Subject A., and *R* = 1.02 for Subject B. The difference in *R* values is proportional to how many trials it took for the Markov Chains to converge, i.e. convergence was faster in Subject A. (*see fig. 2.4.*).

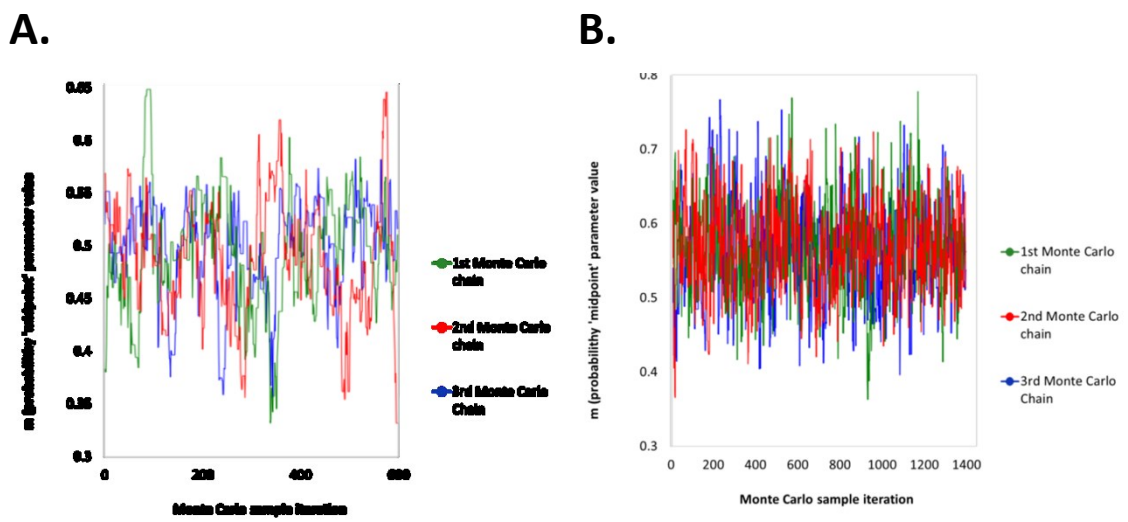

Figure 2.4. PLOTS OF CONVERGENCE TEST OF MCMC. Panel A. Convergence test of MCMC (Markov Chain Monte Carlo) samples for Subject A. Panel B. Convergence test of MCMC (Markov Chain Monte Carlo) samples for Subject B. For each convergence test, three MCMC disparate samples were initiated from the data. Convergence was achieved if R < 1.2, showing that the real posterior distribution of the data is consistent with the Bayesian Inference model.

Prior Parameters

There were four 'prior' parameters of the psychometric function which were determined for the Bayesian Inference model. In a Bayesian model, a prior is an assumption made upon which the data builds to form an estimated 'posterior' distribution, which is then used in analysis (*see Chapter 1, section 1.3.*). The priors set here were the midpoint/mean threshold (m) of the psychometric function, the width upon which the psychometric function rises (w) and the assumed lapse rate (λ) and guessing rate (γ) of healthy subjects. Parameter (m) was modelled by a Gaussian distribution, Gaussian (0.5,3), parameter (w) was modelled as a Gamma distribution (5,3) and the guessing rate (γ) was set to lapse rate (λ) which was

modelled as a Beta distribution (2,20) (*see Chapter 1, section 1.3 for further details about priors*).

Histogram plots composed from the posterior distribution of the sample data (built upon the above parameterised priors) illustrate the Bayesian Inference modelled fit in more detail. Figures 2.5., 2.6. and 2.7. illustrate histogram plots for the midpoint (m), the rise function (w) and the lapse rate (λ) parameter, respectively. In all cases the mean value of the data fell firmly within the 95% confidence intervals suggesting a good, parametric, modelled fit.

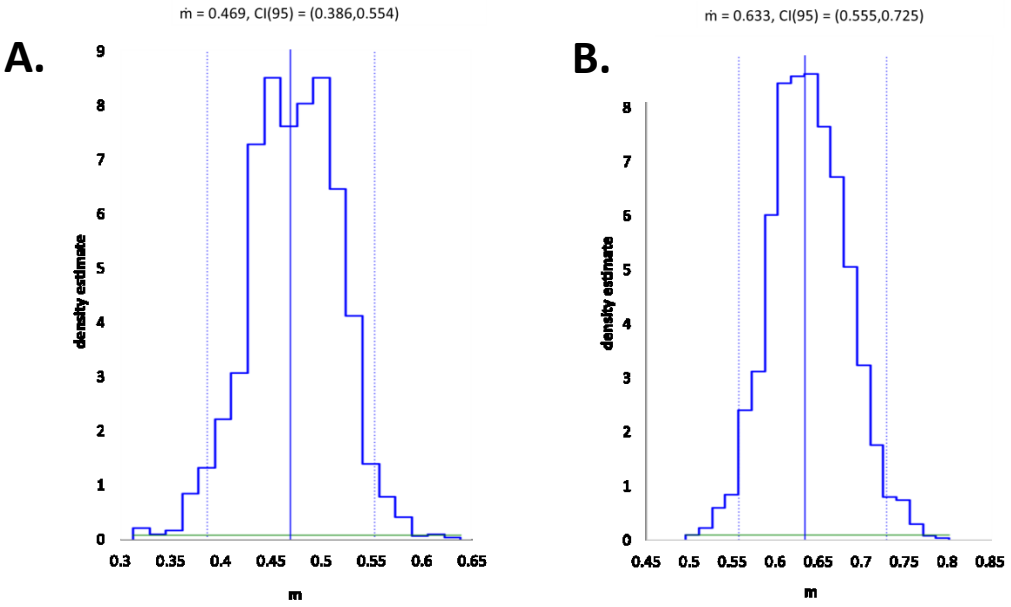

.

Figure 2.5 HISTOGRAM PLOTS OF MIDPOINT PARAMETER. Panel A. Histogram plot of midpoint parameter (m) for Subject A. Panel B. Histogram plot of midpoint parameter (m) for Subject B. Solid vertical blue lines indicate mean midpoint (m) value. Dotted vertical blue lines indicate upper and lower 95% confidence intervals of the sample. Green solid line indicates fit to modelled parameter prior.

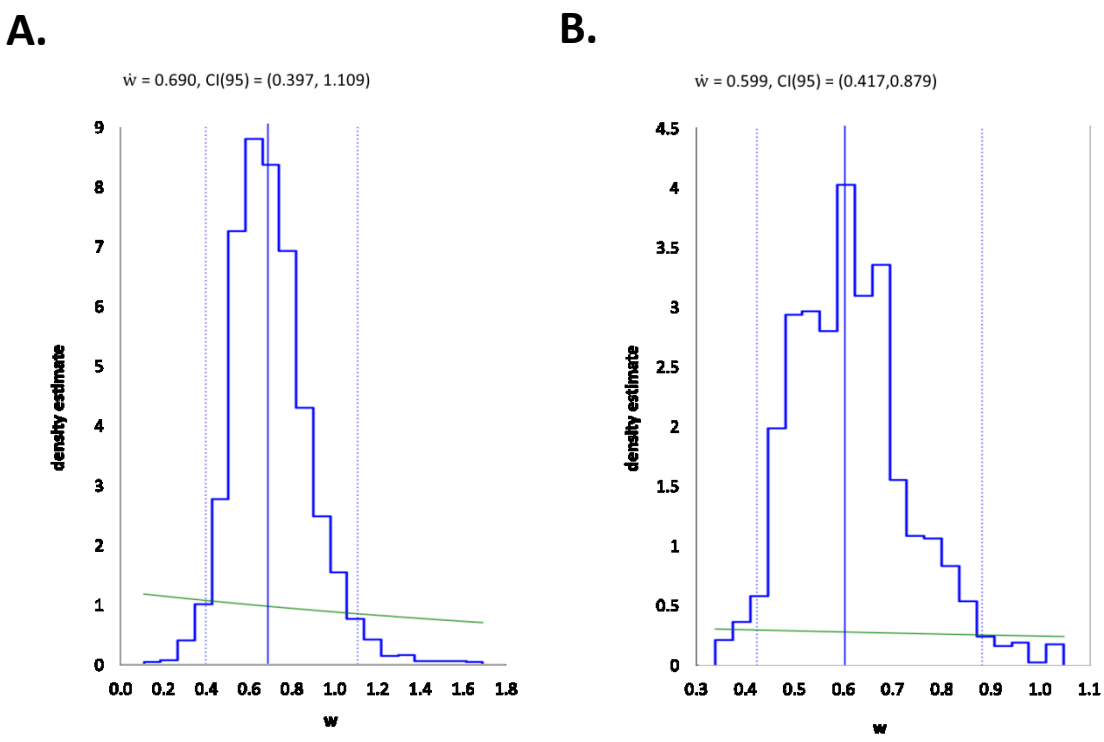

Figure 2.6. HISTOGRAM PLOTS OF RISE FUNCTION PARAMETER. Panel A. Histogram plot of the rise function parameter (w) for Subject A. Panel B. Histogram plot of the rise function parameter (w) for Subject B. Solid vertical blue lines indicate mean rise function (w) value. Dotted vertical blue lines indicate upper and lower 95% confidence intervals of the sample. Green solid line indicates fit to modelled parameter prior.

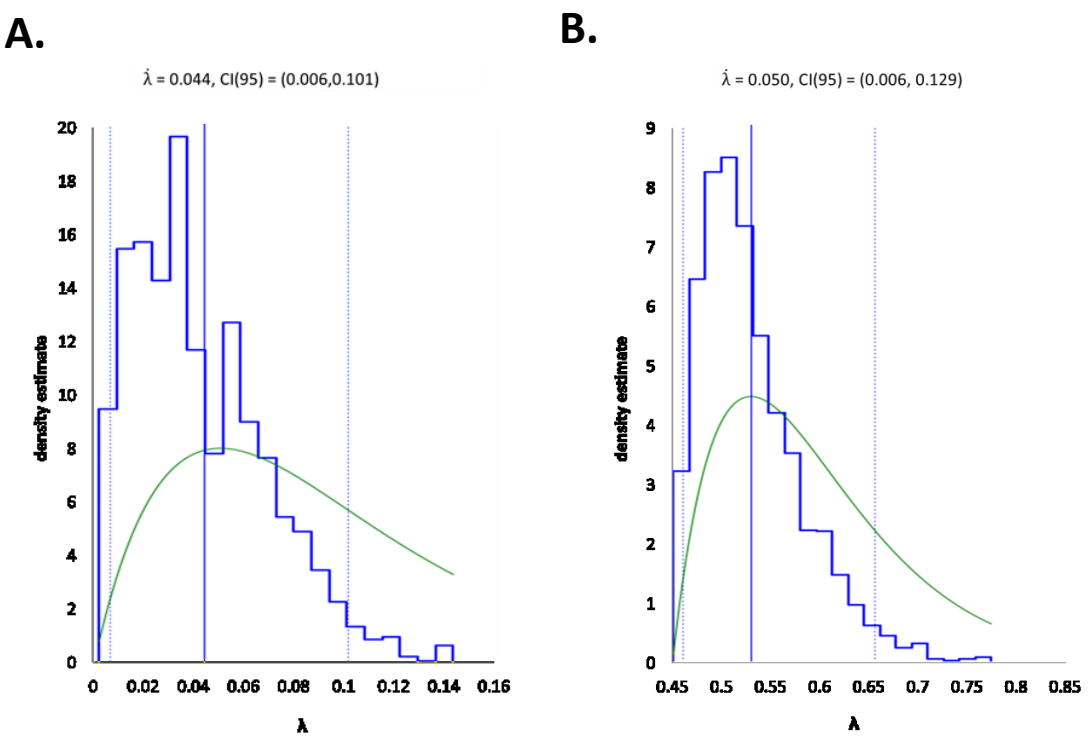

Figure 2.7 HISTOGRAM PLOTS OF LAPSE PARAMETER. Panel A. Histogram plot of the lapse parameter (λ) for Subject A. Panel B. Histogram plot of the lapse parameter (λ) for Subject B. Solid vertical blue lines indicate mean lapse parameter (λ) value. Dotted vertical blue lines indicate upper and lower 95% confidence intervals of the sample. Green solid line indicates fit to modelled parameter prior.

Model Deviance

Deviance residuals between the data and predicted model fit are also useful in searching for systematic deviations between the data and model. Figure 2.8. illustrates such deviance residuals plotted as a function of the model prediction. The slopes of best fit for both Subject A and Subject B have similar slopes suggesting the same types of systematic errors being present (Panels A and B, respectively). However, the line of best fit for subject A more closely cuts through the origin of the y axis (deviance residual magnitude), suggesting less deviation of the data from the model than for Subject B. This is expressed numerically as an Rpd (the correlation

co-efficient of deviance residual and model prediction), with Rpd = 0.46 for Subject A as opposed to Rpd = 0.33 for Subject B.

Deviance residuals were also plotted as a function of block index (i.e. the order of testing in which observations were recorded, correlation which is expressed numerically as the line of best fit, Rkd) and are illustrated in Figure 2.9. This relationship can show how well subjects performed over time and whether learning took place. The lines of best fit for both subjects suggest learning did take place due to their positive slopes (Subject A, Rkd = 0.271. Subject B, Rkd = 0.432), and this suggests that over time the deviation residuals would reverse.

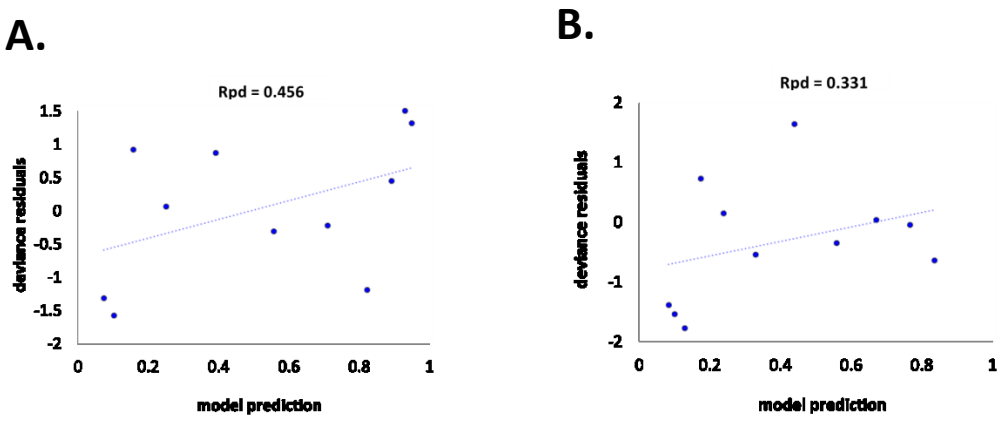

Figure 2.8. PLOTS OF DEVIANCE RESIDUALS BY MODEL PREDICTION. Panel A. Plot of deviance residuals (between data and predicted model fit) by model prediction for Subject A. Panel B. Plot of deviance residuals (between data and predicted model fit) by by model prediction for Subject B. Solid blue lines indicate linear best fit. Rpd is the numerical value of the linear best fit correlation.

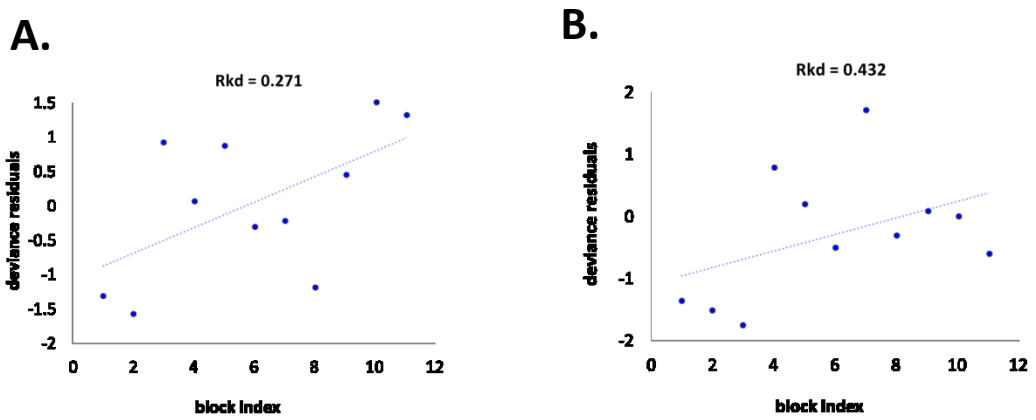

Figure 2.9. PLOTS RKD TO BLOCK INDEX. Panel A. Plot of deviance residuals (between data and predicted model fit) by chronologically ordered block index for Subject A. Panel B. Plot of deviance residuals (between data and predicted model fit) by chronologically ordered block index for Subject B. Solid blue lines indicate linear best fit; a positive slope indicates learning over time. Rkd is the numerical value of the linear best fit correlation.

Correlations of predicted vs. observed deviance (D) are also useful in validating the model. The predicted vs. observed deviance of each of the 2000 samples from the posterior distribution should ideally have a linear 1:1 relationship for a perfect model. Correlations of predicated vs. observed deviance for both subjects are illustrated in Figure 2.10. The data clouds for each subject are dispersed either side of a mean 1:1 linear fit through the origin of each graph. Deviation of the centre of these clouds from a 1:1 linear fit indicates a poorer model fit. The Bayesian p-value of the correlation, Bayesian p (D) is a numerical descriptor of the correlation. Values tending toward 0 or 1 indicate a poor model, with an ideal value of 0.5 precisely. Values of Bayesian p(D) = 0.39 for Subject A and Bayesian p(D) = 0.36 for subject B can be considered respectable in the context described.

Correlations can also be made for the Rpd of observed vs. predicated deviance in a similar fashion as illustrated in Figure 2.11. These are conceptually simplest to understand as equivalent to the correlations in Figure 2.10., but normalised by the model prediction. Hence, they a more conservative measure of model fit. A Bayesian p-value can also be derived for this correlation with values of Bayesian p (Rpd) = 0.24 for Subject A and Bayesian p (Rpd) = 0.31 for Subject B.

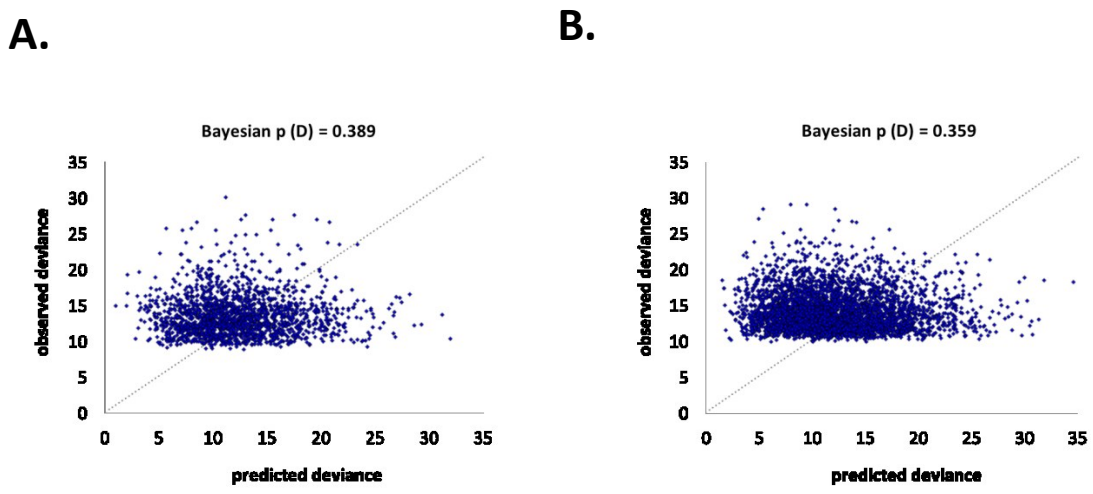

Figure 2.10. PLOTS OF PREDICTED TO OBSERVED DEVIANCE. Panel A. Plot of predicted deviance of the model to the observed deviance of the data sample for Subject A. Panel B. Plot of predicted deviance of the model to the observed deviance of the data sample for Subject B. Data points plotted (n = 2000) are sampled from the posterior distribution of each subject, respectively. Dotted blue line represents a 1:1 correlation between predicted vs. observed deviance. Baysesian p (D) is the Bayesian p value associated with the correlation. Values tending toward 0 or 1 indicate a poor model.

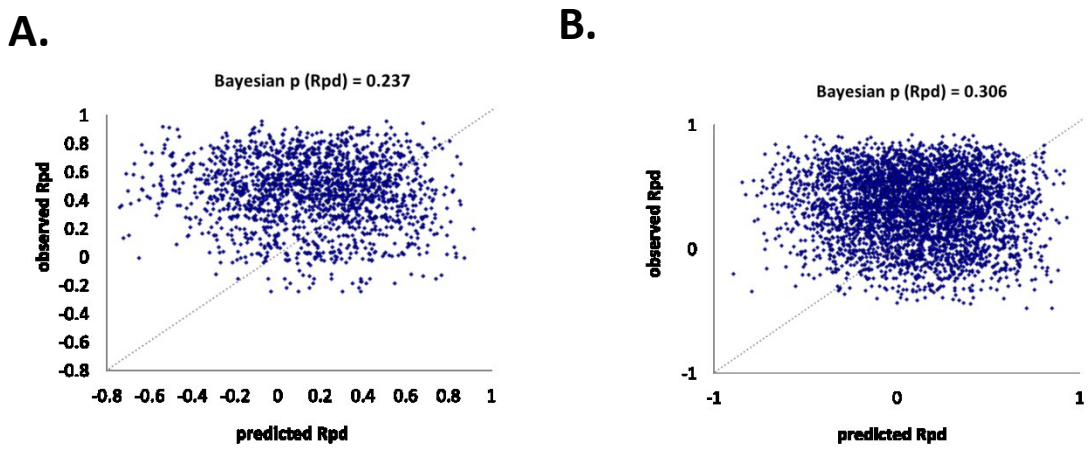

Figure 2.11. PLOTS OF MODEL VS. OBSERVED RPD. Panel A. Plot of Rpd of the model to the observed Rpd of the data sample for Subject A. Panel B. Plot of Rpd of the model to the Rpd of the data sample for Subject B. Data points plotted (n = 2000) are sampled from the posterior distribution of each subject, respectively. Dotted blue line represents a 1:1 correlation between predicted vs. observed Rpd. Baysesian p (Rpd) is the Bayesian p value associated with the correlation. Values tending toward 0 or 1 indicate a poor model.

Discussion

This short proof-of-principle study aimed to highlight the efficacy and power of using Bayesian Inference to exploit the method of constant stimuli in acquiring vestibular perceptual estimates of angular position, and capture learning over the course of an experiment. The method of constant stimuli was used within a two-interval forced choice design (2IFC). This was used to capture the psychometric functions of two independent subjects' vestibular estimates of their angular position in yaw. A Bayesian inference model was used to estimate mean and additional important parameters of these angular position estimates. For an acceptable model fit, key measures which must be satisfied are converged Markov Chains, and acceptable

deviance (D) values. The degree to which the Markov Chains converged is measured by a regression value *R* and in all cases the chains converged within the critical *R* value (R_{crit}) = 1.2. *R* = 1.00 for Subject A., and *R* = 1.02 for Subject B. The deviance (D) of the model is the difference in model fit between the data of the subject and that of the ideal model fit. D = 11.09 for Subject A and D = 11.49 for Subject B. These deviances were well within the maximal deviance permissible (D ≈ 40) for a 'good' model fit (see fig. 2.3.).

This is an important study as most of the research to determine vestibular discrimination thresholds of heading direction have involved linear motion on translational platforms (Gu et al., 2008, Angelaki et al., 2011, Crane, 2012). In these studies the otolith organs rather than the semi-circular canals were stimulated. They are consequently of limited use in resolving how vestibular perceptual estimates of turning angle are involved in 'path integration', the process by which animals calculate current position without an external frame of reference (Mittelstaedt, 1980, Klatzky, 1998).

Markov Chain Monte Carlo Method

The Bayesian Inference technique used (Kuss et al., 2005) takes advantage of an MCMC (Markov Chain Monte Carlo) method to generate random samples from the posterior distribution of the Bayesian model. This method has been empirically shown to provide higher accuracy than simple curve fitting of data to psychometric functions via simple MLE (maximum likelihood estimation) techniques (Wichmann and Hill, 2001b). The addition of MCMC methods can consequently be used to find the same effects but requiring a fraction of the sample size. The elegance of the

current study is that it maximises the information gained from a simple forced choice design experiment with a powerful, non-frequentist inferential analysis. It makes the planning and undertaking of further study more tractable (increased reliability, time and resources saved, error from subject inattention and fatigue reduced).

Increased sample size and multimodal experiments

It was not the aim of this study to reach conclusions about vestibular heading direction measures at the sample level, as evidenced by the testing of only two subjects. It was merely to show that intrasubject variability in the experiment is very low, and that reliable estimates of mean heading direction, and variance of that heading direction can be achieved at the subject level. This is a promising finding which should allow more scope for understanding variance from inter-subject variability when testing larger samples. Critically, it will be important in future studies if combined multimodally with estimates of heading direction from vision. The assumption of optimal multimodal integration in the brain of two (or more) sensory cues is predicated upon having reliable estimates of mean and variance for each sensory modality. These are required to discern how much bias and reliability there is in a mean estimate, using both senses, as a function of the precision (reciprocal of variance $1/\sigma$) of each sense (Ernst and Banks, 2002).

Further work would include increasing the size of the current sample to gain an appreciation of intersubject variability in the estimate of angular position, and also probe a range of angular positions to discern whether the variance of angular position estimates is constant (homoscedastic) or scales with magnitude of angular position from straight ahead (heteroscedastic). This a factor which could undermine the validity of regression tests such as ANOVA (analysis of variance). Furthermore,

similar forced choice techniques could be used to probe visual estimates of angular position. Integration of visual motion cues (optic flow) to produce estimates of angular position is one course of investigation, and which could culminate in combined visual motion and vestibular (motion) cue experiments. The results of such combined analysis could compliment translational visuo-vestibular heading direction work in the macaque (Angelaki et al., 2009b, Angelaki et al., 2009a, Angelaki et al., 2011).

Bayesian Learning

The Bayesian inference technique described here differs from the otherwise similar bootstrap technique described in Chapter 4 in one important aspect. In the Bayesian inference technique, the order of data recordings is taken into account, and used to model the fit based on adapting the fitting procedure over the chronological order of data acquisition. This allows scope for higher accuracy over the bootstrap method if model parameters are chosen correctly (Wichmann and Hill, 2001a, Wichmann and Hill, 2001b). Deviance residuals plotted as a function of block index are illustrated in Figure 2.9. The lines of best fit for both subjects suggest learning took place due to their positive slopes (Subject A, Rkd = 0.271. Subject B, Rkd = 0.432). Given the small sample size of two in the current pilot study, the utility of such measures may not be apparent, save that Subject B learnt at a faster rate than Subject A. I hope that with larger experiments with more subjects, the Rkd measure may become a valuable measure of rate of learning; and could be explored for correlation with accuracy (mean) or reliability (confidence intervals) of vestibular angular position estimation.

Path integration Experiments

In addition visual landmark cues might also be investigated in a similar forced choice, discrimination threshold paradigm. Such analysis is fundamentally different from that of egocentric, visual motion (optic flow) as landmarks are offline, allocentric cues (Klatzky, 1998). Visual landmarks are not known to share the same neural substrate for integration as vestibular signals and optic flow (Gu et al., 2008, Gu et al., 2012). Indeed, the combination of egocentric and allocentric reference frames required for path integration is poorly understood, but is known to be strongly mediated by the hippocampal and entorhinal cortex through the interaction of place, heading direction, grid and border cells (Hafting et al., 2005, McNaughton et al., 2006, Moser et al., 2008, Moser and Moser, 2008, Solstad et al., 2008, Stensola et al., 2012). Hence the research question of how visual landmark and vestibular motion cues are integrated by humans is more pertinent to the understanding of path integration than that of optic flow and vestibular motion cues. I suggest this may not be an optimal multimodal integration, as visual landmarks require object recognition. These are not processed analogously to motion cues, but have shown dependence on the function of the hippocampal entorhinal complex (Braddick et al., 2000, Bar et al., 2001, Hammond et al., 2004, Broadbent et al., 2004, Barker and Warburton, 2011).

Conclusion

The Bayesian Inference model aptly captures the characteristics of vestibular perceptual estimates of angular position in yaw, as transduced by a 2IFC, method of constant stimuli protocol. The technique also holds scope for measuring learning over a course of trials.

Chapter 3.

Angular Heading Direction: Velocity, Position and Time in the brain

Summary

Veridical or biased (dilated or contracted) visual landmark feedback was presented to subjects along with concurrent veridical vestibular feedback from whole-body angular rotation in yaw. Subjects estimated their duration of rotation or angular position in separate experiments. Reliability of visual feedback was in all cases diminished and either subliminal (encoded but not perceived), or intermediary (perceived, with near chance uncertainty) feedback. Biased subliminal presentation of visual landmarks was shown to bias duration estimates of angular rotation (*see fig 4.17a*) [$F(2,16)=6.6$, $P<0.01$], but not estimates of angular position (*see fig 3.20*) [$F(2,16)=1.7$, $P=0.2$]. Biased intermediary presentation of visual landmarks biased position estimates of angular rotation in yaw [$F(2,13)=21.0$, $P<0.00001$] to a greater degree than with subliminal visual feedback.

Introduction

The ecological importance of effective navigation within our environment is unquestioned. In general human navigation is dominated by vision where we use visual landmarks to orientate and hence make our way around our environment. For example to get from my home to the train station I walk to toward the gate at the end of my garden path, turn right at the gate and proceed until I see the station entrance.

In this case I use the garden gate and the station entrance as my visual landmarks. The use of landmarks also invokes the use of a 'world-based' or allocentric reference frame (Klatzky, 1998). Humans can also orientate in the absence of visual cues, e.g. in the dark, from the external environment. In this case, we work within what is known as an egocentric reference frame (Klatzky, 1998); we effectively need to use our knowledge of our body position over time to navigate. Note the wordplay here 'position over time'. From a kinematic viewpoint, one's current position relative to their starting position is the distance one has travelled. Furthermore, distance travelled divided by the duration of travel is equivalent to one's velocity through space. This leads us to the well known relationship:

$$Distance/Time = Velocity \quad (1)$$

Which can also be expressed as the differential equation:

$$dx/dt = v\,(\mathrm{t}) \quad (2)$$

Where dx is an incremental change in distance, dt an incremental change in time and v(t) is velocity.

Thus, in order to calculate our distance travelled and hence our current position, we could argue that we need some external signal of our velocity through space and some analogue of time. Equation (2) can be reversed to derive the integral equation:

$$\int_0^T v(t)dt = X(T) - X(0) \quad (3)$$

Equation (3) shows that by integrating the velocity signal between time points '0' and 'T' the distance travelled can be calculated between them and hence position. Hence, we must then ask ourselves what means we have to execute this

integration? Well, our vestibular system affords us a signal of our head velocity. Although it transduces cues of accelerations of the head, the mechanical properties of the vestibular apparatus transform these to a signal of head velocity also. The way this temporal integration takes place is simply due to the geometry of the vestibular apparatus and viscous forces imposed on the fluid within (Highstein et al., 2005). This mechanical, temporal integration from acceleration cue to head velocity signal leads us to the question of what could temporally integrate the head velocity signal into a position signal of the head? As this velocity signal is transmitted via the vestibular nerve, a mechanical integration is impossible. However, it is well known that there are many neural circuits in the brain which are able to integrate a velocity signal to a position signal. Examples of such neural integrators can be found to form the position signals of the Vestibulo-ocular reflex (VOR) which keep the eyes steady. These integrators are found in the brainstem (Cannon and Robinson, 1987, Crawford et al., 1991). I consider the possibility of other neural integrators, or branches of known neural integrators which feed into the parts of the brain involved in conscious awareness and perception (Mazurek et al., 2003). For instance, what brain regions are involved in the transformation of a head angular velocity signal into a person's perceived estimate of their angular position? One perceives their sensation of motion, but is this, as well as a their perceived estimate of duration of motion, involved in the integration?

In humans and other mammals the ability to estimate their current position based on movement cues since their last position is known as path integration (Mittelstaedt, 1980). The precise mechanisms by which the integration of movement cues takes place is still unknown. However, in mammals a wealth of evidence suggests that

circuitry exists within the hippocampal & entorhinal complex which are involved in our classical understanding of path integration or at least an analogue thereof. Indeed this area is known to contain specialised networks of heading direction (Taube et al., 1990, Sharp, 1996, Taube and Bassett, 2003), place (O'Keefe, 1976, McNaughton et al., 1983, O'Keefe and Burgess, 2005) and grid cells (Hafting et al., 2005) which are thought to work in synergy, again the interaction of which is largely unknown (O'Keefe and Burgess, 2005) . Interestingly, although heading direction cells found in the rat rely heavily on the vestibular system, they are calibrated by means of visual landmarks (Taube et al., 1990). This is consistent with a human study which shows that although the vestibular system is important in path integration involving turning, without the presence of visual feedback, cumulative errors are incurred (Glasauer et al., 2002). Thus, in its use in navigation, this shows that the human vestibular system is 'open loop', requiring allocentric visual feedback for calibration. This is supported by a host of other human studies that show the importance of the vestibular system in human spatial orientation via path integration (Metcalfe and Gresty, 1992, Mergner et al., 1996, Seemungal et al., 2007). Furthermore, in primate study, the PPC (posterior parietal cortex) and DPFC (dorsolateral prefrontal cortex) have already been proposed as communicating brain regions involved in temporal integration of spatial and non-spatial information (Quintana and Fuster, 1993, Quintana and Fuster, 1999).

In this chapter, relationships between the visual and the vestibular-derived perception of angular position and duration of motion were investigated. I hypothesised that vestibular-spatial perception of position requires the use of a perceptual measure of time (or motion duration). This implies that the brain may

store head rotations in the form of an internal model that relates head velocity, position and time (motion duration). Furthermore, I hypothesised that the position estimate of this internal model can be integrated with not only the output of the vestibular head velocity time integral, but also by visual estimates of position (note: the assumption that visual input of position recalibrates estimates of vestibular-derived position was assessed herein).

As a probe of the visual percept of position, I assessed the effect of terminal, subliminal visual feedback (using the technique of *backward visual masking*) on subject estimates of their duration of passive rotation and angular position in the dark. Subliminal visual feedback was chosen as prior pilot visuo-vestibular mismatch experiments were conducted supraliminally. These were conducted by B. Seemungal. He showed that when healthy subjects are rotated passively in the dark, then receive erroneous, terminal, visual feedback of their angular position, they relied completely on their vision to determine their perceived angular position. Without visual feedback, the subjects reverted to relying on their vestibular system. It is hypothesised that this was a prime example of visual capture (Kelso et al., 1975), due to vision providing a less variable, object based percept of one's external surroundings (Mishkin and Ungerleider, 1982), compared to the vestibular system providing only a coarse, spatial estimate (Buettner et al., 1978, Blair, 1981, Galiana and Outerbridge, 1984, Cannon and Robinson, 1985). In addition, B. Seemungal performed almost the same experiment, but this time with subject estimates of duration of rotation rather than position. The results were ambiguous. Figure 3.1. shows the duration estimate results for the experiment for when the terminal visual feedback was not perturbed (control), perturbed 50% further than the veridical

rotation (bigger) and perturbed 50% shorter than the veridical rotation (smaller). Outbound duration estimates for both 'smaller' and 'bigger' conditions are both perceived as longer than the 'control' condition. However, inbound duration estimates show expected outcomes of the 'smaller' condition being perceived as shorter and the 'bigger' condition being perceived as longer. It was posited that outbound responses might be a 'surprised' reaction to an unexpected stimulus when the visual feedback was non-veridical. The surprise having an additive effect upon the underlying estimate of duration of rotation (Pariyadath and Eagleman, 2007). Inbound rotations elicits no 'surprise' effect. Here I assume that the non-veridical visual feedback has already been encoded and a return to the starting position is expected. This proposed phenomena is illustrated in Figure 3.2.

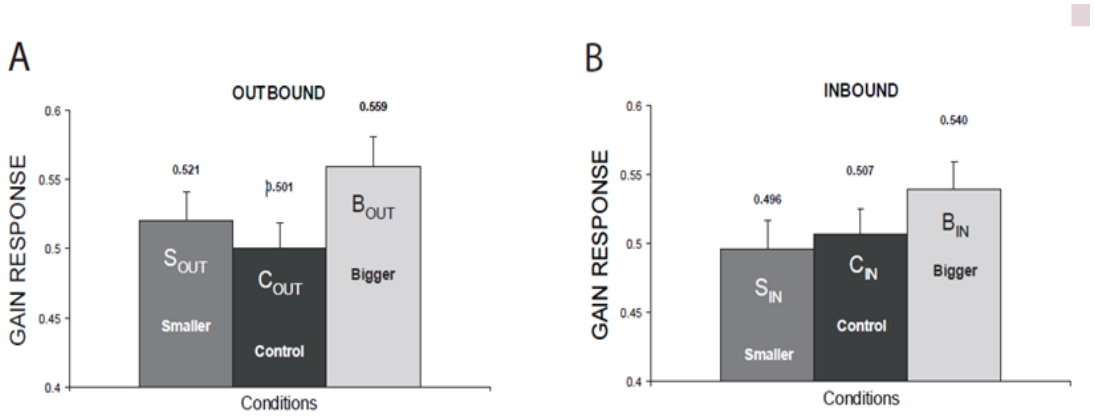

Figure 3.1. GAIN RESPONSES OF DURATION ESTIMATES WITH FULL VISUAL AND VESTIBULAR FEEDBACK. Panel A shows outbound duration estimate responses, Panel B shows inbound duration estimate responses.

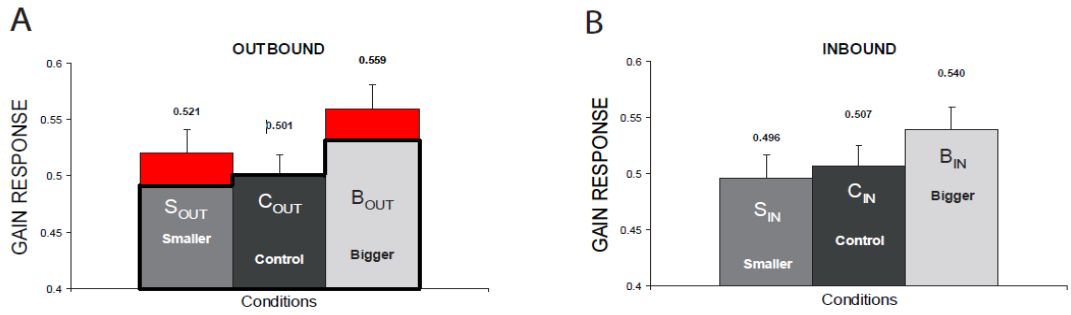

Figure 3.2. ESTIMATING THE EFFECT OF UNEXPECTED VISUAL STIMULUS. Panel A: Visualisation of how the effect of an unexpected stimulus (red sections of graphs) may have affected duration estimates on outbound rotations. The bolded outline indicates the sections of graph which are consistent with duration estimates for inbound rotation in Panel B.

The results of these supraliminal (consciously perceived), visuo-vestibular mismatch (VVM) experiments suggest that disparity in reliability of visual and vestibular cues may play a role in the results observed. Specifically, the visual cues were highly salient as subjects could consciously perceive them with certainty. For the position estimate VVM experiment, the certitude with which subjects estimated their position from visual cues alone made them ignore vestibular cues entirely for this task. For the duration estimate VVM experiment, being consciously aware of a mismatch between erroneous, highly salient visual feedback, and true, but less reliable vestibular feedback, appears to have increased duration responses in cases of visuo-vestibular conflict (Fig. 3.1A).

I hoped to repeat these VVM experiments, but using subliminal, rather than supraliminal visual feedback. I hypothesised that subliminal visual feedback of terminal angular position would permit increased integration of vestibular angular motion cues. This would be effected by the reduced saliency of the visual signal provided and is based on the assumption that the brain integrates spatial sensory

inputs weighted by their reliability (Ernst and Banks, 2002, Kording and Wolpert, 2004). A corollary of this is that estimates of angular position would be biased away from the position indicated by visual cues, and toward those indicated by vestibular cues. I also hypothesised that a saliency of visual feedback midway between subliminal and perfectly clear supraliminal, visual feedback would produce an intermediary result, in keeping with the brain reweighting visual and vestibular cues by their reliability (Ernst and Banks, 2002). I further hypothesised that subliminal visual feedback would remove the disparity in duration estimates between outbound ('surprised') and inbound rotation observed in previous supraliminal experiments (Figure 3.2.). This would be by contravening the mechanisms of conscious perception assumed to increase outbound duration estimates during visuo-vestibular conflict (Pariyadath and Eagleman, 2007).

Methods

Apparatus

In this study subjects experienced both whole body rotation and landmark based visual cues in the yaw plane. The visual cues could be surreptitiously moved to provide erroneous, terminal visual feedback relative to actual whole body rotation experienced. Subjects sat on a vibration-free rotating chair (contraves; torque 120 Nm) with a motorised drum mounted above its neutral axis, and thus aligned to the same axis of rotation. A picture curtain hung from the drum and enveloped the chair. The angular positions of the chair and drum were both under computer, position control and could be moved independently. The basic apparatus is illustrated in figure 3.3.

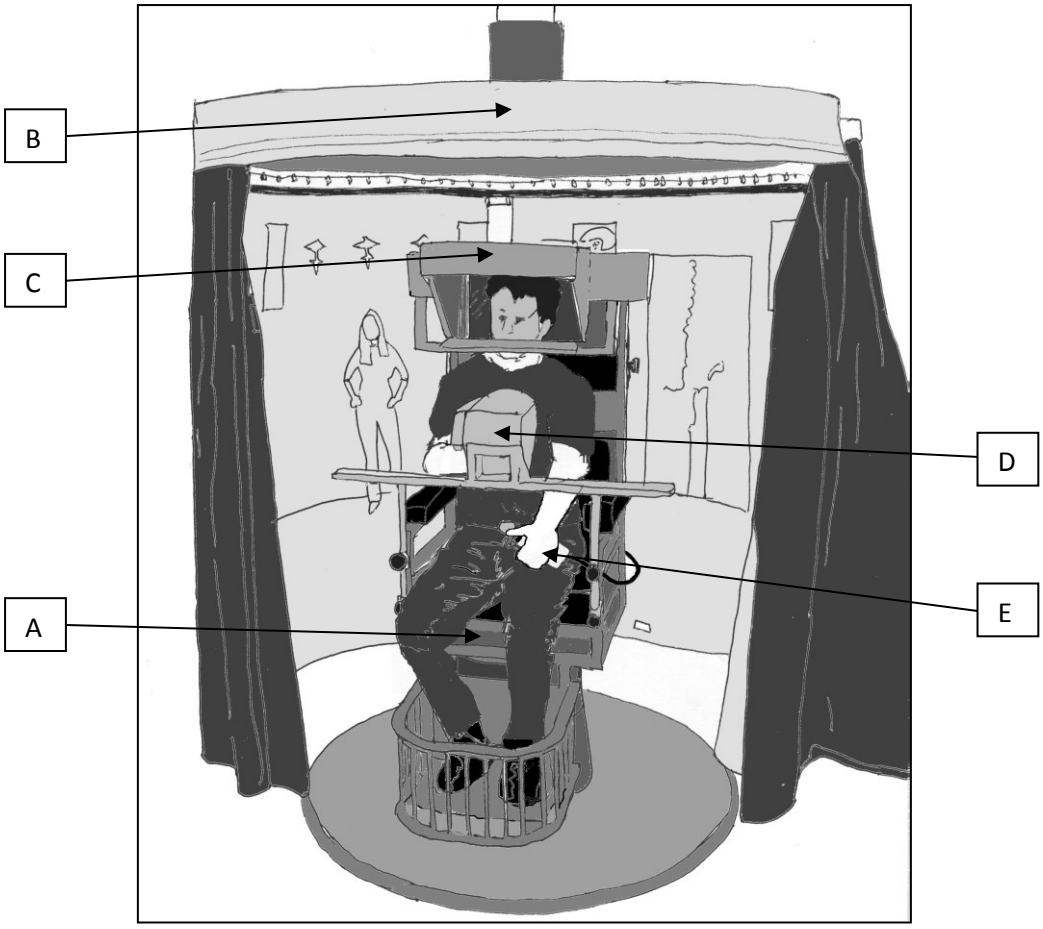

Figure 3.3. MAIN APPARATUS. Subject seated in vibrationless, motorised chair (A) surrounded by a picture curtain (B). The picture curtain is shown withdrawn for visualisation, but during experiments was closed to fully envelop the subject. The chair is mounted with a viewing box (C) (*see fig.3.5.*), a position indicator dial (D) (*see fig. 3.12.*), and a push button (E) (*see fig. 3.12.*) used to indicate perceived duration of rotation (replaced with a dual push button for two alternative forced choice tasks).

Visual Masking

Visual Masking is the use of an additional image before (forward masking) or after (backward masking) a target image, to make the target image harder to see (Breitmeyer, 2007). In this study, I investigated the use of backward masking to interfere with the terminal, landmark based, visual feedback provided to subjects.

This was with the aim of making the landmark, visual signal less reliable and to probe whether less reliable visual signals can be subliminally encoded by subjects, without their conscious awareness.

Assuming human estimates of spatial cues are corrupted by noise, modelled as a Gaussian distribution with a mean estimate (μ) variance (σ^2), the aim of visual masking was to increase the variance (σ^2) of this estimate. This can be illustrated as a probability density function (pdf) shown in Figure 3.4.

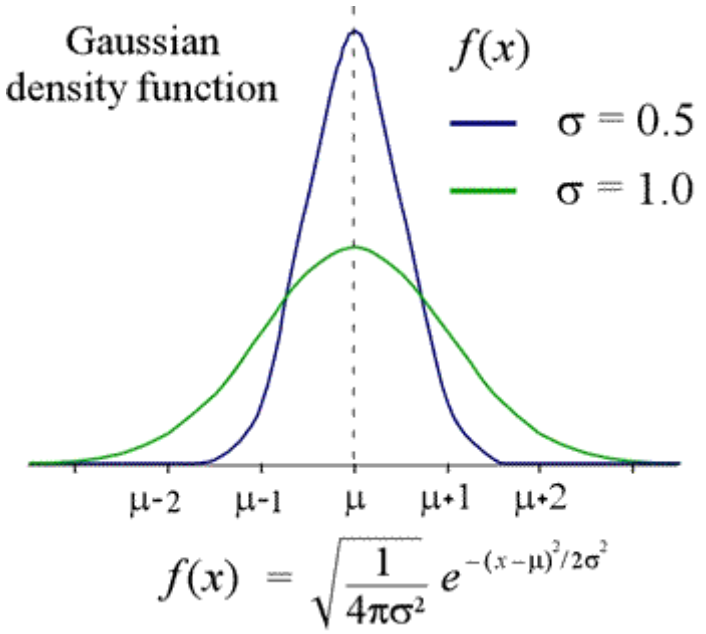

Fig 3.4. PROBABILITY DENSITY FUNCTION OF THE NORMAL/GAUSSIAN DISTRIBUTION OF A RANDOM VARIABLE, X-AXIS (SENSORY ESTIMATE). The coloured graphs indicate changes in mean (μ) and (σ^2) of the normal distribution (Cronk, 2013).

To deliver visual masking, I constructed a viewing box, which allowed subjects to see straight through it, or to see a masking image consisting of greyscale noise. The viewing box was designed for use in the dark. Its function is illustrated in Figure 3.5.

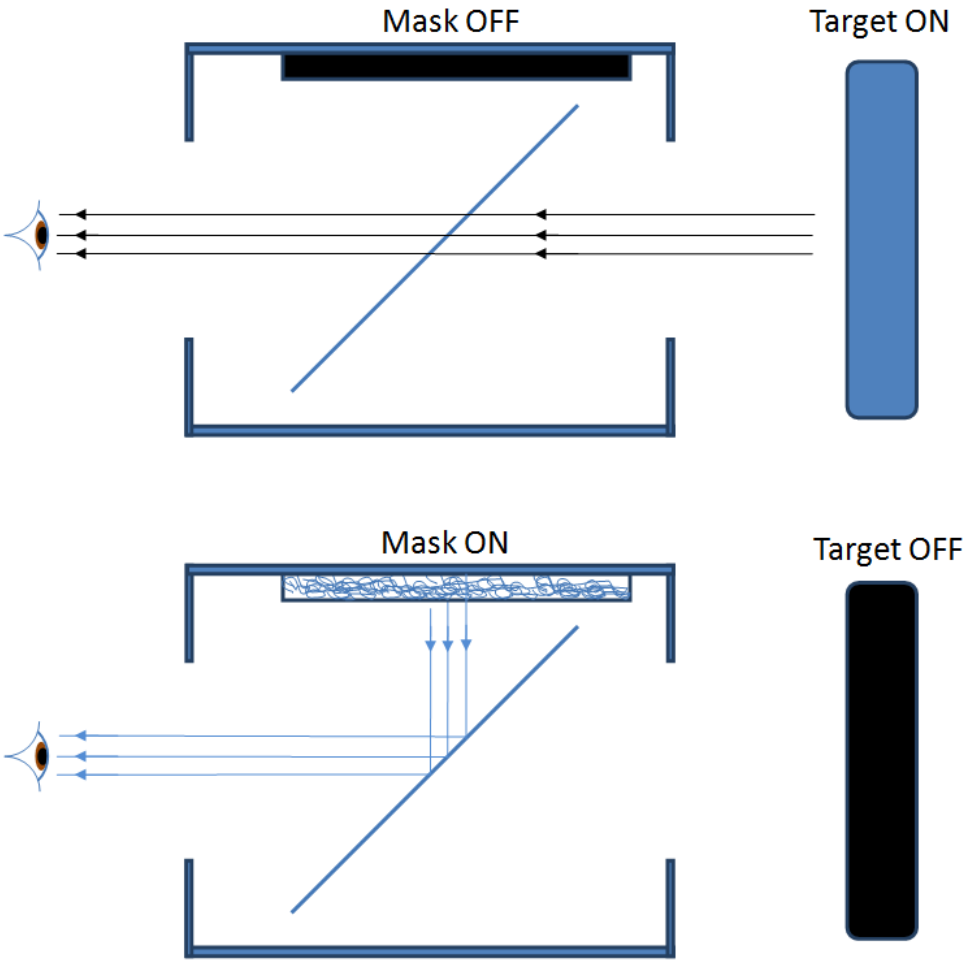

Figure 3.5. FUNCTION OF THE VIEWING BOX. Panel A illustrates the condition where the half silvered mirror is transparent, and parallel rays of light are reflected from an illuminated target to reach the viewer's eyes. In these experiments the target is a picture curtain. Panel B illustrates the condition where only the masking image is illuminated and the half silvered mirror is reflective, bending rays of light 90˚ so that only the mask is seen.

The viewing box housed a half silvered mirror which was mounted at a 45˚ angle between the vertical plane facing the subject, and the horizontal plane facing the ceiling. The roof of the box housed 4 internal LEDs (Light Emitting Diodes) sandwiched between a reflective silvered ceiling above, and a translucent 'masking' image below. These LEDs illuminated the (greyscale noise) masking image and

projected it onto the half silvered mirror, reflecting the masking image into the line of sight of the subject. An external LED was also mounted on top of the viewing box to illuminate the surrounding picture curtain in the dark. The i) external LED and ii) internal LEDs were connected to two separate TTL (Transistor Transistor Logic) input signals under computer control. By modulating the voltage of these inputs, the external and internal LEDs could be independently switched on or off. Thus, a subject looking through the viewing box (in the dark) could be shown the picture curtain, masking image, or neither in any order.

A light meter (LX 1330) measured the intensity of light reaching the subject from the LEDs. The single external LED intensity was 45 Lux. The combined intensity of the 4 internal LEDs was 48 Lux.

To measure the response times/shape of the TTL controlled LEDs, a CED 1401 plus ADC (analogue to-digital converter) connected to a photometer was used. The ADC sampled the photometer readings at a rate of 83.3kHz. The manufacturer tested, maximum error of analogue to digital conversion was 1.6%. The LEDs were accurate to within 0.2ms. The shapes of the step input responses were mildly trapezoidal.

The MOBS program

Threshold values obtained for the single interval forced choice (1IFC) components of this study used a Modified Binary Search (MOBS) staircase algorithm program (Tyrrell and Owens, 1988), *see fig. 3.6*.

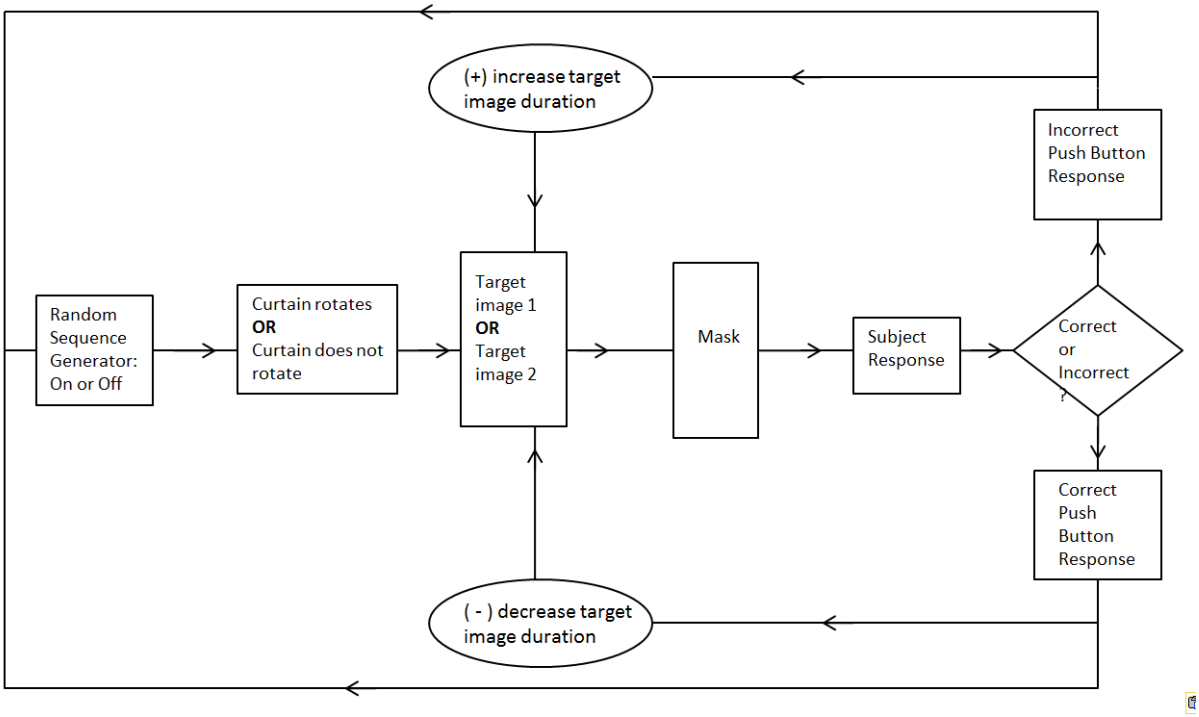

Figure. 3.6. FLOW DIAGRAM ILLUSTRATING FUNCTION OF THE MOBS PROGRAM.

The program responded to dual push buttons, each wired to the left and right 'click' outputs of a computer mouse, USB interfaced with a computer. If the subject indicated correctly to the stimulus presented on the picture curtain, the duration of the next stimulus presentation would be halved. If the subject indicated incorrectly, the duration would double. The first iteration of the program was always a 50ms presentation. The program would always terminate i) when the duration stimulus presentation dropped to 1ms (after a string of correct responses; ii) when it rose to 99ms (after a string of incorrect responses); iii) if the responses of the subject reversed five times between being correct and incorrect.

The MOBS program also presented (greyscale noise) masking for 200ms, at a stimulus onset asynchrony (SOA) of 10ms after any stimulus presentation. Due to

the design of the viewing box, this greyscale noise masking was only functional for the visual threshold task conducted in the dark.

Pilot study/visual threshold task

The efficacy of the viewing box was tested in a pilot study (the methods later became a visual threshold task, used prior to the experimental tasks in the main study).

The pilot study comprised two phases. The first phase was training. It was used to familiarise subjects with the apparatus and two visual stimuli presented. The second phase provided a MOBS threshold to a visual discrimination task: subjects were provided with the same two stimuli as the first phase, but visually masked. They were also tested to discern whether or not the stimuli were being perceived consciously or subliminally. The first and second phases are represented in figures 3.7. and 3.8., respectively.

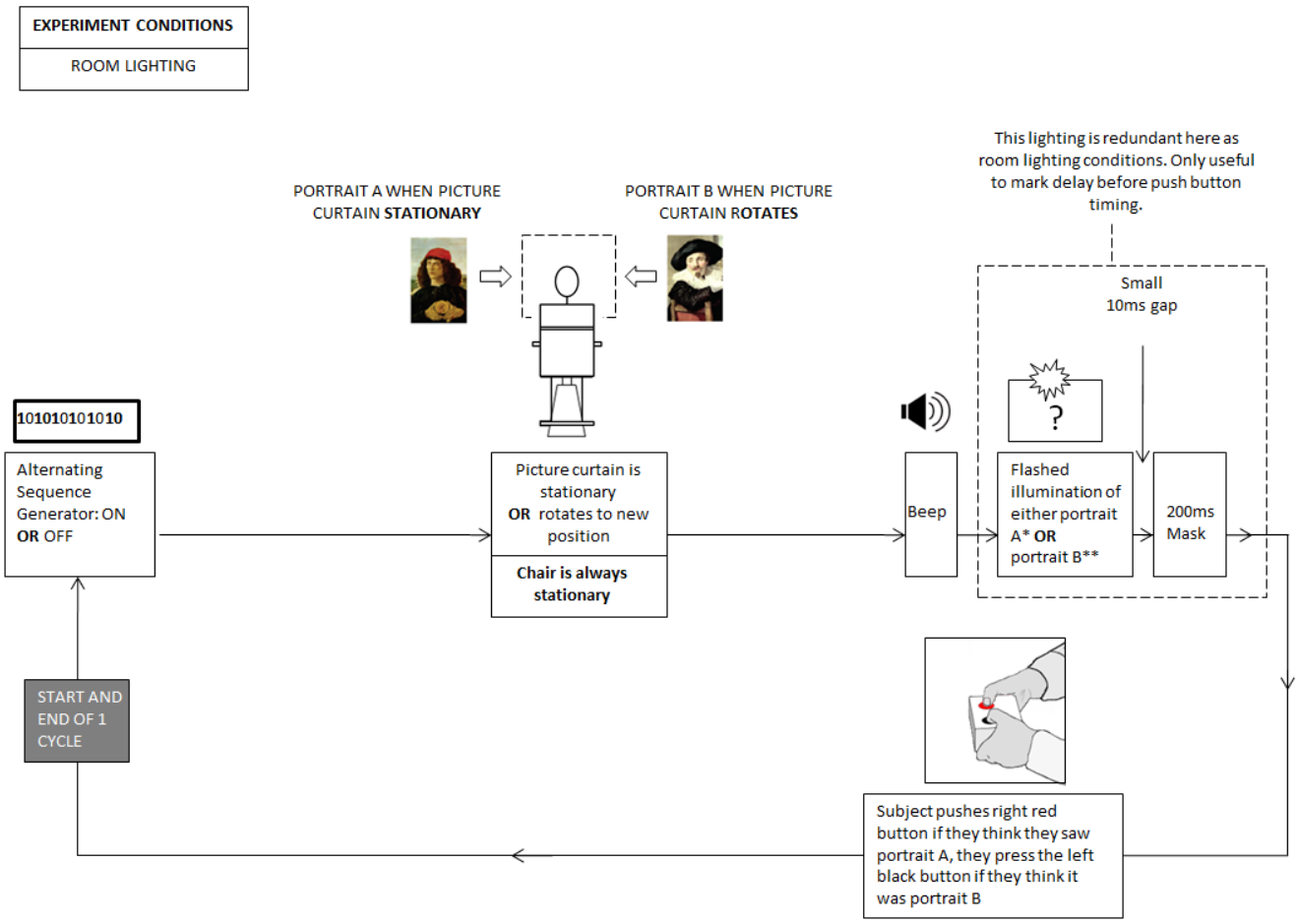

Figure 3.7. FLOW DIAGRAM ILLUSTRATING FIRST PHASE OF PILOT STUDY. The training phase. Each loop of the flow diagram represents one iteration of the MOBS program used to obtain a threshold value for portrait presentation duration.

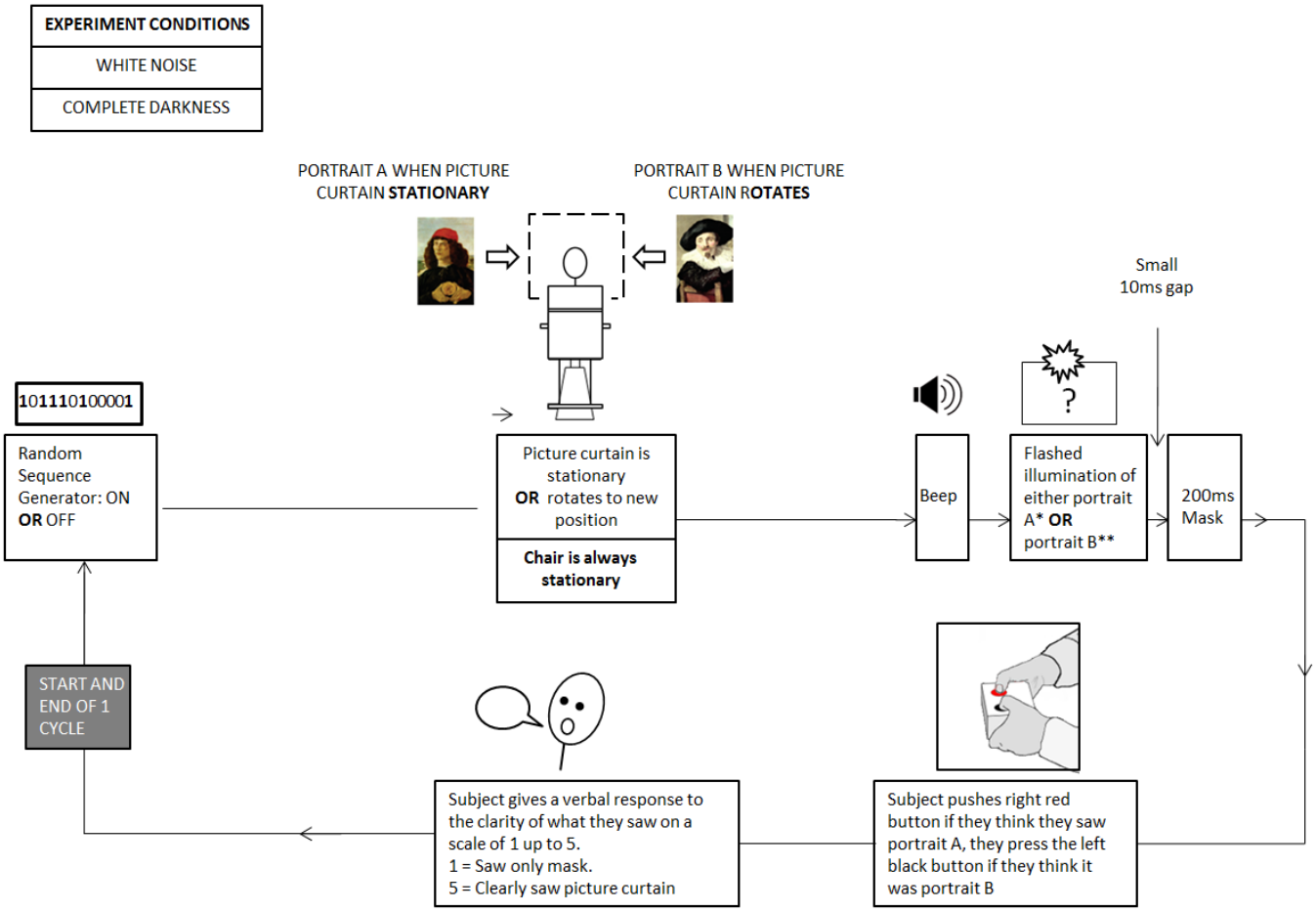

Figure 3.8. FLOW DIAGRAM ILLUSTRATING SECOND PHASE OF PILOT STUDY. Each loop of the flow diagram represents one iteration of the MOBS program used to obtain a threshold value for portrait presentation duration.

The first phase of the pilot study (*see fig.3.7*) comprised a single interval forced-choice (1IFC) task. Subjects were shown two different portraits on a picture curtain, portraits A & B. The task was performed with the room lights on. Instructions were that i) each portrait would be alternately presented, where the chair would not move, but instead the curtain would rotate; ii) subjects must use the dual push buttons to indicate which portrait was observed; iii) after every rotation of the curtain, subjects were to wait for an audible 'beep' (from chair mounted speakers) and visible 'flash' (from the viewing box in figure 3.5.) to pass before they pressed a push button; iv) subjects should press their chosen push button only once.

After instruction, the task was executed via a MOBS (modified binary search) program. The MOBS program recorded all subject responses. The primary, 'threshold search' function of the MOBs program was purposefully rendered redundant by keeping the room lights on. This training task determined i) whether subjects discriminated between the portrait images presented to them, ii) how and when to elicit their response.

The MOBS program iterated the task until a subject always responded correctly. Subjects generally did so, unless they had misunderstood which push button correlated with which portrait, or the timing required to elicit a registered, push button response. In both cases, all errors were remedied with further instruction.

In the second phase of the pilot study (*see fig.3.8*) subjects were informed that the task would be similar to that of the first. However, this task would be randomised, conducted in the dark and would require a subjective verbal response on each iteration of the task, in addition to the objective push button response. The purpose of the viewing box was explained. Black covering panels were placed below and to the sides of the viewing box to ensure subjects had no alternate or inadvertent view of the picture curtain.

Here the 'threshold search' function of the MOBS program was active (room lights off), as opposed to redundant in the first phase (room lights on). During the threshold search, each correct push button response halved the presentation duration of the next presented portrait. For every incorrect response, the duration doubled. Thus, a temporal threshold value for correct perception was approached after multiple iterations of the MOBS program.

To delineate responses to consciously perceived vs. subliminally encoded visual stimuli (Christensen et al., 2008), subjects were asked to give a subjective verbal response after their push button response. This was to indicate how clearly they saw the picture curtain. They were instructed to call out a number from 1 up to 5, with 1 being the lowest and 5 being the highest. Each number on the scale correlated with a graded quality of percept such that:

1. Only see the masking image of the viewing box. Nothing from the curtain.
2. See some artefact from the curtain, but no idea which portrait/image was seen plus the mask.
3. Have a good guess of which image they saw, but uncertain, plus the mask
4. Certain of which image they saw, plus the mask
5. 'Clear as day' (mask has negligible effect)

The subjects were asked to repeat these instructions to confirm they understood.

Subjects were also instructed that i) in the dark, they would only be provided illumination from viewing box ii) the duration of this illumination would be adjusted to make it easier or harder to see the picture curtain; iii) they must indicate which portrait they believe they observed; iv) sometimes they would not 'perceive' anything from the picture curtain and only see the masking image from inside the viewing box. Despite this they should give their best guess as it was a one alternative forced choice (1AFC) exercise.

The room lights were switched off. White noise was activated via the chair-mounted speakers. Subjects were verbally alerted before the MOBS programme was started. The task was executed. A written log was recorded of the subjects' verbal responses

and the associated duration for which the picture curtain was shown. (These would be analysed post hoc). Data from a typical, exemplar subject illustrates the effect of visual masking. With visual masking, the responses were variable, indicating that the reliability of visual stimulus encoding was reduced (*fig. 3.9. Panel A*). With no visual masking, the subject always made correct responses (*fig. 3.9. Panel B*). Furthermore, correct and incorrect push button responses (average of 3 pilot subjects) correlated with verbal subjective estimates of how clearly a portrait was seen (*fig. 3.10*). Thus subliminal encoding of the stimulus was inferred.

A)

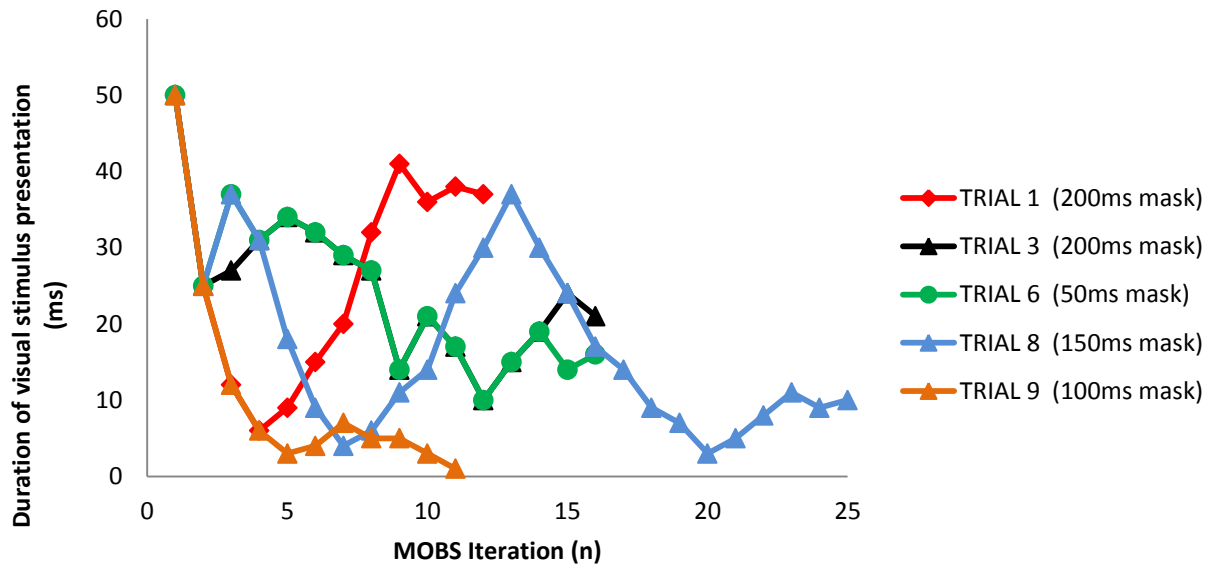

B)

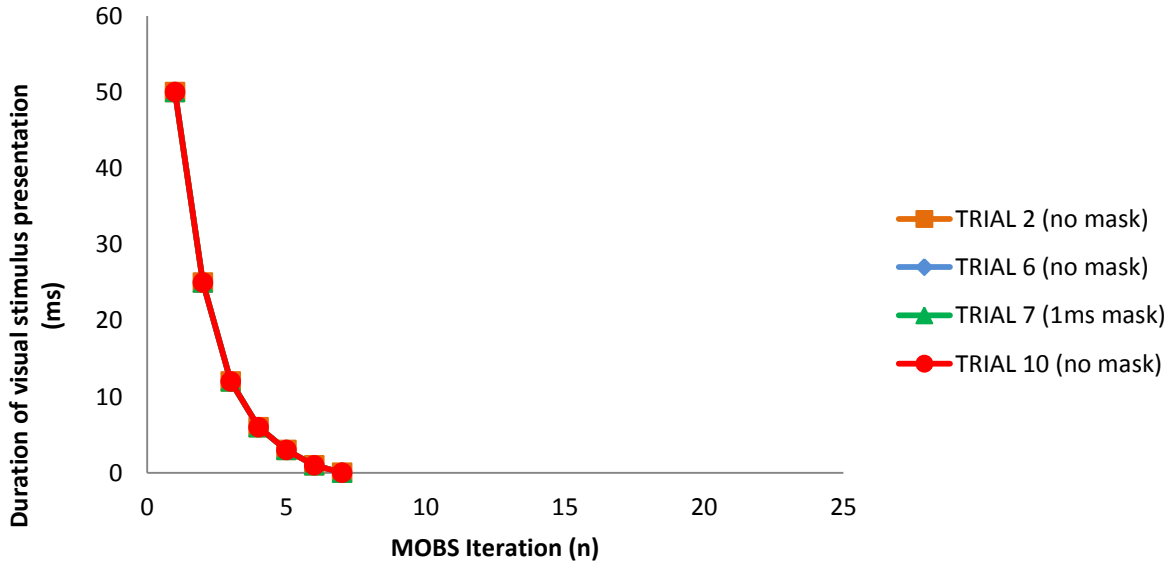

Figure 3.9. EXEMPLAR SUBJECT, VISUAL THRESHOLD TASK. Illustrates the difference between multiple traces of an exemplar subject's binary push button responses produced from repeating the second phase of the pilot study (Fig.5) but with different durations of visual masking presentation (Panel A) or no visual masking at all (Panel B).

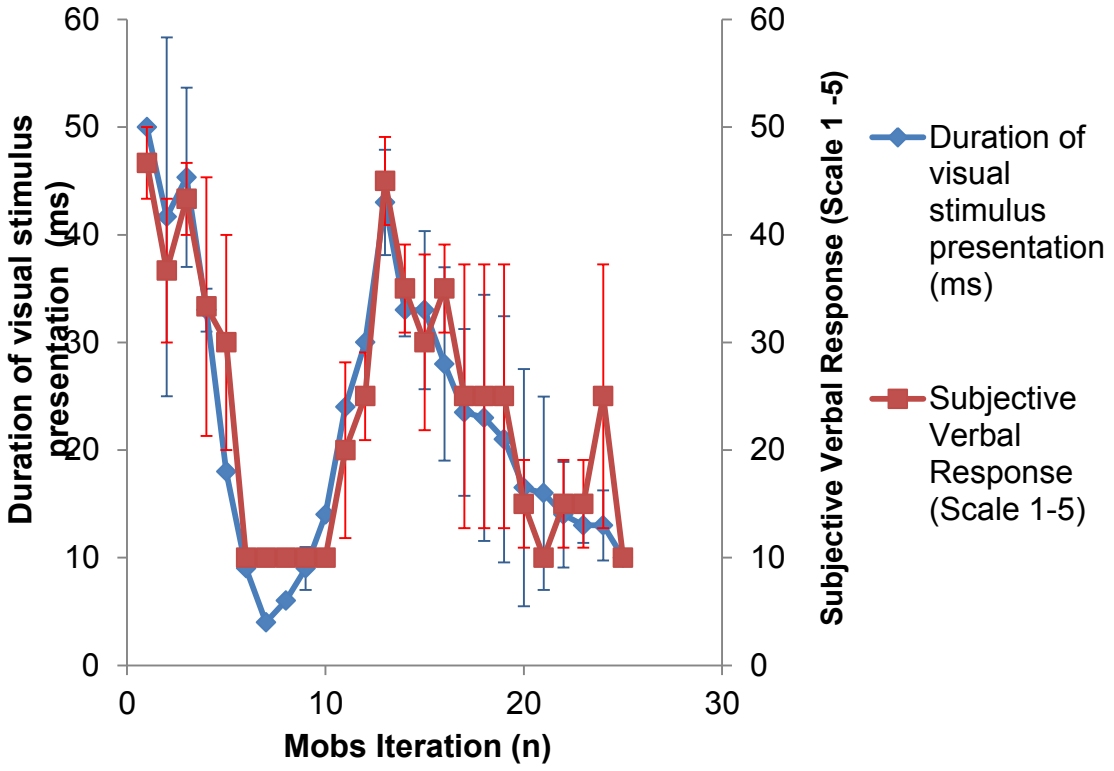

Figure 3.10. AVERAGED (3 PILOT SUBJECTS) TRACE OF OBJECTIVE PUSH BUTTON RESPONSES (FIRST Y AXIS, RED GRAPH) VS. SUBJECTIVE VERBAL RESPONSE TO QUALITY OF VISUAL PERCEPT (2ND Y-AXIS, BLUE GRAPH). A subliminally-encoding subject will make a string of correct push button responses whilst reporting to see only masking (subjective report of 1, on a scale of 1-5 of quality of percept). The push button task is single-interval forced choice (1IFC), hence the probability of making a blind correct choice at each response is *P* = 0.5. For example, the probability of obtaining 6 correct responses by chance (whilst verbally reporting to not see the target visual stimulus) takes the form of Bernoulli trials $P = \binom{6}{6}(0.5^6)\,(0.5^0) = 0.016$ over the 'subliminal' interval, a probability much better than chance. With consecutive correct responses, subsequent presentation of the picture curtain was halved in duration (via the MOBS program). Error bars are SEM (standard error of the mean).

Visual-Vestibular Mismatch (VVM) Study

Subjects were passively rotated in the dark on a computer-controlled motorised chair in yaw, and required to indicate their orientation relative to a surrounding picture curtain (circa 150cm diameter) printed with interspersed images at regular intervals. Reduced saliency, terminal, visual feedback of these images could either be congruent or incongruent with the subjects' true angular position. Incongruent feedback was affected by surreptitiously rotating the picture curtain in the dark. Subjects were naive to the possibility of picture curtain rotations. Incongruent feedback could erroneously indicate an angular excursion of subject rotation 50% bigger or 50% smaller than the true rotation.

Subjects

There were three VVM experiments which contained some of the same and some different test subjects. For the first VVM experiment, self-estimate responses of chair rotation duration were recorded in 16 subjects with subliminal visual feedback (8 female, mean age 25 years, range 19-37yrs). However, in the second experiment, self-estimate responses of angular position were recorded. This was with 16 subjects (8 female, mean age 26 years, range 19-31yrs, 12 of which had performed the first VVM experiment) with subliminal visual feedback. In the third VVM experiment, self-estimate responses of angular position were recorded in 13 subjects (6 female, mean age 24 years, range 19-30 yrs, 8 of which had performed the first and second VVM experiments) with visual feedback in which the subjects received intermediate visual feedback, where they were aware of a visual stimulus, but could not reliably confirm what they saw.

Visual Threshold Task

Prior to each VVM experiment, the visual threshold task was performed. This is identical to the task used in the pilot study (*fig. 3.7 & 3.8*.) and was used to estimate the stimulus durations for which subjects could perceive the images presented at a particular subjective level from 1 (lowest) to 5 (highest). The outcomes of this task were used to estimate the subjective verbal response level 1 (perceiving no stimulus from the curtain) used in both the subliminal duration and position estimate VVM experiments; and the subjective verbal response level 3 (a good guess about curtain stimulus) in the intermediary visual feedback position estimate VVM experiment.

Training for the Visual-Vestibular Mismatch experiments

Prior to each VVM experiment, the subjects undertook training to familiarise them with the picture curtain, and to associate visual landmark stimuli with their sensation of motion over the range of chair rotations performed.

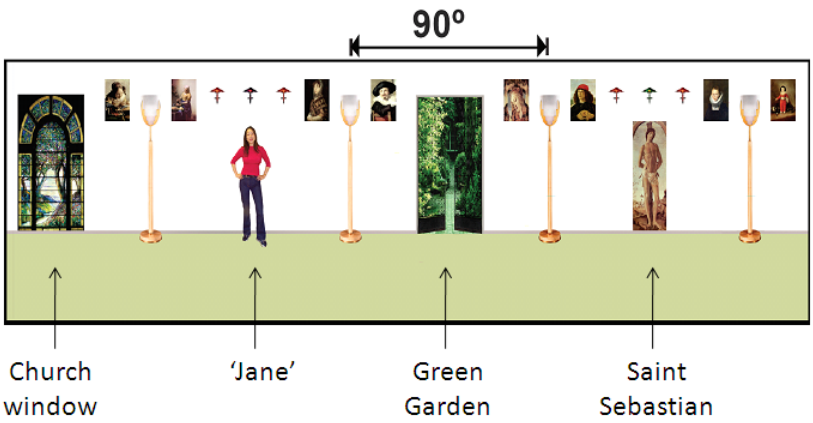

Figure 3.11. PICTURE CURTAIN

Subjects were introduced to four cardinal positions on the picture curtain each 90˚ apart (*see fig.3.11.*). These positions were named as 'Jane' (ahead), 'Saint

Sebastian' (behind), the 'green garden' (left) and the 'church window' (right). Subjects were rotated manually to these positions whilst being asked to move the dial on the position indicator analogously.

Subjects were manually shown that: the angular displacement between each cardinal position was a 'quarter turn or 90˚'; there were 'lampstands' equidistant between each cardinal position - thus spaced 'a quarter turn or 45˚ from adjacent cardinal points; above 'Jane' and 'Saint Sebastian' were 3 lights of different colours; either side of the lampstands were different portraits, with a brief discussion of the differences between these portrait pairs.

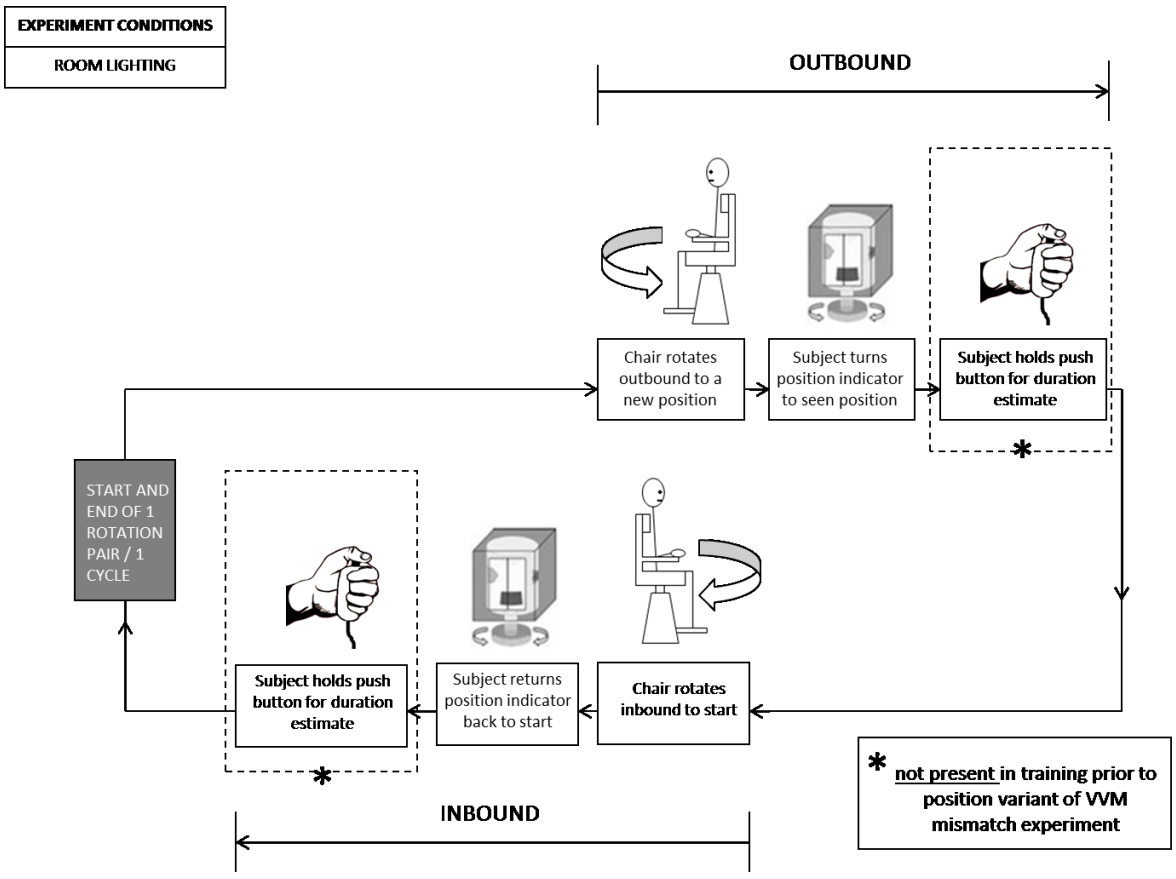

Figure 3.12. FLOW DIAGRAM TO ILLUSTRATE THE TRAINING ROTATIONS UNDER COMPUTER CONTROL.

The last phase of the training was to practise responding to the picture curtain, using the range of rotations subjects would experience in the main Visual-Vestibular Mismatch (VVM) experiments. The training took place with room lighting and under computer control (*see fig.3.12*).

The subjects were instructed that they would rotate from their baseline position (facing 'Jane' on the picture curtain) to a new position. This was termed an 'outbound' rotation. They were instructed to turn the position indicator to its analogous position the moment they stopped rotating. They would then need to press a push button (held in their free hand) to indicate how long they thought the rotation had lasted. Every second rotation would return them to 'Jane'. This was termed an 'inbound' rotation and they would have to repeat their indications of position and rotation duration in an identical fashion to the 'outbound' rotations.

After instruction, subjects were aligned with the image of 'Jane' on the picture curtain. The chair was rotated under computer control with a raised cosine stimulus. Subjects were consecutively moved through the range of rotations they would experience in the experiment. The rotations were non-randomised and progressed from smallest to largest magnitudes of displacement and velocity. Rotations 'outbound' to the right, then inbound' from the right were completed first. Rotations outbound to the left, then inbound from the left were completed last. This was to encourage the subjects to comprehend the increasing angular displacement from their baseline position and make spatial relationships easy as possible. The subjects were told when they were half way through the rotations, with all their responses monitored on a computer.

Visual-Vestibular Mismatch (VVM) Experiments

There were three separate VVM experiments. A duration estimate VVM experiment conducted with subjective level 1 (range 1 to 5) visual feedback (*see fig. 3.13*); a position estimate VVM experiment conducted with subjective level 1 (range 1 to 5) visual feedback (*see fig. 3.14*); and a position estimate VVM experiment conducted with subjective level 3 (range 1 to 5), (*also see fig. 3.14*). In all three types of VVM experiment, the stages at which subliminal visual feedback were presented can be identified by the boxes containing the text "(x) ms". The "(x) ms" represents the duration of visual presentation used which correlated with a value of 1 on the visual threshold task performed for each subject at the beginning of the experiment (range 1 to 5). This value of ""(x) ms" was used consistently throughout each subject's trials. The subjects were asked to inform the experimenter if they perceived any visual feedback that was not a 1. Occasionally, subjects saw what they thought was a value 2 on the rating scale. Here, the experimenter modulated the value of "x" until a value of 1 was again observed consistently across 5 trials, and then the experiment proper was continued.

In the duration estimate VVM experiment, visual feedback was for the purpose of eliciting a duration estimation response from subjects via a held push button and under conditions of subliminal visual feedback. This is illustrated in figure 3.13. For this experiment, a position indication was also required from a subject prior to the primary duration estimate. This is all illustrated in figure. 3.13. The rationale for the additional measure was that a percept of position may be required to calibrate a percept of motion duration (Mergner et al., 1996); and such action would mitigate drift in duration estimates.

Both the position estimate VVM experiments were for the purpose of eliciting a position estimation response by turning a position indicator dial (*fig. 3.14*) to the direction a subject felt they were facing. The difference between the two experiments is that the one experiment was where "(x) ms" represents the duration of visual presentation which previously correlated with a subjective value of 1 on the visual threshold task (range 1 to 5); and the other experiment was where "(x) ms" correlated with a subjective value 3 on the visual threshold task (i.e. intermediary visual feedback).

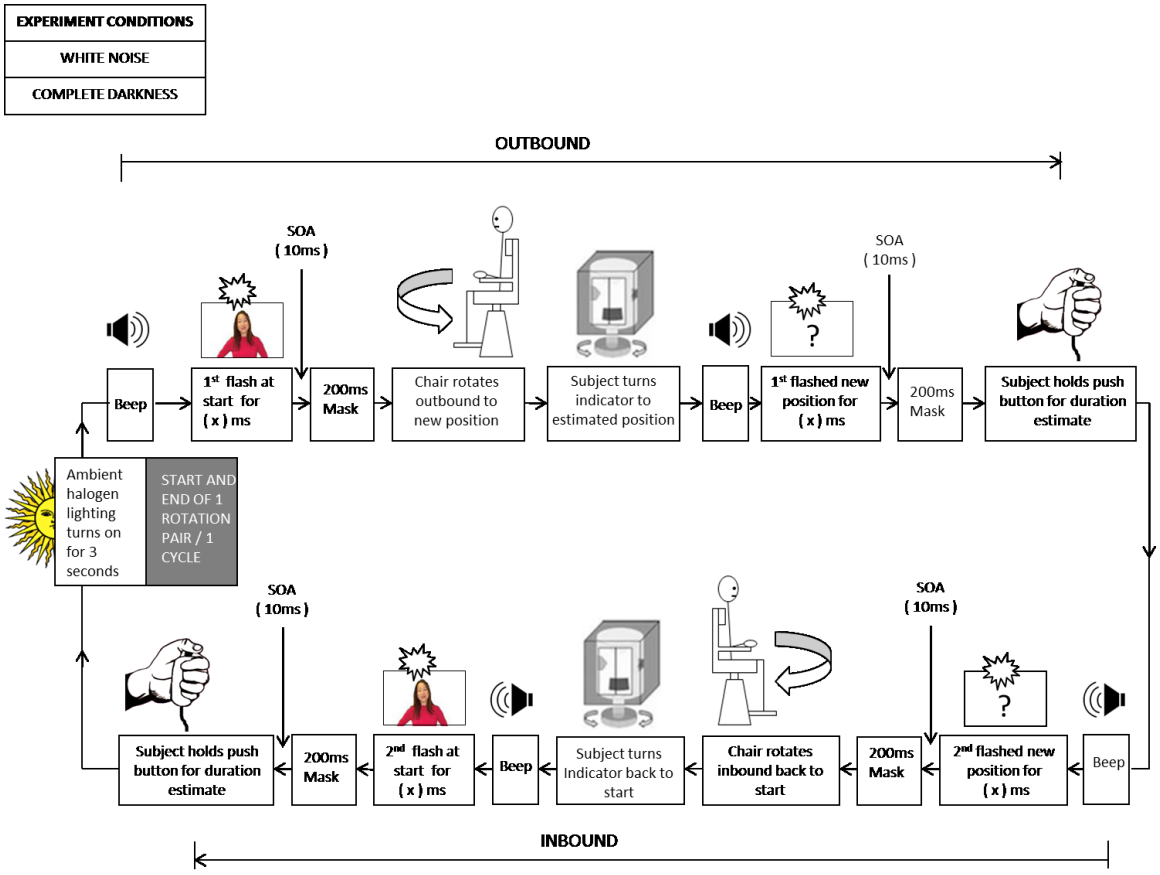

Figure 3.13. FLOW DIAGRAM TO ILLUSTRATE THE DURATION ESTIMATE VVM EXPERIMENT

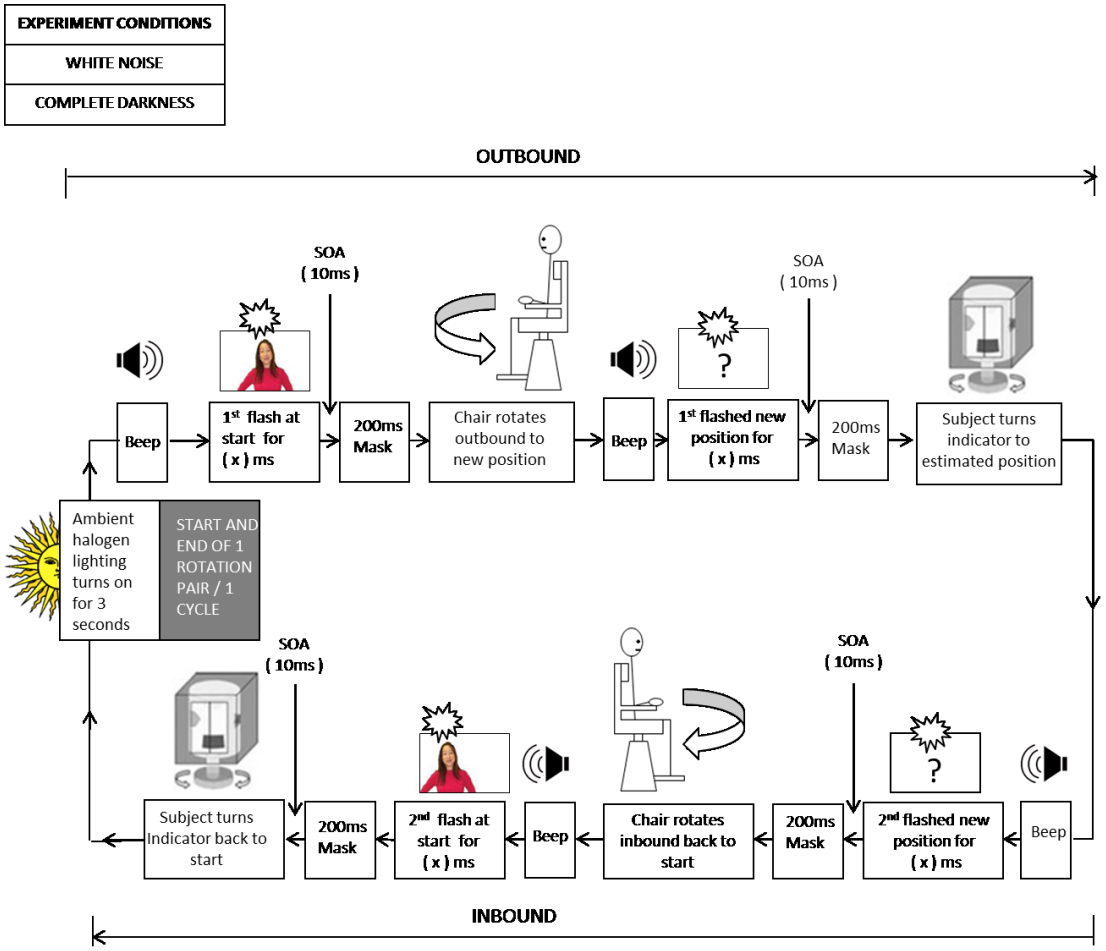

Figure 3.14. FLOW DIAGRAM TO ILLUSTRATE POSITION ESTIMATE VVM EXPERIMENT

In the VVM experiments, subjects were first instructed that the rotations would take place in the dark. They were given the following instructions, with guidance (manual rotation of the chair with verbal cues):

1. They would always rotate out from 'Jane', and then back to her on the second rotation, much like during the training.

2. Before every 'outbound' rotation, the ambient halogen lighting would turn on and provide a few seconds full illumination of the picture curtain before turning off. This would not be present on the 'inbound' rotations.

3. Thereafter, they would receive an audible ‘beep’ followed by a masked ‘flash’ (brief illumination of the picture curtain followed by the ‘masking’ image in the viewing box).

4. After the ‘flash’ the chair would rotate outbound in the dark to a new position.

What subjects were not told is that the picture curtain could surreptitiously move. In a randomised order it would remain static (‘control’ condition), move in the direction of the chair to show an apparent 50% smaller rotation than actual (‘smaller’ condition), or move against the chair to show an apparent 50% larger rotation (‘bigger’ condition)

Instructions for the duration experiment variant

5a. Subjects would indicate their estimated position on the position indicator, the moment they felt they had stopped rotating (thus, they remained consistent with the previous duration experiments conducted supraliminally by B.Seemungal, where perceived position indication was found to be important in giving a correct response of perceived duration).

6a. They were warned that the indication had to come promptly because a second ‘beep’ and ‘flash’ stimulus would follow shortly thereafter, and they had to be looking straight ahead again and paying attention. The end of this second ‘flash’ stimulus was their cue to indicate their duration response with the push button.

Instructions for the position experiment variant

5b. a second ‘beep’ and flash stimulus would shortly follow the rotation, and they had to be looking straight ahead again and paying attention. The end of this second

'flash' stimulus was their cue to indicate their estimated position with the position indicator.

A raised cosine stimulus was used for all rotations. A distinction was made between rotations where the visual feedback was masked and those that were unmasked. The unmasked rotations were only included to prevent subjects becoming accustomed to being unable to see the picture curtain, and losing attention. Pilot studies showed that without the masking, the picture curtain could be reliably seen. The masked rotations will be referred to as 'experimental rotations' and the unmasked rotations will be referred to as 'calibration rotations'.

In total, 108 'experimental rotations' were performed (*see fig.4.15*):

- 9 rotation magnitudes.
- 2 rotations (paired) at each rotation magnitude for 'outbound' and 'inbound' phases.
- 2 directions of outbound rotation, left and right (the inverse for inbound)
- 3 curtain conditions (control and +50%, -50% of apparent rotation, respectively).

In total 28 'calibration rotations' were performed.

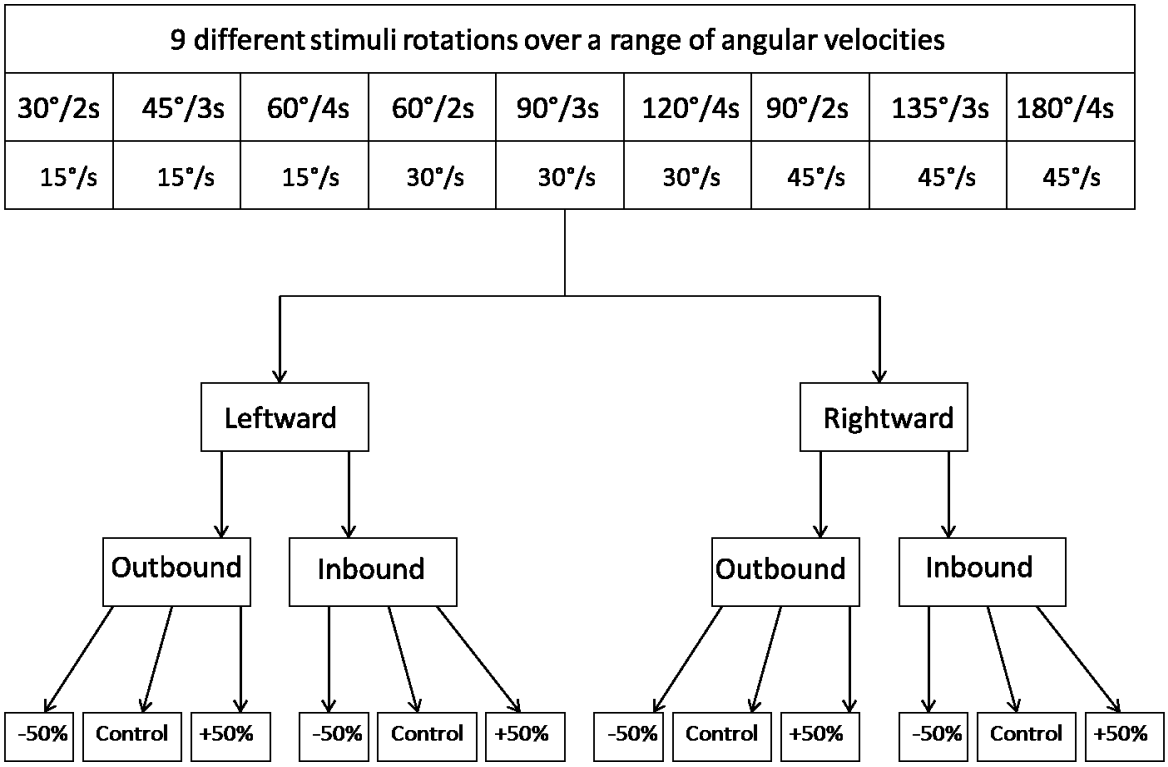

Figure 3.15. A SCHEMATIC OUTLINE OF THE GROUPINGS OF THE EXPERIMENTAL ROTATIONS.

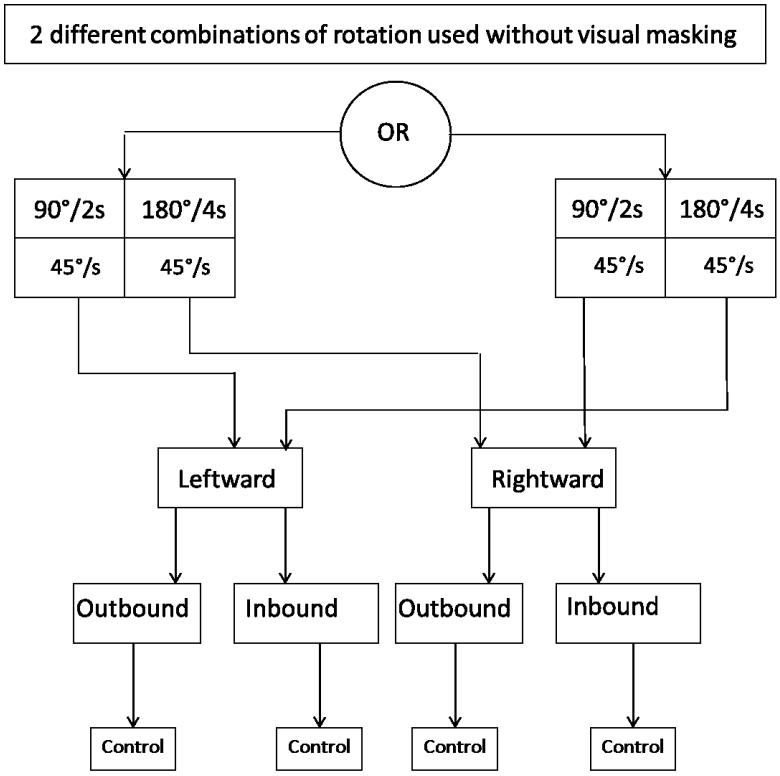

Figure 3.16. A SCHEMATIC OUTLINE OF THE GROUPINGS OF THE CALIBRATION ROTATIONS.

The paired, 'experimental rotations' were randomised and divided into 6 groups. A random order of these groups was presented to each subject. Randomisation was also performed intra-group. The groups were described to the subjects as 'blocks'. They were told that the rotations would be presented in 6 blocks and that they would be informed of their progression upon completion of each block. Between blocks each subject was shown a short series of 'calibration rotations'. They were notified of only the first series, and that these would recur frequently. Two different blocks of calibration rotation were used alternately (*see fig. 3.16*).

Results

Biased subliminal presentation of visual landmarks was shown to bias duration estimates of angular rotation (*see fig 3.17a*), but not estimates of angular position (*see fig 3.21*). Biased intermediary-salience presentation of visual landmarks biased position estimates of angular rotation in yaw (*see fig 3.22*) to a greater degree than with subliminal visual feedback.

Repeated measures ANOVA were performed on the responses for both types of the visuo-vestibular mismatch experiments; with duration estimate response and position estimate response. For the subliminal visual feedback duration experiment, responses from both outbound and inbound rotations were analysed. However, for the position experiments, responses from only the inbound rotations were analysed, as subjects explicitly knew that upon inbound rotation they would return to the same landmark (*see fig. 3.11, 'Jane'*).

Duration estimate VVM experiment

A 3 x 2 Repeated Measures ANOVA was performed on the data from the subliminal visual feedback, duration response experiment. The first factor was the visuo-vestibular mismatch (VVM) and consisted of three levels: '50% smaller', 'control', '50% bigger'. The second factor was the phase of rotation, consisting of two levels, 'outbound' and 'inbound'. There was a significant effect of VVM [$F(2,16)=6.6$, $P<0.01$], but no significant effect of phase [$F(1,16)=0.3$, $P=0.60$]. The result showed that there was no interaction between phase of rotation and VVM [$F(2,16)= 0.9$, $P=0.40$], which suggests that the VVM effect in both phases was the same.

Post hoc paired *t*-tests indicated that there was a significant difference between the 50% smaller vs. control condition ($P<0.02$, Bonferroni corrected $P=0.05$); the 50%

smaller vs. 50% bigger conditions (P<0.01 Bonferroni corrected P=0.01); but no difference between the control and 50% bigger condition (P<0.26 Bonferroni corrected P=0.78).

To further clarify the VVM effect across outbound and inbound rotations, repeated measures ANOVA were performed across the outbound and inbound duration response data independently. There was no significant effect across outbound (F(2,16)=3.2, P=0.06)) estimates, but the inbound estimates were significant (F=(2,16)=6.4, P=0.005). Posthoc analysis with paired t-tests indicated that there were significant differences between the outbound 50% smaller condition and the outbound 50% bigger condition (P=0.02, Bonferroni corrected P=0.30); inbound 50% bigger vs. inbound control (P=0.02, Bonferroni corrected P =0.28); and inbound 50% smaller vs. inbound 50% bigger (P<0.01, Bonferroni corrected P=0.03).

Bar graphs illustrate the differences between VVM conditions for outbound, inbound and combined outbound & inbound rotation data (*see fig. 3.17, graphs a, b, c) respectively*).

Tabulated values of the gain of subject duration response to stimulus show the bias (across all 16 subjects) to indicate a larger gain than 'control' for the 'bigger' VVM condition and a smaller gain than 'control' for the 'smaller' VVM condition (*see table 3.1.*)

A scatter-plot of gain of subject duration response to stimulus (x-axis) vs. the ordering of those gain values (y-axis), takes the form of a cumulative Gaussian, suggesting the data's adherence to a Gaussian (normal) distribution and hence the validity of parametric techniques for analysis (*see fig. 3.20*).

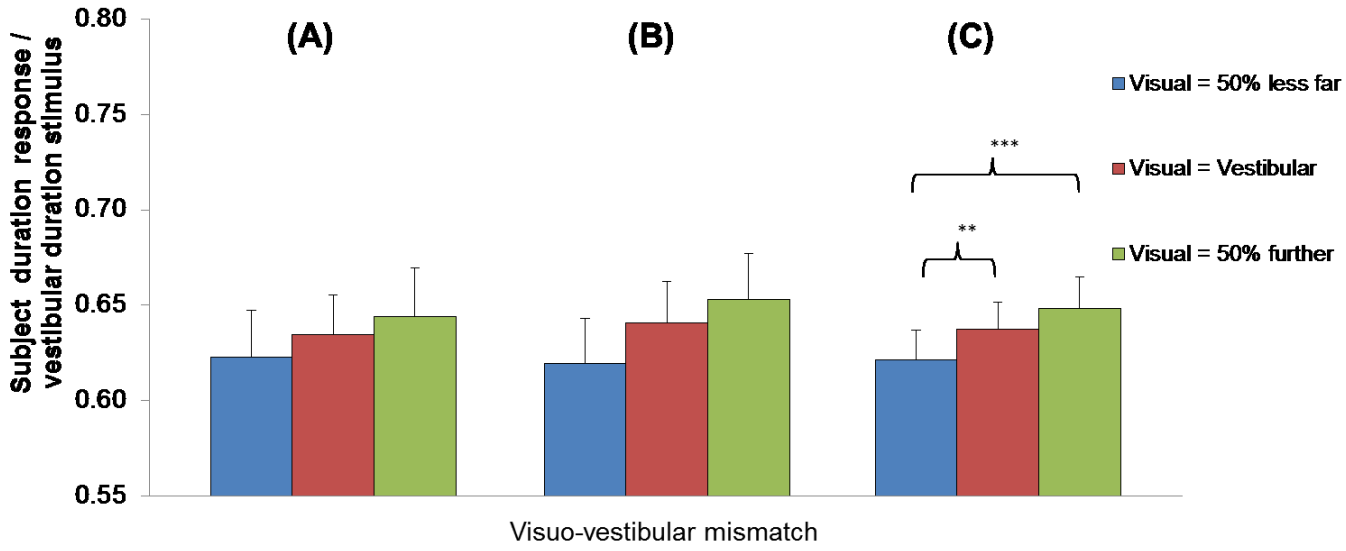

Fig. 3.17 SUBLIMINAL VISUAL FEEDBACK DURATION ESTIMATION EXPERIMENTS. Gain of Outbound (A), Inbound (B), Combined Outbound & Inbound (C) subject perceived response / actual duration of rotation for the three VVM conditions. Blue – 50% smaller condition, Red – control condition, Green – 50% bigger condition. Error bars are Standard Error of the Mean (SEM), N.B. overlapping SEM bars do not directly relate to statistical significance in paired t-tests and rANOVA, as the data are matched in such analyses.

Subject (S)	50% less far (Smaller)	Visual = Vestibular (Control)	50% further (Bigger)
S1	0.41	0.41	0.50
S2	0.34	0.35	0.35
S3	0.60	0.59	0.64
S4	0.45	0.45	0.46
S5	0.73	0.77	0.80
S6	1.18	1.23	1.15
S7	0.72	0.74	0.75
S8	0.47	0.51	0.48
S9	0.77	0.78	0.80
S10	0.19	0.23	0.21
S11	0.82	0.85	0.84
S12	0.73	0.71	0.73
S13	0.54	0.56	0.57
S14	0.52	0.49	0.52
S15	0.86	0.89	0.88
S16	0.62	0.66	0.68
MEAN (μ)	0.62	0.64	0.65
STD(σ)	0.24	0.24	0.23

Table 3.1. GAIN VALUES OF SUBJECT PERCEIVED DURATION RESPONSE / DURATION OF VESTIBULAR STIMULUS. Outbound and inbound chair rotation data are combined. Columns represent a comparison of responses between the '50% smaller', 'control' and '50% bigger conditions of visual mismatch (picture curtain) relative to the veridical vestibular stimulus (chair rotation). Pink fill indicates the gain value is smaller than the control condition. Green fill indicates the gain value is larger than the control condition.

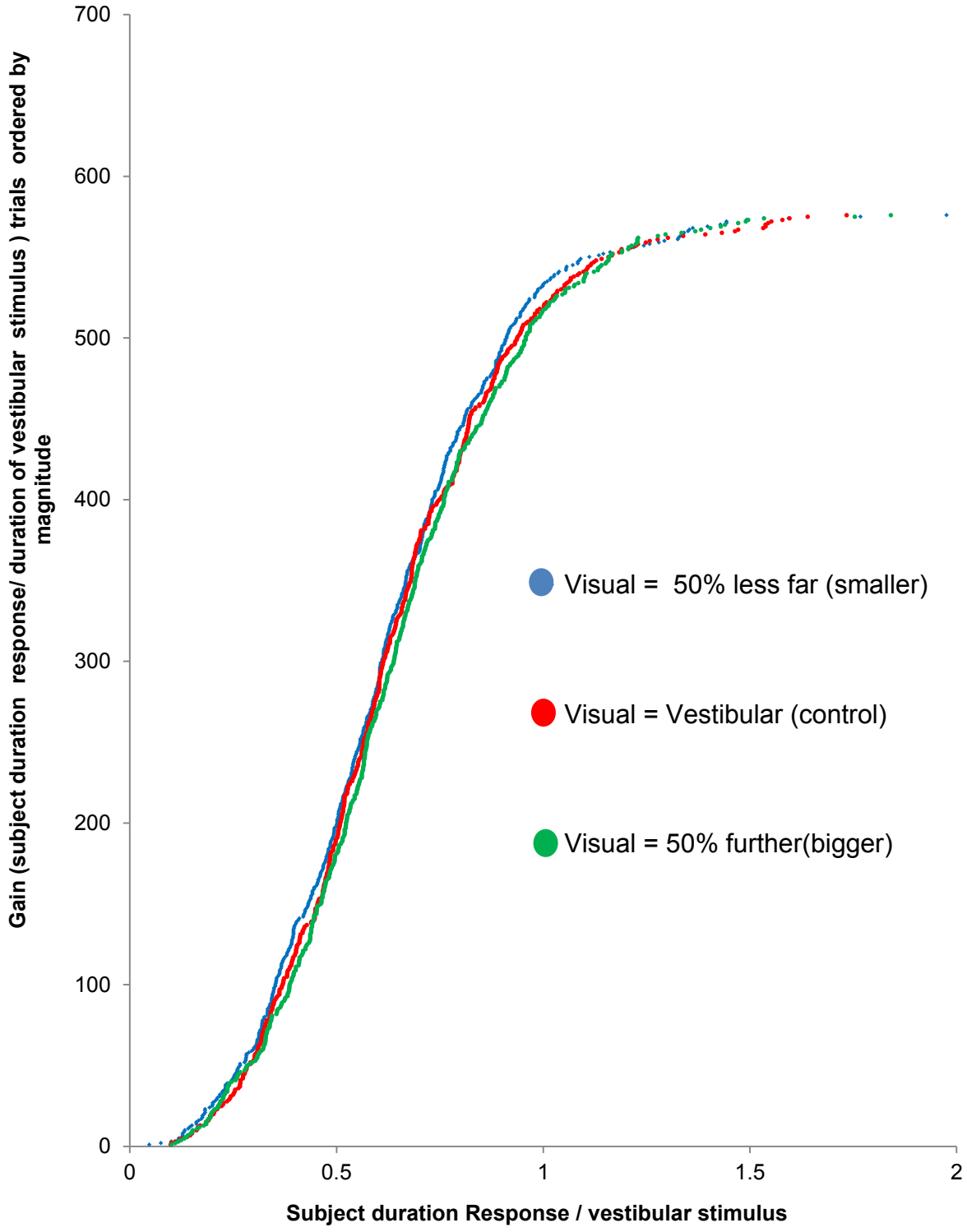

Figure. 3.18. GAIN OF SUBJECT DURATION RESPONSE/VESTIBULAR STIMULUS VS. TRIAL NUMBER. Ordered by magnitude of Gain of subject duration response/vestibular stimulus. Red graph represents control condition, Blue graph the 50% smaller condition, and Green graph the 50% bigger condition.

Position estimate VVM experiments

Subject (S)	50% less far (Smaller)	Visual = Vestibular (Control)	50% further (Bigger)
S1	1.02	0.94	1.02
S2	0.93	0.87	0.91
S3	1.03	1.04	1.32
S4	0.85	0.88	0.85
S5	0.89	1.11	1.09
S6	1.00	1.03	1.04
S7	0.90	1.04	0.87
S8	0.96	1.13	0.91
S9	0.81	1.09	1.12
S10	1.07	0.93	0.96
S11	1.17	0.95	1.03
S12	0.93	0.87	0.91
S13	0.82	1.03	1.28
S14	1.20	1.09	1.13
S15	1.06	1.06	1.05
S16	1.02	1.12	1.23
MEAN (μ)	**0.98**	**1.01**	**1.04**
SD (σ)	**0.11**	**0.09**	**0.15**

Table 3.2. GAIN VALUES OF SUBJECT PERCEIVED POSITION RESPONSE / POSITION CHANGE CUE OF VESTIBULAR STIMULUS. Subliminal visual feedback condition (subject report '1' on visual saliency scale [1-5]). Columns represent a comparison of responses between the '50% smaller', 'control' and '50% bigger conditions of visual mismatch (picture curtain) relative to the veridical vestibular stimulus (chair rotation). Pink fill indicates the gain value is smaller than the control condition. Green fill indicates the gain value is larger than the control condition.

Subject (S)	50% less far (Smaller)	Visual = Vestibular (Control)	50% further (Bigger)
S1	0.80	0.85	1.00
S2	0.83	0.93	0.86
S3	1.03	1.04	1.21
S4	0.59	1.00	1.33
S5	0.53	0.97	0.93
S6	0.59	1.00	1.33
S7	1.06	1.21	1.21
S8	0.62	0.93	1.17
S9	0.71	1.06	1.45
S10	0.78	1.05	1.19
S11	1.04	1.05	1.31
S12	1.07	1.41	1.47
S13	0.67	0.99	0.97
MEAN (μ)	**0.79**	**1.04**	**1.19**
SD (σ)	**0.20**	**0.14**	**0.20**

Table 3.3. GAIN VALUES OF SUBJECT PERCEIVED POSITION RESPONSE / POSITION CHANGE CUE OF VESTIBULAR STIMULUS. Intermediary visual feedback condition (subject report '3' on visual saliency scale [1-5). Columns represent a comparison of responses between the '50% smaller', 'control' and '50% bigger' conditions of visual mismatch (picture curtain) relative to the veridical vestibular stimulus (chair rotation). Pink fill indicates the gain value is smaller than the control condition. Green fill indicates the gain value is larger than the control condition.

Repeated Measures ANOVA was also performed on the outbound rotation data for both position response experiments. For the subliminal visual feedback variant, there was no significant effect of VVM [$F(2,16)=1.7$, $P=0.2$]. However, for the variant with visual feedback in which the subjects were aware of a visual stimulus, but could not reliably confirm what they saw, there was a significant effect of VVM

(F(2,13)=21.0, *P*<0.00001). Bar graphs representing the differences between VVM conditions for these experiments are shown in figures 3.21 and 3.22, respectively.

Tabulated values of the gain of subject position response to stimulus show the bias (across all 16 subjects) to indicate a larger gain than 'control' for the 'bigger' VVM condition and a smaller gain than 'control' for the 'smaller' VVM condition (*see table 3.2 for subliminal visual feedback, see table 3.3. for intermediary visual feedback.*)

Scatter-plots of gain of subject position response to stimulus (x-axis) vs. the ordering of those gain values (y-axis), and probability density functions further illustrate VVM (*see fig. 3.23. for subliminal visual feedback, see fig. 3.24. for intermediary visual feedback.*)

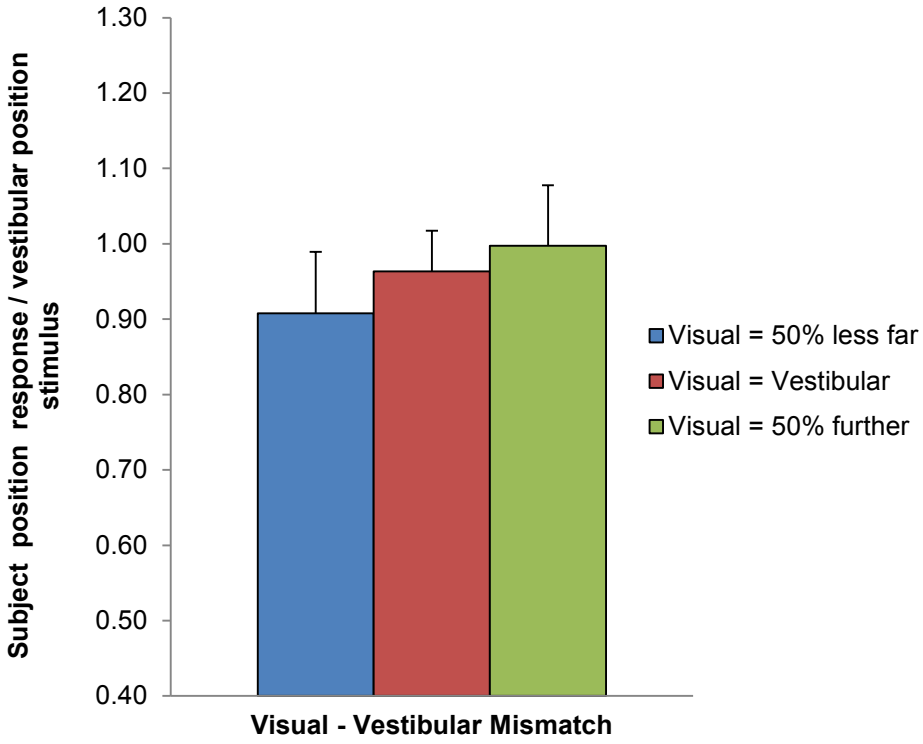

Figure 3.19. SUBLIMINAL VISUAL FEEDBACK POSITION ESTIMATION EXPERIMENT. Gain of subject perceived response / actual angular position for the three VVM conditions. Blue – 50% smaller condition, Red – control condition, Green – 50% bigger condition. Error bars are Standard Error of the Mean (SEM), N.B. overlapping SEM bars do not directly relate to statistical significance in paired t-tests and rANOVA, as the data are matched in such analyses.

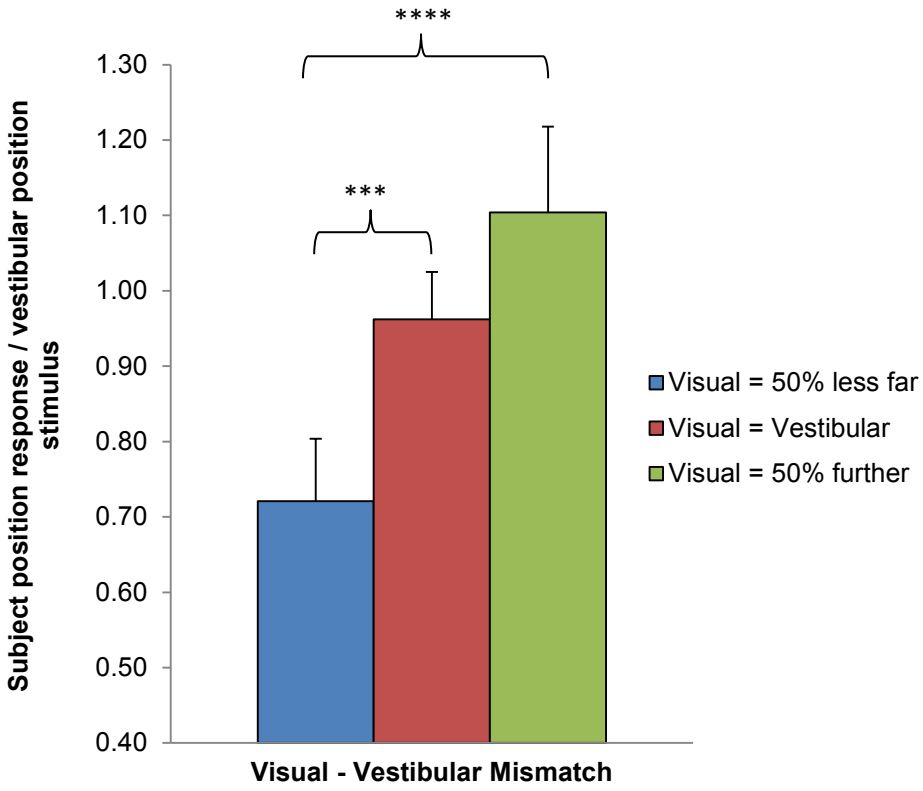

Figure 3.20. INTERMEDIARY VISUAL FEEDBACK POSITION ESTIMATION EXPERIMENT. Gain of subject perceived response / actual angular position for the three VVM conditions. Blue – 50% smaller condition, Red – control condition, Green – 50% bigger condition. Asterisks indicate significant differences with paired *t*-tests. Error bars are Standard Error of the Mean (SEM), N.B. overlapping SEM bars do not directly relate to statistical significance in paired t-tests and rANOVA, as the data are matched in such analyses.

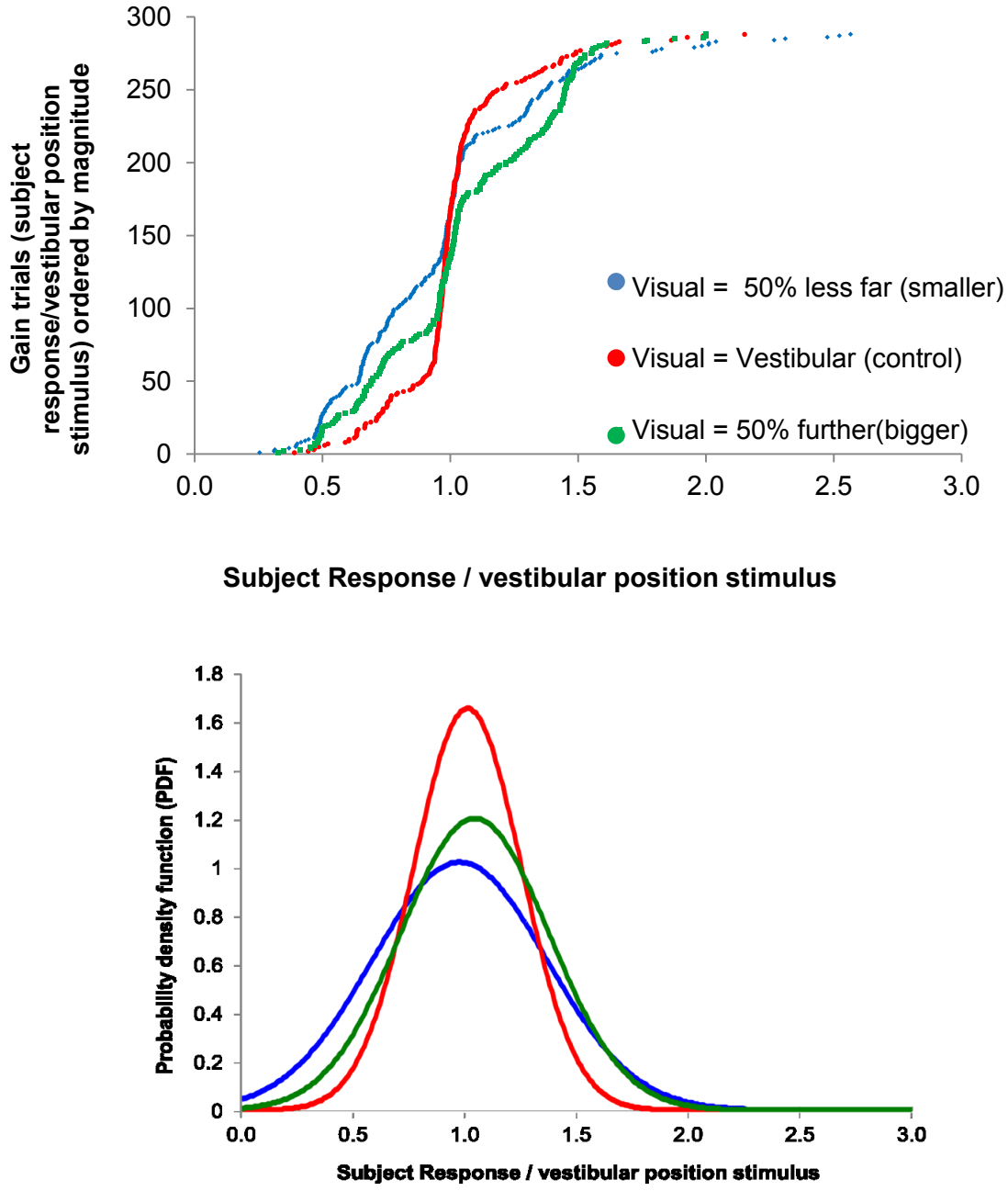

Figure 3.21. POSITION EXPERIMENT: SUBLIMINAL VISUAL FEEDBACK CONDITION (subject report '1' on visual saliency scale [1-5]). 16 subjects. Panel A. Gain of subject position response/vestibular stimulus vs. trial no. ordered by magnitude of Gain of subject position response/vestibular stimulus. Red graph represents control condition, Blue graph the 50% smaller condition, and Green graph the 50% bigger condition. All 16 subject data pooled. Panel B. Probability Density Function of the Gain of subject position response/vestibular stimulus. Curves fit via MLE in Matlab. Data averaged over all 16 subjects prior to curve fitting.

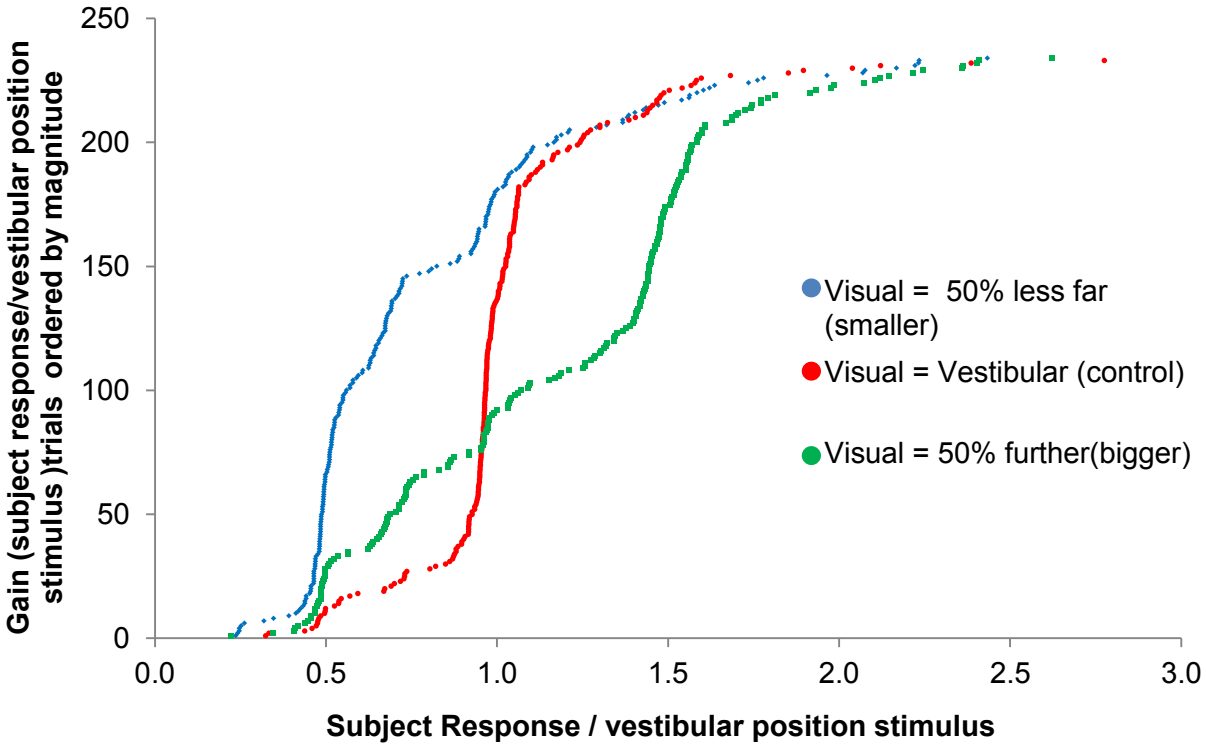

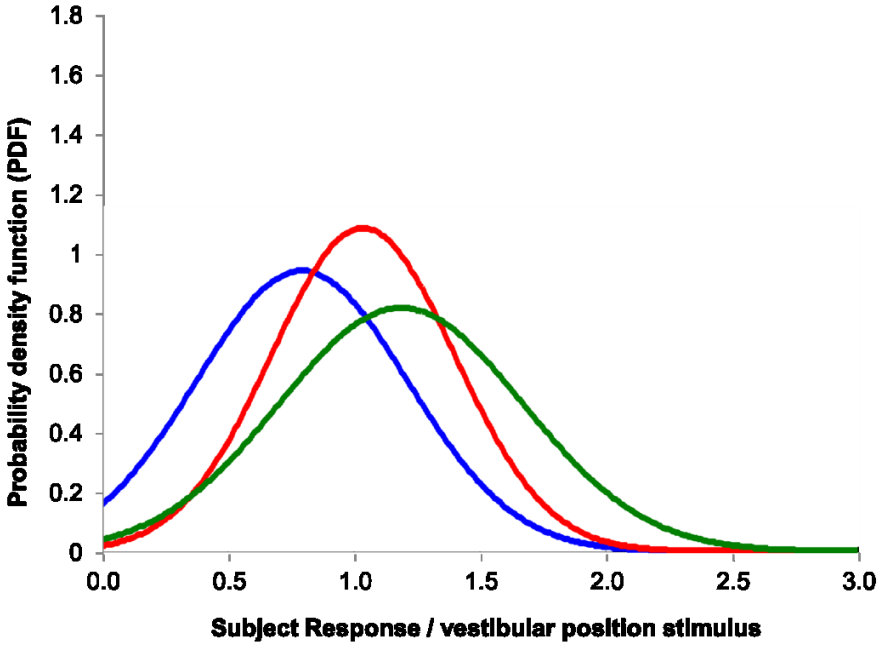

Fig 3.22. POSITION EXPERIMENT: INTERMEDIARY VISUAL FEEDBACK CONDITION (subjects report '3' on visual saliency scale [1-5]). 13 subjects. Panel A. Gain of subject position response/vestibular stimulus vs. trial no. ordered by magnitude of Gain of subject position response/vestibular stimulus. Red graph represents control condition, Blue graph the 50% smaller condition, and Green graph the 50% bigger

condition. All 16 subject data pooled. Panel B. Probability Density Function of the Gain of subject position response/vestibular stimulus. Curves fit via MLE in Matlab. Data averaged over all 13 subjects prior to curve fitting.

Discussion

The experiments in this study set out to explore interactions of the visual and vestibular system: to elucidate how, by combining these sensory modalities, the brain forms a percept of human angular motion duration, and angular position in space. The interaction of terminal, visual landmark based feedback with online vestibular feedback (from passive whole body rotation) was used to probe how visual landmark feedback updates vestibular encoding to provide estimates of duration of rotation or angular position. Visuo-vestibular mismatch (VVM) was used as a tool to probe the relative contributions of either visual or vestibular sensory modalities. Biased subliminal presentation of visual landmarks was shown to bias duration estimates of angular rotation (*see fig 3.17a*), but not estimates of angular position (*see fig 3.19*). Biased intermediary-salience presentation of visual landmarks biased position estimates of angular rotation in yaw (*see fig 3.20*) to a greater degree than with subliminal visual feedback.

Duration estimate VVM experiment

The duration estimate VVM experiment succeeded in confirming the hypothesis that differential effects between outbound and inbound duration estimates in VVM are attributable to conscious perception of an unexpected visual stimulus. The experiments previously conducted by Dr. B. Seemungal are suggestive of such effects during supraliminal visual feedback conditions. In that study, the differential

effects take the form of markedly increased duration estimates for the perturbed visual feedback conditions in outbound, relative to inbound rotation data. The inbound data conforms to what would be expected if duration of rotation estimates were biased toward the perturbed visual feedback conditions presented (*see fig. 3.1.*). The current study shows that by honing the visual feedback to subliminal levels of perception (with visual masking), these differential effects disappear from outbound duration estimates for the perturbed visual feedback condition. Repeated measures ANOVA show that in the current study, there is also no interaction between outbound (*fig. 3.17a*) and inbound (*fig.3.17b*) duration estimates [$F(1,16)=0.3$, $P=0.60$]. Furthermore, although the outbound estimates were not significant [$F(2,16)=3.2$, $P=0.06$)], the inbound estimates were significant [$F=(2,16)=6.4$, $P=0.005$]. This suggests that the outbound estimates may have tended toward significance. However, on these outbound rotations, the neuronal circuitry involved in subliminally encoding, and perhaps also integrating visual stimuli were insufficiently activated for the result to become significant. On inbound rotations, a priming effect from prior neuronal activation from outbound rotations of the same neuronal population may explain the shift to significance (Simons et al., 2003). As this data shows that subliminal visual stimuli have been successfully integrated with veridical vestibular stimuli, it must be asked what neuronal circuitry may be responsible. Masked visual feedback causing subliminal perception of visual stimuli, as used in the current study, is well established (Breitmeyer, 2007). Indeed, it has been argued that the masking of visual stimuli prevents activation of top-down attentional mechanisms of the brain, which are essential for conscious perception, but allows bottom up processing of visual information involved in unconscious perception. It has further been shown that visual distractors may also act to prevent

top-down attentional mechanisms from bringing a target stimulus to conscious awareness (Kouider and Dehaene, 2007).

Here I argue that the human hippocampal and entorhinal complex has been accessed without the involvement of top-down attentional areas of the brain being involved in visual landmark encoding. It is the hippocampal and entorhinal complex of cortex which has been shown to be responsible for the integration of multimodal sensory cues, including visual landmark with vestibular cues, in the formation of cognitive maps of allocentric space (O'Keefe, 1976, O'Keefe and Conway, 1978, O'Keefe and Burgess, 2005). It has also been argued that the formulation of such cognitive maps is informed not only by the current sensory information, but the recruitment of a-priori knowledge from previous experience (Rotenberg and Muller, 1997, McNaughton et al., 2006). I therefore stipulate that the training subjects performed prior to the main VVM tasks may constitute this type of a-priori knowledge. The training involved subject rotation to all positions of the picture curtain used under full illumination. Subjects haptically reported estimates of their angular position and motion duration. Hence, associations between congruent vestibular stimuli and visual landmark stimuli should have already been present in the hippocampal and entorhinal complex prior to the main VVM tasks. There could be an interaction in this area between top-down a-priori knowledge, bottom-up supraliminal vestibular information, and bottom-up subliminal visual landmark information. It is reasonable to assume that if a memory of the picture curtain is already held in the brain, far less must be encoded from the subliminal visual landmark information during the task, than if it had not. Thus it may be the training on the picture curtain that allows subliminal visual encoding.

As this relates to the elicitation of an appropriate estimate of duration of rotation by the subjects, it may be that neural integrators in the hippocampal and entorhinal complex used in path integration (Glasauer et al., 2002, Tcheang et al., 2011) are accessible by perceptual decision making areas of the brain, such as may be found in prefrontal cortex. For example it has been shown with fMRI of the macaque brain, that myriad brain areas are involved in the planning and decision making involved in choosing which of two routes to take through a given environment. Activity in prefrontal cortex (PFC) and posterior parietal cortex (PPC) were associated with decision making elements of the task, whilst activity in the parahippocampal gyrus was shown to be strongly associated with remembering the visual scene (Viard et al., 2011). It may be that in my study, the subliminal visual feedback feeds forward from visual cortex to hippocampal and entorhinal complex (which updates the spatial maps therein) and on to the body position and external object integration area, posterior parietal cortex (PPC); and the decision making (and working memory) centre, dorsolateral prefrontal cortex (PFC). However, critically without 'conscious' perception by attentional areas of the brain, which may not be activated due to the weak subliminal signal and additionally distraction by attention being paid to encoding the supraliminal vestibular cue which forms the primary sensory input in this task (Kouider and Dehaene, 2007).

Specifically regarding the neural substrate of subject estimates of duration, it can be assumed that the measure of duration perceived is a function of path integration performed in the hippocampal and entorhinal complex. It follows that the path

integration is of the vestibular angular velocity signal taking place over an analogue of time in a known spatial reference frame (Samsonovich and McNaughton, 1997), i.e., a 'continuous attractor network'. A continuous attractor network is the standard neuronal network approach to model networks which have memory and represent continuous spaces (Stringer et al., 2005), and it has been shown that even in the absence of allocentric (landmark) visual cues, idiothetic (on-line) cues such as vestibular cues are able to update activity of neuronal firing in one dimension, as is the case for head direction cells (Skaggs et al., 1995, Redish et al., 1996, Zhang, 1996, Sharp et al., 2001, Hahnloser, 2003) and two-dimensions as is the case for place cells (Samsonovich and McNaughton, 1997, Redish and Touretzky, 1998, Redish, 1999, Tsodyks, 1999). The hypothetical continuous attractor network described herein would receive prior calibration by the allocentric spatial map encoded during training on the picture curtain (*see fig 3.11*). It is well known how neuronal properties of an array of head direction cells in the rat may globally change their alignment given an allocentric visual stimulus which is incongruent with their expected head orientation. For example, in the case of the rat being inserted into a known environment, if this array has drifted since the last time the rat was present, it will promptly re-align itself with known visual landmarks (Taube et al., 1990, Taube, 1998, Valerio and Taube, 2012). In the context of a continuous attractor network, a duration estimate may be a function of online vestibular (velocity) input and a-priori veridical visual landmark (position) input (where distance/velocity = time, *see Eq. 1*.); the estimate may be held in the network until it is updated with non-veridical visual landmark input. If so, the estimate could be updated and either dilated or constricted dependent upon whether the landmark appeared further, or less far, relative to the prior veridical visual landmark input. A critical question to ask about the current

model is where does comparison and re-weighting of the allocentric (visual) and egocentric (vestibular) sensory cues take place? In the introduction to this chapter I discussed the concept of neural integrators, and the scope for perceptual neural integrators in the brain. It seems highly unlikely that reweighting of sensory cues according to their reliability takes place in decision making areas, as I assume integration of sensory cues is continuous and not amenable to discrete computation. It is more likely to occur in the hippocampal & entorhinal complex as a function of a continuous attractor network. To start breaking the problem down, variance in vestibular input can readily be explained as a neuro-mechanical phenomena in transducing (mechanical) and incrementally integrating a (neuronal) vestibular velocity signal in the vestibular cortex (analogue of monkey parieto-insular vestibular cortex [PIVC]). This does not involve object recognition as the velocity signal is idiothetic and not predicated on external, allocentric cues. However, the converse is true of the visual landmark position cue. I assume variance in this cue is based on the visual saliency of external discrete cues, requiring object recognition which partly occur in the hippocampus (Broadbent et al., 2004), but also require processing in visual and associated areas of cortex (Zhaoping and Guyader, 2007). I do not believe the answers to the questions posed in this section are readily deducible given our current, limited knowledge of the neural substrate underlying human navigation, such as the hippocampal and entorhinal complex. How navigation is orchestrated between the known heading direction, place, boundary and grid cells, and neural components which may remain unknown, is still not understood. What has been learned would often not have been predicted, such as the uniform firing of grid cells (triangular grid), that is based on an internal framework for computation not

dependent on regularity (or the lack thereof) in the external environment (Moser et al., 2008).

Position estimate VVM experiment

The objective of the current position estimate experiment differs to that described for the duration estimate experiment. In the context of a prior supraliminal, position estimate experiment (conducted by B. Seemungal, *see fig. 3.23*), the current study set out to establish the efficacy of visual masking for degrading the terminal (landmark) visual feedback signal for position estimation. The objective being to avoid visual capture (Pavani et al., 2000) and allow the brain to integrate the terminal (landmark) visual signal with (online) vestibular feedback. The experiment showed that visual capture exerts such a strong influence that subjects will always override their veridical vestibular sensation and indicate their position accurately according to the visual landmark (picture curtain) presented. It is clear that with a supraliminal duration estimate there is more scope for error and non-visual bias than with a supraliminal position estimate on an otherwise identical VVM experiment. This may be due to differential neuronal computation required to implicitly estimate duration as compared to that necessary for explicit estimation of position. This could be partially dependent on how the hippocampal and entorhinal complex processes and communicates information to perceptual areas of the brain (Solstad et al., 2008, Moser et al., 2008). Indeed a dearth of studies collectively suggest that the hippocampus and entorhinal complex are at least partially responsible for object recognition, definitely responsible for spatial recognition, with the remainder of object recognition substrate contained within cortex (Hammond et al., 2004, Broadbent et al., 2004).

Thus, in keeping with the objective of preventing visual capture with estimates of position in the current study, two position estimation VVM experiments were conducted. The first using subliminal, terminal visual feedback (subjective saliency scale level 1, *see fig. 3.21.*) and the second an intermediary level of visual feedback (subjective saliency scale level 3, *see fig. 3.22.*). The objective was achieved in both the subliminal visual feedback and intermediary visual feedback VVM experiments. The intermediary visual feedback experiment does indeed give a bias in position estimates clearly demarked between the estimates shown by subliminal visual feedback and fully supraliminal visual feedback. The comparative data is illustrated in figure 3.26. and shows that increased visual feedback correlates with a divergence of perturbed VVM conditions relative to a comparatively constant control VVM condition.

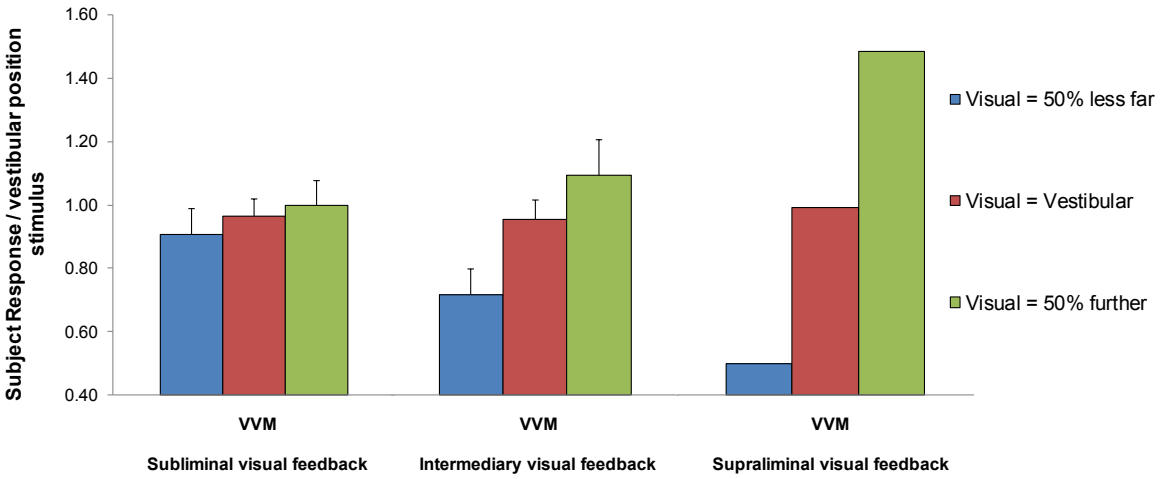

Figure 3.23. Comparison of subject position estimate responses by VVM condition across all visual saliency conditions tested. Error bars are Standard Error of the Mean (SEM), N.B. overlapping SEM bars do not directly relate to statistical significance in paired t-tests and rANOVA, as the data are matched in such analyses. N.B. Supraliminal visual feedback data was collected previously by BM Seemungal.

For the perturbed VVM conditions, an instance where the gain of position responses is 1 would be indicative of where subjects accurately encoded their veridical vestibular feedback and completely ignored visual feedback. Interestingly, it can be observed that in the subliminal visual feedback experiment, perturbed VVM condition gain responses most closely tend to a value of 1, with small non-significant biases (Gain of response ~ 1) toward visual feedback indications of angular position (Repeated Measures ANOVA [$F(2,16)=1.7$, $P=0.2$]). Conversely, in the supraliminal visual feedback experiment, perturbed VVM condition responses agreed precisely with visual feedback indications of subjects' angular position (Note the lack of SEM error bars on this graph). Hence for the perturbed VVM condition where visual feedback indicated subjects had erroneously travelled further (50% bigger condition) the gain of position response was 1.5 and for the opposite VVM perturbation (50% smaller condition) the gain of position response was 0.5. However, for intermediary visual feedback, the average gain for these responses was 1.2 and 0.8 respectively. If these gain response values are plotted against the subjective values (verbal scale of 1-5) used to describe the associated saliency of visual feedback, a near linear relationship is observed. As these correlations consist of only the median and end points of the psychophysical scale used, they may overlie psychometric functions which describe absolute sensory thresholds to the perception of the visual landmark feedback. For example figure 3.24. illustrates how subject responses for the perturbed VVM conditions deviate from that of the control condition with changes in saliency of visual feedback. The responses might overlay psychometric functions starting at chance level for perceiving the picture curtain when the visual feedback is subliminal (saliency level 1), to full visual capture of the picture curtain with complete supraliminal visual feedback (saliency level 5).

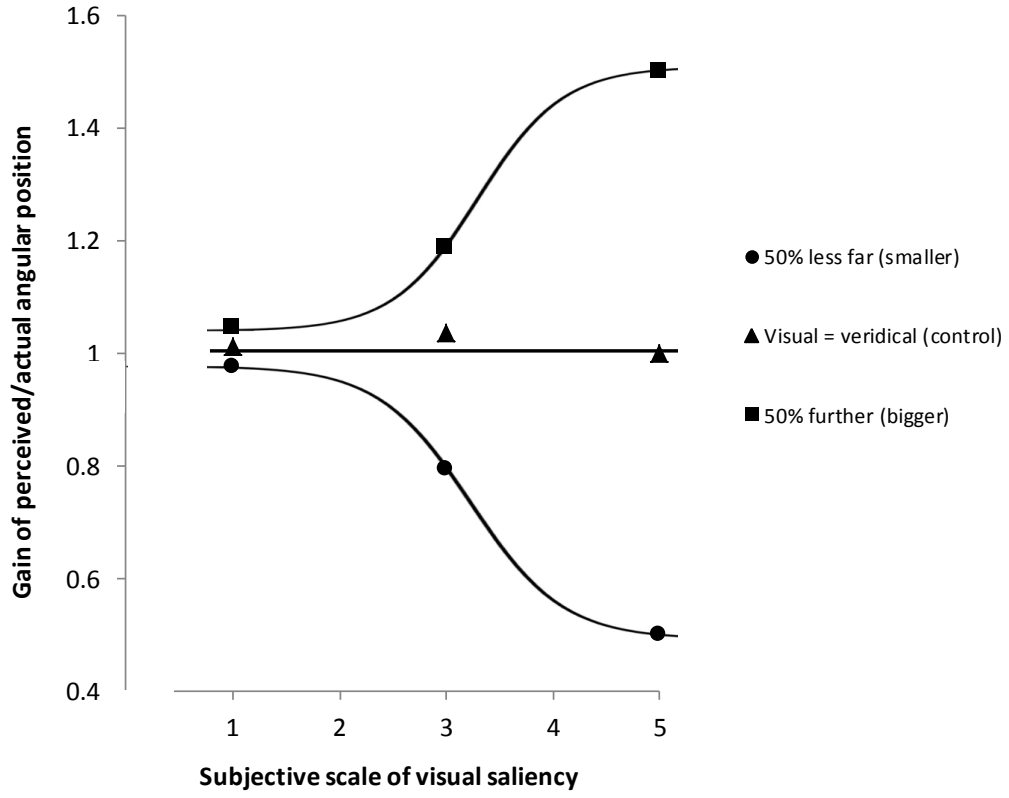

Figure. 3.24. CORRELATIONS OF SUBJECTIVE SCALE OF VISUAL SALIENCY AGAINST GAIN OF SUBJECT RESPONSE ESTIMATE/ VESTIBULAR POSITION STIMULUS. Graphs shown for the 'smaller' , 'control' and 'bigger' conditions from each position estimate VVM experiment. Sigmoid functions fits to the data points of the perturbed VVM conditions in concordance with psychometric functions. Linear fit to the data points of the control condition.

Analogue vs. Binary responses

A drawback of the current VVM experiments was the analogue nature of the response data used to maintain consistency with the prior supraliminal VVM experiments conducted (*see fig. 3.1. & 3.23*). To exploit the power of modern psychometric techniques, two alternative/interval (2AFC/2IFC) forced choice methods are far more powerful. Critically, they do not incur noise from the motor

system, and are widely used and tested analytically (Bogacz et al., 2006). Despite this drawback, the analogue duration estimate data approximates well to a normal distribution (*see fig 3.18.*) Indeed, the comparison of the position estimation experiments were amenable to Maximum Likelihood Estimation (MLE) (performed in MATLAB, The Mathsworks Inc.) to obtain estimates of mean (μ) and variance (σ) for the subliminal, and intermediary visual feedback conditions. This allowed representation of the data in the form of probability density functions (PDFs) illustrated in Panel B of figure 3.21. and Panel B. of figure 3.22, respectively. However, in these cases of position estimate, it is clear that in the perturbed VVM conditions, some erroneous transpositions of encoding the 'bigger' condition as 'smaller' and vice versa have occurred, corrupting the unimodality of a normal distribution. Panel A of figure 3.21. shows frequency-distribution data for the subliminal position experiment. The control data fits a cumulative Gaussian consistent with a unimodal, normal distribution. The perturbed conditions data vary in their slope about the mean (μ), and display signs of skew and increased variance relative to control. Panel A of figure 3.22. shows frequency-distribution data for the intermediary feedback position experiment. Here again, the control data model a normal distribution, the 'smaller' condition data model an offset normal distribution with a larger variance(σ) than control. Critically, however, the graph of the 'bigger' condition crosses that of the 'control', with increased variance (σ) relative to control, and is suggestive of a bimodal distribution. A possible explanation for this is that the brain has difficulty integrating a visual estimate that it believes is significantly 'further' than the vestibular estimate, as compared to a visual estimate that is 'less far' or indeed the same. Such 'further' visual estimates may be evaluated as non-sensical. Ecologically speaking, a position estimate path integrated by means of the vestibular

system may be underestimated due to an inefficiency to integrate the velocity signal into a position (Glasauer et al., 2002). The converse may not be true as it is impossible for any system to operate at more than 100% efficiency. Thus the brain may have evolved to be conducive to integrating visual landmark signals that may be indicative of a position signal that not has not been fully transduced by the vestibular system.

Probability density functions (*see fig. 3.21 & 3.22*) illustrate an anomalous difference between the subliminal and intermediary visual feedback VVM position experiments. Namely, that with intermediary visual feedback the estimate for the control VVM condition is less precise relative to that elicited with subliminal visual feedback. This suggests that with subliminal visual feedback subjects are relying more on their veridical vestibular feedback than with intermediary visual feedback. However, with intermediary visual feedback they bias their response further toward what they see despite this signal decreasing their precision (the reciprocal of the variance of their response, thus $\frac{1}{\sigma}$). Interestingly, this result undermines what one would typically expect to observe when the brain combines the estimates of two sensory cues. In this instance, a Maximum Likelihood Estimation (MLE) integrator model (Ernst and Banks, 2002) dictates that the reciprocal of the combined-cue variance (thus the precision of the combined-cue) is simply the addition of the reciprocals of the variances of the independent cues alone. Thus by increasing the effect of a visual cue, if the brain integrated this cue in a statistically optimal fashion with a constant vestibular cue, the variance of the estimate with combined cues could only decrease.

There are a number of factors which may contribute to the disparity between this effect observed and that of an MLE integrator model. The most obvious is that the visual feedback used consists of discrete landmark cues of varying salience. Typically, the cues combined in an MLE integrator are continuous, and simply vary in magnitude across a measure. As a basic example, in the case of using optic flow as a visual cue, a cloud of uniform white dots may be presented to a subject upon a black background, with a particular uniform direction and velocity to the dots' suggesting motion. The variable to be modulated in this visual cue, in terms of magnitude, would be the velocity of the dots and thus velocity of apparent motion. This type of cue is considered egocentric as it informs the subject of their relative position to where they started. The main areas of the brain to be activated are the areas processing visual motion such as V5/MT+ and area MST (Smith et al., 2006). Conversely, by using a picture curtain for terminal visual feedback, the interaction between the visual elements on the curtain of differing size, colour, contrast and subjective meaning, are certain to engage a number of different brain areas. Those involved in object recognition (Riesenhuber and Poggio, 1999) and place, head direction and grid cells of the hippocampal and entorhinal complex may all be involved in the processing of this allocentric visual cue (Solstad et al., 2008, Moser et al., 2008) with a number of interactions (Barker and Warburton, 2011). Furthermore, as this feedback is not continuous, subjects may sometimes, erroneously use it to 'warp' their vestibular sense toward estimates of the wrong visual feedback, as all three types of visual feedback position (50% smaller, control, 50% bigger) were delivered in a randomised order. As a basic example, if the perturbed visual landmark feedback is the 50% bigger condition, and the subject erroneously perceives it as the 50% smaller condition, then this will skew the result

accordingly. In addition, seven angular positions were presented visually, for either direction of rotation, within the current VVM experiments (*see fig. 3.15.*). Hence there is an argument that a whole range of transposition errors could be made across the spectrum of what could be presented visually on the picture curtain. Over the course of the experiment and averaged across all the subjects tested, this might be considered to tend toward a form of Gaussian noise. Therefore, Gaussian noise from this source would obviously reduce the precision (the reciprocal of the variance of subject response, thus $\frac{1}{\sigma}$) of the data.

Another factor that could explain discordance of the data with an MLE integrator model is that the nature of the task in the current study may be too complex, and thus violate terms of the model. Due to its complexity, the VVM position task may necessitate conscious perception of supraliminal visual feedback, and may not be possible with the unconscious perception of subliminal feedback. Therefore, a comparison between the subliminal and supraliminal position experiments may violate the terms of the MLE integrator model, due to the difference in neuronal circuitry required at the two levels of visual feedback. For example, with a 2 alternative forced choice (2AFC) task of visual landmarks, subjects can respond better than chance to masked visual feedback. This may be partly due to the simplicity of the task involved, such as reporting the perception or not of one of only two target stimuli, or basic discrimination tasks, which one could argue are based primarily on pre-attention and bottom up processing of this visual information (Zhaoping and Guyader, 2007). It may also depend on the method of masking used. Metacontrast or 'backward' visual masking operates on the principle that the mask temporally follows the target visual stimulus. It is proposed that this type of

backward visual masking has far more of an effect on top-down feedback to visual processing areas, such as the primary visual cortex (V1), from higher brain areas influencing conscious perception, than early feed-forward information from the target, which is encoded unconsciously (Lamme and Roelfsema, 2000). Hence bottom up processing dominates the response given during backward masking and allow the processing of simpler tasks. However, in the current study, the task is not a forced choice, and the subject able to make only an analogue representation of where they feel they have rotated to in space relative to what they ostensibly believe to be an always stationary picture curtain. This greatly increased level of choice and decision making could most certainly be dependent on top down processing to delineate features presented and organise an appropriate response. Thus in this case, subliminal visual feedback may not provide the higher order level of information at the pre-cognitive, feed-forward levels of visual processing to complete the position estimation task demanded and thus make subliminal perception unviable. However, it has previously been described in this chapter how subliminal encoding was achieved in the duration estimation VVM experiment. The significant effect being present in responses to visual landmark presentation after the inbound rotations of trials ($F(2,16)=6.4$, $P=0.005$). It may then be asked why duration estimates may have been encoded subliminally, whilst position estimates were not. I have already argued that the visual feedback for the VVM position estimation task may be too complex for subliminal encoding, and that this may be on the basis that top down feedback is required to process numerable complex visual stimuli from the picture curtain. This may be why supraliminal intermediary feedback shows a significant result for modulation of position estimation via visual feedback, as the top down feedback is not prevented by backward visual masking in this case. However, the

subliminal duration estimation experiment uses the same picture curtain, with the same number of presentations of each point of the picture curtain. For the result of the subliminal duration estimate experiment to be significant for responses to the inbound rotation it may be that it is not top down processing, but caused by a priming effect from presentation of the masked picture curtain on outbound rotations. By the very nature of the VVM position estimation experiment, data can only be collected for outbound rotations, as subjects know the position to which they will return. Both the data for the subliminal duration estimation experiment and position estimation experiment show that for responses to outbound rotation, there are trends in the data which suggest encoding of the picture curtain is taking place, yet neither yields a significant effect: Outbound duration ($F(2,16)=3.2$, $P=0.06$); Outbound position ($F(2,16)=1.7$, $P=0.2$). Hence, the significant effect in the subliminal duration experiment for inbound responses may simply be due to two iterations of bottom up processing of the picture curtain.

All aspects of the subliminal duration estimation and position estimation experiments were the same apart from the responses given and type of response recorded. With the duration estimation experiment a duration response was given, but then followed with a position estimation response (*see fig.3.13.*), even though it was the duration estimation response only that was recorded. The position estimation response was included as it was believed that as the duration estimate engages neuronal circuits involved in path integration, an allocentric visual position estimate may also be required to calibrate an otherwise open loop vestibular signal (Glasauer et al., 2002, Metcalfe and Gresty, 1992, Mergner et al., 1996, Seemungal et al., 2007) hence if subjects know they will have to give a position estimate as well as a duration

estimate, this might modulate the way spatial information is encoded during the actual rotation.

To further the investigations of the current study it would be necessary to conduct experiments in which visual landmark and vestibular estimates for duration of rotation and angular position are obtained separately, and then in combination in VVM experiments. This would be required to verify the relative contributions of each sensory modality by using a maximum likelihood integrator (Ernst and Banks, 2002). An example of how two sensory estimates can be combined in such a fashion can be found in Chapter 1, section 1.3. Furthermore, to perform accurate psychometric fits, the data must be obtained with an experiment of two interval forced choice design (2IFC), by the method of constant stimuli (Ehrenstein and Ehrenstein, 1999). According to the method of constant stimuli, relative to the current design of VVM experiment, these would differ in so far as the data would be binary rather than analogue. Specific angular positions of the chair (vestibular) and picture curtain (visual landmark) would have to be chosen as datum positions. About these datums a range of test positions would be set at equidistant intervals either side and compared relative to the datum position with two interval forced choice responses to a specific question. To probe perception of duration of rotation this question could be 'which rotation took longer?', to which subjects could respond 'first' or 'second'. To probe perception of position the question could be asked 'which rotation did you travel further?'. Over a number of trials comparing datum with test positions, probabilities of responding to a question with the test position over the datum position can be graphically plot over the range of test positions generated for each datum position. Psychometric functions can then be fit to this data and measures of

the mean (μ) and variance (σ) obtained for use in a maximum likelihood integrator to determine whether these sensory cues are combined in a statistically optimal fashion (Ernst and Banks, 2002).

.

Conclusion

This study suggests that it is possible for masked visual feedback to be encoded subliminally by the brain, when presented before and after passive rotation in the dark. The study suggests that visuo-vestibular mismatch perceived consciously has a dilative effect on subject's perception of time, which is absent when the same sensory mismatch is perceived subliminally. The study suggests that to derive a percept of duration of motion or angular position, the brain combines allocentric visual landmark cues with ego centric vestibular cues with weightings that are dependent upon the reliability of each cue. However, further studies will need to be conducted to clarify whether this integration is performed in a near statistically optimal fashion. These studies would take the form of two interval forced choice (2IFC) tasks using the method of constant stimuli on measures of vestibular sensed angular velocity and visually sensed landmark position with and without visual masking.

Chapter 4.

Probing Visual Motion Perception with TMS (transcranial magnetic stimulation)

Summary

I found that the strength of TMS intensity used to probe visual cortex (visual motion area V5/MT+) had a significant effect upon the measurements and changes between measurements recorded (either excitatory or inhibitory) and is an important factor in understanding how to interpret changes in cortical excitability in response to a visual motion stimulus. However, I also probed different visual motion coherence stimuli using this measurement technique, and found no statistical difference between coherence groups. The results suggests that the sample sizes used were not large enough to effectively employ the sophisticated modelling algorithms used to analyse the data.

Introduction

Our response to visual motion is critical to our day to day survival. For example, when crossing the street, we may be aware of the motion of a car coming towards us without having to register very much about what it looks like. Our prior experience of crossing the street may suggest to us that this moving object is a vehicle, but we do not necessarily have to encode this attribute to be able to take the appropriate action

of getting out of the way. It can simply be the motion of the image of the car across the retina that provides the cue to move, not the recognition of its form. Hence, the brain's perception of visual motion does not necessitate an understanding of what it is that is actually moving, and this underlies the cortical pathways that encode motion (Ungerleider and Haxby, 1994, Braddick et al., 2000).

As described in Chapter 1, the function of visual area V5/MT+ is to process visual motion. A common stimulus used to elicit activity in V5/MT+ is visual dot motion (consisting a number of round or sometimes square dots moving with a particular arrangement of trajectories and usually presented in two dimensions on a computer monitor)(Guzman-Lopez et al., 2011a).

Many studies have investigated how V5/MT+ responds to both coherent (dots all move in the same direction) and random visual dot motion. The results have been discordant. Studies involving single electrode recordings in monkey suggest that directionally selective neurons in V5/MT+ are driven maximally by coherent visual dot motion as opposed to conditions of mixed direction (random) dot motion (Allman et al., 1990, Snowden et al., 1991). Conversely, a Positron Emission Tomography (PET) study in humans (McKeefry et al., 1997) suggests that it is incoherent (random) visual motion that activates human visual area V5/MT+ more than coherent motion. To further confound matters, fMRI studies (Braddick et al., 1998, Braddick et al., 2000, Smith et al., 2006) and a Magnetoencephalography (MEG) study (Lam et al., 2000) suggest no net difference between the effects of coherent and incoherent visual motion.

A differential activation of V5/MT+ is conceptually simple to understand, whether it be coherent or random visual motion that provides maximal activation of neurons – one modality of visual motion provides a stronger stimulus than the other. However, in the studies where coherent and random visual motion do not elicit any differential activation, a less parsimonious explanation is required. One theory posited by Lam et al. (2000), is that coherent motion could highly activate fewer dedicated, direction specific neurones (tuned to the direction of the coherent motion), whereas random motion could activate a much larger population of direction specific neurones, but to a lesser degree. With either mode of visual motion a comparable net effect in neuronal activation may be created.

It is clear that further study is required to elucidate the fundamental mechanisms driving V5/MT+ response to coherent vs. random motion, and that this may require a new approach.

TMS (transcranial magnetic stimulation) is a type of non-invasive brain stimulation used over human, visual brain areas to modulate cortical activity. It is an approach that has been developed over the past two decades (Kobayashi and Pascual-Leone, 2003). TMS delivers a magnetic pulse through the skull and is thought to effectively penetrate and activate superficial layers of cortex (Wagner et al., 2009). Some studies have involved the use of TMS over visual motion area V5/MT+ as an intervention (a high frequency form called 'repetitive' rTMS) and assess its effect on a visual task (Beckers and Homberg, 1992, Laycock et al., 2009, Tadin et al., 2011). Whilst this approach has its merits, the actual performance of the task engenders ambiguity regarding the primary sites of cortical activity. Conversely, other studies

utilise the transient visual percept evoked by TMS (known as a phosphene) as a direct measure of V5/MT+ cortical excitability (Silvanto et al., 2005a, Silvanto et al., 2005b, Taylor et al., 2010, Kammer and Baumann, 2010) of which a proportion use TMS in combination with visual dot motion stimuli either presented as coherent dot motion (Silvanto et al., 2005b) or random dot motion (Guzman-Lopez et al., 2011a). Guzman-Lopez et al. (2011b) utilised a range of dot motion coherences using data from this thesis. It is with consideration of this last study that the argument for investigation of visual motion coherences between the coherent and random states is made. The argument is predicated on the assumption that intermediary levels of dot motion coherence could not elicit the same net neuronal activation as either the coherent or random states. There should be a continuous transition from high activation of few direction specific neurons, to low activation of many direction specific neurons. Consequently, the visual dot motion parameters chosen for the current study probed an exponential scale of dot motion coherence extending from a minimal coherence level where subjects perceived the dot motion as random (from a pilot study this was found to be with a σ= 128° from mean dot trajectory) to a maximal coherence level where subjects perceived coherent motion (σ= 1° from mean dot motion trajectory).

The current study also investigated the effect of intensity of TMS used as a mensuration tool of cortical excitability. Traditionally, TMS is delivered at a subject's 50% threshold to phosphene perception, also known as the absolute threshold to a sensory stimulus (Bouman, 1955). By honing the objective output intensity of the TMS stimulator to a subjective measure of phosphene perception, this relative intensity of TMS is acquired and variability in response due to intrasubject and

intersubject factors may be circumvented (Roy Choudhury et al., 2011). However it is unknown how the relative intensity of TMS used affects the modulation of cortex by an intervening stimulus. For example, a TMS study (Seemungal et al., 2012) used the probability of observing V5/MT+ phosphenes evoked at a 50% threshold intensity as a measure of cortical excitability before and after a vestibular stimulus. The authors showed that the probability of observing a V5/MT+ phosphene is reduced after the intervention of the vestibular stimulus (a caloric irrigation). This reduction is interpreted as V5/MT+ becoming less excitable and the vestibular stimulus producing an inhibitory effect.

Here we must ask, how might the relative intensity of TMS used as a probe of cortical excitation influence the outcome? If a relative intensity of TMS at a 70% threshold to phosphene perception had been used in lieu of a 50% threshold, how might this have modulated the effect of the vestibular stimulus? Should the authors have expected the same magnitude of inhibition? To answer these questions a similar mensuration technique was used in the current study to measure changes in cortical excitability before and after a visual stimulus (moving dot kinematogram). Critically, the experiment was repeated at a range of relative TMS intensities, at, above and below the 50% threshold, to afford a comprehensive picture of the relationship between i) intensity of objective TMS output, ii) subjective phosphene perception, iii) cortical modulation elicited by an intervening stimulus.

In summary, the aim of the current study was two-fold: i) to explore the effect of visual dot motion of a range of motion coherences upon the cortical excitability of

V5/MT+ ii) to explore the influence of TMS intensity upon changes in V5/MT+ at a range of TMS stimulation levels as measured with subject reported phosphenes.

Methods

Subjects and apparatus

6 healthy subjects were recruited (2 male) mean age 29. Range (23-38). All subjects were right handed. 2 subjects were authors and all 6 of the subjects had experienced phosphenes before.

Subjects were seated comfortably in a barber's chair and rested their face on an adjustable chinrest with forehead support. TMS stimulation was provided by a Magventure Mag-Pro (Model X-100) device using a figure of 8 coil (MC B70). The coil was mounted on a poseable, lockable arm rigidly affixed to the rear of the barber's chair. The waveform of the pulses delivered was biphasic. To mitigate cumulative thermic induction at the scalp from prolonged TMS elicitation, and ensure subject comfort, a cooling fan (39.5 cubic feet per minute) was mounted above the coil.

Moving dot kinematograms (MDK) were presented on a 17 inch CRT monitor (resolution 800 x 640 pixels) viewed from a distance of 28.5 cm (subtending 62° horizontal field of view). Each moving dot kinematogram consisted 100 white dots moving across a black background which filled the whole CRT display. Each moving dot was circular with a radius of 5 pixels and subtended a visual angle of 0.38°. The dots were randomly assigned a start position on the screen and each dot was randomly assigned a linear motion direction drawn from a Gaussian distribution with

a mean dot motion trajectory of either 45° (right) or 135° (left) and a standard deviation (σ) of either σ =1°, σ =32°, σ = 64°. σ =128° . Thus there were a total of eight moving dot kinematogram conditions which were presented to subjects in a randomised order. At the centre of the of the display was a static fixation circle (radius 15 pixels, subtending a visual angle of 1.14°).

Phosphene observation took place in the dark. Wide angle occluding goggles were worn by subjects to prevent exposure to any residual low level ambient illumination. They were easily removed from line of sight for viewing the random dot kinematograms.

Each run of the last 15 trials (out of 20) of the experiment at a particular TMS intensity was considered a block. Each session of testing consisted four blocks, pseudo randomised from the entire set of block conditions. Only the last 15 trials of each block were used, as it was shown in the RANOVA analyses that a differential effect between areas V1 and V5/MT+ was noted in the first 5 trial (30 second) epoch of testing. As I simply want to assess the effect of TMS intensity upon the probability of observing a phosphene I removed the first epoch of data from analysis.

Experimental Procedure

Phosphene Localisation

Phosphene perception had to fulfil a series of criteria. Subjects had to be able to perceive the phosphenes with desk lamp lighting as well as in the dark. The phosphenes also had to be observable with eyes open and eyes closed (Kammer and Baumann, 2010). All subjects were trained to experience phosphenes by first stimulating the area V1 approximately 2cm above the inion. This was with the aim of

eliciting a strong percept of a coloured phosphene, appearing across the mid-line of the visual field (Silvanto et al., 2007). To probe V5/MT+ the coil was then moved laterally about the occipital area in approximately 5mm increments until phosphenes were observed firmly in the right visual field and could be differentiated from the phosphenes previously observed with V1 stimulation, by i) presence of motion ii) lack of colour. The TMS coil was oriented with the handle horizontal and directed left of the coil, lateral to the location being stimulated (Meyer et al., 1991) (*see fig. 4.1.*).

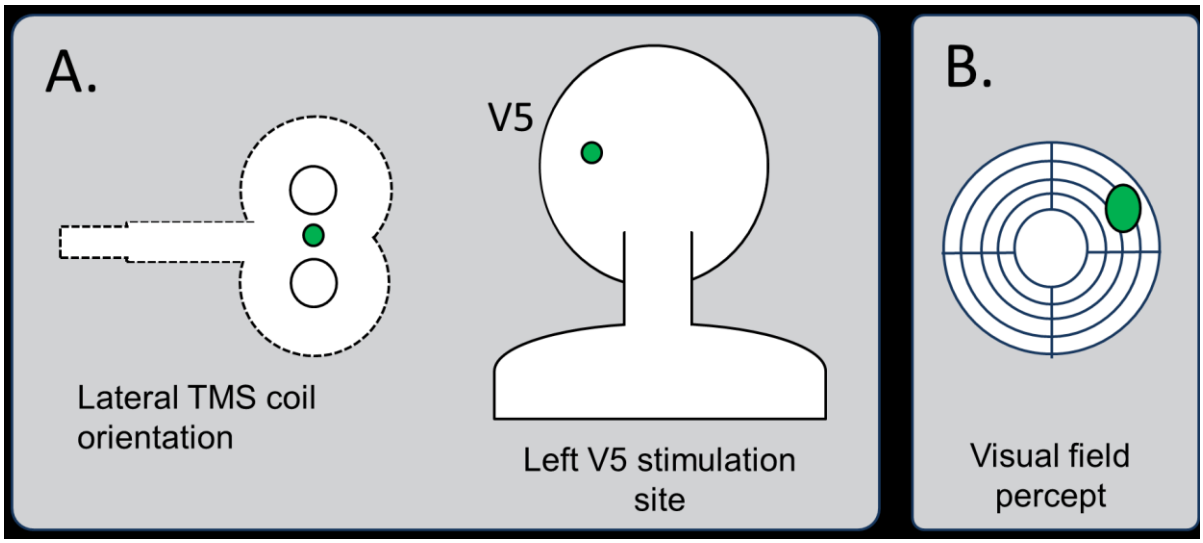

Figure 4.1. TMS COIL LOCALISATION. Panel A. Lateral orientation of TMS coil relative to rear view of subject head. Green dots illustrate required co-location of TMS coil and stimulation site at left V5/MT+. Panel B. Target representation of subject visual field. Centre of target is straight ahead, concentric circles represent eccentricity from straight ahead. Orthogonal lines demarcate quadrants of visual field. Green dot illustrates region of right visual hemifield in which phosphene appears (with left V5/MT+ stimulation) and a representation of its size. N.B. the green colour is only used for illustrative purposes as V5/MT+ phosphenes are colourless. V5/MT+ phosphenes are also characterised by movement across the hemifield.

Main Experiment

Once the phosphenes were localised, subjects were delivered a series of pulses which followed a modified binary search (MOBS) algorithm (Tyrrell and Owens, 1988). They were asked to answer 'yes' or 'no' via dual push buttons to ascertain whether they observed a phosphene with the pulse or not. Push button responses were necessary, as verbal reports could displace the TMS coil with respect to the subject's head. For every response of the subject, the TMS stimulator varied the intensity of the next TMS pulse delivered via a MOBS program. The MOBS program works with an adaptive bounds structure. Initially, bounds of the program were set at 100% (upper) and 0% (lower) of the maximum output intensity of the TMS stimulator, which elicited the first TMS pulse equidistantly between the bounds at 50% of maximum TMS output intensity. If a subject perceived a phosphene from this pulse, the program would decrease the intensity of the next TMS pulse to 25% maximum output intensity (taking 50% as the new upper bound and maintaining 0% as the lower bound). However, if the subject did not perceive a phosphene, the program would increase the intensity of the next TMS pulse to 75% (taking 50% as the new lower bound and maintaining 100% as the lower bound). Hence, the program would adapt TMS pulse intensity to the subject's successive responses and terminate at its estimate of the subject's 50% threshold to phosphene perception after five reversals of the subject's phosphene response.

As obtained with MOBS, at each subject's 50% threshold to phosphene perception a series of 20 TMS pulses was then delivered at 6 second intervals which lasted two minutes. At each pulse they reported if they observed a phosphene or not. If the series of 20 pulses elicited the ratio of 'yes' to 'no' responses required, this was

taken as the subject's 'Baseline' response, with the response count and TMS stimulator intensity of the pulses recorded. If not, a further 20 pulses were delivered at a higher or lower TMS stimulator intensity, using a staircase approach, until the required ratio was elicited. After the pulses were delivered, a description of the position and trajectory of the phosphenes was requested from the subject to check for drift of the coil (in no case was this recorded).

Experiments were conducted at four relative TMS intensities, to populate a psychometric function of TMS stimulator intensity (dependent variable) to probability of observing a phosphene (independent variable). The four relative TMS intensities were 0.5 'threshold' (~50% chance of observing a phosphene, approximate ratio of 10:10 'yes' to 'no' responses, range 8:12 and 12:8 inclusive); the 0.3 threshold (~30% chance of observing a phosphene, approximate ratio of 6:14 'yes' to 'no' responses, range 4:16 and 8:12 inclusive); 0.7 threshold (~70% chance of observing a phosphene, approximate ratio of 14:6 'yes' to 'no' responses, range 16:4 and 12:8 inclusive); 0.9 threshold (~90% chance of observing a phosphene, approximate ratio of 18:2 'yes' to 'no' responses, range 20:0 and 16:4 inclusive).

In order to obtain the 'other than 0.5 threshold or chance' levels, the 0.5 threshold (or weighted equivalent) obtained via MOBS was used as a datum bound. Dependent upon whether a lower or higher threshold level was required, a further series of 20 pulses was used to probe initially at a 6% increment of TMS maximal output below or above the datum 0.5 threshold bound value. Once the amount of acceptable phosphene responses was observed, an additional caveat was that there must be at least 2 less (or more) phosphenes observed than for the 0.5 threshold (or weighted equivalent). If the required count was not achieved the TMS output was modulated by plus or minus 2% of maximal TMS output. As with the 0.5 threshold, the 0.7

threshold was weighted, thus if 15 phosphenes were observed, then this would constitute a 0.75 threshold value for phosphene perception and included in the analysis of 0.7 threshold responses.

After the Baseline phosphene responses were elicited, subjects were presented with a visual motion discrimination task (moving dot kinematogram) for a period of 2 minutes. They were instructed that for its duration they must look toward a central, hollow fixation circle, but must also attend to the visual dot motion stimuli presented and attempt to discern whether the mean dot motion trajectory was in a direction 45˚ or at 135˚ in the frontal plane. Six seconds before the end of the kinematogram, they were requested to give a verbal two-forced choice response of their perceived mean dot motion which was recorded. For simplicity they were asked to answer 'left' for the 45˚ mean dot motion condition and 'right' for the 135 ˚ mean dot motion condition. As the kinematogram ended, there immediately followed a further series of 20 TMS pulses delivered at the same rate, and intensity as Baseline TMS for a further 2 minutes. Subject responses to these constituted the 'Post' phosphene response (see fig. 4.2.).

Upon completion a description of the position and trajectory of the phosphenes observed across Baseline and Post phosphene responses were requested from the subject. The phosphene reports of each subject for both Baseline and Post responses respectively, were converted to a probability of phosphene observation derived from the number of phosphenes observed divided by the number of TMS pulses delivered. It was in this format that analysis was performed on the acquired data.

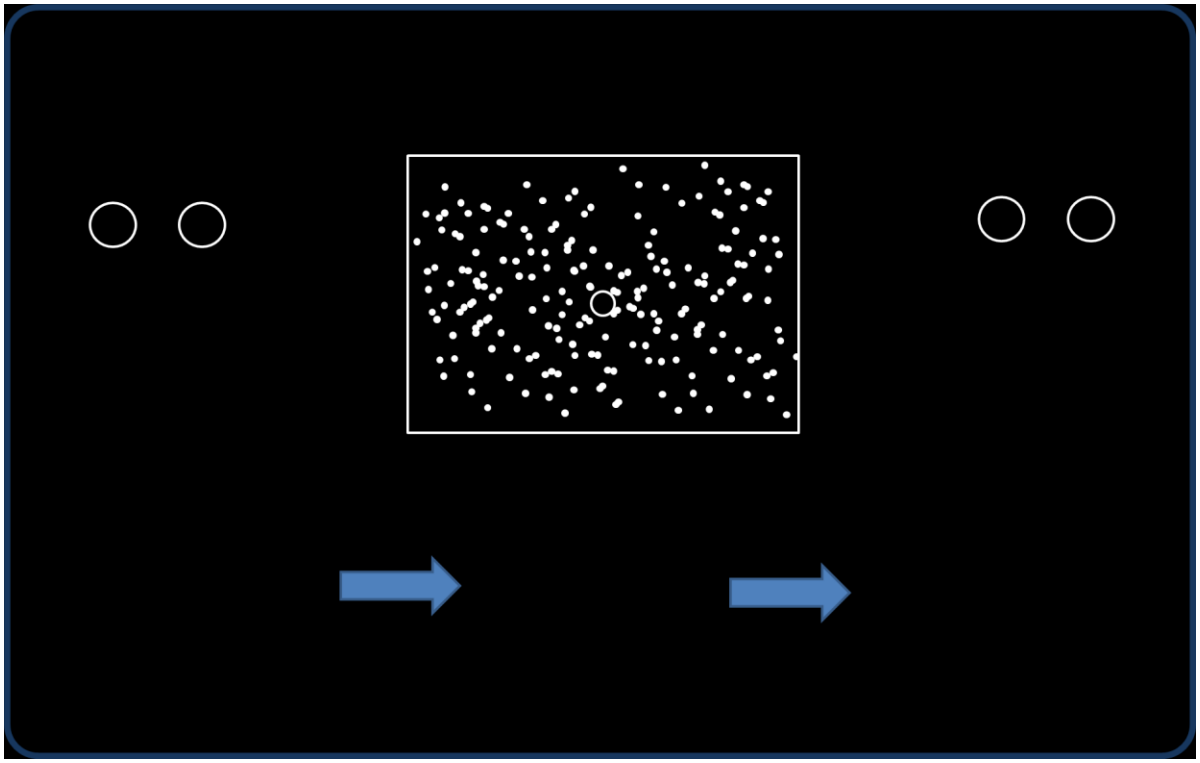

Figure. 4.2. EXEMPLAR TRIAL. 2 minutes of BASELINE TMS consisting 20 pulses at 6 second intervals; 2 minutes of Moving Dot Kinematogram presentation; 2 minutes of POST TMS consisting 20 pulses at 6 second intervals. BASELINE and POST TMS varied in like-for-like intensity at each trial (30%, 50%, 70%, 90% threshold to phosphene perception). Moving Dot Kinematogram varied in coherence at each trial (four levels at σ =1°, σ =32°, σ = 64°. σ =128° from mean dot motion trajectory). Central hollow fixation circle at centre of CRT screen of 100 moving dots.

In summary, thirty two trials were performed per subject of Baseline phosphene responses to TMS -> random dot kinematogram -> Post phosphene responses to TMS. These trials comprised of three variables: dot motion coherence presented (four levels at σ =1°, σ =32°, σ = 64°. σ =128°); relative intensity of TMS delivered (four levels at 30% subthreshold, 50% threshold, 70% suprathreshold and 90%

suprathreshold); and direction of mean dot motion trajectory (two levels at 45˚ or 135 ˚ mean dot motion).

A separate control experiment was conducted in which the intervening visual stimulus was an array of static dots of the same size and shape as the visual moving dot stimuli. Eight trials were performed per subject of Baseline phosphene responses to TMS -> static dot array -> Post phosphene responses to TMS. Two trials were performed at each relative intensity of TMS delivered.

Data Analysis

Parametric statistics were performed in SPSS (IBM Corporation).

Constrained Bootstrap modelling using Maximum likelihood Estimation was performed in Psignifit (Wichmann and Hill, 2001b) with constraints of guessing (γ) and lapse rate (λ) of subjects modelled upon a Beta(2,20) distribution (*see Chapter 1, section 1.3.*).

Results

The strength of TMS intensity used to probe visual cortex (visual motion area V5/MT+) had a significant effect upon the measurements and changes between measurements recorded (either excitatory or inhibitory). However, I also probed different visual motion coherence stimuli using this measurement technique, and found no statistical difference between coherence groups. This was with analyses of both the threshold (see fig. 4.3, then 4.5-4.9) and slope (*see fig. 4.10*) of psychometric function data. The results suggests that the sample sizes used were not large enough to effectively employ the sophisticated modelling algorithms required to analyse the psychometric functions.

rANOVA analysis of phosphene response

For each trial of the experiment post phosphene responses to visual dot motion were divided by Baseline phosphene responses to provide a gain term. These gain values were averaged across all 6 subjects and were analysed with a Repeated Measures ANOVA (rANOVA) performed in SPSS (IBM Corporation) across the four factors described in the experimental procedure. There was a significant effect of the relative TMS intensity used ($F(3,6)=6.8$, $P = 0.004$). There was no corresponding difference between coherence level conditions collapsed across intensities of TMS ($F(3,6)=3.0$, $P=0.06$). There was no effect of the direction of visual dot motion presented ($F(3,6)=4.7$, $P=0.17$). There was no interaction recorded between the relative TMS intensity used and the coherence of visual dot motion presented ($F(3,6)=1.4$, $P=0.2$)).

Psychometric function fitting to phosphene responses

The data were averaged across all 6 subjects. In the first instance, data across all motion coherence levels was assessed within the same psychometric function for Baseline and Post phosphene responses, respectively. Hence 32 data points populated each function: four relative TMS intensities; four coherence levels tested at each TMS intensity; two directions of visual dot motion tested. The psychometric functions are illustrated in figure 4.3.

As exemplars, analyses of the 'goodness of fit' to both Baseline and Post psychometric functions are illustrated in figure 4.4. The control data was then analysed in a similar fashion to the combined motion coherence data, but with only four data points per psychometric function (*see fig. 4.5.*). Analyses of each motion

coherence (eight data points per psychometric function) are shown in figures 4.6., 4.7., 4.8., 4.9. (order of σ = 1°, 32°, 64°,128°, respectively).

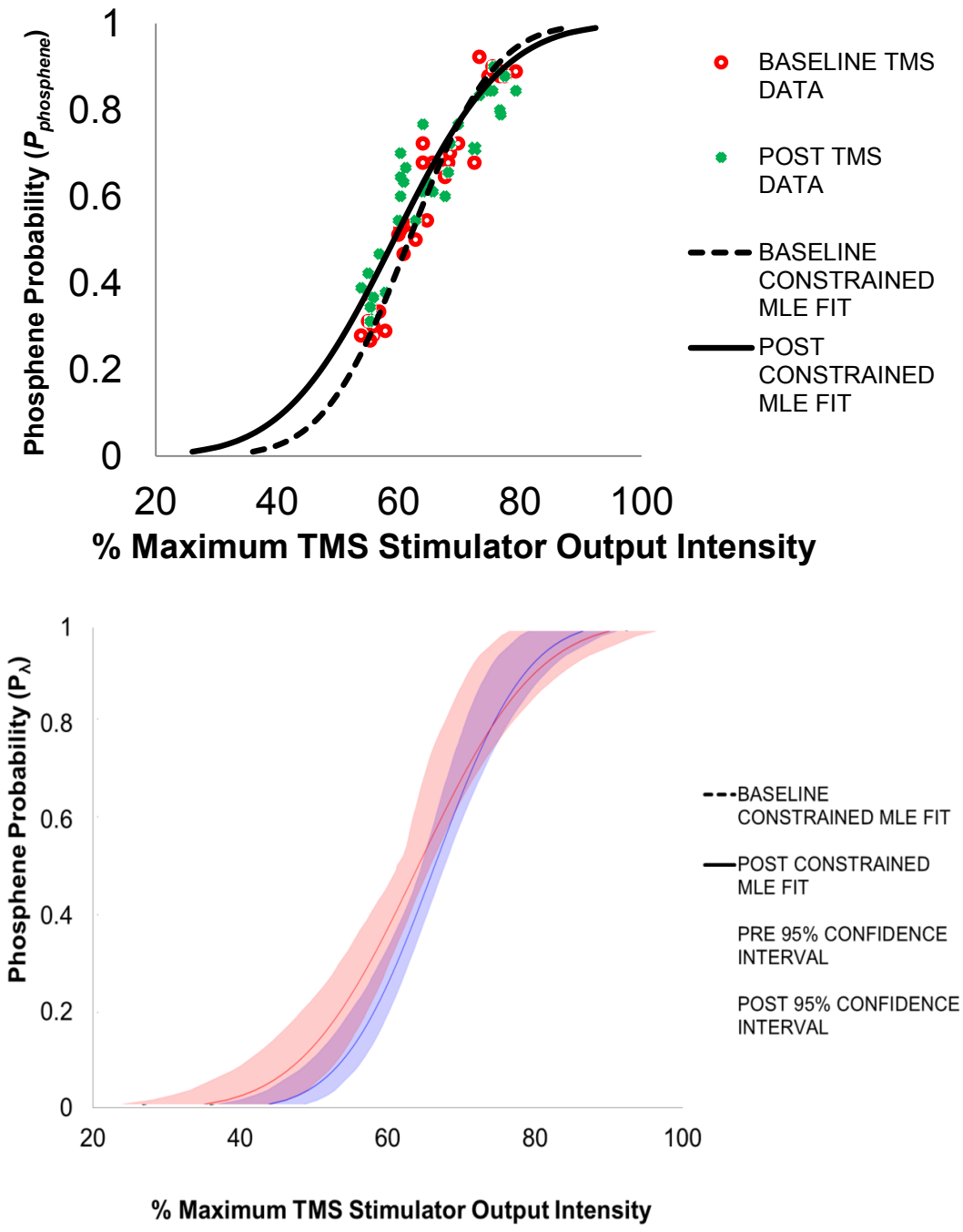

Figure. 4.3. PSYCHOMETRIC FITS TO ALL MOTION COHERENCE DATA (n=32). Panel A. Plot of Phosphene probability (*Pphosphene*) by % Maximum TMS stimulator Output Intensity. Baseline TMS data represented by red circles, Post TMS data by green crosses. Dotted sigmoid indicates constrained MLE fit to Baseline TMS data. Solid sigmoid indicates constrained MLE fit to Post TMS data. Constraints: γ = λ = beta (2,20). Panel B. Baseline TMS (Blue) and Post TMS (Red) Constrained Bootstrap MLE Fits. Shaded error areas represent 95% Confidence Intervals (CI).

Figure. 4.4. GOODNESS OF FIT ANALYSES FOR COMBINED MOTION COHERENCE CONDITION (below) Left Column: Baseline TMS bootstrapped fit. Right Column: Post bootstrapped fit.

<table>
<tr>
<td>BASELINE TMS
 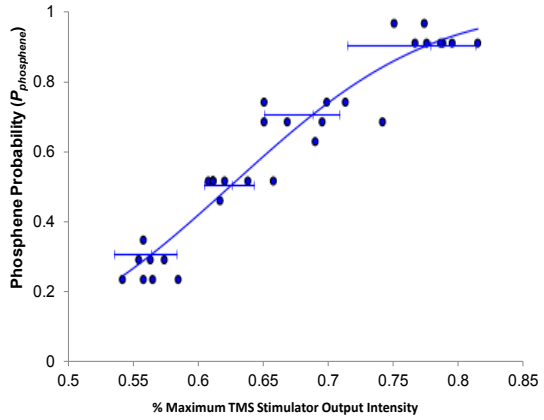
</td>
<td>POST TMS
 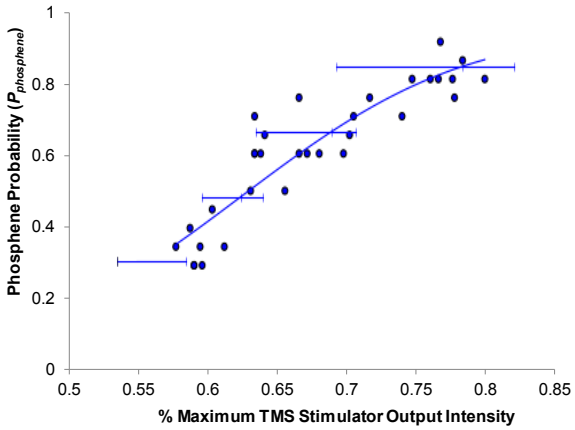
</td>
</tr>
<tr>
<td>PANEL A) Data point fit to the psychometric function. Error bars indicate 95% confidence intervals at Threshold Cuts (0.3, 0.5, 0.7, 0.9). Constrained MLE fit parameters: Sigmoid = Gaussian; core = ab; nAFC = 1 (yes/no); Deviance (D) = 11.396</td>
<td>PANEL B) Data point fit to the psychometric function. Error bars indicate 95% confidence intervals at Threshold Cuts (0.3,0.5,0.7,0.9). Constrained MLE fit parameters: Sigmoid = Gaussian; core = ab; nAFC = 1 (yes/no); Deviance (D) = 15.776</td>
</tr>
<tr>
<td>BASELINE TMS
 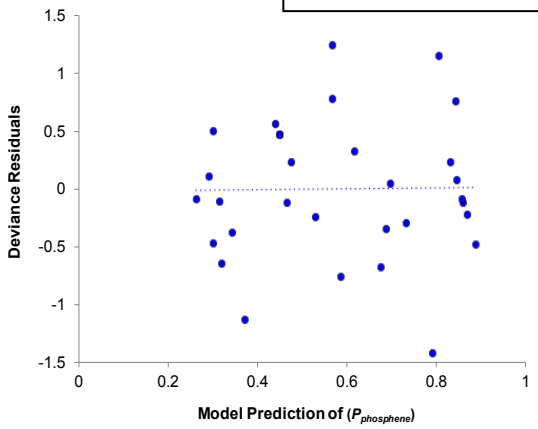
</td>
<td>POST TMS
 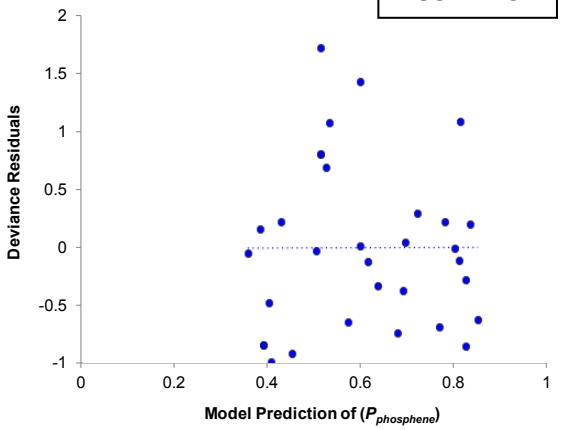
</td>
</tr>
<tr>
<td>PANEL C) Deviance residuals plotted as a function of the predicted correct response rate of the model. Dotted line is best linear fit. Numerical value of correlation is the ‘Rpd’ (Residual Prediction Deviance) = 0.014.</td>
<td>PANEL D) Deviance residuals plotted as a function of the predicted correct response rate of the model. Dotted line is best linear fit. Numerical value of correlation is the ‘Rpd’ (Residual Prediction Deviance) = 0.018.</td>
</tr>
</table>

BASELINE TMS

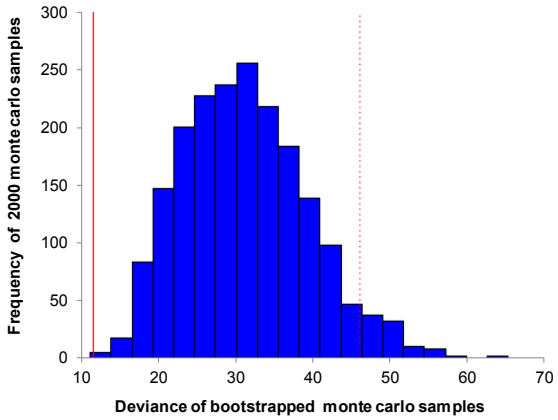

PANEL E) Histogram of sampled model deviance. Observed Deviance (D) = 11.396 indicated by solid red line. 95% confidence interval of Model Deviance (D_crit)=45.347 and indicated by dotted red line.

POST TMS

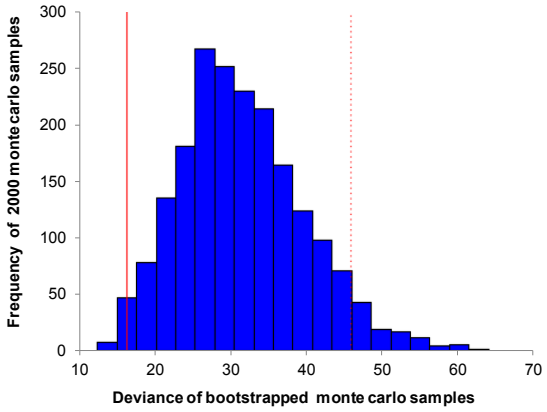

PANEL F) Histogram of sampled model deviance. Observed Deviance (D) = 15.776 indicated by solid red line. 95% confidence interval of Model Deviance (D_crit)=46.227 and indicated by dotted red line.

BASELINE TMS

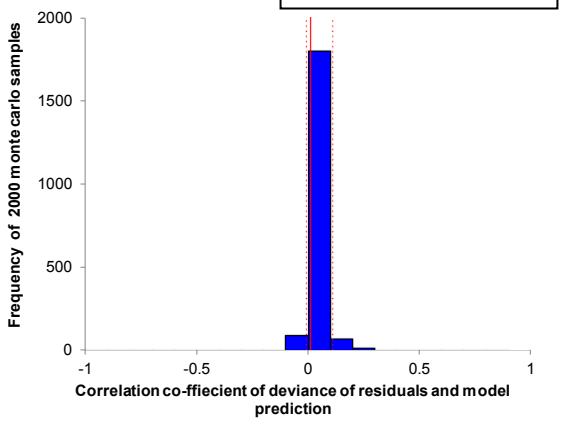

PANEL G) Histogram of bootstrapped correlation coefficients for the correlation between deviance residuals and predicted correct response rate of the model. Dotted lines demarcate 95% intervals of the sampled correlation coefficients, solid line marks the observed correlation between deviance residuals and model prediction.

POST TMS

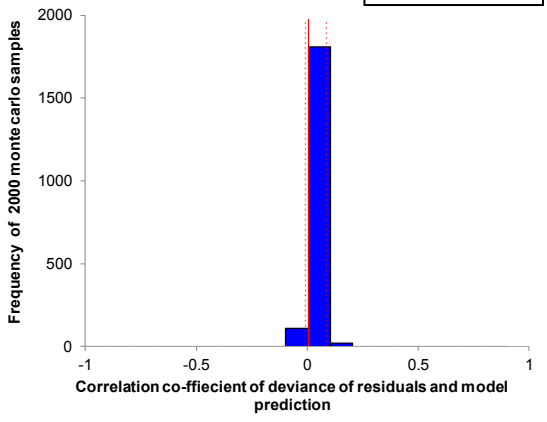

PANEL H) Histogram of bootstrapped correlation coefficients for the correlation between deviance residuals and predicted correct response rate of the model. Dotted lines demarcate 95% intervals of the sampled correlation coefficients, solid line marks the observed correlation between deviance residuals and model prediction.

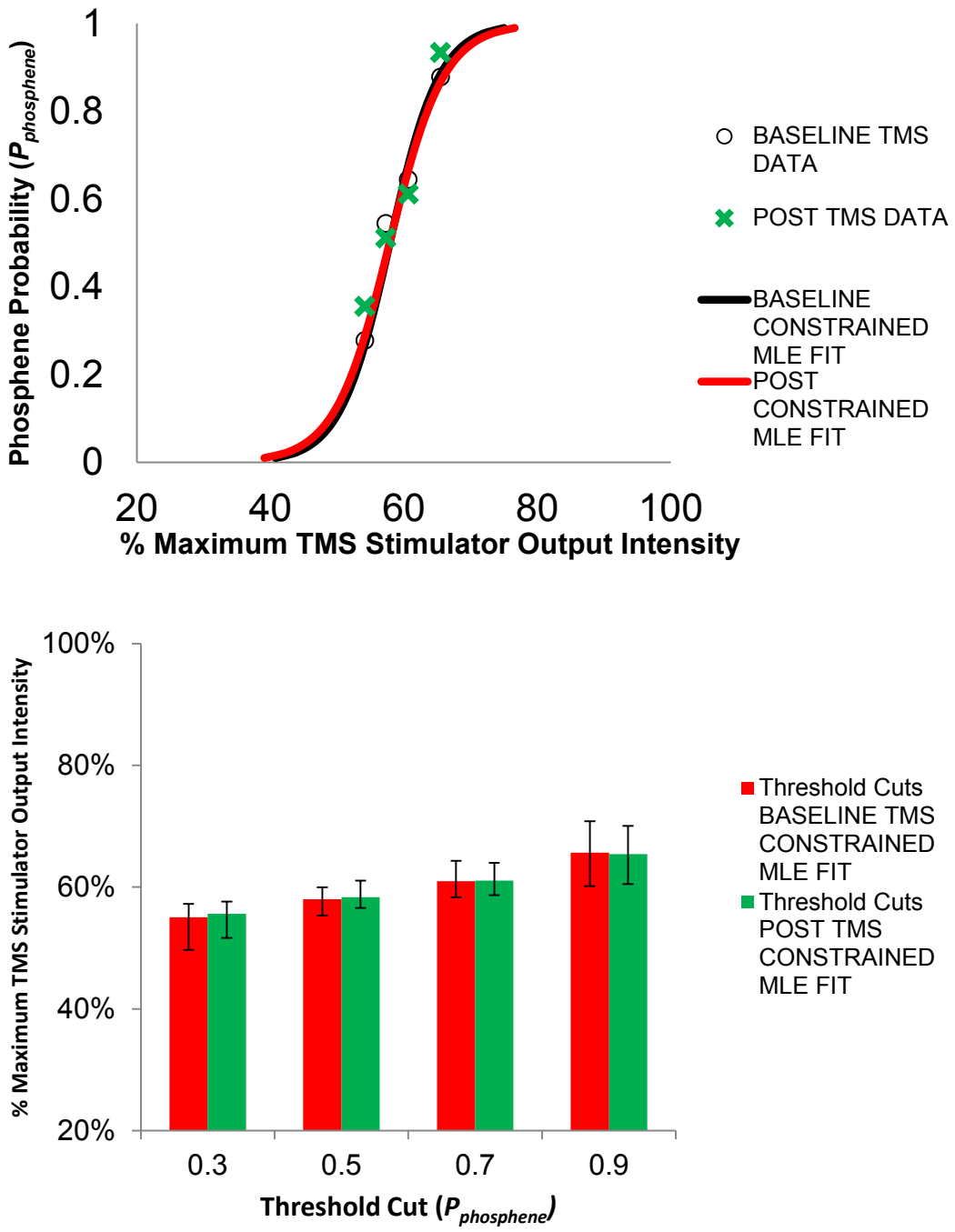

Figure. 4.5. PSYCHOMETRIC FITS TO CONTROL DATA (n=4). Panel A. Plot of Phosphene probability (Pphosphene) by % Maximum TMS stimulator Output Intensity. Baseline TMS data represented by red circles, Post TMS data by green crosses. Black sigmoid indicates Constrained Bootstrap MLE fit to Baseline TMS data. Red sigmoid indicates Constrained Bootstrap MLE fit to Post TMS data. Constraints: γ = λ = beta (2,20). Panel B. Baseline TMS (Red) and Post TMS(Green) Constrained Bootstrap MLE Fits. Error bars represent 95% Confidence Intervals (CI).

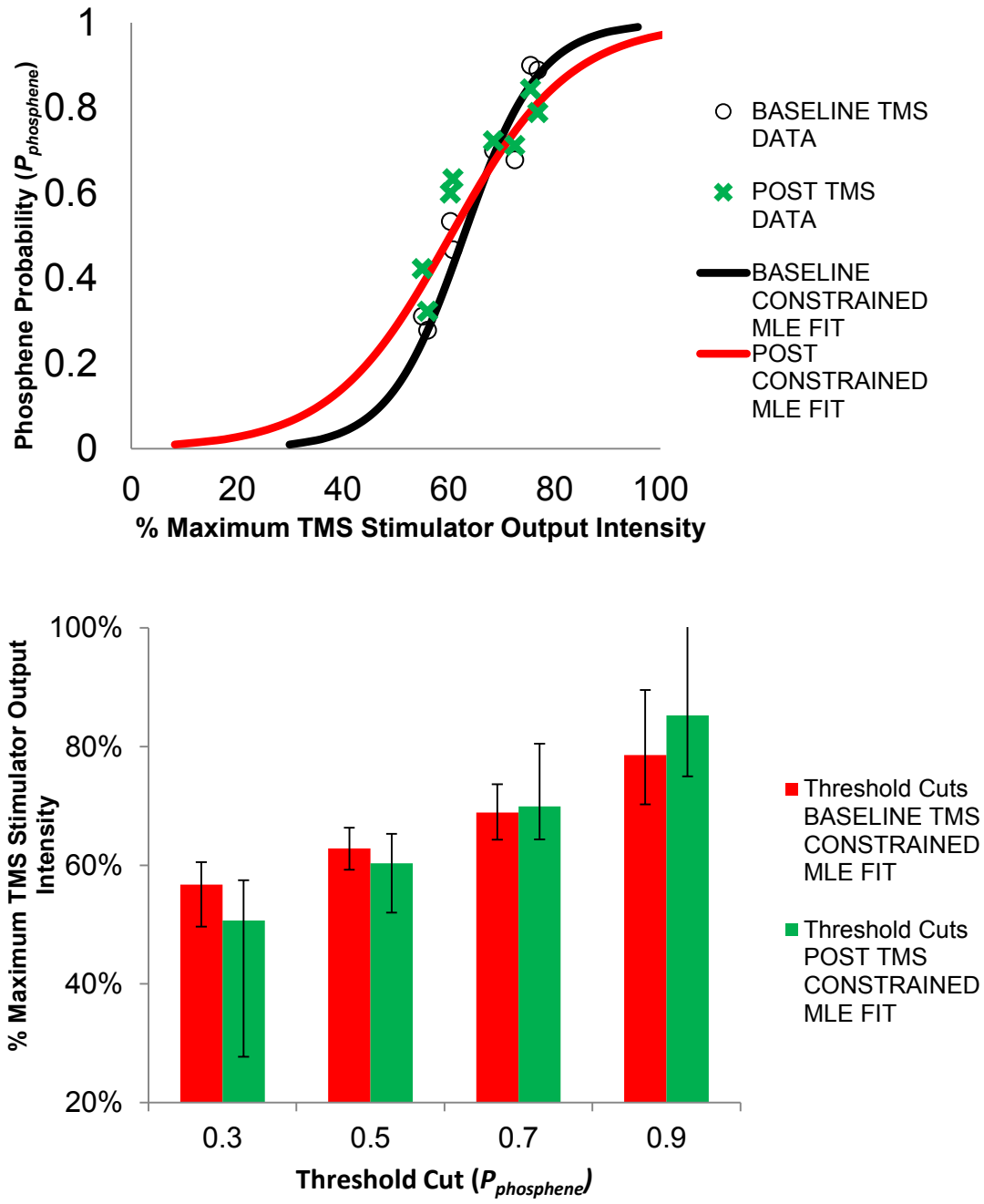

Figure. 4.6. Psychometric fits to (σ=1°) coherent motion data (n=8). Panel A. Plot of Phosphene probability ($P_{phosphene}$) by % Maximum TMS stimulator Output Intensity. Baseline TMS data represented by red circles, Post TMS data by green crosses. Black sigmoid indicates Constrained Bootstrap MLE fit to Baseline TMS data. Red sigmoid indicates Constrained Bootstrap MLE fit to Post TMS data. Constraints: γ = λ = beta (2,20). Panel B. Baseline TMS (Red) and Post TMS(Green) Constrained Bootstrap MLE Fits. Error bars represent 95% Confidence Intervals (CI).

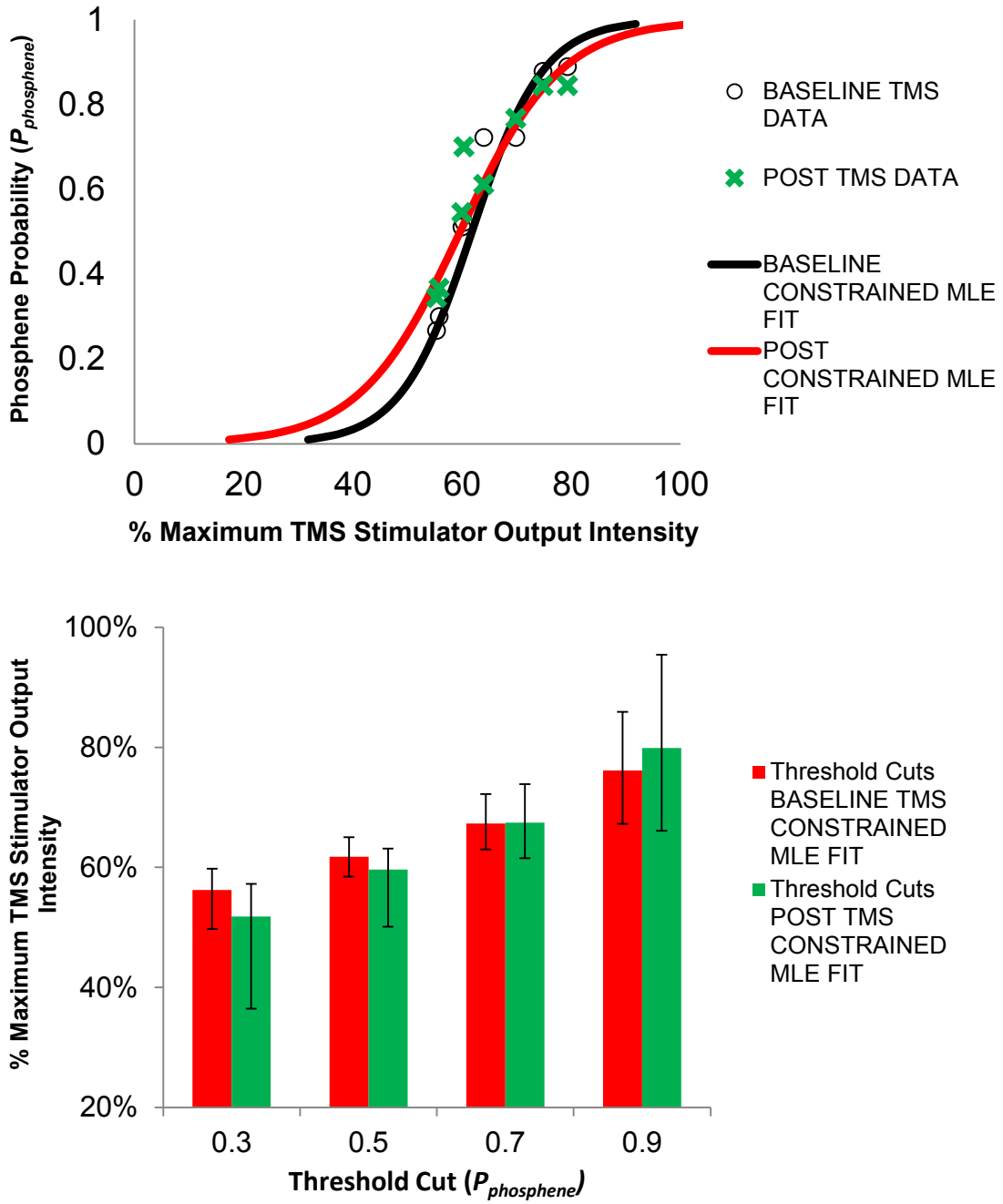

Figure. 4.7. PSYCHOMETRIC FITS TO (Σ=32°) MOTION COHERENCE DATA (n=8). Panel A. Plot of Phosphene probability (Pphosphene) by % Maximum TMS stimulator Output Intensity. Baseline TMS data represented by red circles, Post TMS data by green crosses. Black sigmoid indicates Constrained Bootstrap MLE fit to Baseline TMS data. Red sigmoid indicates Constrained Bootstrap MLE fit to Post TMS data. Constraints: γ = λ = beta (2,20). Panel B. Baseline TMS (Red) and Post TMS(Green) Constrained Bootstrap MLE Fits. Error bars represent 95% Confidence Intervals (CI).

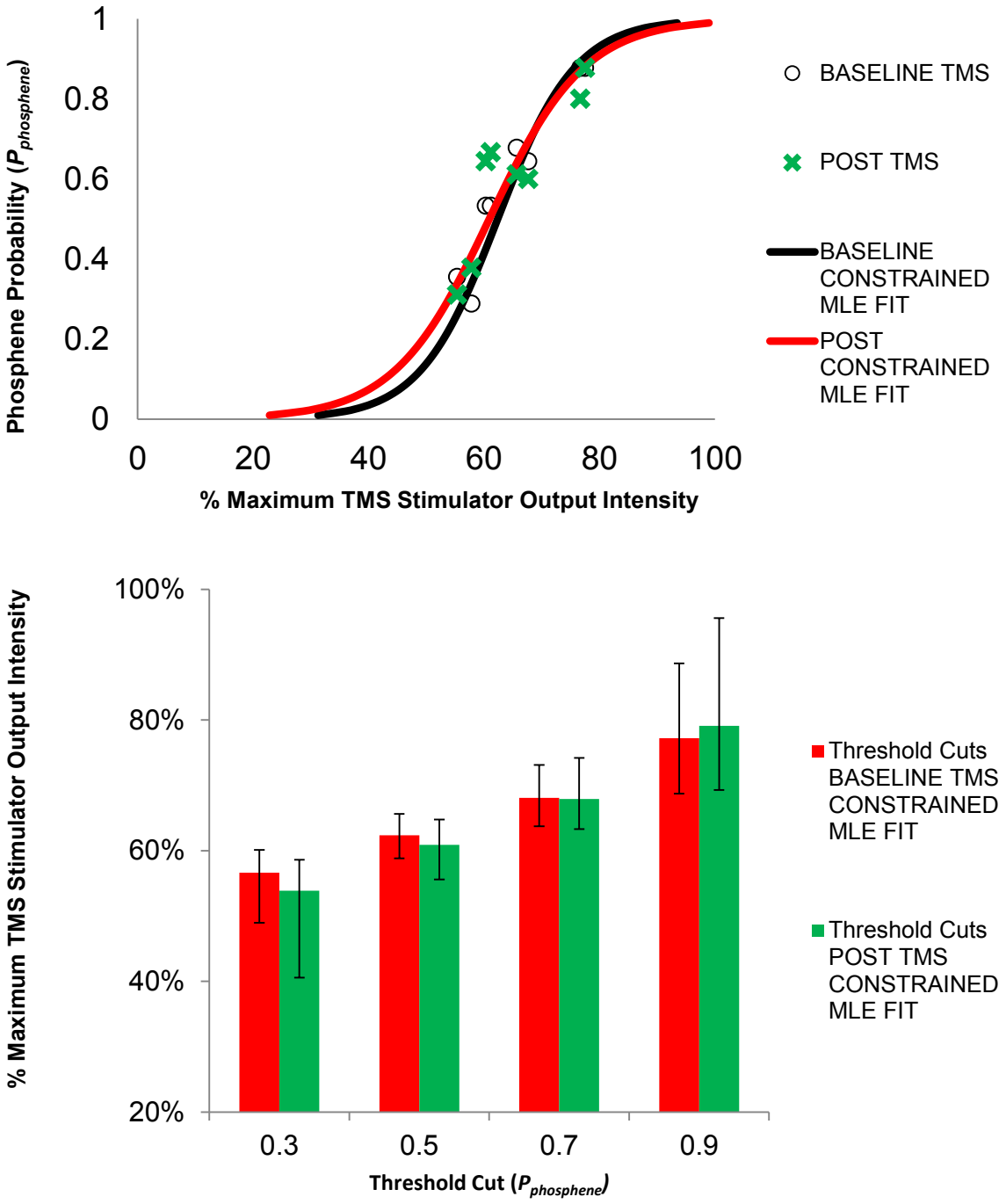

Figure. 4.8. PSYCHOMETRIC FITS TO (Σ=64°) MOTION COHERENCE DATA (n=8). Panel A. Plot of Phosphene probability (Pphosphene) by % Maximum TMS stimulator Output Intensity. Baseline TMS data represented by red circles, Post TMS data by green crosses. Black sigmoid indicates Constrained Bootstrap MLE fit to Baseline TMS data. Red sigmoid indicates Constrained Bootstrap MLE fit to Post TMS data. Constraints: γ = λ = beta (2,20). Panel B. Baseline TMS (Red) and Post TMS (Green) Constrained Bootstrap MLE Fits. Error bars represent 95% Confidence Intervals (CI).

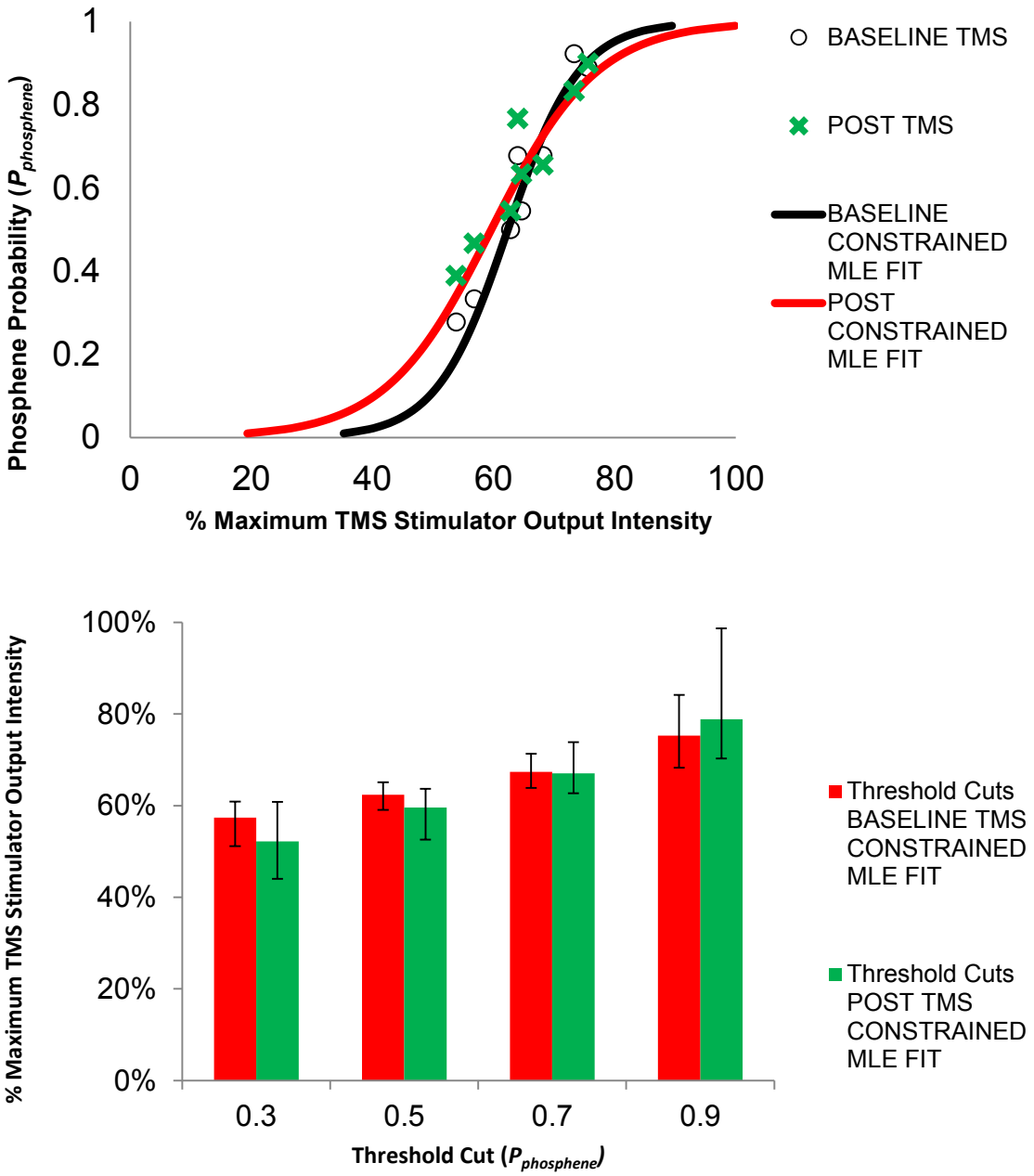

Figure. 4.9. PSYCHOMETRIC FITS TO (Σ=128°) RANDOM MOTION DATA (n=8). Panel A. Plot of Phosphene probability (Pphosphene) by % Maximum TMS stimulator Output Intensity. Baseline TMS data represented by red circles, Post TMS data by green crosses. Black sigmoid indicates Constrained Bootstrap MLE fit to Baseline TMS data. Red sigmoid indicates Constrained Bootstrap MLE fit to Post TMS data. Constraints: γ = λ = beta (2,20). Panel B. Baseline TMS (Red) and Post TMS (Green) Constrained Bootstrap MLE Fits. Error bars represent 95% Confidence Intervals (CI).

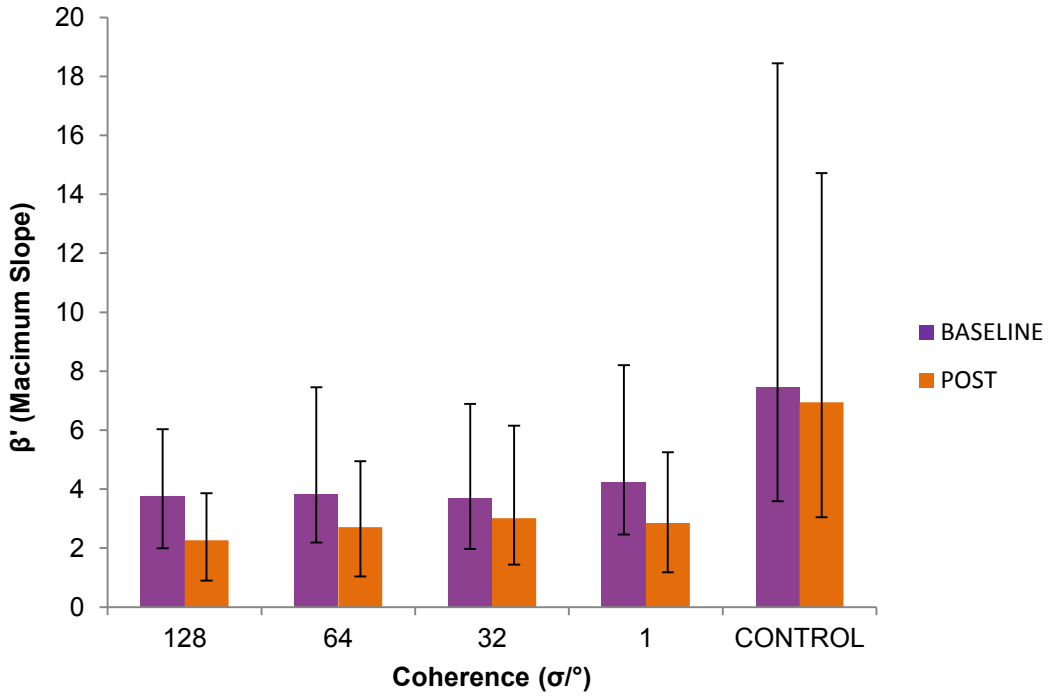

Figure 4.10. COMPARISON OF MAXIMUM SLOPE (β') FOR POST TMS VS. BASELINE TMS FOR EACH MOTION COHERENCE (σ/°) CONDITION. Maximum slope (β') is found at P = 0.5 on the psychometric function. Error bars represent 95% Confidence Intervals (CI).

Time course data

The data was also analysed in terms of its time course across both 'baseline' and 'post' epochs of phosphene response. This data was averaged across all 6 subjects and is illustrated in Figure 4.10. A comparison of these time course plots suggests that within the first 10 pulses delivered in the 'post' epoch, there is a gradual, average increase in phosphenes observed relative to baseline. A comparison of the (averaged) motion vs. control conditions was performed as a gain of post/baseline response, and binned into four epochs of 30 second duration (i.e. representing 5 TMS pulses) and is illustrated in figure 4.11. Repeated measures ANOVA performed across the data by epoch do corroborate a differential modulation of phosphene perception for moving dots ($F(5,6)= 6.313$, $P = 0.006$), but interestingly,

not for static (control) dots ($F(5,6)= 0.639$, $P = 0.601$), which could be indicative of processing by differential neuronal pathways.

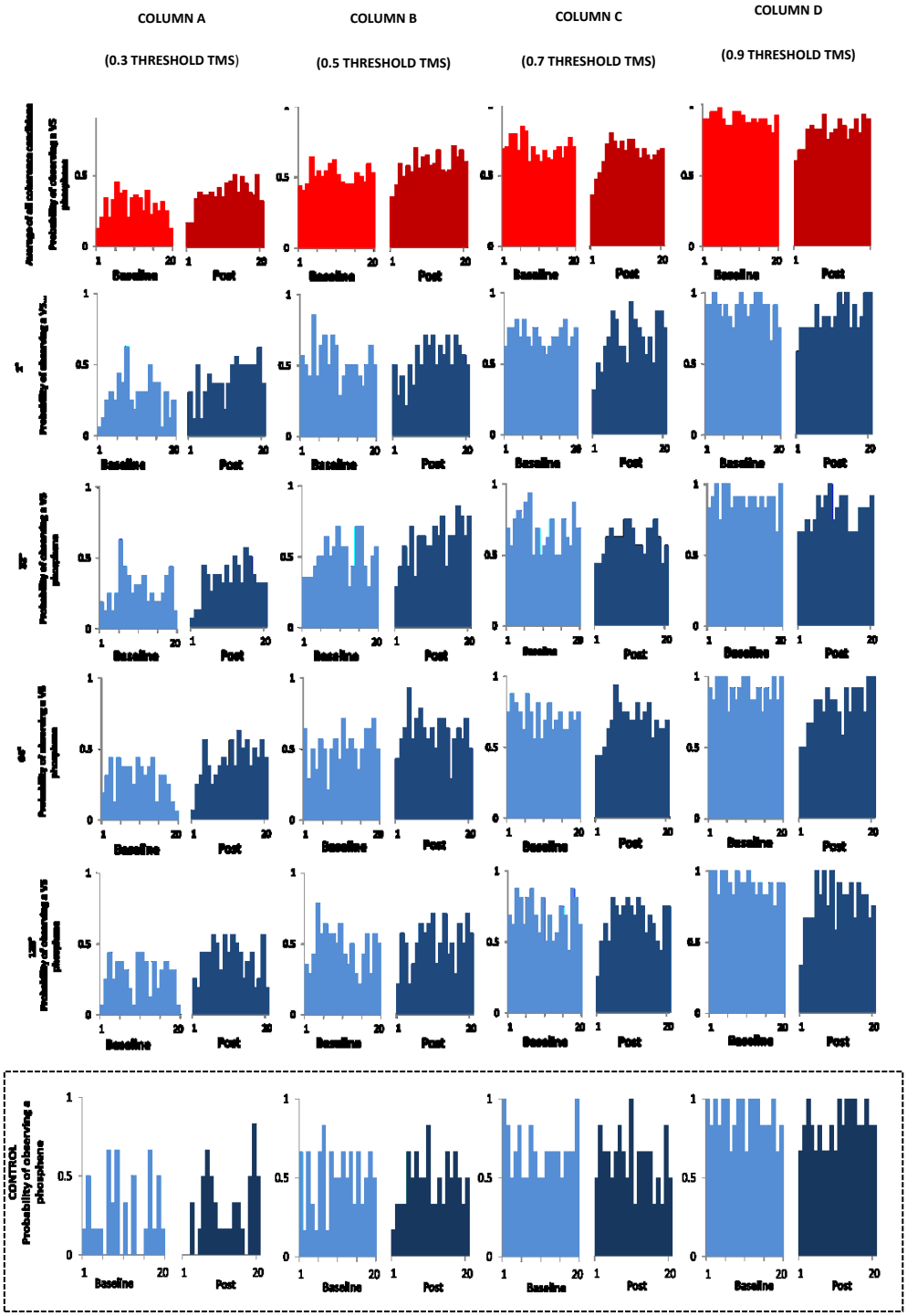

Figure 4.11. V5/MT+ DATA - PROBABILITY OF PHOSPHENE OBSERVATION DURING TMS PULSE SERIES. Average 6 subjects. Columns A, B, C and D show the series for TMS pulses delivered at 0.3, 0.5, 0.7 and 0.9 thresholds, respectively. In each case the top Panel (red) shows the averaged frequencies across all dot motion coherence conditions. The lower panels (blue) show the series' for coherence levels of σ=1˚, σ=32˚, σ=64˚, σ=128˚ , CONTROL (static dots) in descending order from top to bottom. The CONTROL condition is outlined with a dotted line.

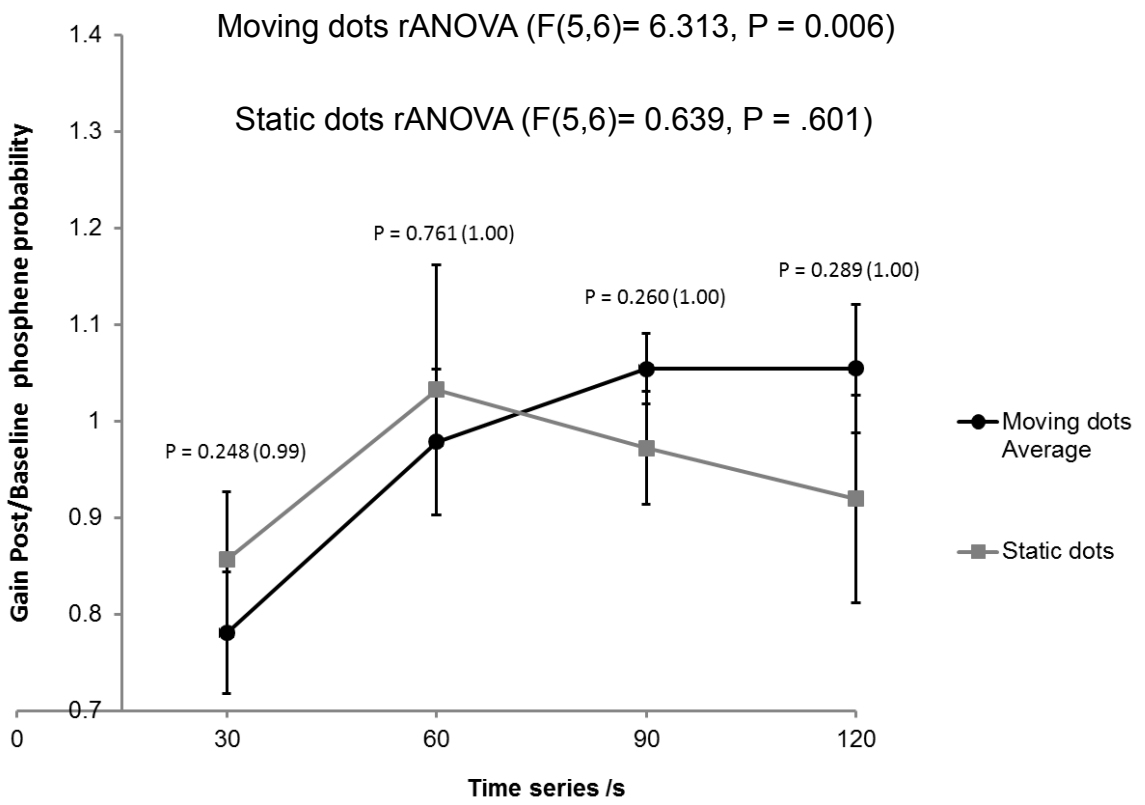

Figure. 4.12. COMPARISON OF GLOBALLY AVERAGED MOVING DOTS VS. STATIC DOTS TIME SERIES DATA. Data binned into 30 second (5 pulse) epochs. Error bars indicate standard error of the mean (SEM). P-values indicate paired t-tests by subject between moving dot and static dot (control) conditions. Bracketed P-values indicate Bonferroni correction. rANOVA = repeated measures analysis of variance.

Perceived visual dot motion direction

The subjects' responses to perceived mean direction of visual dot motion at each level of dot motion coherence was recorded. The percentage of correct responses averaged across all 6 subjects was calculated at each level for either rightward or leftward mean direction of visual dot motion (*see fig. 4.13*).

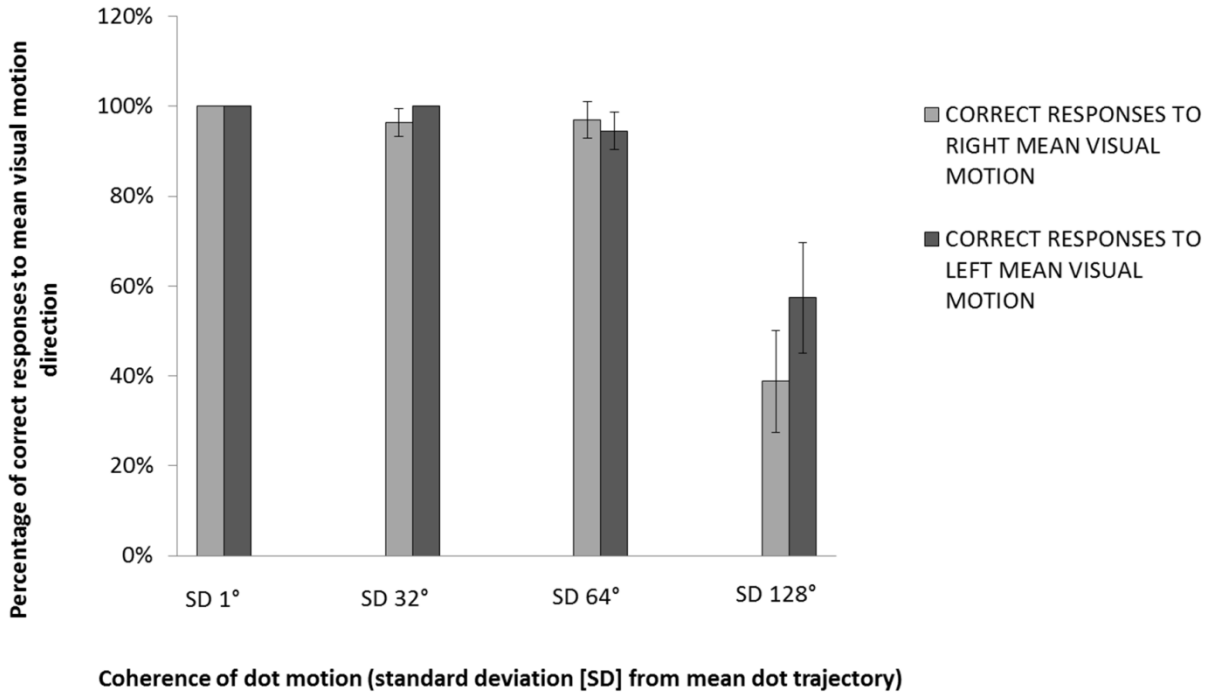

Figure 4.13. CORRECT RESPONSES TO MEAN DIRECTION OF VISUAL DOT MOTION IN V5/MT+ TRIALS. Averaged across all 6 subjects. Error bars represent SEM (standard error of the mean).

Discussion

This study has investigated the responsivity of visual motion area V5/MT+ to TMS intensities at and other than the subjects' 50% threshold level for phosphene perception, after adaptation to visual motion discrimination tasks of varying difficulty. To my knowledge, these parameters of motion coherence and TMS intensity have not yet been explored in the same study.

The strength of TMS intensity used to probe visual cortex (visual motion area V5/MT+) had a significant effect upon the measurements and changes between measurements recorded (either excitatory or inhibitory). However, I also probed different visual motion coherence stimuli using this measurement technique, and found no statistical difference between coherence groups. This was with analyses of

both the threshold (*see fig. 4.3, then 4.5-4.9*) and slope (*fig. 4.10*) of psychometric function data. The results suggest that the sample sizes used were not large enough to effectively employ the sophisticated modelling algorithms required to analyse the psychometric functions.

Differential activation by coherent and random motion

The first aim of this study was to clarify how neurons of V5/MT+ may be differentially activated by coherent and incoherent (random) visual motion. Previous studies have provided discordant results, with arguments for a differential activation (Allman et al., 1990, Snowden et al., 1991, McKeefry et al., 1997); and for no net difference (Braddick et al., 1998, Braddick et al., 2000, Lam et al., 2000, Smith et al., 2006).

The analyses I performed show that the sample sizes in the current study were within the lower boundary of being able to apply the analyses (goodness of fit, *see fig. 4.4*), yet too small to show significant differences between treatments using the standard measurement procedures of the analyses (*see overlapping CI shaded areas fig. 4.3 & CI error bars in figures 4.5 to 4.9. & 4.10*). Nonetheless, the constrained bootstrap modelling of the data (*fig. 4.3 & 4.5 - 4.9*) suggested that visual dot motion stimuli affected excitability of V5/MT+ as opposed to a static dot stimulus (control) when presented for the same duration. This was shown by a decrease in slope (ϭ) of the psychometric function at the 50% threshold after the visual dot motion stimulus (POST TMS) as compared to before (BASELINE TMS). The gain in slope for the motion condition = ($ϭ_P/ϭ_B$) = 0.78 (see *fig. 4.3*). Conversely, there was a small, positive change in slope for the control condition of static dots. The gain in slope for the control condition was $ϭ_P/ϭ_B$ = 1.09. (*see fig. 4.5*). A breakdown of the visual dot motion stimuli by coherence (randomness of dot motion)

also suggests a reduced differential modulation by coherence level. At the 50% threshold, the gain in slope ($ϐ_P/ϐ_B$) of the σ=1° (coherent), σ=32°, σ=64° and σ=128° (random) psychometric functions were $ϐ_P/ϐ_B$ = 0.67, 0.82, 0.71 and 0.63 respectively (*see fig. 4.5-4.9*) The trends in the data support the argument made by Lam et al. (2000) that coherent ($ϐ_P/ϐ_B$ = 0.67) and random motion stimuli ($ϐ_P/ϐ_B$ = 0.63) differentially activate V5/MT+ to produce a similar net neuronal activation. Hence, these trends are consistent with a transition from maximal activation of few direction specific neurons (in the direction of coherent visual motion) to moderate activation of many neurons with different direction specificities (random visual motion).

The reduction in width of 95% confidence intervals for the grouped motion stimuli (data points for all coherence levels plotted on the same psychometric function; n trials=640; *see fig 4.3*) as compared to each motion stimulus alone (n trials=160, *see fig. 4.5-4.9*) show that in this measure, statistical significance of the findings is predicated upon sample size (n observations), rather than the magnitude of the differential effects measured (changes in slope (ϐ) and horizontal separation (α) of psychometric functions of BASELINE TMS and POST TMS, which remain largely indeterminate of sample size). It can thus be inferred that the size of our subject cohort (6) was sufficiently large to produce reliable, subject-averaged estimates but was not large enough to disambiguate significant effects between different treatments. Hence, there is further scope for repeated testing of the same subjects to increase the reliability of such estimates at individual motion coherence levels (i.e. increase sample size from n trials =160 to n trials >=640). An excellent review of techniques used in the modelling of data with psychometric functions, with especial focus on (β) the slope parameter; differences in its definition and usage; and which

include the techniques used in this chapter (Wichmann and Hill 2001a, Wichmann and Hill 2001b), is that of Klein (2001).

Theory of preferential activation of non-signal carrying neurons

Trends in the data suggest that in response to adaptation to visual dot motion, 30% threshold as well as 50% threshold TMS elicit a facilitatory effect upon probability of perceiving a phosphene, (70%) threshold TMS elicits approximately no change, and 90% threshold TMS elicits an inhibitory effect (*see fig.4.3, 4.6.-4.9.*). I suggest this may be due to an interaction between two factors: the first being a dose effect of increased neuronal activation with increased intensity of TMS stimulation (assuming that with a stronger TMS pulse there is increased activation of individual neurons and also a larger population of neurons activated) and the second being the theorised preferential activation of less active, non-signal carrying neurons (Silvanto et al., 2007). This second factor operates on the argument that signal carrying neurons are less excitable to TMS stimulation than non-signal carrying neurons. It can be used to explain why TMS applied as an intervention prior to a task may produce very different effects to application during a task (Beckers and Homberg, 1992, Laycock et al., 2009, Tadin et al., 2011): prior to a task all neurons are at their baseline level of excitability, thus TMS may stimulate them more equally. During a task however, neurons involved in that task are already activated and hence less susceptible to excitation by TMS. It is also worth considering a saturation effect, whereby direction specific neurons involved in the perception of visual dot motion may not be activated. The form of TMS used to elicit phosphenes was of a single pulse modality of low frequency (0.1Hz), as opposed to high frequency repetitive

TMS (Gersner et al., 2011), thereby having no carry-over effect into the visual dot motion discrimination task from baseline TMS stimulation.

Recurrent feedback between V5/MT+ and V1

In this study, perception of phosphenes in V5/MT+ was used as a probe of how the brain responds to visual motion. However, this is a complex issue, and it has been shown that the perception of phosphenes in V5/MT+ seems not only to involve the site of stimulation, but requires processing in other brain regions, including a strong influence of primary visual cortex (V1). Indeed, subthreshold TMS of V1 5-40ms after TMS of V5/MT+ has been shown to severely disrupt phosphene perception in V5/MT+ (Bullier, 2001). This suggests that V5/MT+ phosphene perception necessitates processing in V1 and that information flows 'backward' from V5/MT+ to V1. When a TMS pulse is delivered to V1, it may be directly stimulating shared neuronal circuitry necessary for phosphene perception in both V1 or V5/MT+. However, when a TMS pulse is delivered to V5/MT+ it may filtered by the neuronal circuitry of this visual area, and additionally limited by the bandwidth of the afferent pathways from V5/MT+ to V1, to reach the suggested, common neuronal circuitry required for phosphene perception.

Interestingly, a differential pattern between TEPS (TMS Evoked Potentials) show that multiple posterior brain areas are also activated 160-200ms after TMS of V1 when phosphenes are elicited, as compared to when they are not (Taylor et al., 2010). In combination with the evidence that phosphene perception in V5/MT+ necessitates V1 activation (Bullier, 2001), it can be argued that a feed forward chain of information from V5/MT+ through V1 and on to other posterior brain areas may be required for V5/MT+ phosphene perception. It must also be reminded that I discuss

V5/MT+ as feeding forward to V1 for the purpose of phosphene explication and that V5/MT+ receives the majority of its input from V1 in the first instance (Pascual-Leone and Walsh, 2001). Interestingly, it has also been argued that fast visual motion input is processed by V5/MT+ without the need of input from V1 (Zeki et al., 1993). It has also subsequently been shown that conscious perception of fast visual motion is possible even with extensive damage to V1 in the 'blind' field (Cragg, 1969) and that this is dependent upon V5/MT+ activity (Zeki and Ffytche, 1998). In addition, anatomical studies show that there is a direct retinal pathway to V5/MT+ that by passes V1 (Cragg, 1969, Sincich et al., 2004).

Nonetheless, a feed forward model does not take into account possible top-down influences of posterior brain areas shown to be activated by phosphenes (Taylor et al., 2010). It has been argued that in visual perception, a feed-forward 'sweep' of cortical processing is only involved in pre-attentive, unconscious visual processing, and that it is recurrent feedback from higher and parallel cortical areas that result in attentive, conscious, visual perception (Lamme and Roelfsema, 2000). Indeed, spatial attention to moving visual stimuli has been shown to modulate the activity in V5/MT+ of the macaque. It has been shown in a single-unit electrode recording study that when two competing visual motion stimuli are presented within the receptive field of a V5/MT+ neuron, and attention is directed to one of them, the response of the neuron is dominated by the attended stimulus. Its activity rises when the attended visual motion is in its 'preferred' direction of firing, and falls when the visual motion opposes this preferred direction, with a median effect of attention amongst trials recorded at over 80% (Treue and Maunsell, 1996).

A similar single-unit electrode recording study was subsequently conducted by a separate group, with one aim being to reproduce this strong effect. This study confirmed the presence of an attentional effect, but of the much smaller effect size of 8.7%. The authors suggest this order of magnitude difference could critically depend upon the precise parameters of the visual task presented, and method by which attention was directed. Furthermore, the smaller attentional effects were recorded at a long latency of ~300ms after the onset of the visual motion stimulus, and increased throughout the duration of its presentation, peaking at the offset of the stimulus (Seidemann and Newsome, 1999) . The ~300ms latency of attention effects can be juxtaposed with i) the combination of the ~5-40ms latency required to inhibit V5/MT+ phosphene perception with TMS of V1 after V5/MT+ (Bullier, 2001) and ii) the 160-200ms latency shown in activation of posterior brain areas after TMS of V1 in perception of V1 phosphenes. The maximum combined latency of 240ms suggests that visual motion information fed forward from V5/MT+ to V1 to posterior brain areas is within the latency of information fed forward from V5/MT+ to higher areas involved in spatial attention (~300ms). Hence activation of the same neuronal circuitry. It would also suggest a minimal latency of ~60ms for top-down attentional information to reach visual cortical areas, which could potentially feedback to V5/MT+ through V1, directly to V5/MT+, or feedback solely to V1. Hence top down, feedback information may travel faster than bottom up feed-forward, visual information.

Furthermore, both short latency feed-forward processing from V5/MT+ to V1 and longer latency recurrent processing have been shown in motion detection, and interestingly in single word recognition (Laycock et al., 2007, Laycock et al., 2009). Hence, there seems to exist a dichotomy between V5/MT+ being a cortical area

which feeds external visual information forward to higher cortical areas, and which recurrently feeds back information to area V1.

Therefore, both phosphene perception and motion detection may involve feed-forward or horizontal processing as well as longer latency recurrent processing between V5/MT+, V1 and other surrounding areas (Lamme and Roelfsema, 2000). Hence, it is not solely the baseline excitation of the stimulated site which will determine whether a phosphene is perceived or not.

Extending the study to primary visual cortex (V1)

The reciprocity of V5/MT+ and V1 interactions might cause differential and congruent effects observed between V5/MT+ and V1 elicited phosphenes. As described in Chapter 2., V1 also possess columns of neurons selective for motion orientation. An interesting extension of the current study would be to repeat the paradigm for V1 also, under the hypothesis that with visual motion stimulation to V5/MT+ and V1 independently, there will be some overlap in the characteristics of the respective responses due to shared neuronal circuitry required for phosphene perception. Congruent effects observed between V5/MT+ and V1 elicited phosphenes might partially be attributed to the filtering of information between V5/MT+ to V1. Single and multiunit electrode recordings in the macaque V5/MT+ area suggest that although small clusters of V5/MT+ neurons are attributed to parvocellular pathways, the majority are magnocellularly dependent (Maunsell et al., 1990)(See Chapter 1.). In contrast V1 has been widely shown to have strong magnocellular, parvocellular and koniocellular input (Hendry and Reid, 2000, Vidyasagar et al., 2002). As it is

also known that first order motion is based on luminance contrasts transmitted via magnocellular pathways (Baloch et al., 1999), it may also be assumed that the percept of V5/MT+ moving phosphenes is a manifestation of magnocellular throughput to V1 and communication with other posterior brain areas. Therefore, if the bulk of the processing of visual dot motion is assumed to take place in V5/MT+, irrespective of whether it is V5/MT+ or V1 that is being probed with TMS, it would stand to reason that any gross similarities observed between V5/MT+ and V1 would be indicative of recurrent processing via magnocellular circuitry between these areas (Bullier, 2001, Pascual-Leone and Walsh, 2001, Block, 2005).

Here, it may be asked what neuronal architecture might account for the effect that occurs within the first epoch of post phosphene perception. An interesting conjecture is that it may be due to a fast acting, direct connection to V5/MT+ from the lateral geniculate nucleus (LGN) which completely bypasses V1, the main input to V5/MT+. Interestingly it has been shown that a koniocellular pathway exists from the LGN to V5/MT+ which sends virtually no collateral axons to V1. (Sincich et al., 2004). Furthermore, it has also been shown that despite visual motion processing being largely considered to be mediated via magnocellular pathways, primate studies and human behavioural studies have also shown that there exist koniocellular pathways which are also able to process visual motion. Indeed, these pathways convey spatial information faster than magnocellular pathways (Morand et al., 2000).

Interestingly, stimulation of parvocellular neurons in V1 result in the perception of a coloured phosphene, however this does not mean to say that V1 is the cortical site for colour phosphene perception, simply that it is necessary for colour information to

be conveyed to perceptual areas of the brain (Pollen, 1999). The lack of functional parvocellular architecture in V5/MT+ (Baloch et al., 1999) has been shown and could explain the absence of colour in phosphenes elicited from TMS stimulation to V5/MT+.

Obtaining accurate thresholds to phosphene perception

In addition to the Modified Binary Search (MOBS) adaptive staircase approach used to establish a 50% baseline to phosphene perception (See Methods) it must also be stated that there are other adaptive procedures which may also have been incorporated into the experimental design to afford potentially more efficient and reliable methods of establishing the 'other than 50% chance' thresholds to phosphene perception. In my current study these subthreshold (30%) and suprathreshold (70% and 90%) rates of phosphene perception are obtained solely with a 20 pulse approach, using the 50% threshold Baseline obtained with the MOBS adaptive staircase procedure as a datum. However additional approaches in obtaining a stimulus threshold either expound upon the method of searching with 20 pulses at fixed step intervals (Parameter Estimation by Sequential Testing), or equally use adaptive staircase techniques (transformed up-down methods) to probe 'other than 50% threshold' levels of phosphene perception.

As the first example, Parameter Estimation by Sequential Testing (PEST) is an adaptive approach where a number of trials are given at a particular stimulus level and a test statistic run to evaluate these trials. In theory, this technique can be used at any specified target stimulus threshold. If the rules of the test statistic are not met at that stimulus level , the PEST procedure increases or decreases the intensity by a

specified step size and proceeds with a series of trials at the new stimulus level, which again is re-evaluated against a test statistic. This process is continued until a trial stimulus level does meet those rules which satisfy the test statistic and it is this stimulus level which constitutes the stimulus threshold (Taylor and Creelman, 1967) . Variations of the PEST adaptive approach have modified this original design to allow faster convergence of the procedure (Findlay, 1978) and formed a hybrid design which allows all of the sequential trial data over the course of the procedure to be used in the formation of a threshold level estimate (Hall, 1981) rather than simply the final stimulus level. This hybrid PEST also overcomes many of the shortcomings of the original PEST as it is more robust to such effects as subject lapses and inappropriate starting levels or step sizes (Leek, 2001).

Conversely, transformed up-down methods are adaptive staircase approaches which bias the number of responses of incorrect to correct responses to a test stimulus, in order to be able to obtain 'other than chance' stimulus thresholds. They differ from PEST procedures in that they require far fewer assumptions (Levitt, 1971). Given that in traditional up-down methods the step size is not altered, this results in a very few stimulus thresholds that can be obtained with this technique, and it is up to the experimenter to decide whether these threshold values suit their experimental design. For example, there is the '1 up 2 down' method where two incorrect responses are required to force the procedure to decrease a step, but only one required to increase a step. With this staircase procedure, the probability of a 'down' sequence of responses (to effect a step) must equal that of an 'up' sequence. The probability of an 'up' step from one incorrect response is 0.5, therefore a step down from two correct responses is also 0.5. This means that, following the 'AND' rule of

probability theory, the probability of each of these individual correct responses (p) must be multiplied together to form the resultant step probability of 0.5, where p x p = 0.5. Re-arranging this equation, p = $\sqrt{0.5}$ = 0.707, which would target the 70.7% stimulus threshold. With the same token, a '3 down, 1 up' method would require that p x p x p = 0.5. This time the cube root of the resultant step probability is taken to derive p, thus p = $\sqrt[3]{0.5}$ = 0.794, hence this method targets the 79.4% stimulus threshold.

It can be seen from the '2 down 1 up' and '3 down 1 up' procedures that transformed up-down methods are unsuitable when specific stimulus threshold levels are required. Although, if our current experiment had been probing only subjects' 50% and 70% thresholds to phosphene perception, a '1 up, 1 down' method (such as the MOBS) could again afford a 50% threshold estimate, but in addition, a '2 down 1 up' method may have sufficed for the 70% threshold, as it affords a 70.7% stimulus threshold which is a good approximation.

A further type of adaptive staircase technique, rather than reach 'other than 50% stimulus thresholds' by biasing the step size for correct vs. incorrect answers (Levitt, 1971), actually modulates the step size (Kaernbach, 1991). This method allows targeting of any stimulus threshold by biasing the correct to incorrect responses as multiples of each other, such that the probability ratio of incorrect to correct responses takes the form (1-p)/p where the denominator p represents the probability of a correct response. For example, this technique can be used to target the 75% threshold of a sensory stimulus with the probability ratio of 0.25/0.75 = 1/3. As compared to the current study, this technique could reduce the time taken and

reliability of estimates of baseline phosphene perception, and normalise the method by which all relative TMS thresholds (30%,50%,70% and 90%) are obtained.

Conclusion

The current study has used a novel combination of measurement and analysis techniques, and has shown that whilst such combination of techniques holds promise, the intrasubject sample sizes need to be increased to have the statistical power necessary to show (or not show) convincing results. The current results are promising in that the trends in the data are concordant with the theory that differential activation of V5/MT+ by coherent and random motion may achieve the same net neuronal activation (Lam et al., 2000). By testing a range of TMS intensities it also probed the interaction of TMS intensity and visual motion signal, with trends in the data being concordant with the theory that TMS preferentially activates non-signal carrying neurons (Silvanto et al., 2007).

Chapter 5.

Differential effects of whole body rotation in yaw on TMS-induced phosphene perception in V5/MT+

Summary

V5/MT excitability was measured by TMS, under whole-body rotation, and thus vestibular stimulation in yaw. Both vestibular stimulation and TMS intensity were modulated in a 2x2 factorial design, and a significant interaction was found ($F(1,21) = 4.72$, $P=0.042$). Nonetheless, no significant main effects were found. Additional analysis indicates that the stimulus onset asynchrony (SOA) between whole-body rotation and TMS pulse onset, differentially affects excitability of V5/MT $F(3,21) = 3.52$ $P = 0.02$).

Introduction

The vestibular system is phylogenetically ancient and predates the evolution of the eye. As vision has come to be the dominant sense in humans, this begs the question of how the visual system developed in the context of an established, reliable sense of self motion. Vestibulo-ocular reflexes (VOR) were present in vertebrates, such as fish, prior to the development of mammals and thus humans. Hence the use of the earlier vestibular system in the functioning of the later visual system has been clearly established in vertebrates. However, this only indicates a gross one-way relationship between these two sensory modalities. With the

development of the mammalian cortex it must be asked what other interactions take place between the visual and vestibular systems and for what purpose. How has the enrichment of our visual world engendered changes in cortex and our vestibular system?

There is some debate as to whether or not visuo-cortical processing is reciprocally inhibited by vestibular stimulation and vice versa. The rationale for an interaction being that dependent upon which of these two cortices is activated, the other is inhibited to avoid a potentially confusing sensory mismatch. The most compelling evidence for the interaction comes from Positron Emission Tomography (PET) scans of these cortices under stimulation of unilateral caloric irrigation, showing that as vestibular cortex is activated, visual cortex is concurrently inhibited (Bottini et al., 1994, Deutschlander et al., 2002, Dieterich et al., 2003). However, the concept of reciprocal inhibition suggests the brain is trying to ignore the information from the weaker sensory stimulus as it is more likely to be erroneous. It is therefore discordant with the widely espoused optimal integration model of sensory integration, in which it has been shown that the brain acts as a near optimal integrator of sensory cues based on their reliability, and that this occurs across multiple sensory modalities (Ernst and Banks, 2002, Kording and Wolpert, 2004, Alais and Burr, 2004, Gu et al., 2008, Angelaki et al., 2011). The key factor being that no matter how unreliable the weaker sensory signal, the brain will still use that information.

Furthermore, it is well known that caloric irrigation is a strong, artificial, vestibular stimulus, which can induce the corollaries of vertigo and nausea (Seemungal et al., 2012). It may also be that visual cortex is only inhibited above a threshold vestibular

stimulus and that with weaker, real-world vestibular stimulation, the effect on visual cortex may be quite different. Therefore, in this study I used a 2x2 Factorial design to interrogate the interaction of phosphene perception in visual motion area V5/MT+ (direct visuo-cortical activation) against whole body rotation in the horizontal plane ('real world' vestibular cortical activation). Phosphene perception is evoked by TMS (transcranial magnetic stimulation) and affords a subjective measure of visuo-cortical neuronal activity which is not derived from blood flow analysis as found with PET. Consequently, TMS may provide a better measure of visuo-cortical activity associated with signal processing rather than metabolic activity. I use magnitudes of acceleration of whole-body rotation in yaw toward the just perceptible end of vestibular sensation, and do this to contravene symptoms of vertigo and nausea which are associated with stronger vestibular stimulation, and more realistically simulate ecologically normal activity.

Methods

The main analysis in this study was a repeated measures ANOVA performed across all subjects; across two levels of vestibular stimulation; and across two levels of phosphene/TMS intensity within a 2 x 2 factorial design. Additional analyses were required to gauge perceptual thresholds for both phosphene and vestibular perception prior to the main experiment and analysis. These threshold tasks incorporated a Modified Binary Search, staircase algorithm. Lastly, SOA (stimulus onset asynchrony) which, here, is the delay between the onset of the vestibular stimulation (chair rotation) and visual probe (TMS evoked phosphene), was

investigated, again with repeated measures ANOVA across all four SOA levels tested.

Subjects

34 subjects, all right handed were recruited. Of these 6 subjects were unable to see phosphenes and 3 subjects were excluded due to non-compliance with the experiment or technical fault. 2 subjects were excluded due to undisclosed unilateral amblyopia (validated by history, poor visual acuity in the affected eye both near and far, and lack of normal stereo acuity as measured by the fly dot stereo test). Therefore, 23 subjects (13 female) (mean age 25.2 yrs range 14.5 yrs) took part in the study.

Apparatus

The equipment comprised a vibrationless motorised chair under computer control, which was free to rotate in the horizontal plane. All rotations were of a raised cosine waveform and under velocity control of the computer. Loudspeakers mounted on the chair provided white noise to eliminate ambient, spatial auditory cues. Subject psychophysical responses were recorded via push button. TMS pulses were delivered by a Magventure Mag-Pro (Model X-100) device using a figure of 8 coil (MC B70). The coil was mounted on a poseable, lockable arm. The waveform of the pulses delivered was biphasic and the direction of the current set to 'normal'. Figure 5.1. illustrates the setup used for the vestibular threshold pre-test with chin rest, head rest and left-right push buttons (Panel A), and the set up used for both the phosphene threshold pre-test and the final visuo-vestibular interaction experiment (Panel B). This used a forehead rest only with the TMS coil located at left V5/MT+,

providing additional support from behind the head. The poseable arm used to locate the TMS coil was omitted from the diagram for clarity.

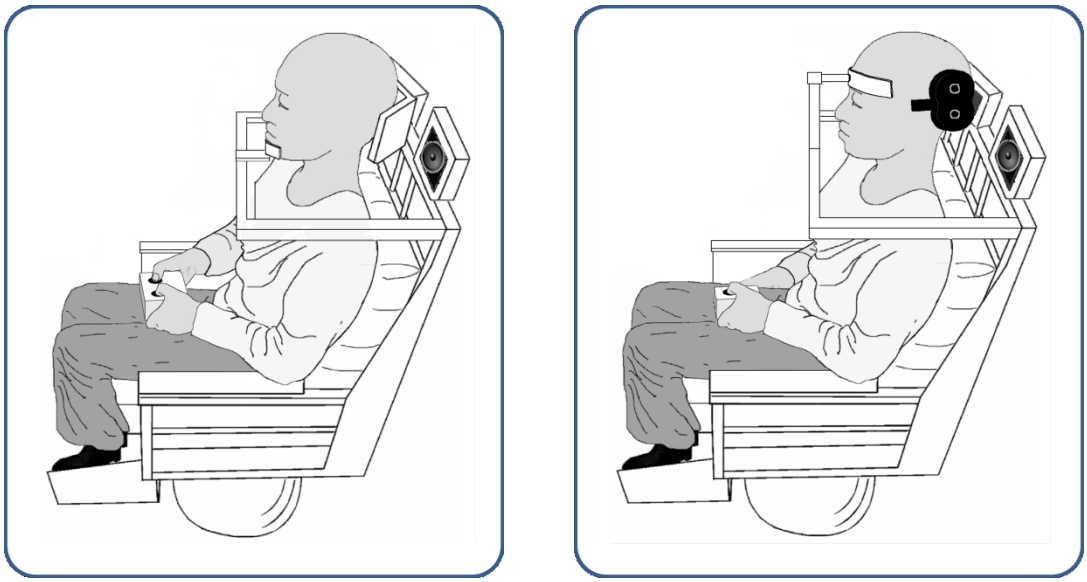

Figure 5.1. THRESHOLD TESTS SETUP. Panel A. Vestibular Threshold Pre-Test Setup. Left and Right push buttons. Chin and head rests. Panel B. Phosphene Threshold Pre-Test & Visuo-vestibular Interaction Experiment. Single push button. TMS Coil at left V5/MT+. Forehead rest and Loudspeakers provide white noise.

Localisation of V5/MT+ phosphenes with TMS.

Phosphenes were localised as in Chapter 4.

Vestibular threshold pre-test

Subjects were seated in the chair in the dark and instructed to keep their eyes open. They were told that they could be randomly rotated to the left or to the right, and to indicate with twin-push buttons which direction they felt they had rotated. If they felt no sensation of rotation they should not press either button. Rotations of 5 seconds ramp input (and 5 seconds ramp down) were delivered randomly by the chair, either

to the left or to the right, by a MOBS program (*see Chapter 3.*) (Tyrrell and Owens, 1988). Subjects provided 2 alternative forced choice (2AFC) push button responses to their perceived direction of motion which modulated the velocity of subsequent rotations. The modulation was a staircase of correct responses reducing chair velocity, and incorrect responses increasing chair velocity. The program ceased after 5 reversals of response to output a vestibular threshold value of rotation velocity (subject average 0.87°/s^2, range 0.67 – 1.18 °/s^2). The vestibular thresholds were used to program the magnitudes of chair rotation in the final visuo-vestibular interaction experiment and as such were tailored to the vestibular thresholds of each subject. By its very nature, MOBS affords 50% threshold detection. The 50% threshold was multiplied 1.5 times to afford an approximation of subject 75% threshold to vestibular perception. It is worth note that prolonged rotation in darkness causes spatial disorientation and confusion in subjects. Hence a gross suprathreshold level of vestibular activation, without further thresholding, was a compromise for time.

Phosphene threshold pre – tests

50% - Threshold - Mobs test

Subjects were presented V5/MT+ phosphenes controlled by a MOBS program (Tyrrell and Owens, 1988, Seemungal et al., 2004), see Chapter 3. Starting at an objective output of 50% of the maximum intensity of the TMS machine, subject 2 alternative forced choice (2AFC) push button responses modulated the intensity of the next phosphene delivered. This was in a staircase fashion of phosphene observation reducing phosphene intensity, and lack of phosphene observation increasing phosphene intensity. The program ceased after 5 reversals of responses

to output a 50% threshold value for phosphene perception. This threshold value was used in the final visuo-vestibular interaction experiment and as such was tailored to each subjects' phosphene threshold.

50% Threshold - Pulse series test

At 6 second intervals, a series of 20 pulses of TMS were then delivered to the subject at the threshold value obtained from the MOBS test. If 8-12 phosphenes were observed out of a total of 20, this series was accepted and graded as a weighted function of the 50% threshold MOBS value. For example, if the MOBS threshold value was 53% of the maximum output intensity of the TMS machine and a count of 12 phosphenes were observed, then this 53% output intensity would constitute the 60% threshold value for phosphene perception.

If the series produced more or less than 8-12 phosphene observations, the output intensity of the TMS machine was either raised or lowered 2% and another 20 pulse series recorded. This process was repeated until a value within the required range of observations was reached.

70% Threshold - Pulse series test

Thereafter a 70% threshold to phosphene perception was obtained. With the 50% threshold (or weighted equivalent) used as a lower bound, a series of 20 pulses was used to probe the 70% threshold of each subject. This was achieved by probing initially at a 6% increment of TMS maximal output above the lower bound value. The range of acceptable responses was 12-16 phosphenes observed, with the additional caveat that there must be at least 2 more phosphenes observed than for the 50% threshold (or weighted equivalent). If the required count was not achieved the TMS

output was modulated by plus or minus 2% of maximal TMS output. As with the 50% threshold, the 75% threshold was weighted, thus if 15 phosphenes were observed, then this would constitute the 70% threshold value for phosphene perception.

Visuo-vestibular interaction experiment

Subjects were seated in the chair in the dark. They wore opaque goggles to ensure they could see no light. They were instructed to keep their eyes open and that for each trial of the experiment, they would be rotated to the left or right and that this motion would be preceded by a warning beep. They were told that during the rotation a TMS pulse would be delivered and that they might perceive a phosphene. Hence they should attend to their visual field in anticipation.

The progression of a typical trial is illustrated in figure 5.2. A 0.5s warning beep was given to alert the subjects to trial onset. This was followed by a variable delay rotation of the chair in the form of a 5 second ramp input, 1 second plateau and 4 second ramp down. The delay could randomly be 1s, 1500ms, 2000ms or 2500ms seconds after beep onset. This was used to undermine a temporal strategy by which subjects could correlate the onset of the TMS pulse from the beep with the onset of chair rotation. Thus not attend to their perception of motion from the rotation. The TMS pulse was delivered 4 seconds after onset of chair rotation. Post TMS, subjects indicated that they saw a phosphene or not with a single press of a push button (phosphene observed), or a rapid double press (phosphene not observed). Upon each trial, the chair rotation could either be delivered at a velocity equal to the magnitude obtained with the subject's vestibular threshold pre-test (50% threshold to vestibular activation) or at a magnitude 1.5 larger (70% threshold to vestibular

activation). Note that as the form of the rotation signal is consistent between the vestibular threshold pre-test and the visuo-vestibular experiment

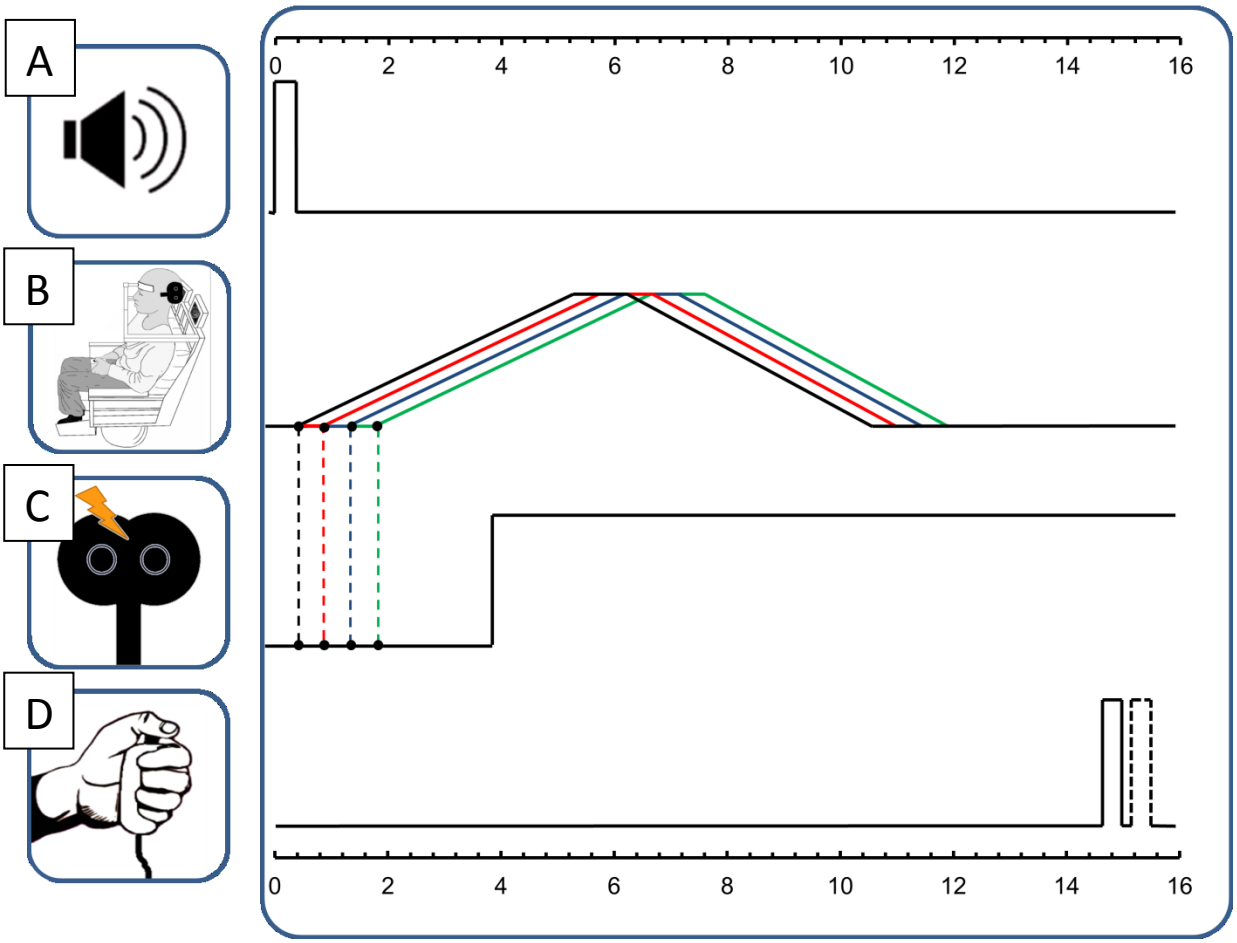

Figure. 5.2. TRACE DIAGRAM OF A TYPICAL TRIAL. Trace A indicates an auditory warning beep. Trace B. indicates the ramp onset, plateau and offset of chair rotation. Delay to chair rotation onset is indicated by colour of trace. Black = 500ms, Red = 1000ms, Blue = 1500ms, Green = 2000ms. Trace C indicates the onset of TMS pulse at 4000ms. Trace D. indicates subjects yes/no push button response to the perception of a phosphene. In this example the subject double clicks a push button to indicate that a phosphene was not observed. A single click indicates a phosphene was observed.

Each trial lasted 18 seconds and this allowed time for the vestibular system to 'washout' ready for the next trial. In total, there were 128 trials per subject. These were divided into 8 blocks with checking of the apparatus and subject in between (subject was attentive, could see no light, TMS coil was firmly against subject's head, TMS coil lead was slack). There were 4 blocks each for the high and low phosphene perception conditions, respectively. These blocks were presented randomly, and within each block the trials were balanced and randomised for direction of rotation (left or right), for speed of rotation (low or high vestibular perception conditions) and for delay to onset of chair rotation (0.5, 1, 1.5, 2s).

Results

In summary, both vestibular stimulation and TMS intensity were modulated in a 2x2 factorial design, and a significant interaction was found ($F(1,21) = 4.72$, P=0.042). Nonetheless, no significant main effects were found. Additional analysis indicates that the stimulus onset asynchrony (SOA) between whole-body rotation and TMS pulse onset, differentially affects excitability of V5/MT $F(3,21) = 3.52$ $P = 0.02$).

Outliers

Pearson correlations were performed between subject 50% thresholds to phosphene perception obtained with MOBS and independently to their 50% and 70% thresholds obtained with the 20 pulse technique, respectively. For each correlation, casewise diagnostics were performed upon the residuals of linear regression between correlation variables. These used a 2 standard deviation (σ) threshold to search for outliers. Two such outliers were found in the 70% threshold correlation and remained the only outliers with a sensitivity upon reanalysis of $\sigma = 1.5$. One outlier was found in the 50% threshold correlation and belonged to the same subject as the largest

outlier in the 70% threshold correlation. The correlations before and after removal of outliers are shown in figure. 6.3.

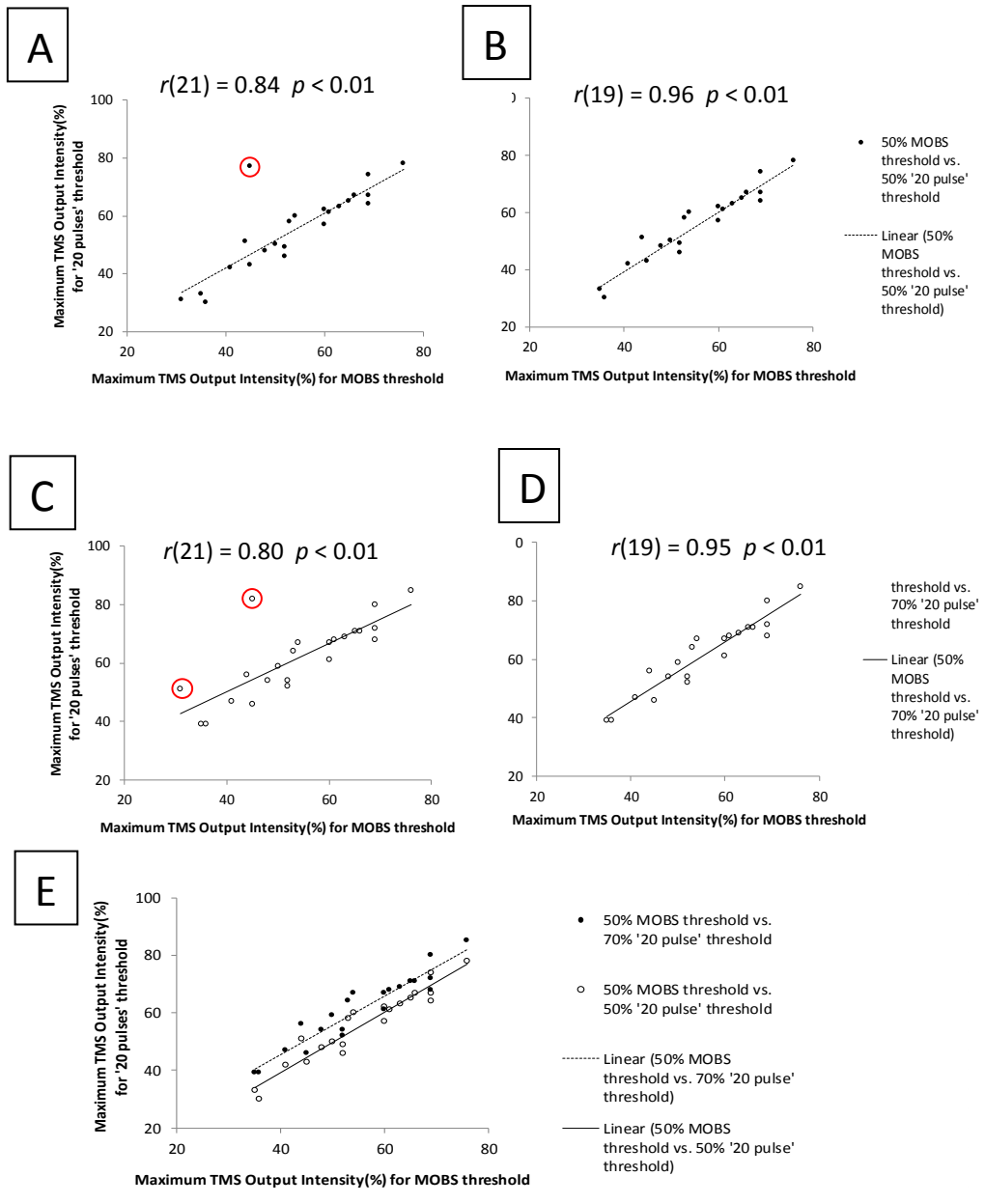

Figure 5.3. CORRELATIONS OF THRESHOLDS TO PHOSPHENE PERCEPTION AS DERIVED BY MOBS VS. '20 PULSES' TECHNIQUE. Panel A. 50% MOBS Threshold vs. 50% '20 pulses' Threshold with outliers larger than (2σ) present. Panel B. 50% MOBS Threshold vs. 50% '20 pulses' Threshold with outliers removed. Panel C. 50% MOBS Threshold vs. 70% '20 pulses' Threshold with outliers larger than (2σ) present. Panel D. 50% MOBS Threshold vs. 70% '20 pulses' Threshold with outliers removed. Panel

E. Comparison of 50% MOBS threshold with both 50% and 70% ’20 pulse threshold. Pearson correlation statistics are shown on Panels A,B,C,D respectively.

A Factorial Design, four-way Repeated Measures ANOVA was used to analyse the data. The four factors were threshold level for phosphene perception (2 levels); threshold level for vestibular perception (2 levels); direction of rotation / laterality (2 levels), and delay to rotation onset (4 levels). An overview of the preliminary SPSS output indicated no effect of direction of rotation ($F(1,21) = 0.25$, $P = 0.624$) and a test for outliers was performed across the remaining factors, which showed no outliers present (*see fig 5.4.*).

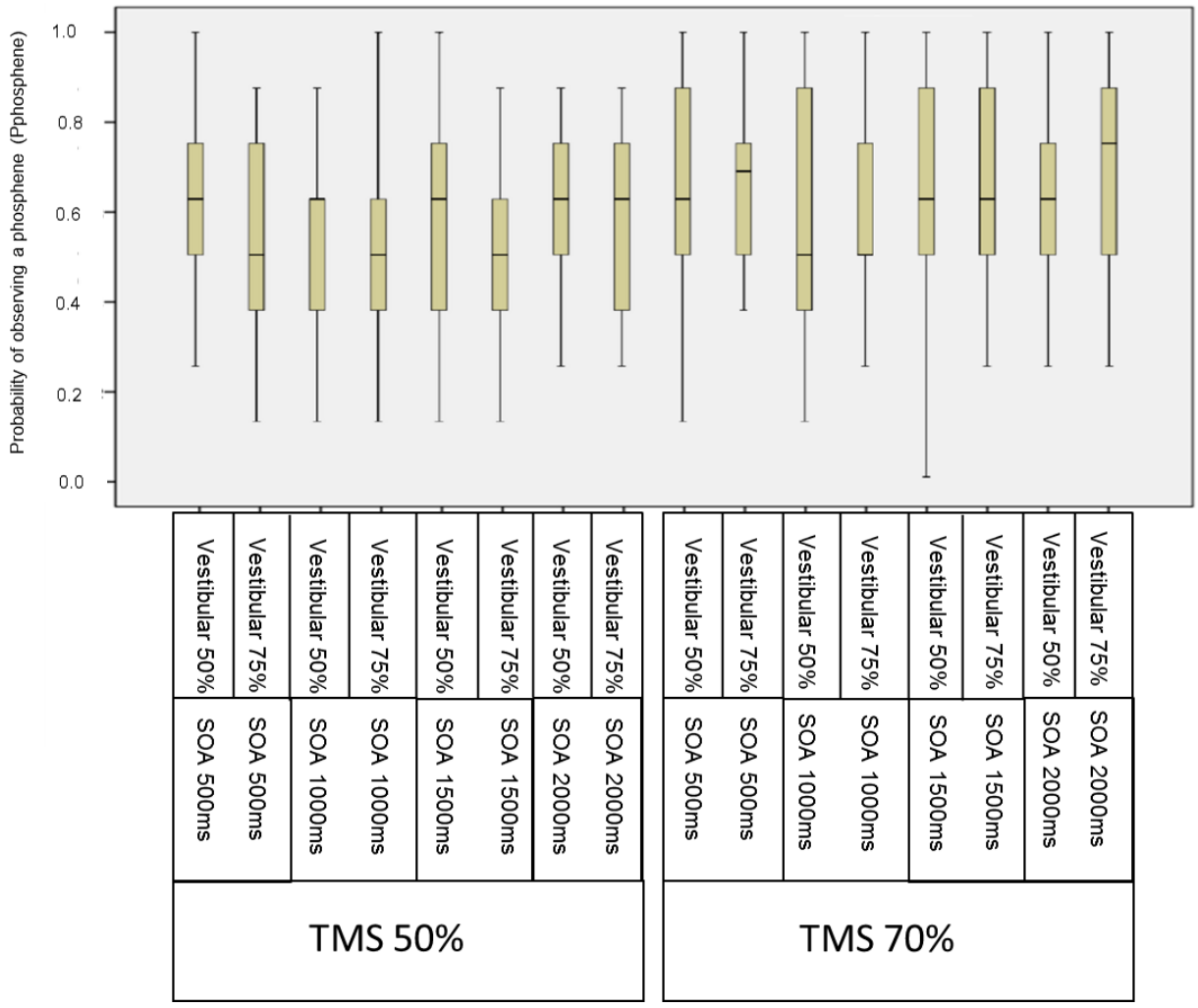

Figure 5.4. BOX AND WHISKERS PLOT FOR OUTLIERS. Box and whiskers plot indicating mean & interquartile ranges across factors of vestibular perception; TMS threshold; and delay to onset of rotation. No outliers present. If present, potential outliers would be indicated by subject ID number at each measure.

Four-way repeated measures ANOVA

There was a significant effect of threshold level to phosphene perception (F(1,21) =16.67, *P* =0.001). There was no effect of vestibular perception level (F(1,21) =1.80, *P*=0.194). There was a significant interaction between phosphene threshold level and vestibular threshold level (F(1,21) = 4.72, *P*=0.042). There was no laterality effect upon phosphene threshold level (F(1,21) = 0.25, *P*=0.624) or upon vestibular threshold level (F(2,21) =0.02, *P*=0.906). There was no interaction between visual threshold level, vestibular threshold level and laterality (F(1,21) = 0.02 *P*=0.483). Plots of both 50% and 70% threshold to phosphene perception at 50% threshold and 75% (actual 50% x 1.5) threshold levels of vestibular perception are illustrated in figure 5.5. The converging plots are indicative of the significant interaction between phosphene perception and vestibular perception.

There were no significant main effects. A paired *t*-test performed at 50% phosphene threshold level, between 50% and 75% threshold vestibular perception levels showed no significant difference (P=0.075). Similarly, a paired t-test performed at 70% phosphene threshold level, between 50% and 75% threshold vestibular perception levels showed no significant difference also(P=0.459).

At 50% vestibular threshold level, there was no significant difference between the two strengths (50% and 70%) of phosphene used, paired *t*-test (P=0.098). However, at 70% phosphene threshold level, there was a significant difference between the two strengths (50% and 70%) phosphene used, paired *t*-test (P<0.001).

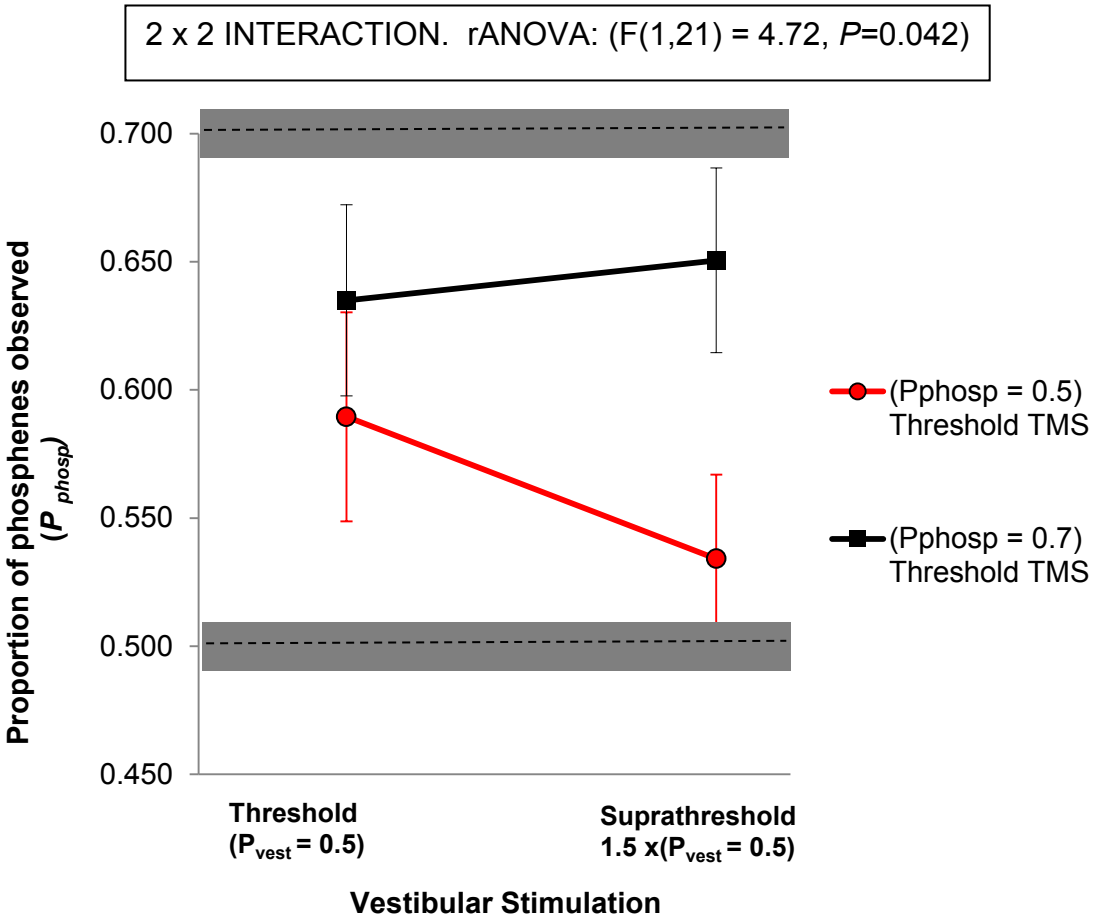

Figure 5.5. PLOT OF VISUO-VESTIBULAR INTERACTION. Line graphs of vestibular activation against (averaged) probability of observing a phosphene ($P_{phosphene}$). Top graph (black) represents 70% threshold TMS. Bottom graph (grey) represents 50% threshold TMS. Error bars indicate standard error of the mean (SEM).

Individual phosphene responses are illustrated in figure 5.6. We had hypothesised that a suprathreshold level of vestibular stimulation would further reduce the amount of phosphenes observed relative to threshold vestibular stimulation, irrespective of the strength of phosphenes used. However, 5 out of 21 subjects expressed an increase in the number of threshold phosphenes observed with suprathreshold as compared to threshold vestibular stimulation. 14 out of 21 subjects expressed the

same effect with suprathreshold phosphenes. 5 subjects were common to both results.

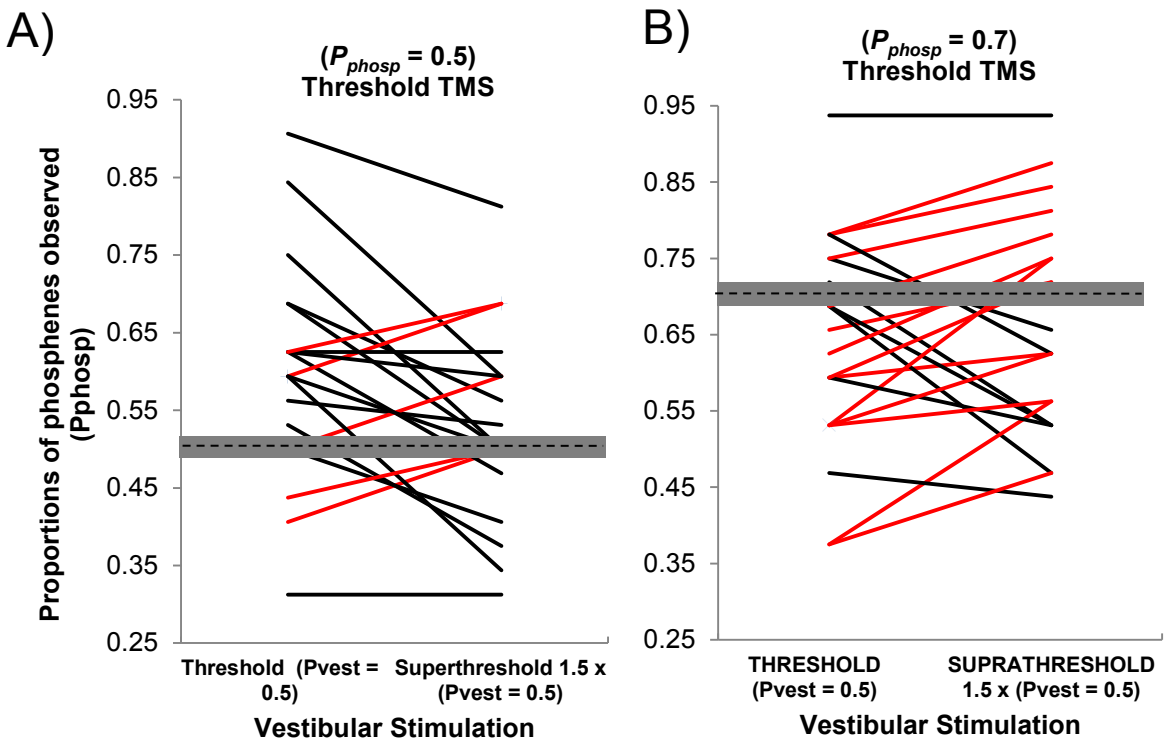

Figure. 5.6. PROPORTIONS OF PHOSPHENES OBSERVED TO VISUAL-VESTIBULAR STIMULATION BY SUBJECT. Pane A) illustrates (P_{phosp} = 0.5) threshold phosphene responses. Pane B) illustrates 1.5 x (P_{phosp} = 0.5) suprathreshold phosphene responses. Dotted lines on grey bars indicate baseline phosphene response threshold (P_{phosp} = 0.5) and suprathreshold (P_{phosp} = 0.7) levels and respective standard errors (SEM_{phosp} = 0.01).

Effect of delay to chair rotation onset

There was additionally an effect of the delay to chair rotation onset (F(3,21) =3.52, *P*=0.020), which is equivalent to the stimulus onset asynchrony (SOA) between the visual TMS pulse, and vestibular chair rotation. There was no interaction between delay of chair rotation onset and phosphene perception (F(3,21) =0.95, *P*=0.963), or vestibular perception (F(3,21) =0.81, *P*=0.491), respectively. Furthermore, the effect

of delay of chair rotation upon phosphene perception followed a quadratic trend as evidenced by an analysis polynomial contrast (F(1,21) =8.02, *P*=0.010). A plot of delay of chair rotation against averaged probability of observing a phosphene, clearly shows the quadratic trend (*see fig. 5.7*).

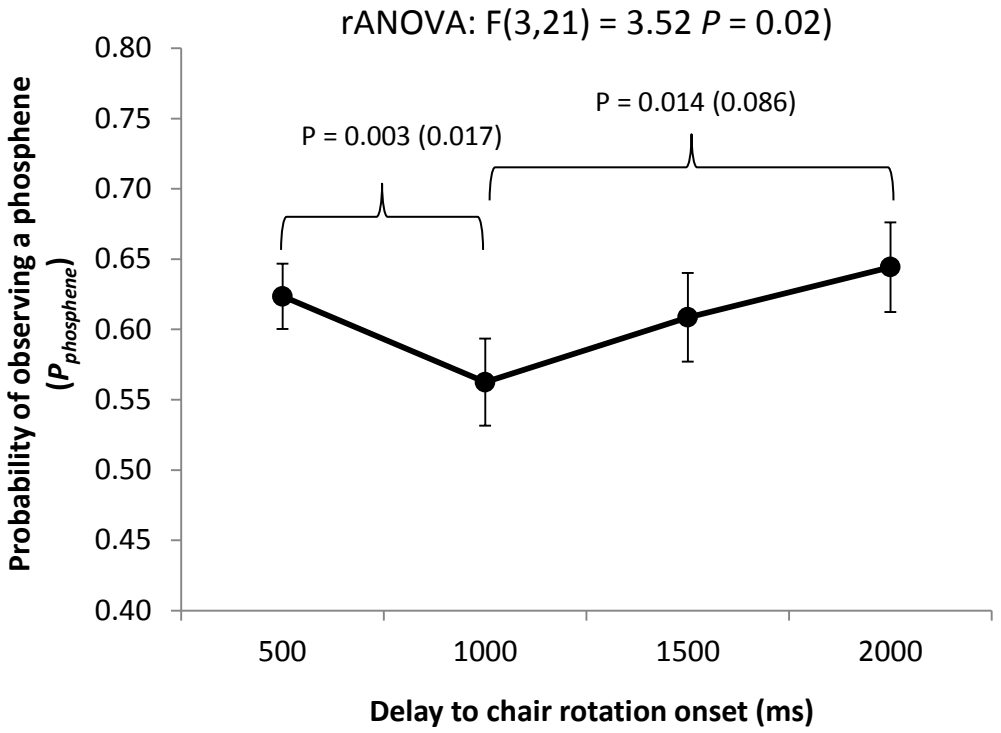

Figure 5.7. EFFECT OF DELAY TO CHAIR ROTATION ONSET. Line graph of delay to chair rotation onset against (averaged) probability of observing a phosphene ($P_{phosphene}$). Error bars indicate standard error of the mean (SEM). Bracketed P-values indicate Bonferroni corrected paired *t*-test.

Discussion

The purpose of this study was to lend further evidence to the debate over whether vestibular and visual cortices reciprocally inhibit one another, using a real world vestibular stimulus and an alternative measure of visual cortical excitability

modulation (TMS evoked phosphenes) as compared to PET (positron emission topography) (Muehllehner and Karp, 2006).

V5/MT excitability was measured via TMS evoked phosphenes, under whole-body rotation, and thus vestibular stimulation in yaw. Both vestibular stimulation and TMS intensity were modulated in a 2x2 factorial design, and a significant interaction was found ($F(1,21) = 4.72$, $P=0.042$). Nonetheless, no significant main effects were found. Additional analysis indicates that the stimulus onset asynchrony (SOA) between whole-body rotation and TMS pulse onset, differentially affects excitability of V5/MT $F(3,21) = 3.52$ $P = 0.02$).

Argument for reciprocal inhibition of visual and vestibular cortices

The most convincing argument to date for a reciprocal inhibition has been built from a series of PET studies conducted over the last 14 years. The first of these studies was prompted by a surprising PET finding for a patient with opsoclonus, a condition which consists of rapid, multivectoral, conjugate (both eyes moving together), unpredictable, involuntary eye movements (Digre, 1986). This result, conducted with [F^{18}]deoxyglucose (FDG) showed a significant bilateral decrease in glucose metabolism in both the striate and exstriate cortices. This prompted the question of what the functional significance of deactivation of the visual cortices with eye movement might be. Consequently, this was probed with a PET study in healthy subjects whereby caloric irrigation of the ear canals was used to promote involuntary movement of the eyes in the form of nystagmus. Caloric irrigation consists of water entering the ear canal, and the differential thermic effect of the water temperature stimulating the nearby distal fibres of the vestibular nerve, causing an artificial stimulation of the vestibulo-ocular reflex (VOR). The VOR drives eye movement

involuntarily. The PET result showed that in addition to bilaterally inhibiting visual cortical areas (area V1 then V2 being most affected), areas of vestibular cortex were simultaneously activated. This effect occurred with caloric irrigation of either ear, and was maximal with the use of ice cold water as an irrigant, but still present with warm water of 44˚C. The interpretation at the time was that visual cortex was inhibited to prevent oscillopsia (a visual disturbance in which elements of the visual scene appear to oscillate) produced by visual input during involuntary ocular oscillations (Wenzel et al., 1996, Brandt et al., 1998, Dieterich et al., 2003). The converse modulations of the vestibular and visual cortices with vestibular activation in this study suggested a potential reciprocal inhibition of these cortices.

This possibility was further investigated in a PET study in which the sensory stimulus was instead visual motion, thus probing whether increased activity in visual cortex was accompanied by a concurrent inhibition of vestibular cortex to support the concept of reciprocal inhibition (Brandt et al., 1998). Indeed this proved to be the case. The visual motion stimulus used afforded large field stimulation, resulting in the perception in subjects of circular vection (CV). CV is the perception of self-motion against a stationary environment caused by constant velocity visual motion. Interestingly, it was found that during CV, although visual areas were activated, these were primarily a medial parieto occipital area. Surprisingly, neither middle temporal (V5/MT+) or medial superior temporal (MST) areas were major sites of activation, despite their importance in the processing of visual motion and optic flow (Duffy and Wurtz, 1997, Smith et al., 2006, Nadler et al., 2009). These areas were actually activated more by a control condition of random motion rather than CV. However, the vestibular area concurrently deactivated during CV, located in the deep

posterior insular, was entirely consistent with the areas activated by caloric vestibular stimulation as measured with similar PET techniques (Bottini et al., 1994). Furthermore, this area also represents the human analogue of the monkey parieto-insular vestibular cortex (PIVC), an area well known for multisensory vestibular integration (Grüsser et al., 1990, Brandt et al., 1994).

Activation of the human homologue of PIVC has also been shown with caloric vestibular stimulation in another PET study. Here it was additionally and comprehensively shown that there is a bias in activation of this multisensory vestibular network toward the non-dominant hemisphere of the subject - the hemisphere ipsilateral to the dominant hand. In addition, increased activation was produced in the hemisphere ipsilateral to caloric irrigation. Consequently, caloric irrigation of the ipsilateral ear to the dominant hand will produce maximal activation of the PIVC in the ipsilateral hemisphere (Dieterich et al., 2003).

A PET study has also been conducted which specifically probes the cortical correlates of human vestibulo-ocular reflex (VOR) modulations (Naito et al., 2003). Caloric vestibular stimulation (irrigation) was used to induce VOR responses of nystagmus. With this stimulation, as would be expected, areas including the strongly vestibular PIVC were activated. However, additional visual cortical areas were also activated including the fusiform and lingual gyrii. Although these areas are typically associated with responses to faces (Sergent et al., 1992, Puce et al., 1995, Kanwisher et al., 1997) they have also been activated when discriminating the direction of motion of a random dot pattern (Cornette et al., 1998), judging the speed of motion of a random dot pattern (Orban et al., 1998) and in the processing of visual

orientation (Orban et al., 1998, de Jong et al., 1999). Thus it could be argued the reason these ostensibly visual areas are activated with caloric vestibular stimulation (and here in complete darkness), is that they are involved in the processing of sensation of self and spatial motion which are not solely dependent on visual cues. Furthermore, this study also analysed cortical responses when visual target fixation was used to suppress the nystagmus engendered by caloric irrigation. During visual fixation broad areas of visual cortex were shown to be activated, including striates cortices, V5/MT+ and MST, areas more typically involved in the processing of visuo-spatial information than those described to be activated with caloric vestibular stimulation. Concurrently during visual fixation, areas including hippocampus and the hippocampal gyrii were deactivated, areas which use vestibular input to form maps of space for development of spatial memory during learning tasks (Zheng et al., 2001).

Hence, it is clear from the studies described that there do exist reciprocal inhibitions of the visual and vestibular cortices which are dependent upon whether a vestibular or visual cue is administered. It is posited that the cortex of the sensory cue that is not being dominantly encoded is inhibited to reduce potential sensory mismatch of an erroneous signal interfering with the veridical dominant signal (Dieterich and Brandt, 2008). However, it is also evident that there are activations of visual cortex with vestibular stimulation, and myriad other cortical activations and deactivations which may have an unknown bearing on the processing of spatial sensory cues (Wenzel et al., 1996, Brandt et al., 1998, Dieterich et al., 2003, Naito et al., 2003). Thus, a concrete, consistent pattern of co-activation and deactivation has not been established between studies thus far.

Argument for optimal integration of visual and vestibular stimuli

However, arguing against the utility of reciprocal inhibition of the visual and vestibular cortices may be equally as evocative. Numerous studies show that the brain is capable of integrating multimodal sensory stimuli in a near statistically optimal fashion. This holds true for visuo-haptic interactions (Ernst and Banks, 2002, Kording and Wolpert, 2004), visuo-auditory interactions (Alais and Burr, 2004) and of course visuo-vestibular interactions (Angelaki et al., 2011, Gu et al., 2008). It has specifically been shown that with visuo-vestibular integration, perception of linear heading direction in monkey is formed from a near optimal combined estimate of the vestibularly derived heading direction (derived from translatory motion in the horizontal plane to activate the linear acceleration transduction organs, the otoliths in the inner ear) and from visually derived heading direction (formed from exposure to full field optic flow stimulation). In addition, it is the precision, i.e. the reciprocal of the variance, inherent in each sensory cue that determines the weighting it is given in the integration. This entails that the precision of the combined estimate is always higher than with either sensory modality alone. This may mean that the mean heading direction perceived may be erroneous due to one or both of the sensory cues being erroneously biased, yet still the brain uses each signal as a function of its reliability (Angelaki et al., 2009a, Angelaki et al., 2011). The basic method of multimodal integration using Maximum Likelihood Estimation (MLE) and Bayesian Inference is outlined in Chapter 1, section 1.3.

At first viewing the well substantiated finding of optimal sensory integration may be considered in diametric disagreement with the findings of the PET studies described, illustrating reciprocal inhibition of visual and vestibular cortices. However, it must be

understood that in these PET studies, the sensory stimulus was unimodal. Thus, it could be suggested that they describe an extreme situation in which there is little to no competition between the visual and vestibular senses for cortical control, and consequently it appears there may be an 'all or nothing' gating to which of these senses 'wins out'. However, this has been shown not to be the case. A PET study was conducted which utilised a bimodal activation of cortex with simultaneous vestibular and visual stimuli (Deutschlander et al., 2002). Given the confines of the PET apparatus and placement of subjects, it was impossible to obtain a naturalistic whole body rotation to simulate normal vestibular activation in one's environment. As in previous studies the caloric irrigation was used as a substitute, providing a sensation of rotation in the frontal plane. The visual stimulus was small field visual motion stimulation in roll – a rotating disk at which subjects focused at the centre and did not induce perception of self-motion i.e. circular vection. It must be noted that in multimodal sensory interactions, to simulate locomotion and movement in the natural environment bilateral activation of the sensory organs (eyes, inner ears) must occur. However, due to the practicalities of the experimental set up this could not be the case. Nonetheless, it was shown that with bimodal, visual and vestibular stimulation, activations were apparent in both visual and vestibular cortices. No deactivations were apparent. The visual cortical activations occurred bilaterally in Brodmann areas 17 and 18, but not in area 19. Brodmann area 17 is anatomically equivalent to the exstriate, primary visual cortex V1. Brodmann areas 18 to 19 are equivalent to the exstriate cortices which are jointly considered as the 'visual association areas' involved in image interpretation (Gazzaley et al., 2007). Vestibular cortical deactivations were biased toward the right hemisphere and the posterior insula and retroinsular regions which have been shown to be the human analogue of monkey

PIVC, and considered to be the core region of the multisensory vestibular cortical network (Grüsser et al., 1990, Guldin and Grüsser, 1996). In the same study under unimodal vestibular stimulation, temporo-parietal vestibular areas were activated including the posterior insular and retroinsular (human analogue of PIVC). Visual cortical areas were also deactivated consisting Brodmann areas 17-19 and Brodmann junction 19/37 where the human homologues of monkey V5/MT and MST are located (Heide et al., 1996). Conversely, under visual motion stimulation, temporo-parietal vestibular areas were deactivated and visual cortical areas including visual motion area V5/MT+ were activated.

These findings suggest that it is entirely possible that a reciprocal inhibitory interaction of the visual and vestibular cortices caused by antagonistic sensory stimuli is consistent with an optimal integration of these sensory stimuli by the brain. Concomitant activation of these cortices by motion transduction between visual (rotating disk stimulus in frontal roll plane) and vestibular (unilateral right caloric irrigation) displays a gross integration of the visual and vestibular signals (evidenced by PET) consistent with that expected from a weighting of the relative contributions of both sensory stimuli. Specifically, a unimodal visual stimulus incurs an activation of visual cortices and deactivation of vestibular cortices, a unimodal vestibular stimulus the converse result, and concurrent bimodal stimuli incurs a reduced and more moderate activation of both cortices than either stimulus alone, with no concurrent cortical deactivations. It can consequently be argued that the reciprocal inhibitory function of these two sensory modalities underpins the weighting of each by the brain when their information reaches conscious perception. A stronger activation of cortex may then be argued to relate to a higher precision of the sensory

stimulus, and thus weighting in a multisensory integration. Even from such a gross interaction, it is clear that cortical activations of either sensory modality are stronger than respective deactivations, which is apparent in the solely moderate activation of both visual and vestibular cortices with bimodal stimulation (Deutschlander et al., 2002).

Response of V5/MT+ to a vestibular stimulus as measured by TMS evoked phosphenes.

The current study took a TMS approach to the study of visuo-vestibular cortical interactions. The dependent variable measured is the probability of observing a phosphene with TMS stimulation over visual cortex (in this instance, LEFT visual motion area V5/MT+). The argument for this approach being that the probability of phosphenes observed out of a number of trials ($P_{phosphene}$) represent an interaction of i) the magnitude of neuronal activation caused by the TMS stimulus, and ii) the concomitant baseline activation of the neuronal substrate of visual cortex (Seemungal et al., 2012). The latter factor predicated upon other independent variables (i.e. not TMS) expected from the research question. The term 'excitability' refers to the capacity of the neuronal substrate of cortex to be activated relative to a specified datum state. For example, when the neuronal activation of cortex is hypothetically nil, it is maximally 'excitable'. When cortex is maximally neuronally activated (saturated), it is no longer excitable.

It has already been shown that the ability to observe (TMS evoked) phosphenes in V5/MT+ are reduced when the brain is under concomitant vestibular stimulation (unilateral caloric irrigation) (Seemungal et al., 2012). In that study, the phosphenes

were elicited at subjects' 50% threshold to phosphene perception, and concomitant caloric irrigation engendered symptoms of nausea and fatigue which were difficult to disambiguate from the specific perception of a vestibular stimulus (Seemungal et al., 2012). In the current study I took measures to disambiguate the effect of vestibular perception from nausea by choosing a 'real-world' vestibular stimulus (whole body rotation in yaw) and delivering non-vertiginous magnitudes of vestibular activation from the lowest signal required to elicit a perception (50% threshold to vestibular perception) to a moderate real-world activation (1.5 x 50% threshold, assumed ≈ 75%). Furthermore, in the context of studies indicating effects of laterality on visual-vestibular cortical interaction (Deutschlander et al., 2002, Dieterich et al., 2003) the independent variables, other than the TMS used to elicit phosphenes, were expected to comprise: magnitude of vestibular activation, direction of vestibular activation in yaw, with the prediction that a temporal, stimulus onset asynchrony (SOA) of vestibular and visual TMS stimuli may play a part in the interaction due to cueing effects (Barnett-Cowan and Harris, 2009). Hence all these were included as variables in the experiment and analysed as factors in the analysis.

The interaction of relative TMS intensity and magnitude of vestibular activation.

I found an interaction between the relative intensity of TMS delivered to produce phosphenes (50% and 70% thresholds) and the intensity of the relative vestibular activation delivered (50% threshold, 1.5 x 50% threshold) as evidenced by a 2 x 2 repeated measures ANOVA, ($F(1,21) = 4.72$, $P=0.042$). The interaction is illustrated in figure 5.5. and suggests that phosphene perception with 50% threshold TMS is reduced by increased vestibular activation (from 50% threshold to suprathreshold

levels), phosphene perception, whereas 70% threshold TMS remained unaffected. However, it must be stressed that no significant main effect was observed; paired t-test performed at 50% phosphene threshold level, between 50% and 1.5 x 50% threshold vestibular perception levels showed no significant difference (P = 0.075).

I propose an explanation for the interaction observed that comprises two factors, i) the relative signal strengths of visual and vestibular stimuli ii) increased vestibular activation causes a temporal cueing effect to increase the probability of correct perception a phosphene thereafter. The first factor expounds reciprocal inhibition of the visual and vestibular cortices; phosphenes induced with a 70% threshold, relative intensity of TMS are less affected/may not be affected by concurrent vestibular activation, whilst phosphenes induced at the weaker, 50% threshold are reduced. The second factor is predicated upon the perception of vestibular activation. A higher, suprathreshold perception of vestibular activation provides a more reliable, temporal cue to attend to the impending presence of a TMS pulse than a threshold perception; despite the same stimulus reducing the ability of phosphenes to be perceived from V5/MT+. These two factors could therefore cancel each other out.

Temporal cueing effect of vestibular perception dependent on visuo-vestibular stimulus onset asynchrony.

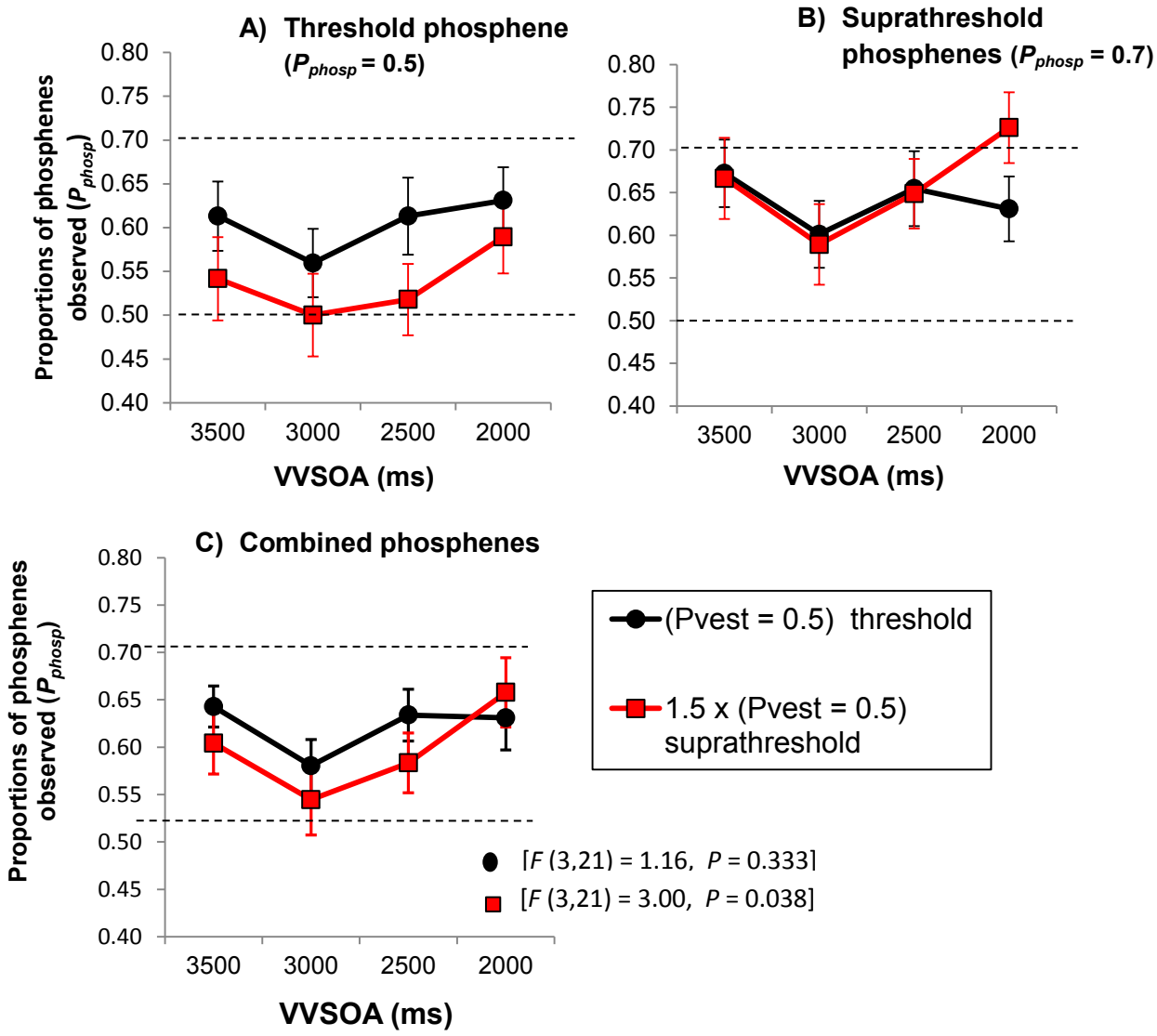

Figure 5.8. PROPORTIONS OF PHOSPHENES OBSERVED WITH LEVEL OF VVSOA (visual-vestibular stimulus onset asynchrony). Pane A) Threshold phosphene responses (P_{phosp} = 0.5). Pane B) Suprathreshold phosphene responses (P_{phosp} = 0.7), Pane C) Combined phosphene responses. Black graphs represent (V_{est} = 0.5) threshold vestibular stimulation, red graphs represent (1.5 x V_{est} = 0.5) suprathreshold vestibular stimulation. Dotted lines indicate average, baseline phosphene threshold (P_{phosp} = 0.5) and suprathreshold (P_{phosp} = 0.7) levels. Error bars represent standard error of the mean (SEM).

The temporal cueing effect is also dependent upon the delay to chair rotation onset as evidenced by the plot in figure 5.7. However, this data can be split by level of phosphene perception, and vestibular perception, and also put in terms of stimulus onset asynchrony (SOA) between onset of the vestibular activation and onset of the TMS pulse evoking a phosphene, to more clearly describe the effect of delay to chair rotation onset (*see fig. 5.8.*). To be clear, as the onset to the TMS pulse delivered on each trial was constant at 4000ms, the variable chair delay onset of 500ms, 1000ms, 1500ms, and 2000ms is synonymous with an SOA between chair rotation and TMS pulse of 3500ms, 3000ms, 2500ms and 2000ms, respectively (i.e. the temporal cueing effect is only present at 2000ms SOA between chair rotation onset and TMS pulse).

A differential cueing effect caused by high vestibular activation was observed only when the SOA was as small as 2000ms (equivalent to a delay to chair rotation onset as late as 2000ms). Comparison of 50% vs. 75% threshold vestibular activation in panes (a), (b) and (c) in figure 5.8. provide a comprehensive illustration to make the temporal cueing effect clear. Pane (c) includes rANOVA tests across all SOA, which shows that this cueing effect is only apparent for suprathreshold phosphenes [F (3,21) = 3.00, P = 0.038], and not threshold phosphenes ([F (3,21) = 1.16, P = 0.333].

It may be that an increase in phosphenes observed due to the temporal cueing effect is associated with attentional resources priming V5/MT+ for when visuo-cortical stimulation is delivered (Treue and Maunsell, 1996).

Intersubject and intrasubject variability

Figure 5.6 illustrates intersubject variability of responses in the experiment. A moderate sample of subjects was required to take part (21 subjects), and it is clear that subject variability in this study was high relative to the small effect and the possible reasons for this numerous. Aside from currently unknown intersubject factors which could include the anatomical differences and genetic polymorphisms proposed in models of TMS in motor cortex (Kleim et al., 2006), there are myriad other variables which are amenable to modulation and improvement.

Visual Thresholds

One factor could be the accuracy of obtaining visual thresholds to phosphene perception. I was able to use two types of measure to obtain values for each subject's 50% threshold to phosphene perception; the MOBS (Tyrrell and Owens, 1988) and a 20 TMS pulse count. However, due to its very nature, I was unable to use the MOBS to obtain a 70% threshold. I thus took measures to ensure congruence between the 20 pulse technique used to obtain both 50% and 70% thresholds and the adaptive staircase MOBS used to obtain datum 50% thresholds for each subject, and all relationships considered were linear (*see fig. 5.4*). MOBS is a powerful determinant of 50% (absolute) sensory thresholds and lacking this tool for the 70% threshold, it may have been more appropriate to minimise error by choosing a higher suprathreshold value closer to 100%. For example, if one considers a psychometric function of probability of observing a phosphene as a response to TMS, a 90% threshold value should engender less variability than a 70% threshold due to heteroscedasticity of sensory responses with magnitude of stimulus. As a corollary of this, performing a 2 x 2 Repeated Measures ANOVA between the levels

of phosphene and vestibular perception would benefit from both i) a larger difference between the levels of phosphene perception ii) lower response variability at suprathreshold phosphene perception. An alternative to this approach would be to use an adaptive staircase technique other than the standard MOBS. There are such techniques where a bias may be introduced between upward and downward steps of the staircase which allow for thresholds other than 50%, and these techniques are termed 'transformed up-down methods'. A number of these methods are described in the discussion section of Chapter 4, but a good example is that developed by (Kaernbach, 1991) in which a weighted approach step size is used, producing a ratio between upward and downward steps which permits a threshold of any magnitude to be achieved.

In addition, an adaptive staircase technique could also have been used to obtain a like for like datum for the 70% phosphene threshold obtained with the 20 pulse technique (*see methods*). As outlined in the Discussion section of Chapter 4, there is a fast, adaptive staircase technique that can theoretically obtain any threshold value, which should be used in future experiments that compare phosphene responses obtained with TMS of disparate thresholds (Kaernbach, 1991).

Vestibular Thresholds

A second factor contributing to inter-subject variability could lie in the accuracy of obtaining vestibular perception thresholds. Here, within a fixed 5 second time frame, the velocity of chair rotation used was adapted to independent left and right 50% thresholds. This was performed by a MOBS program and utilised a 'boundary difference' parameter which set a minimum limit to the disparity between the magnitude of consecutive rotation velocities. As such, this set the 'floor' beyond which the accuracy of vestibular thresholds could not be measured; with a minimum achievable threshold of approximately $0.85^{\circ}/s^2$. As a comparison, and using a similar MOBS approach, it has previously been shown that the vestibular perceptual thresholds of a cohort of 14 young adults was $1.18^{\circ}/s^2$ (Seemungal et al., 2004). Removing the boundary difference parameter theoretically allows very fine discrimination of vestibular thresholds, below $0.85^{\circ}/s^2$. Practically though, at these levels of discrimination, subjects were found to get highly disoriented and their responses over time erratic. Indeed, without the boundary difference parameter (set to the minimum integer value of 1), subjects would often converge on a threshold value, lose it and then become unable to discriminate their motion from even high angular accelerations. I also found that if the result of a vestibular threshold test appeared erroneous and required repeating, a break in testing was needed before a second attempt was made. Without this break, involving the room lights being turned on and the subject being able to see visual landmarks, the second attempt further confused them. With the break, however, the subjects then usually performed the task without complication. I am confident that this improvement in performance is related to a recalibration of visual-and vestibular spatial orientation. Despite its drawbacks and as far as I know, the MOBS approach affords the most reliable

measure of vestibular perceptual threshold available (Seemungal et al., 2004). There is an alternative approach, which utilises fixed duration velocity steps, which increase in magnitude until the subject perceives the rotation. However this was only formulated for use in vertiginous patients, who could not attend for the number of trials required with the MOBS approach (Cutfield et al., 2011).

It must also be stated that as with the visual thresholds to phosphene perception, there may have been scope to increase the ~75% (1.5 x 50%) threshold magnitude of vestibular activation relative to the 50% threshold magnitude of vestibular activation for each subject. This would have been in order to maximise the power of factorial analysis. However, a concern here was what level of vestibular activation would make subjects feel symptoms of dizziness, such as prove nauseogenic. I did not want to engender any such symptoms as these could engage additional parts of the brain and thus confound analysis of the visuo-vestibular interaction in terms of visual and vestibular cortices. A previous study shows a specific down regulation effect of caloric irrigation on perception of phosphenes in area V5/MT+ (Seemungal et al., 2012), but this must be considered in the context of how much of this effect was due to the perception of the vestibular activation itself in addition to the corollaries of such a high activation of the vestibular system; such as nausea and fatigue. Thus, in this study, a conservative measure of suprathreshold vestibular activation was sought. It could be argued that a further pre-test or pilot study could have been conducted to ascertain the magnitude of vestibular activation that precipitated any noxious symptoms, to establish that this was well above those magnitudes used in the main visuo-vestibular experiment. This could be expected as the stimulus used was a velocity ramp input of short duration (5 seconds) with no

sinusoidal component. It is well known that symptoms of motion sickness are strongly associated with the sense of translational, sinusoidal motion in the region of 0.2Hz (Golding et al., 2001) and circumstances of sensory conflict (Denise et al., 2009). In the example of a caloric irrigation, sensory conflict is engendered by vestibular activation in the absence of motion. Therefore, further studies could investigate the scope for increased suprathreshold vestibular activation above the ~75% (1.5 x 50%) threshold magnitude.

Attention and fatigue

A third factor that could account for inter subject variability was attention level and fatigue. I tested subjects between the hours of 9am and 3.30pm and asked them if they were feeling fatigued from their days' or previous night's exertions. In some instances subjects returned to perform the experiment when they were feeling more alert. During the experiment, I also gave subjects verbal feedback to motivate them and give them a sense of their progress. During the main visuo-vestibular interaction experiment, I informed subjects of when they were half way through a 'block' of trials. Between blocks I also asked how subjects were feeling and offered them water or a short break from the task if they were finding it repetitive and becoming inattentive. Subjects were also informed of how many out of the 8 blocks they had completed and given feedback of their progress. Subjects generally reported that the encouragement and feedback was useful. They also reported that over the duration of the experiment, it became more difficult for them to discriminate their self-motion during trials and thus they found attending to rotations in the chair harder. As well as fatigue, this can also be explained by the vestibular system becoming effectively open loop in darkness. Without visual feedback, path integration via vestibular

means accrues errors (Glasauer et al., 2002, Tcheang et al., 2011). Unfortunately, it was impossible to provide subjects with intermittent visual landmark feedback to recalibrate their vestibular rotary path integration. It was imperative to maintain the subject's dark adaptation (Pianta and Kalloniatis, 2000) and changing this would alter the conditions with which they saw phosphenes.

Effect of delay to chair rotation onset a pre-attentional response

Variability could also be caused by temporal noise affecting the perception of phosphenes (*see fig. 5.6.*). Indeed, the variable delay to rotation onset, after the warning beep, was used to afford such temporal noise (*see fig. 5.2*). The purpose being to mitigate a strategy of purely timing when a TMS pulse was due to observe a phosphene. If such a strategy were used, this could undermine a subject's attendance to the chair rotation and thus encoding of the vestibular stimulus. Hence, a compromise was to allow the subject to use their perception of the vestibular stimulus as a cue for attendance to the possibility of observing a phosphene from the TMS pulse, but vary the cue temporally to probe its effect. Indeed there was an effect of delay to chair rotation onset $F(3,21) = 3.52$ $P = 0.02$) (*see fig 5.6.*). The interpretation is that there is a minima in phosphene perception when chair rotation begins 3s prior to TMS delivery, itself delivered at a constant 4s from trial onset (*see fig 5.2.*). This is independent of either relative strength of TMS ($F(3,21) =0.95$, $P=0.963$) or vestibular activation delivered ($F(3,21) =0.81$, $P=0.491$). A plot of delay of rotation onset against averaged probability of observing a phosphene clearly shows the quadratic trend (*see fig. 5.6.*). Interestingly, this effect seems independent of the cueing effect to phosphene perception previously described, and which only occurred at a delay to chair rotation onset of 2000ms (or equivalently

SOA prior to TMS pulse of 2000ms) (*see fig. 5.8.*). The effect currently described could be due to a subconscious pre-attenional, bottom up response of V5/MT+, models of which have previously been described to occur in primary visual cortex V1 (Zhaoping and Guyader, 2007). This would explain why it is not modulated by suprathreshold levels of visuo-cortical and vestibular activation any differently to threshold levels. Assuming the cueing effect was pre-attentional, and given it occurs in concert with a shorter latency, supraliminal cueing effect, this raises the intriguing possibility that each cueing effect uses different pathways to V5/MT+. It has already been shown that with lesion to V1 (the main input to V5/MT+) visual signals still reach V5/MT+ subconsciously via a fast pathway that bypasses V1 in a form of 'blindsight' (Zeki and Ffytche, 1998), and it has been suggested that vestibular input may also possess a direct pathway to V5/MT+ (Seemungal et al., 2012).

Conclusion

To my knowledge this is the first time that non-caloric, whole body vestibular stimulation in yaw has been shown to modulate visual motion area V5/MT+. This modulation is consistent with a reciprocally inhibitive interplay between visual and vestibular cortex, although does not show such a relationship. This study also shows that stimulus onset asynchrony (SOA) between vestibular and visual stimuli is a factor in resultant phosphene perception.

Chapter 6.
Conclusions

Introduction

The primary objectives of this thesis were to discern whether visual motion area (V5/MT+) differentially encodes visual motion coherence and how allocentric visual cues interact with vestibular system to tell us where and when we are in physical space. I did not show a differential encodement of visual motion coherence by V5/MT+, although I argue how larger sample size was required to fully satisfy the analyses used. I also showed that reweighting of visual (allocentric) and vestibular (egocentric) signals of angular motion occurs with reduction in reliability of the visual signal, and that the visual signal can even be encoded subliminally.

A secondary objective was to develop current techniques for the recording and analysis of visuo-vestibular sensory information for the purpose of multisensory, multimodal integration. Although I did not show differential encodement of coherent vs. random motion by V5/MT+, in the same experiment, I did show how the relative intensity of TMS used to elicit phosphenes impacts upon the modulation of V5/MT+ by a visual motion stimulus; which is important in understanding what an excitation or inhibition of cortex practically means.

I also showed in a factorial design experiment, that a visuo-vestibular interaction takes place between TMS evoked phosphenes in V5/MT+, and real-world vestibular

stimulation from whole body rotation in yaw. I also showed that a Bayesian approach to estimating vestibularly derived angular position in yaw exhibits a high enough resolution to model responses at the subject level.

In this chapter, I will also discuss how the current work could be furthered in future work.

Mode of visuo-vestibular integration

Visual motion & vestibular motion

To afford enhanced spatial orientation in human navigation, there are two perceptual modes by which visual system interacts with vestibular system. The first mode involves the processing of visual motion cues for integration with vestibular motion cues in the estimation of egocentric positioning during path integration (Kearns et al., 2002, Glasauer et al., 2002). Translational combinations of optic flow and linear whole body motion (activating the otoliths) have shown integration in monkey MSTd, and with visual motion input from visual motion area V5/MT+ (Angelaki et al., 2009a, Angelaki et al., 2011, Gu et al., 2007, Gu et al., 2008, Gu et al., 2012). A similar integration of angular orientation cues is yet to be shown in either monkey or human. However, in humans, visual motion is shown to differentially activate V5/MT+ as a function of visual motion coherence (see Chapter 4.). This is a key finding as V5/MT+ provides the primary input to MST which is critical for the processing of optic flow and hence heading direction. I hypothesised that V5/MT+ may be used as a surrogate marker for MST activity, with encoding of motion coherence (noise) in

V5/MT+ a correlate of the motion coherence of full field optic flow constructs in MST (Duffy and Wurtz, 1997).

I did not find the differential encodement of visual motion coherences by V5/MT+ that I was looking for, and found that my sample size was too small to form reliable estimates with the analytical methods used. I do believe there is much scope for performing a further study with larger samples and the current data could form the basis of a power calculation to do this.

I also hypothesised that V5/MT+ activity would be modulated by whole body motion in yaw (Chapter 6.). The rational being that as a function of vestibular perceptual threshold, the faster the whole body rotation, the less excitable V5/MT+ becomes to TMS evoked phosphene induction (a measurable analogue of external visual stimulation). Reciprocally, the more reliable the phosphene induction (as a function of relative TMS intensity used), the less whole body rotation diminished V5/MT+ excitability. Such a finding would expound the reciprocal inhibitory model of visual and vestibular cortex (Brandt et al., 1998, Deutschlander et al., 2002, Dieterich et al., 2003). Critically, it would illustrate a differential modulation of V5/MT+ dependent upon intensity of vestibular stimulation.

I cannot conclude such a reciprocally inhibitive interaction was found. Although my experiment (Chapter 5) showed a significant interaction between visual phosphenes and vestibular stimulation perceived, there were no significant main effects. I argue that this experiment be considered a feasibility study, and further experiments using a similar paradigm be conducted using the current knowledge gained. As outlined in the discussion of Chapter 6, especially fruitful might be to increase the disparity in magnitude between levels of visual phosphene and vestibular stimulation used,

respectively; and improve the methods used to establish both visual and vestibular thresholds. The results from the current study could also inform power calculations for sample sizes in future studies.

Future work investigating reciprocal inhibition of visual and vestibular cortices, could also explore the two sensory factors in more detail. For example, using the method of constant stimuli, a range of TMS thresholds could be probed between 50% threshold and 70% threshold, with a range of vestibular perceptual thresholds similarly probed. Exploring these factors within the same study could determine whether reciprocal inhibition of visual and vestibular cortices (if such is the case) accords with an optimal, multimodal integration of the cues predicated on their relative reliability. This is best described by a Bayesian inference model (Deneve and Pouget, 2004).

Visual landmarks & vestibular motion

The second mode of visual-vestibular spatial interaction also relates to human path integration. Recognition of object form and encoding of visual landmarks is used as a calibrator of online vestibular spatial orientation which 'leaks' over time (Glasauer et al., 2002). Human spatial orientation in yaw is dominated by allocentric cues from visual landmarks, which override egocentric, vestibular derived estimates of heading direction. It has been shown that in circumstances of sensory conflict, erroneous visual presentation of the environment is used exclusively (see Chapter 3.) However, I have shown that under circumstances of a 'noisy' visual environment and unreliable visual landmark cues, the brain does allow for integration of veridical vestibular cues. Furthermore, integration occurs as a function of the 'noisiness' of the visual landmark cues used (see Chapter 3.) Indeed, I also show that vestibular

spatial ‘time’ signals, i.e. percepts of motion duration, are modulated by visual landmark cues at the subliminal level. This suggests some of the pathways which allow calibration of vestibular spatial information by visual landmarks are bottom-up, pre-attentional and thus bypass the perceptual networks of the brain involved in conscious awareness (Zhaoping and Guyader, 2007). What remains unclear is the manner in which the integration of visual landmark and vestibulospatial information takes place. In Chapter 2. I show the utility of forced choice data acquisition methods to obtain reliable estimates of the characteristics of vestibular orientation such as mean angular position and variance. The characteristics were modelled by a non-frequentist, Bayesian Inference model which exploits parametric measures (Wichmann and Hill, 2001a, Wichmann and Hill, 2001b, Kuss et al., 2005). In combination these are powerful tools to explore visual and vestibular interactions. Bayesian inference has proven effective for modelling multimodal interactions (Deneve and Pouget, 2004) and it is critical that sensory stimuli within different frames of reference be recorded in a way that is interpretable by a Bayesian model, i.e. the method of constant stimuli (Klein, 2001, Ernst and Banks, 2002).

Utility of using differential TMS of visual area V5/MT+

In the studies of Chapters 4. & 5. I used TMS to probe the activity of V5/MT+ through the induction of phosphenes. In Chapter 4. I showed the utility of probing V5/MT+ response to visual motion at a range of relative TMS intensities using the method of constant stimuli. I showed modulation of V5/MT+ excitability independent of visual motion stimulus used, but dependent upon the relative TMS intensity. I also provided a theory of how to interpret the modulation based on the existing theory that TMS preferentially facilitates the activity of non-signal carrying neurons (Silvanto et

al., 2007). The utility of this finding is that modulation of visual cortex in prior and future studies may be better understood as a function of the relative intensity of TMS used. This provides the framework for a baseline by which phosphene induction studies may be measured and to further clarify the response of visual cortex to TMS. Indeed, the finding of a differential effect between 50% and 70% TMS thresholds (during the study in Chapter 4.) was utilised in the study in Chapter 5. which was performed subsequently.

Summary

The work undertaken in this thesis fulfils some of the objectives outlined in the Abstract. This body of work adds a significant contribution to knowledge in the fields of systems neuroscience, visual psychophysics and neuro-otology. The work has been conducted under critical review of prior research and has been justified within that context.

Bibliography

AITKEN, C. G. 1999. Sampling--how big a sample? *J Forensic Sci,* 44**,** 750-60.

ALAIS, D. & BURR, D. 2004. The ventriloquist effect results from near-optimal bimodal integration. *Curr Biol,* 14**,** 257-62.

ALBRIGHT, T. D. 1984. Direction and orientation selectivity of neurons in visual area MT of the macaque. *J Neurophysiol,* 52**,** 1106-30.

ALLMAN, J., MIEZIN, F. & MCGUINESS, E. 1990. Effects of background motion on the responses of neurons in the first and second cortical visual areas. *In:* EDELMAN, G., GALL, W. & COHEN, W. (eds.) *Signal and Sense: Local and Global Order in Perceptual Maps.* New York: Wiley.

ANDERSEN, R. A., SNYDER, L. H., BRADLEY, D. C. & XING, J. 1997. Multimodal representation of space in the posterior parietal cortex and its use in planning movements. *Annu Rev Neurosci,* 20**,** 303-30.

ANGELAKI, D. E., GU, Y. & DEANGELIS, G. C. 2009a. Multisensory integration: psychophysics, neurophysiology, and computation. *Curr Opin Neurobiol,* 19**,** 452-8.

ANGELAKI, D. E., GU, Y. & DEANGELIS, G. C. 2011. Visual and vestibular cue integration for heading perception in extrastriate visual cortex. *J Physiol,* 589**,** 825-33.

ANGELAKI, D. E., KLIER, E. M. & SNYDER, L. H. 2009b. A vestibular sensation: probabilistic approaches to spatial perception. *Neuron,* 64**,** 448-61.

ASHER, D. L. & SANDO, I. 1981. Perilymphatic communication routes in the auditory and vestibular system. *Otolaryngol Head Neck Surg,* 89**,** 822-30.

BALOCH, A. A., GROSSBERG, S., MINGOLLA, E. & NOGUEIRA, C. A. 1999. Neural model of first-order and second-order motion perception and magnocellular dynamics. *J Opt Soc Am A Opt Image Sci Vis,* 16**,** 953-78.

BAR, M., TOOTELL, R. B., SCHACTER, D. L., GREVE, D. N., FISCHL, B., MENDOLA, J. D., ROSEN, B. R. & DALE, A. M. 2001. Cortical mechanisms specific to explicit visual object recognition. *Neuron,* 29**,** 529-35.

BARKER, G. R. & WARBURTON, E. C. 2011. When is the hippocampus involved in recognition memory? *J Neurosci,* 31**,** 10721-31.

BARMACK, N. H. 2003. Central vestibular system: vestibular nuclei and posterior cerebellum. *Brain Res Bull,* 60**,** 511-41.

BARNETT-COWAN, M. & HARRIS, L. R. 2009. Perceived timing of vestibular stimulation relative to touch, light and sound. *Exp Brain Res,* 198**,** 221-31.

BECKERS, G. & HOMBERG, V. 1992. Cerebral visual motion blindness: transitory akinetopsia induced by transcranial magnetic stimulation of human area V5. *Proc Biol Sci,* 249**,** 173-8.

BELTON, T. & MCCREA, R. A. 2000. Role of the cerebellar flocculus region in the coordination of eye and head movements during gaze pursuit. *J Neurophysiol,* 84**,** 1614-26.

BENSE, S., STEPHAN, T., YOUSRY, T. A., BRANDT, T. & DIETERICH, M. 2001. Multisensory cortical signal increases and decreases during vestibular galvanic stimulation (fMRI). *J Neurophysiol,* 85**,** 886-99.

BLAIR, S. M., GAVIN, M., 1981. Brainstem commissure and control of time constant of vestibular nystagmus. *Acta otolar.,* 91**,** 1–8.

BLANKE, O., LANDIS, T., SPINELLI, L. & SEECK, M. 2004. Out-of-body experience and autoscopy of neurological origin. *Brain,* 127**,** 243-58.

BLANKE, O., MOHR, C., MICHEL, C. M., PASCUAL-LEONE, A., BRUGGER, P., SEECK, M., LANDIS, T. & THUT, G. 2005. Linking out-of-body experience and self processing to mental own-body imagery at the temporoparietal junction. *J Neurosci,* 25**,** 550-7.

BLANKE, O., ORTIGUE, S., LANDIS, T. & SEECK, M. 2002. Stimulating illusory own-body perceptions. *Nature,* 419**,** 269-70.

BLOCK, N. 2005. Two neural correlates of consciousness. *Trends Cogn Sci,* 9**,** 46-52.

BOGACZ, R., BROWN, E., MOEHLIS, J., HOLMES, P. & COHEN, J. D. 2006. The physics of optimal decision making: a formal analysis of models of performance in two-alternative forced-choice tasks. *Psychol Rev,* 113**,** 700-65.

BOTTINI, G., KARNATH, H. O., VALLAR, G., STERZI, R., FRITH, C. D., FRACKOWIAK, R. S. & PAULESU, E. 2001. Cerebral representations for egocentric space: Functional-anatomical evidence from caloric vestibular stimulation and neck vibration. *Brain,* 124**,** 1182-96.

BOTTINI, G., STERZI, R., PAULESU, E., VALLAR, G., CAPPA, S. F., ERMINIO, F., PASSINGHAM, R. E., FRITH, C. D. & FRACKOWIAK, R. S. 1994. Identification of the central vestibular projections in man: a positron emission tomography activation study. *Exp Brain Res,* 99**,** 164-9.

BOUMAN, M. A. 1955. Absolute threshold conditions for visual perception. *J Opt Soc Am,* 45**,** 36-43.

BRADDICK, O., HARTLEY, T., O'BRIEN, J., ATKINSON, J., WATTAM-BELL, J. & TURNER, R. 1998. Brain areas differentially activated by coherent visual motion and dynamic noise. *Neuroimage,* 7.

BRADDICK, O. J., O'BRIEN, J. M., WATTAM-BELL, J., ATKINSON, J. & TURNER, R. 2000. Form and motion coherence activate independent, but not dorsal/ventral segregated, networks in the human brain. *Curr Biol,* 10**,** 731-4.

BRANDT, T., BARTENSTEIN, P., JANEK, A. & DIETERICH, M. 1998. Reciprocal inhibitory visual-vestibular interaction. Visual motion stimulation deactivates the parieto-insular vestibular cortex. *Brain,* 121 (Pt 9)**,** 1749-58.

BRANDT, T., DIETERICH, M. & DANEK, A. 1994. Vestibular cortex lesions affect the perception of verticality. *Ann Neurol,* 35**,** 403-12.

BRANDT, T., MARX, E., STEPHAN, T., BENSE, S. & DIETERICH, M. 2003. Inhibitory interhemispheric visuovisual interaction in motion perception. *Ann N Y Acad Sci,* 1004**,** 283-8.

BREITMEYER, B. G. 2007. Visual masking: past accomplishments, present status, future developments. *Adv Cogn Psychol,* 3**,** 9-20.

BREMMER, F., DUHAMEL, J. R., BEN HAMED, S. & GRAF, W. 2002a. Heading encoding in the macaque ventral intraparietal area (VIP). *Eur J Neurosci,* 16**,** 1554-68.

BREMMER, F., KLAM, F., DUHAMEL, J. R., BEN HAMED, S. & GRAF, W. 2002b. Visual-vestibular interactive responses in the macaque ventral intraparietal area (VIP). *Eur J Neurosci,* 16**,** 1569-86.

BROADBENT, N. J., SQUIRE, L. R. & CLARK, R. E. 2004. Spatial memory, recognition memory, and the hippocampus. *Proc Natl Acad Sci U S A,* 101**,** 14515-20.

BUCKINGHAM, T. 1987. The influence of temporal frequency and wavelength on beta movement. *Ophthalmic Physiol Opt,* 7**,** 5-8.

BUETTNER, U. W., BUTTNER, U. & HENN, V. 1978. Transfer characteristics of neurons in vestibular nuclei of the alert monkey. *J Neurophysiol,* 41**,** 1614-28.

BULLIER, J. 2001. Feedback connections and conscious vision. *Trends Cogn Sci,* 5**,** 369-370.

CAMPOS, A., CANIZARES, F. J., SANCHEZ-QUEVEDO, M. C. & ROMERO, P. J. 1990. Otoconial degeneration in the aged utricle and saccule. *Adv Otorhinolaryngol,* 45**,** 143-53.

CANNON, S. C. & ROBINSON, D. A. 1985. An improved neural-network model for the neural integrator of the oculomotor system: more realistic neuron behavior. *Biol Cybern,* 53**,** 93-108.

CANNON, S. C. & ROBINSON, D. A. 1987. Loss of the neural integrator of the oculomotor system from brain stem lesions in monkey. *J Neurophysiol,* 57**,** 1383-409.

CARLETON, S. C. & CARPENTER, M. B. 1984. Distribution of primary vestibular fibers in the brainstem and cerebellum of the monkey. *Brain Res,* 294**,** 281-98.

CHOWDHURY, S. A., TAKAHASHI, K., DEANGELIS, G. C. & ANGELAKI, D. E. 2009. Does the middle temporal area carry vestibular signals related to self-motion? *J Neurosci,* 29**,** 12020-30.

CHRISTENSEN, M. S., KRISTIANSEN, L., ROWE, J. B. & NIELSEN, J. B. 2008. Action-blindsight in healthy subjects after transcranial magnetic stimulation. *Proc Natl Acad Sci U S A,* 105**,** 1353-7.

CLARKE, A. H., SCHONFELD, U. & HELLING, K. 2003. Unilateral examination of utricle and saccule function. *J Vestib Res,* 13**,** 215-25.

COLBY, C. L. & GOLDBERG, M. E. 1999. Space and attention in parietal cortex. *Annu Rev Neurosci,* 22**,** 319-49.

CORNETTE, L., DUPONT, P., ROSIER, A., SUNAERT, S., VAN HECKE, P., MICHIELS, J., MORTELMANS, L. & ORBAN, G. A. 1998. Human brain regions involved in direction discrimination. *J Neurophysiol,* 79**,** 2749-65.

COURTNEY, S. M., UNGERLEIDER, L. G., KEIL, K. & HAXBY, J. V. 1996. Object and spatial visual working memory activate separate neural systems in human cortex. *Cereb Cortex,* 6**,** 39-49.

COUSINS, S., KASKI, D., CUTFIELD, N., SEEMUNGAL, B., GOLDING, J. F., GRESTY, M., GLASAUER, S. & BRONSTEIN, A. M. 2013. Vestibular perception following acute unilateral vestibular lesions. *PLoS One,* 8**,** e61862.

CRAGG, B. G. 1969. The topography of the afferent projections in the circumstriate visual cortex of the monkey studied by the Nauta method. *Vision Res,* 9**,** 733-47.

CRANE, B. T. 2012. Direction specific biases in human visual and vestibular heading perception. *PLoS One,* 7**,** e51383.

CRAWFORD, J. D., CADERA, W. & VILIS, T. 1991. Generation of torsional and vertical eye position signals by the interstitial nucleus of Cajal. *Science,* 252**,** 1551-3.

CRAWFORD, J. D. & VILIS, T. 1991. Axes of eye rotation and Listing's law during rotations of the head. *J Neurophysiol,* 65**,** 407-23.

CRONK, J. 2013. Gaussian density function [Chart]. Retrieved from http://guweb2.gonzaga.edu/faculty/cronk/CHEM240/images/Gaussian_graph_and_eqn.gif.

CUTFIELD, N. J., COUSINS, S., SEEMUNGAL, B. M., GRESTY, M. A. & BRONSTEIN, A. M. 2011. Vestibular perceptual thresholds to angular rotation in acute unilateral vestibular paresis and with galvanic stimulation. *Ann N Y Acad Sci,* 1233**,** 256-62.

DAS, A. 2000. Optimizing coverage in the cortex. *Nat Neurosci,* 3**,** 750-2.

DE JONG, B. M., FRACKOWIAK, R. S., WILLEMSEN, A. T. & PAANS, A. M. 1999. The distribution of cerebral activity related to visuomotor coordination indicating perceptual and executional specialization. *Brain Res Cogn Brain Res,* 8**,** 45-59.

DE RIDDER, D., VAN LAERE, K., DUPONT, P., MENOVSKY, T. & VAN DE HEYNING, P. 2007. Visualizing out-of-body experience in the brain. *N Engl J Med,* 357**,** 1829-33.

DENEVE, S. & POUGET, A. 2004. Bayesian multisensory integration and cross-modal spatial links. *J Physiol Paris,* 98**,** 249-58.

DENISE, P., VOURIOT, A., NORMAND, H., GOLDING, J. F. & GRESTY, M. A. 2009. Effect of temporal relationship between respiration and body motion on motion sickness. *Autonomic Neuroscience,* 151**,** 142-146.

DEUTSCHLANDER, A., BENSE, S., STEPHAN, T., SCHWAIGER, M., BRANDT, T. & DIETERICH, M. 2002. Sensory system interactions during simultaneous vestibular and visual stimulation in PET. *Hum Brain Mapp,* 16**,** 92-103.

DIETERICH, M., BENSE, S., LUTZ, S., DRZEZGA, A., STEPHAN, T., BARTENSTEIN, P. & BRANDT, T. 2003. Dominance for vestibular cortical function in the non-dominant hemisphere. *Cereb Cortex,* 13**,** 994-1007.

DIETERICH, M. & BRANDT, T. 2008. Functional brain imaging of peripheral and central vestibular disorders. *Brain,* 131**,** 2538-52.

DIGRE, K. B. 1986. Opsoclonus in adults. Report of three cases and review of the literature. *Arch Neurol,* 43**,** 1165-75.

DUBNER, R. & ZEKI, S. M. 1971. Response properties and receptive fields of cells in an anatomically defined region of the superior temporal sulcus in the monkey. *Brain Res,* 35**,** 528-32.

DUFFY, C. J. & WURTZ, R. H. 1997. Medial superior temporal area neurons respond to speed patterns in optic flow. *J Neurosci,* 17**,** 2839-51.

DUHAMEL, J. R., COLBY, C. L. & GOLDBERG, M. E. 1998. Ventral intraparietal area of the macaque: congruent visual and somatic response properties. *J Neurophysiol,* 79**,** 126-36.

EHRENSTEIN, W. & EHRENSTEIN, A. 1999. Psychophysical methods. *In:* WINDHORST, U. & JOHANSSON, H. (eds.) *Modern techniques in neuroscience research.* Har/Cdr edition ed.: Springer (1 Oct 1999).

EICKHOFF, S. B., WEISS, P. H., AMUNTS, K., FINK, G. R. & ZILLES, K. 2006. Identifying human parieto-insular vestibular cortex using fMRI and cytoarchitectonic mapping. *Hum Brain Mapp,* 27**,** 611-21.

ENGELHARDT, H., FEDDERSEN, B., BOETZEL, K. & NOACHTAR, S. 2007. The influence of caloric nystagmus on flash evoked transient and steady-state potentials. *Clin Neurophysiol,* 118**,** 2282-6.

ERNST, M. O. & BANKS, M. S. 2002. Humans integrate visual and haptic information in a statistically optimal fashion. *Nature,* 415**,** 429-33.

FASOLD, O., VON BREVERN, M., KUHBERG, M., PLONER, C. J., VILLRINGER, A., LEMPERT, T. & WENZEL, R. 2002. Human vestibular cortex as identified with caloric stimulation in functional magnetic resonance imaging. *Neuroimage,* 17**,** 1384-93.

FERNBERGER, S. W. 1949. Coefficients of precision in the method of constant stimuli. *Am J Psychol,* 62**,** 591.

FETSCH, C. R., TURNER, A. H., DEANGELIS, G. C. & ANGELAKI, D. E. 2009. Dynamic reweighting of visual and vestibular cues during self-motion perception. *J Neurosci,* 29**,** 15601-12.

FINDLAY, J. 1978. Estimates on probability functions: A more virulent PEST. *Attention, Perception, & Psychophysics,* 23**,** 181-185.

FISCHL, B. & DALE, A. M. 2000. Measuring the thickness of the human cerebral cortex from magnetic resonance images. *Proc Natl Acad Sci U S A,* 97**,** 11050-5.

FLUUR, E. 1970. The interaction between the utricle and the saccule. *Acta Otolaryngol,* 69**,** 17-24.

GALIANA, H. L. & OUTERBRIDGE, J. S. 1984. A bilateral model for central neural pathways in vestibuloocular reflex. *J Neurophysiol,* 51**,** 210-41.

GATTASS, R. & GROSS, C. G. 1981. Visual topography of striate projection zone (MT) in posterior superior temporal sulcus of the macaque. *J Neurophysiol,* 46**,** 621-38.

GAZZALEY, A., RISSMAN, J., COONEY, J., RUTMAN, A., SEIBERT, T., CLAPP, W. & D'ESPOSITO, M. 2007. Functional interactions between prefrontal and visual association cortex contribute to top-down modulation of visual processing. *Cereb Cortex,* 17 Suppl 1**,** i125-35.

GERSNER, R., KRAVETZ, E., FEIL, J., PELL, G. & ZANGEN, A. 2011. Long-term effects of repetitive transcranial magnetic stimulation on markers for neuroplasticity: differential outcomes in anesthetized and awake animals. *J Neurosci,* 31**,** 7521-6.

GLASAUER, S., AMORIM, M. A., VIAUD-DELMON, I. & BERTHOZ, A. 2002. Differential effects of labyrinthine dysfunction on distance and direction during blindfolded walking of a triangular path. *Exp Brain Res,* 145**,** 489-97.

GOLDING, J. F., MUELLER, A. G. & GRESTY, M. A. 2001. A motion sickness maximum around the 0.2 Hz frequency range of horizontal translational oscillation. *Aviat Space Environ Med,* 72**,** 188-92.

GRUNFELD, E. A., MORLAND, A. B., BRONSTEIN, A. M. & GRESTY, M. A. 2000. Adaptation to oscillopsia: a psychophysical and questionnaire investigation. *Brain,* 123 (Pt 2)**,** 277-90.

GRÜSSER, O. J., PAUSE, M. & SCHREITER, U. 1990. Localization and responses of neurones in the parieto-insular vestibular cortex of awake monkeys (Macaca fascicularis). *J Physiol,* 430**,** 537-57.

GU, Y., ANGELAKI, D. E. & DEANGELIS, G. C. 2008. Neural correlates of multisensory cue integration in macaque MSTd. *Nat Neurosci,* 11**,** 1201-10.

GU, Y., DEANGELIS, G. C. & ANGELAKI, D. E. 2007. A functional link between area MSTd and heading perception based on vestibular signals. *Nat Neurosci,* 10**,** 1038-47.

GU, Y., DEANGELIS, G. C. & ANGELAKI, D. E. 2012. Causal links between dorsal medial superior temporal area neurons and multisensory heading perception. *J Neurosci,* 32**,** 2299-313.

GULDIN, W. O. & GRÜSSER, O.J. 1996. The anatomy of the vestibular cortices of primates. *In:* COLLARD, M., JEANNEROD, M. & CHRISTEN, Y. (eds.) *Le cortex vestibulaire.* IRVINN ed. Paris: Ipsen.

GULDIN, W. O., AKBARIAN, S. & GRÜSSER, O. J. 1992. Cortico-cortical connections and cytoarchitectonics of the primate vestibular cortex: a study in squirrel monkeys (Saimiri sciureus). *J Comp Neurol,* 326**,** 375-401.

GULDIN, W. O. & GRÜSSER, O. J. 1998. Is there a vestibular cortex? *Trends Neurosci,* 21**,** 254-9.

GUZMAN-LOPEZ, J., SILVANTO, J. & SEEMUNGAL, B. M. 2011a. Visual motion adaptation increases the susceptibility of area V5/MT to phosphene induction by transcranial magnetic stimulation. *Clin Neurophysiol,* 122**,** 1951-5.

GUZMAN-LOPEZ, J., SILVANTO, J., YOUSIF, N., NOUSI, S., QUADIR, S. & SEEMUNGAL, B. M. 2011b. Probing V5/MT excitability with transcranial magnetic stimulation following visual motion adaptation to random and coherent motion. *Ann N Y Acad Sci,* 1233**,** 200-7.

HAFTING, T., FYHN, M., MOLDEN, S., MOSER, M. B. & MOSER, E. I. 2005. Microstructure of a spatial map in the entorhinal cortex. *Nature,* 436**,** 801-6.

HAHNLOSER, R. H. 2003. Emergence of neural integration in the head-direction system by visual supervision. *Neuroscience,* 120**,** 877-91.

HALL, J. L. 1981. Hybrid adaptive procedure for estimation of psychometric functions. *J Acoust Soc Am,* 69**,** 1763-9.

HAMMOND, R. S., TULL, L. E. & STACKMAN, R. W. 2004. On the delay-dependent involvement of the hippocampus in object recognition memory. *Neurobiol Learn Mem,* 82**,** 26-34.

HANSSON, E. E., BECKMAN, A. & HAKANSSON, A. 2010. Effect of vision, proprioception, and the position of the vestibular organ on postural sway. *Acta Otolaryngol,* 130**,** 1358-63.

HASEGAWA, S. 1970. [Frequency characteristics of the system of the semi-circular canals]. *Nihon Jibiinkoka Gakkai Kaiho,* 73**,** 444-8.

HEIDE, W., KURZIDIM, K. & KOMPF, D. 1996. Deficits of smooth pursuit eye movements after frontal and parietal lesions. *Brain,* 119 (Pt 6)**,** 1951-69.

HENDRY, S. H. & REID, R. C. 2000. The koniocellular pathway in primate vision. *Annu Rev Neurosci,* 23**,** 127-53.

HERRICK, R. M. 1967. Psychophysical methodology: comparison of thresholds of the method of limits and of the method of constant stimuli. *Percept Mot Skills,* 24**,** 915-22.

HIGHSTEIN, S. M. & HOLSTEIN, G. R. 2006. The anatomy of the vestibular nuclei. *Prog Brain Res,* 151**,** 157-203.

HIGHSTEIN, S. M., RABBITT, R. D., HOLSTEIN, G. R. & BOYLE, R. D. 2005. Determinants of spatial and temporal coding by semicircular canal afferents. *J Neurophysiol,* 93**,** 2359-70.

HORTON, J. C. & HOYT, W. F. 1991. The representation of the visual field in human striate cortex. A revision of the classic Holmes map. *Arch Ophthalmol,* 109**,** 816-24.

IIDA, M., SAKAI, M. & IGARASHI, M. 1997. Visual-vestibular interaction--an evoked potential study in normal human subjects. *Tokai J Exp Clin Med,* 22**,** 137-9.

IONTA, S., HEYDRICH, L., LENGGENHAGER, B., MOUTHON, M., FORNARI, E., CHAPUIS, D., GASSERT, R. & BLANKE, O. 2011. Multisensory mechanisms in temporo-parietal cortex support self-location and first-person perspective. *Neuron,* 70**,** 363-74.

ITO, J., SASA, M., MATSUOKA, I. & TAKAORI, S. 1982. Afferent projection from reticular nuclei, inferior olive and cerebellum to lateral vestibular nucleus of the cat as demonstrated by horseradish peroxidase. *Brain Res,* 231**,** 427-32.

KAERNBACH, C. 1991. Simple adaptive testing with the weighted up-down method. *Percept Psychophys,* 49**,** 227-9.

KALLONIATIS, M. & LUU, C. 2013. Psychometric function for a YES-NO paradigm [Chart]. Retrieved from http://webvision.med.utah.edu/book/part-viii-gabac-receptors/psychophysics-of-vision/.

KAMMER, T. & BAUMANN, L. W. 2010. Phosphene thresholds evoked with single and double TMS pulses. *Clin Neurophysiol,* 121**,** 376-9.

KANWISHER, N., MCDERMOTT, J. & CHUN, M. M. 1997. The fusiform face area: a module in human extrastriate cortex specialized for face perception. *J Neurosci,* 17**,** 4302-11.

KEARNS, M. J., WARREN, W. H., DUCHON, A. P. & TARR, M. J. 2002. Path integration from optic flow and body senses in a homing task. *Perception,* 31**,** 349-74.

KELSO, J. A., COOK, E., OLSON, M. E. & EPSTEIN, W. 1975. Allocation of attention and the locus of adaptation to displaced vision. *J Exp Psychol Hum Percept Perform,* 1**,** 237-45.

KLAM, F. & GRAF, W. 2003. Vestibular signals of posterior parietal cortex neurons during active and passive head movements in macaque monkeys. *Ann N Y Acad Sci,* 1004**,** 271-82.

KLATZKY, R. L. 1998. Allocentric and egocentric spatial representations: definitions, distinctions, and interconnections. *In:* FREKSA, C. H., C. WENDER K.F. (ed.) *Spatial Cognition: An interdisciplinary approach to representing and processing spatial knowledge.* New York: Springer Verlag.

KLEIM, J. A., CHAN, S., PRINGLE, E., SCHALLERT, K., PROCACCIO, V., JIMENEZ, R. & CRAMER, S. C. 2006. BDNF val66met polymorphism is associated with modified experience-dependent plasticity in human motor cortex. *Nat Neurosci,* 9**,** 735-7.

KLEIN, S. A. 2001. Measuring, estimating, and understanding the psychometric function: a commentary. *Percept Psychophys,* 63**,** 1421-55.

KOBAYASHI, M. & PASCUAL-LEONE, A. 2003. Transcranial magnetic stimulation in neurology. *Lancet Neurol,* 2**,** 145-56.

KOLSTER, H., PEETERS, R. & ORBAN, G. A. 2010. The retinotopic organization of the human middle temporal area MT/V5 and its cortical neighbors. *J Neurosci,* 30**,** 9801-20.

KORDING, K. P. & WOLPERT, D. M. 2004. Bayesian integration in sensorimotor learning. *Nature,* 427**,** 244-7.

KOUIDER, S. & DEHAENE, S. 2007. Levels of processing during non-conscious perception: a critical review of visual masking. *Philos Trans R Soc Lond B Biol Sci,* 362**,** 857-75.

KUSS, M., JAKEL, F. & WICHMANN, F. A. 2005. Bayesian inference for psychometric functions. *J Vis,* 5**,** 478-92.

LAM, C. F., DUBNO, J. R. & MILLS, J. H. 1999. Determination of optimal data placement for psychometric function estimation: a computer simulation. *J Acoust Soc Am,* 106**,** 1969-76.

LAM, K., KANEOKE, Y., GUNJI, A., YAMASAKI, H., MATSUMOTO, E., NAITO, T. & KAKIGI, R. 2000. Magnetic response of human extrastriate cortex in the detection of coherent and incoherent motion. *Neuroscience,* 97**,** 1-10.

LAMME, V. A. & ROELFSEMA, P. R. 2000. The distinct modes of vision offered by feedforward and recurrent processing. *Trends Neurosci,* 23**,** 571-9.

LAMME, V. A., SUPER, H., LANDMAN, R., ROELFSEMA, P. R. & SPEKREIJSE, H. 2000. The role of primary visual cortex (V1) in visual awareness. *Vision Res,* 40**,** 1507-21.

LAPLACE, P. S. 1814. *Essai philosophique sur les probabilités*, Courcier.

LAYCOCK, R., CREWTHER, D. P., FITZGERALD, P. B. & CREWTHER, S. G. 2007. Evidence for fast signals and later processing in human V1/V2 and V5/MT+: A TMS study of motion perception. *J Neurophysiol,* 98**,** 1253-62.

LAYCOCK, R., CREWTHER, D. P., FITZGERALD, P. B. & CREWTHER, S. G. 2009. TMS disruption of V5/MT+ indicates a role for the dorsal stream in word recognition. *Exp Brain Res,* 197**,** 69-79.

LEEK, M. R. 2001. Adaptive procedures in psychophysical research. *Percept Psychophys,* 63**,** 1279-92.

LENGGENHAGER, B., MOUTHON, M. & BLANKE, O. 2009. Spatial aspects of bodily self-consciousness. *Conscious Cogn,* 18**,** 110-7.

LENGGENHAGER, B., SMITH, S. T. & BLANKE, O. 2006. Functional and neural mechanisms of embodiment: importance of the vestibular system and the temporal parietal junction. *Rev Neurosci,* 17**,** 643-57.

LEVITT, H. 1971. Transformed up-down methods in psychoacoustics. *J Acoust Soc Am,* 49**,** Suppl 2:467+.

LEWIS, J. W. & VAN ESSEN, D. C. 2000. Mapping of architectonic subdivisions in the macaque monkey, with emphasis on parieto-occipital cortex. *J Comp Neurol,* 428**,** 79-111.

LOBEL, E., KLEINE, J. F., BIHAN, D. L., LEROY-WILLIG, A. & BERTHOZ, A. 1998. Functional MRI of galvanic vestibular stimulation. *J Neurophysiol,* 80**,** 2699-709.

LOBEL, E., KLEINE, J. F., LEROY-WILLIG, A., VAN DE MOORTELE, P. F., LE BIHAN, D., GRÜSSER, O. J. & BERTHOZ, A. 1999. Cortical areas activated by bilateral galvanic vestibular stimulation. *Ann N Y Acad Sci,* 871**,** 313-23.

MAGNUM, G. 2009. Inner Ear [Diagram]. Retrieved from http://puttingzone.com/graphics/Anatomy/innerear.jpg.

MARCAR, V. L., XIAO, D. K., RAIGUEL, S. E., MAES, H. & ORBAN, G. A. 1995. Processing of kinetically defined boundaries in the cortical motion area MT of the macaque monkey. *J Neurophysiol,* 74**,** 1258-70.

MATESZ, C., NAGY, E., KULIK, A. & TONKOL, A. 1997. Projections of the medial and superior vestibular nuclei to the brainstem and spinal cord in the rat. *Neurobiology (Bp),* 5**,** 489-93.

MAUNSELL, J. H., GHOSE, G. M., ASSAD, J. A., MCADAMS, C. J., BOUDREAU, C. E. & NOERAGER, B. D. 1999. Visual response latencies of magnocellular and parvocellular LGN neurons in macaque monkeys. *Vis Neurosci,* 16**,** 1-14.

MAUNSELL, J. H., NEALEY, T. A. & DEPRIEST, D. D. 1990. Magnocellular and parvocellular contributions to responses in the middle temporal visual area (MT) of the macaque monkey. *J Neurosci,* 10**,** 3323-34.

MAUNSELL, J. H. & VAN ESSEN, D. C. 1983. Functional properties of neurons in middle temporal visual area of the macaque monkey. I. Selectivity for stimulus direction, speed, and orientation. *J Neurophysiol,* 49**,** 1127-47.

MAZUREK, M. E., ROITMAN, J. D., DITTERICH, J. & SHADLEN, M. N. 2003. A role for neural integrators in perceptual decision making. *Cereb Cortex,* 13**,** 1257-69.

MCFADZEAN, R., BROSNAHAN, D., HADLEY, D. & MUTLUKAN, E. 1994. Representation of the visual field in the occipital striate cortex. *Br J Ophthalmol,* 78**,** 185-90.

MCGILL UNIVERSITY 2013. The various visual cortexes [Flow Chart]. Retrieved from http://thebrain.mcgill.ca/flash/a/a_02/a_02_cr/a_02_cr_vis/a_02_cr_vis.html.

MCKEEFRY, D. J., WATSON, J. D., FRACKOWIAK, R. S., FONG, K. & ZEKI, S. 1997. The activity in human areas V1/V2, V3, and V5 during the perception of coherent and incoherent motion. *Neuroimage,* 5**,** 1-12.

MCNAUGHTON, B. L., BARNES, C. A. & O'KEEFE, J. 1983. The contributions of position, direction, and velocity to single unit activity in the hippocampus of freely-moving rats. *Exp Brain Res,* 52**,** 41-9.

MCNAUGHTON, B. L., BATTAGLIA, F. P., JENSEN, O., MOSER, E. I. & MOSER, M. B. 2006. Path integration and the neural basis of the 'cognitive map'. *Nat Rev Neurosci,* 7**,** 663-78.

MERGNER, T., RUMBERGER, A. & BECKER, W. 1996. Is perceived angular displacement the time integral of perceived angular velocity? *Brain Res Bull,* 40**,** 467-70; discussion 470-1.

MESULAM, M. M. 1998. From sensation to cognition. *Brain,* 121 (Pt 6)**,** 1013-52.

METCALFE, T. & GRESTY, M. 1992. Self-controlled reorienting movements in response to rotational displacements in normal subjects and patients with labyrinthine disease. *Ann N Y Acad Sci,* 656**,** 695-8.

MEYER, B. U., DIEHL, R., STEINMETZ, H., BRITTON, T. C. & BENECKE, R. 1991. Magnetic stimuli applied over motor and visual cortex: influence of coil position and field polarity on motor responses, phosphenes, and eye movements. *Electroencephalogr Clin Neurophysiol Suppl,* 43**,** 121-34.

MINOR, L. B., MCCREA, R. A. & GOLDBERG, J. M. 1990. Dual projections of secondary vestibular axons in the medial longitudinal fasciculus to extraocular motor nuclei and the spinal cord of the squirrel monkey. *Exp Brain Res,* 83**,** 9-21.

MISHKIN, M. & UNGERLEIDER, L. G. 1982. Contribution of striate inputs to the visuospatial functions of parieto-preoccipital cortex in monkeys. *Behav Brain Res,* 6**,** 57-77.

MITTELSTAEDT, M. L. A. M., H. 1980. Homing by path integration in a mammal. *Naturwissenschaften* 67**,** 566–567.

MORAND, S., THUT, G., DE PERALTA, R. G., CLARKE, S., KHATEB, A., LANDIS, T. & MICHEL, C. M. 2000. Electrophysiological evidence for fast visual processing through the human koniocellular pathway when stimuli move. *Cereb Cortex,* 10**,** 817-25.

MOSER, E. I., KROPFF, E. & MOSER, M. B. 2008. Place cells, grid cells, and the brain's spatial representation system. *Annu Rev Neurosci,* 31**,** 69-89.

MOSER, E. I. & MOSER, M. B. 2008. A metric for space. *Hippocampus,* 18**,** 1142-56.

MUEHLLEHNER, G. & KARP, J. S. 2006. Positron emission tomography. *Phys Med Biol,* 51**,** R117-37.

NADLER, J. W., ANGELAKI, D. E. & DEANGELIS, G. C. 2008. A neural representation of depth from motion parallax in macaque visual cortex. *Nature,* 452**,** 642-5.

NADLER, J. W., NAWROT, M., ANGELAKI, D. E. & DEANGELIS, G. C. 2009. MT neurons combine visual motion with a smooth eye movement signal to code depth-sign from motion parallax. *Neuron,* 63**,** 523-32.

NAITO, Y., TATEYA, I., HIRANO, S., INOUE, M., FUNABIKI, K., TOYODA, H., UENO, M., ISHIZU, K., NAGAHAMA, Y., FUKUYAMA, H. & ITO, J. 2003. Cortical correlates of vestibulo-ocular reflex modulation: a PET study. *Brain,* 126**,** 1562-78.

NEALEY, T. A. & MAUNSELL, J. H. 1994. Magnocellular and parvocellular contributions to the responses of neurons in macaque striate cortex. *J Neurosci,* 14**,** 2069-79.

O'KEEFE, J. 1976. Place units in the hippocampus of the freely moving rat. *Exp Neurol,* 51**,** 78-109.

O'KEEFE, J. & BURGESS, N. 2005. Dual phase and rate coding in hippocampal place cells: theoretical significance and relationship to entorhinal grid cells. *Hippocampus,* 15**,** 853-66.

O'KEEFE, J. & CONWAY, D. H. 1978. Hippocampal place units in the freely moving rat: why they fire where they fire. *Exp Brain Res,* 31**,** 573-90.

ORBAN, G. A., DUPONT, P., DE BRUYN, B., VANDENBERGHE, R., ROSIER, A. & MORTELMANS, L. 1998. Human brain activity related to speed discrimination tasks. *Exp Brain Res,* 122**,** 9-22.

PARIYADATH, V. & EAGLEMAN, D. 2007. The effect of predictability on subjective duration. *PLoS One,* 2**,** e1264.

PASCUAL-LEONE, A. & WALSH, V. 2001. Fast backprojections from the motion to the primary visual area necessary for visual awareness. *Science,* 292**,** 510-2.

PAVANI, F., SPENCE, C. & DRIVER, J. 2000. Visual capture of touch: out-of-the-body experiences with rubber gloves. *Psychol Sci,* 11**,** 353-9.

PIANTA, M. J. & KALLONIATIS, M. 2000. Characterisation of dark adaptation in human cone pathways: an application of the equivalent background hypothesis. *J Physiol,* 528**,** 591-608.

POLLEN, D. A. 1999. On the neural correlates of visual perception. *Cereb Cortex,* 9**,** 4-19.

PROBST, T., BRANDT, T. & DEGNER, D. 1986. Object-motion detection affected by concurrent self-motion perception: psychophysics of a new phenomenon. *Behav Brain Res,* 22**,** 1-11.

PROBST, T., STRAUBE, A. & BLES, W. 1985. Differential effects of ambivalent visual-vestibular-somatosensory stimulation on the perception of self-motion. *Behav Brain Res,* 16**,** 71-9.

PUCE, A., ALLISON, T., GORE, J. C. & MCCARTHY, G. 1995. Face-sensitive regions in human extrastriate cortex studied by functional MRI. *J Neurophysiol,* 74**,** 1192-9.

QUINTANA, J. & FUSTER, J. M. 1993. Spatial and temporal factors in the role of prefrontal and parietal cortex in visuomotor integration. *Cereb Cortex,* 3**,** 122-32.

QUINTANA, J. & FUSTER, J. M. 1999. From perception to action: temporal integrative functions of prefrontal and parietal neurons. *Cereb Cortex,* 9**,** 213-21.

REDISH, A. D. 1999. *Beyond the Cognitive Map: From Place Cells to Episodic Memory* Cambridge, MIT Press.

REDISH, A. D. & TOURETZKY, D. S. 1998. The role of the hippocampus in solving the Morris water maze. *Neural Comput,* 10**,** 73-111.

REDISH, A. D., TOURETZKY, D. S., TOURETZKY, D. S., MOZER, M. C. & HASSELMO, M. E. 1996. Modeling Interactions of the Rat's Place and Head Direction Systems. *In:* D. S. TOURETZKY, M. C. M. A. M. E. H. (ed.) *Advances in Neural Information Processing Systems 8.* MIT Press.

RIESENHUBER, M. & POGGIO, T. 1999. Hierarchical models of object recognition in cortex. *Nat Neurosci,* 2**,** 1019-25.

ROSA, M. G. 2002. Visual maps in the adult primate cerebral cortex: some implications for brain development and evolution. *Braz J Med Biol Res,* 35**,** 1485-98.

ROTENBERG, A. & MULLER, R. U. 1997. Variable place-cell coupling to a continuously viewed stimulus: evidence that the hippocampus acts as a perceptual system. *Philos Trans R Soc Lond B Biol Sci,* 352**,** 1505-13.

ROY CHOUDHURY, K., BOYLE, L., BURKE, M., LOMBARD, W., RYAN, S. & MCNAMARA, B. 2011. Intra subject variation and correlation of motor potentials evoked by transcranial magnetic stimulation. *Ir J Med Sci,* 180**,** 873-80.

RUWALDT, M. M. & SNIDER, R. S. 1956. Projections of vestibular areas of cerebellum to the cerebrum. *J Comp Neurol,* 104**,** 387-401.

SAMSONOVICH, A. & MCNAUGHTON, B. L. 1997. Path integration and cognitive mapping in a continuous attractor neural network model. *Journal of Neuroscience,* 17**,** 5900-5920.

SANABRIA, D., SOTO-FARACO, S., CHAN, J. S. & SPENCE, C. 2004. When does visual perceptual grouping affect multisensory integration? *Cogn Affect Behav Neurosci,* 4**,** 218-29.

SEEMUNGAL, B. M., GLASAUER, S., GRESTY, M. A. & BRONSTEIN, A. M. 2007. Vestibular perception and navigation in the congenitally blind. *Journal of Neurophysiology,* 97**,** 4341-4356.

SEEMUNGAL, B. M., GUNARATNE, I. A., FLEMING, I. O., GRESTY, M. A. & BRONSTEIN, A. M. 2004. Perceptual and nystagmic thresholds of vestibular function in yaw. *J Vestib Res,* 14**,** 461-6.

SEEMUNGAL, B. M., GUZMAN-LOPEZ, J., ARSHAD, Q., SCHULTZ, S. R., WALSH, V. & YOUSIF, N. 2012. Vestibular Activation Differentially Modulates Human Early Visual Cortex and V5/MT Excitability and Response Entropy. *Cereb Cortex*.

SEIDEMANN, E. & NEWSOME, W. T. 1999. Effect of spatial attention on the responses of area MT neurons. *Journal of Neurophysiology,* 81**,** 1783-1794.

SERGENT, J., OHTA, S. & MACDONALD, B. 1992. Functional neuroanatomy of face and object processing. A positron emission tomography study. *Brain,* 115 Pt 1**,** 15-36.

SHARP, P. E. 1996. Multiple spatial/behavioral correlates for cells in the rat postsubiculum: multiple regression analysis and comparison to other hippocampal areas. *Cereb Cortex,* 6**,** 238-59.

SHARP, P. E., BLAIR, H. T. & BROWN, M. 1996. Neural network modeling of the hippocampal formation spatial signals and their possible role in navigation: A modular approach. *Hippocampus,* 6**,** 720-734.

SHARP, P. E., BLAIR, H. T. & CHO, J. 2001. The anatomical and computational basis of the rat head-direction cell signal. *Trends Neurosci,* 24**,** 289-94.

SHERBACK, M., VALERO-CUEVAS, F. J. & D'ANDREA, R. 2010. Slower visuomotor corrections with unchanged latency are consistent with optimal adaptation to increased endogenous noise in the elderly. *PLoS Comput Biol,* 6**,** e1000708.

SILVANTO, J., COWEY, A., LAVIE, N. & WALSH, V. 2005a. Striate cortex (V1) activity gates awareness of motion. *Nat Neurosci,* 8**,** 143-4.

SILVANTO, J., LAVIE, N. & WALSH, V. 2005b. Double dissociation of V1 and V5/MT activity in visual awareness. *Cereb Cortex,* 15**,** 1736-41.

SILVANTO, J., MUGGLETON, N. G., COWEY, A. & WALSH, V. 2007. Neural adaptation reveals state-dependent effects of transcranial magnetic stimulation. *Eur J Neurosci,* 25**,** 1874-81.

SIMONS, J. S., KOUTSTAAL, W., PRINCE, S., WAGNER, A. D. & SCHACTER, D. L. 2003. Neural mechanisms of visual object priming: evidence for perceptual and semantic distinctions in fusiform cortex. *Neuroimage,* 19**,** 613-26.

SINCICH, L. C., PARK, K. F., WOHLGEMUTH, M. J. & HORTON, J. C. 2004. Bypassing V1: a direct geniculate input to area MT. *Nat Neurosci,* 7**,** 1123-8.

SKAGGS, W. E., KNIERIM, J. J., KUDRIMOTI, H. S. & MCNAUGHTON, B. L. 1995. A model of the neural basis of the rat's sense of direction. *Adv Neural Inf Process Syst,* 7**,** 173-80.

SMITH, A. T., GREENLEE, M. W., SINGH, K. D., KRAEMER, F. M. & HENNIG, J. 1998. The processing of first- and second-order motion in human visual cortex assessed by functional magnetic resonance imaging (fMRI). *J Neurosci,* 18**,** 3816-30.

SMITH, A. T., WALL, M. B. & THILO, K. V. 2012. Vestibular inputs to human motion-sensitive visual cortex. *Cereb Cortex,* 22**,** 1068-77.

SMITH, A. T., WALL, M. B., WILLIAMS, A. L. & SINGH, K. D. 2006. Sensitivity to optic flow in human cortical areas MT and MST. *Eur J Neurosci,* 23**,** 561-9.

SNOWDEN, R. J., TREUE, S., ERICKSON, R. G. & ANDERSEN, R. A. 1991. The response of area MT and V1 neurons to transparent motion. *J Neurosci,* 11**,** 2768-85.

SNYDER, L. H., GRIEVE, K. L., BROTCHIE, P. & ANDERSEN, R. A. 1998. Separate body- and world-referenced representations of visual space in parietal cortex. *Nature,* 394**,** 887-91.

SOLSTAD, T., BOCCARA, C. N., KROPFF, E., MOSER, M. B. & MOSER, E. I. 2008. Representation of geometric borders in the entorhinal cortex. *Science,* 322**,** 1865-8.

STEINMAN, R. M., PIZLO, Z. & PIZLO, F. J. 2000. Phi is not beta, and why Wertheimer's discovery launched the Gestalt revolution. *Vision Res,* 40**,** 2257-64.

STENSOLA, H., STENSOLA, T., SOLSTAD, T., FROLAND, K., MOSER, M.-B. & MOSER, E. I. 2012. The entorhinal grid map is discretized. *Nature,* 492**,** 72-78.

STEPHAN, T., DEUTSCHLANDER, A., NOLTE, A., SCHNEIDER, E., WIESMANN, M., BRANDT, T. & DIETERICH, M. 2005. Functional MRI of galvanic vestibular stimulation with alternating currents at different frequencies. *Neuroimage,* 26**,** 721-32.

STRINGER, S. M., ROLLS, E. T. & TRAPPENBERG, T. P. 2005. Self-organizing continuous attractor network models of hippocampal spatial view cells. *Neurobiol Learn Mem,* 83**,** 79-92.

SUAREZ, C., DIAZ, C., TOLIVIA, J., ALVAREZ, J. C., GONZALEZ DEL REY, C. & NAVARRO, A. 1997. Morphometric analysis of the human vestibular nuclei. *Anat Rec,* 247**,** 271-88.

SUZUKI, M., KITANO, H., ITO, R., KITANISHI, T., YAZAWA, Y., OGAWA, T., SHIINO, A. & KITAJIMA, K. 2001. Cortical and subcortical vestibular response to caloric stimulation detected by functional magnetic resonance imaging. *Brain Res Cogn Brain Res,* 12**,** 441-9.

TADIN, D., SILVANTO, J., PASCUAL-LEONE, A. & BATTELLI, L. 2011. Improved motion perception and impaired spatial suppression following disruption of cortical area MT/V5. *J Neurosci,* 31**,** 1279-83.

TAUBE, J. S. 1998. Head direction cells and the neurophysiological basis for a sense of direction. *Prog Neurobiol,* 55**,** 225-56.

TAUBE, J. S. & BASSETT, J. P. 2003. Persistent neural activity in head direction cells. *Cereb Cortex,* 13**,** 1162-72.

TAUBE, J. S., MULLER, R. U. & RANCK, J. B., JR. 1990. Head-direction cells recorded from the postsubiculum in freely moving rats. II. Effects of environmental manipulations. *J Neurosci,* 10**,** 436-47.

TAYLOR, M. M. & CREELMAN, C. D. 1967. PEST: Efficient Estimates on Probability Functions.
Journal of the Acoustical Society of America, 41**,** 782-787.

TAYLOR, P. C., WALSH, V. & EIMER, M. 2010. The neural signature of phosphene perception. *Hum Brain Mapp,* 31**,** 1408-17.

TCHEANG, L., BULTHOFF, H. H. & BURGESS, N. 2011. Visual influence on path integration in darkness indicates a multimodal representation of large-scale space. *Proc Natl Acad Sci U S A,* 108**,** 1152-7.

THUT, G., NIETZEL, A. & PASCUAL-LEONE, A. 2005. Dorsal posterior parietal rTMS affects voluntary orienting of visuospatial attention. *Cereb Cortex,* 15**,** 628-38.

TOFT, N., INNOCENT, G. T., GETTINBY, G. & REID, S. W. 2007. Assessing the convergence of Markov Chain Monte Carlo methods: an example from evaluation of diagnostic tests in absence of a gold standard. *Prev Vet Med,* 79**,** 244-56.

TOOTELL, R. B., REPPAS, J. B., KWONG, K. K., MALACH, R., BORN, R. T., BRADY, T. J., ROSEN, B. R. & BELLIVEAU, J. W. 1995. Functional analysis of human MT and related visual cortical areas using magnetic resonance imaging. *J Neurosci,* 15**,** 3215-30.

TREUE, S. & MAUNSELL, J. H. 1996. Attentional modulation of visual motion processing in cortical areas MT and MST. *Nature,* 382**,** 539-41.

TSODYKS, M. 1999. Attractor neural network models of spatial maps in hippocampus. *Hippocampus,* 9**,** 481-9.

TYRRELL, R. & OWENS, D. 1988. A rapid technique to assess the resting states of the eyes and other threshold phenomena: The Modified Binary Search (MOBS). *Behavior Research Methods, Instruments, & Computers,* 20**,** 137-141.

UNGERLEIDER, L. G. & HAXBY, J. V. 1994. 'What' and 'where' in the human brain. *Curr Opin Neurobiol,* 4**,** 157-65.

VALERIO, S. & TAUBE, J. S. 2012. Path integration: how the head direction signal maintains and corrects spatial orientation. *Nat Neurosci,* 15**,** 1445-53.

VIARD, A., DOELLER, C. F., HARTLEY, T., BIRD, C. M. & BURGESS, N. 2011. Anterior hippocampus and goal-directed spatial decision making. *J Neurosci,* 31**,** 4613-21.

VIDYASAGAR, T. R., KULIKOWSKI, J. J., LIPNICKI, D. M. & DREHER, B. 2002. Convergence of parvocellular and magnocellular information channels in the primary visual cortex of the macaque. *Eur J Neurosci,* 16**,** 945-56.

VOLCIC, R. & KAPPERS, A. M. 2008. Allocentric and egocentric reference frames in the processing of three-dimensional haptic space. *Exp Brain Res,* 188**,** 199-213.

WAGNER, T., RUSHMORE, J., EDEN, U. & VALERO-CABRE, A. 2009. Biophysical foundations underlying TMS: setting the stage for an effective use of neurostimulation in the cognitive neurosciences. *Cortex,* 45**,** 1025-34.

WANDELL, B. A., BREWER, A. A. & DOUGHERTY, R. F. 2005. Visual field map clusters in human cortex. *Philos Trans R Soc Lond B Biol Sci,* 360**,** 693-707.

WATANABE, T., NANEZ, J. E., SR., KOYAMA, S., MUKAI, I., LIEDERMAN, J. & SASAKI, Y. 2002. Greater plasticity in lower-level than higher-level visual motion processing in a passive perceptual learning task. *Nat Neurosci,* 5**,** 1003-9.

WENZEL, R., BARTENSTEIN, P., DIETERICH, M., DANEK, A., WEINDL, A., MINOSHIMA, S., ZIEGLER, S., SCHWAIGER, M. & BRANDT, T. 1996. Deactivation of human visual cortex during involuntary ocular oscillations. A PET activation study. *Brain,* 119 (Pt 1)**,** 101-10.

WEST VIRGINIA UNIVERSITY 2013. Optic Flow and Mobility [Computer generated image]. Retrieved from http://www.hsc.wvu.edu/wvucn/Faculty-Lab-Personnel/Odom/Research-Topics/Optic-Flow-and-Mobility.

WICHMANN, F. A. & HILL, N. J. 2001a. The psychometric function: I. Fitting, sampling, and goodness of fit. *Percept Psychophys,* 63**,** 1293-313.

WICHMANN, F. A. & HILL, N. J. 2001b. The psychometric function: II. Bootstrap-based confidence intervals and sampling. *Percept Psychophys,* 63**,** 1314-29.

WILSON, V. J., WYLIE, R. M. & MARCO, L. A. 1967. Projection to the spinal cord from the medial and descending vestibular nuclei of the cat. *Nature,* 215**,** 429-30.

WILSON, V. J. & YOSHIDA, M. 1969. Comparison of effects of stimulation of Deiters' nucleus and medial longitudinal fasciculus on neck, forelimb, and hindlimb motoneurons. *J Neurophysiol,* 32**,** 743-58.

WIST, E. R., BRANDT, T. & KRAFCZYK, S. 1983. Oscillopsia and retinal slip. Evidence supporting a clinical test. *Brain,* 106 (Pt 1)**,** 153-68.

ZEKI, S. & FFYTCHE, D. H. 1998. The Riddoch syndrome: insights into the neurobiology of conscious vision. *Brain,* 121 (Pt 1)**,** 25-45.

ZEKI, S., WATSON, J. D. & FRACKOWIAK, R. S. 1993. Going beyond the information given: the relation of illusory visual motion to brain activity. *Proc Biol Sci,* 252**,** 215-22.

ZEKI, S., WATSON, J. D., LUECK, C. J., FRISTON, K. J., KENNARD, C. & FRACKOWIAK, R. S. 1991. A direct demonstration of functional specialization in human visual cortex. *J Neurosci,* 11**,** 641-9.

ZEKI, S. M. 1974. Functional organization of a visual area in the posterior bank of the superior temporal sulcus of the rhesus monkey. *J Physiol,* 236**,** 549-73.

ZHANG, K. 1996. Representation of spatial orientation by the intrinsic dynamics of the head-direction cell ensemble: a theory. *J Neurosci,* 16**,** 2112-26.

ZHAOPING, L. & GUYADER, N. 2007. Interference with bottom-up feature detection by higher-level object recognition. *Curr Biol,* 17**,** 26-31.

ZHENG, Y., HORII, A., APPLETON, I., DARLINGTON, C. L. & SMITH, P. F. 2001. Damage to the vestibular inner ear causes long-term changes in neuronal nitric oxide synthase expression in the rat hippocampus. *Neuroscience,* 105**,** 1-5.